



HAL
open science

Genetic and environmental control of microfibril angle on eucalyptus wood: its effects on wood traits and implication for selection

Paulo Ricardo Gherardi Hein

► **To cite this version:**

Paulo Ricardo Gherardi Hein. Genetic and environmental control of microfibril angle on eucalyptus wood: its effects on wood traits and implication for selection. Life Sciences [q-bio]. Université Montpellier II - Sciences et Techniques du Languedoc, 2011. English. NNT: . tel-00623042

HAL Id: tel-00623042

<https://theses.hal.science/tel-00623042>

Submitted on 13 Sep 2011

HAL is a multi-disciplinary open access archive for the deposit and dissemination of scientific research documents, whether they are published or not. The documents may come from teaching and research institutions in France or abroad, or from public or private research centers.

L'archive ouverte pluridisciplinaire **HAL**, est destinée au dépôt et à la diffusion de documents scientifiques de niveau recherche, publiés ou non, émanant des établissements d'enseignement et de recherche français ou étrangers, des laboratoires publics ou privés.

**UNIVERSITE MONTPELLIER 2
SCIENCES ET TECHNIQUES DU LANGUEDOC**

THESE

pour obtenir le grade de

DOCTEUR DE L'UNIVERSITE MONTPELLIER 2

Discipline : Mécanique et Génie Civil

Ecole Doctorale : Information, Structures et Systèmes

présentée et soutenue publiquement

par

Paulo Ricardo GHERARDI HEIN

Le 16 juin 2011

Titre :

**GENETIC AND ENVIRONMENTAL CONTROL OF MICROFIBRIL ANGLE
ON *Eucalyptus* WOOD: ITS EFFECTS ON WOOD TRAITS AND
IMPLICATION FOR SELECTION**

JURY

M. Kambiz POURTAHMASI
M. Joseph GRIL
M. Philippe ROZENBERG
M. Jean-Michel LEBAN
M. Gilles CHAIX
M. Loic BRANCHERIAU
M. José Tarcísio LIMA
M. Bruno CLAIR

Président
Directeur de Thèse
Rapporteur
Rapporteur
Examineur
Examineur
Examineur
Invité

PREFACE

This thesis was based on research done at the “Bois Tropicaux” unit of research (UR40) of the PERSYST department and at the “Genetic improvement and adaptation of mediterranean and tropical plants” unit of research (UMR AGAP) of the BIOS department of the *Centre de Coopération Internationale en Recherche Agronomique pour le Développement* (CIRAD, France); at the “Laboratoire de Mécanique et Génie Civil” of the *Université de Montpellier 2* (UM2, France) and at the “Laboratório de Ciência e Tecnologia da Madeira” of the *Universidade Federal de Lavras* (UFLA, Brazil).

The trees used in this study were provided by the *Centre de Recherche sur la Durabilité et la Productivité des Plantations Industrielles* (CRDPI, Republic of Congo) and by *Celulose Nipo-Brasileira S.A.* (CENIBRA, Brazil). Financial support for the study was provided by CNPq (*Conselho Nacional de Desenvolvimento Científico e Tecnológico*, Brazil), CIRAD and CENIBRA. My scholarship was granted by CNPq through the process no. 200970/2008-9.

I would like to thank many people who have assisted me to achieve this accomplishment, through encouragement and help along the way during my doctoral thesis at University of Montpellier 2. I wish to thank my Thesis director Dr. Joseph GRIL whose experience steered me in the right direction during this endeavour and co-advisors Dr. Gilles CHAIX, Dr. Loic BRANCHERIAU and Dr. José Tarcísio LIMA for their helpful, precise guidance. Special thanks to Bruno CLAIR, Tancrede ÁLMERAS and Bernard THIBAUT for their passion, their fruitful tracks and advice.

Thanks to the members of my advisory committee: Dr. Philippe ROZENBERG, Dr. Jean-Michel LEBAN, Dr. Jean-Marc BOUVET, Dr. Bruno CLAIR, Dr. Bernard THIBAUT, Dr. Alfredo NAPOLI, Mr. Gilles CALCHERA, Dr. Kambiz POURTAHMASI and Dr. Jean GÉRARD, whose insights and knowledge guided this process. Thanks also to Dr. José Tarcísio LIMA for helping us to find wood, his valuable insights, and dedication to the scientific process and Dr. Jean Marc BOUVET and Dr. Marie DENIS for their statistic assistance.

Thanks also to the staff of the CIRAD teams *Bois Tropicaux* and *Genetic improvement and adaptation of mediterranean and tropical plants* for technical, experimental and scientific support. Special thanks to Isabelle CHALON and Roselyne LANNES for their helpful assistance. Thanks to *Departamento de Ciências Florestais, Universidade Federal de Lavras*, Brazil, for experimental support. Special thanks to Paulo Fernando TRUGILHO and José Reinaldo Moreira da SILVA for critical reading of my project proposal in 2008, when I submit it for evaluation at CNPq.

To all of my colleagues, I am truly grateful for the support, assistance, and inspiration during my stay at Montpellier, France. I realize that so many individuals helped me, that I cannot name them all. However, special recognition is given to: Luc MARTIN and Cecílio FROIS.

To my parents who have encouraged me over the years. Agradeço aos meus pais, minhas tias e tios, minhas irmãs e irmãos pelos conselhos e apoio ao longo dos últimos anos.

Finally, I would like to thank my mate Aline for her patience, love and understanding.

“For scientists, wood remains a fascinating adventure. On the one hand, solutions used by nature to solve its mechanical problems are fully up to date: nano structured materials, smart structures, light and low energy materials... Understanding more and more both the ‘making of wood’ and the wood properties will surely be very profitable for the progress of man-made materials and structures. On the other hand, humanity will have in future to deal with the struggling problem of avoiding ‘troublesome’ energy solutions, for the making of materials for example. Wood is a striking demonstration of making a useful material using very simple and renewable factors: solar energy, water and carbon dioxide.

We can try to copy this system for producing 100% man-made materials. We can also try to harvest with care these marvellous gifts from nature that trees are, and use them the best we can, like generations of genius craftsmen did before us, through the making of structures, furniture, musical instruments and so on. If so, the first thing to do is to restore to wood its proper rank among other materials (data bank, material selection software, material teaching...), and admit that diversity is a treasure, not a pledge, for smart engineers”.

(B THIBAUT, J GRIL and M FOURNIER, 2001)

CONTROLE GENETIQUE ET ENVIRONNEMENTAL DE L'ANGLE DES MICROFIBRILLES DANS LE BOIS D'*Eucalyptus* : EFFETS SUR LES PROPRIETES DU BOIS ET IMPLICATION POUR LA SELECTION

Le contrôle génétique et l'environnemental de l'angle des microfibrilles (MFA), les corrélations génétiques du MFA avec d'autres caractères du bois et de croissance, et par conséquent les implications pour la sélection sont très peu documentés pour les *Eucalyptus*. Les objectifs de cette étude étaient d'établir la variation spatiale du MFA, de la densité du bois (ρ) et de sa rigidité (E); de déterminer les relations entre MFA et propriétés du bois et enfin d'estimer le contrôle génétique et environnemental des caractères du bois et de la croissance dans le cadre de tests clonaux et de test de descendances d'*Eucalyptus* au Brésil et au Congo. Méthodes classiques, résonance, diffraction des rayons-X et la spectroscopie proche infrarouge ont été combinées pour évaluer les propriétés du bois. La variation du MFA représente 44% de la variation du module spécifique (E/ ρ) du bois. La densité du bois est le principal déterminant de la rigidité et de la résistance du bois alors que le MFA joue un rôle secondaire. Les estimations de l'héritabilité sont de modéré à élevées pour le MFA, ρ , E, la lignine de Klason (KL) et les caractères de croissance, selon la position spatiale et le dispositif expérimental. Le contrôle génétique du MFA, ρ et E et leurs corrélations génétiques avec KL et la circonférence à 1.3 mètre des arbres varient avec l'âge. Les résultats suggèrent que les arbres à forte croissance sont génétiquement plus aptes à produire du bois de faible densité et un MFA plus faible pour assurer la rigidité du bois nécessaire à leur développement. La plupart des propriétés du bois sont génétiquement corrélées négativement avec la croissance, bien que corrélations génétiques favorables entre propriétés du bois sont observés. Les corrélations génétiques et environnementales sont parfois de signes opposés selon les caractères considérés. Ceci peut s'expliquer par l'effet pléiotropique des gènes et/ou par le déséquilibre de liaison. Les conséquences de ces résultats sur les stratégies de sélection sont discutées selon l'usage final du bois d'*Eucalyptus*.

GENETIC AND ENVIRONMENTAL CONTROL OF MICROFIBRIL ANGLE ON *Eucalyptus* WOOD: ITS EFFECTS ON WOOD TRAITS AND IMPLICATION FOR SELECTION

The genetic and environmental control of microfibril angle (MFA), the genetic correlations with other wood and growth traits, and therefore the implications for selection are poorly documented for *Eucalyptus*. Thus, the objectives of this study were to determine the spatial variation of the MFA, wood density (ρ) and stiffness (E); to determine the relationship between MFA and wood traits and finally to estimate the genetic and environmental control of wood and growth traits from clonal and progeny tests of *Eucalyptus* in Brazil and Congo. Conventional methods, resonance, X-ray diffraction and spectroscopy were combined to evaluate the wood properties. MFA variation accounted for 44 percent of the variation in specific modulus (E/ ρ) of wood. The ρ was the prime determinant on wood stiffness and strength while the MFA played a secondary role. The heritability estimates were moderate to high for the MFA, ρ , E, Klason lignin (KL) and growth traits according to the spatial position and the experimental design. Genetic control of the MFA, ρ and E and their genetic correlations with KL and circumference at 1.3 meters of trees varied with age. The results suggest that tree with potential to grow fast are genetically more prone to produce low ρ and also to decrease the MFA for ensuring stiffness required for their development. Most wood properties were genetically negatively correlated with growth, although favorable genetic correlations between many wood traits were observed. Genetic and environmental correlations were sometimes of opposite signs according to the considered trait. This can be explained by the pleiotropic effect of genes and / or linkage disequilibrium. The implications of these findings for selection strategies are discussed according to the final use of *Eucalyptus* wood.

DISCIPLINE

Mechanical and Civil Engineering

KEYWORDS

Wood, quality, stiffness, microfibril angle, breeding, quantitative genetic, genetic control, genotype by environment interaction, Clonal propagation, progeny trials

**CIRAD - Production and Processing of Tropical Woods (UR40) TA B-40/16 and UMR - Genetic improvement and adaptation of mediterranean and tropical plants TA A-108/C - 34398 - Montpellier
CNRS - Laboratoire de Mécanique et Génie Civil - 34090 - Montpellier**

CONTENTS

PREFACE	3
CONTENTS	9
EXPANDED SUMMARY	11
RÉSUMÉ ÉTENDU	15
Matériel végétal	16
Stratégie de la recherche	16
Phénotypage des propriétés du bois	16
Les modèles SPIR	17
Approches en génétique quantitative	18
Résultats principaux	19
Considérations finales	20
LIST OF NOTATIONS	21
LIST OF WOOD TRAITS	21
LIST OF PAPERS	23
1 INTRODUCTION	25
1.1 BACKGROUND	25
1.2 <i>Eucalyptus</i> as a timber source	26
1.2.1 Problems of <i>Eucalyptus</i> wood	27
1.2.2 What is wood quality?	29
1.2.3 Selecting traits for wood improvement	30
1.2.4 MFA controls wood quality	31
1.3 <i>Eucalyptus</i> breeding programs	36
1.3.1 Quantitative genetic of wood	38
1.3.2 <i>Eucalyptus</i> breeding programs	39
1.3.3 Challenges	43
1.3.4 Strategies for wood phenotyping	43
1.4 Scientific strategy	48
1.4.1 Lacks of knowledge	48
1.4.2 Hypothesis of this study	51
1.4.3 Purposes of this study	51
1.4.4 Strategy of this study	53
2 MATERIAL AND METHODS	57
2.1 Origin of the material	57
2.1.1 Progeny test	57
2.1.2 Clonal test	57
2.2 Sampling preparation	59
2.2.1 Progeny test	59
2.2.2 Clonal test	60
2.3 Methods for phenotyping	62
2.3.1 Sonic resonance	62
2.3.2 Static bending test	64
2.3.3 Basic density and shrinkage of wood	65
2.3.4 X-ray diffraction	66
2.3.5 Wet-lab chemistry	67
2.3.6 NIR spectroscopy	67
2.3.7 Resume of wood traits measurements	68
2.4 STATISTICAL ANALYSIS	69
2.4.1 Descriptive statistics and correlations	69
2.4.2 Developing NIR spectroscopy models	69

2.4.3	Genetic parameter estimation	71
3	RESULTS AND DISCUSSION.....	75
3.1	Growth traits.....	75
3.2	Wood phenotyping of progeny tests.....	76
3.2.1	Wood chemical composition	76
3.2.2	Microfibril angle and wood density.....	77
3.2.3	Effect of wood chemical components on MFA.....	79
3.3	Phenotyping the wood of clonal tests.....	79
3.3.1	Kiln-dried scantlings	79
3.3.2	Wood specimens from scantlings.....	81
3.3.3	Small wood samples	83
3.3.4	Correlations between wood traits of <i>Eucalyptus</i> from clonal test	87
3.4	Near infrared spectroscopic models	91
3.4.1	NIR spectra.....	91
3.4.2	Reference data	92
3.4.3	NIRS-based calibrations and validations.....	93
3.5	Genetic studies from progeny test	99
3.5.1	Heritability of growth and wood traits	99
3.5.2	Genetic and residual correlations	101
3.5.3	Age trends of additive genetic, residual and phenotypic correlations	103
3.5.4	Implications for selection	105
3.6	Genetic studies from clonal test.....	106
3.6.1	Growth traits.....	106
3.6.2	Genetic studies from the kiln-dried scantlings	108
3.6.3	Genetic studies from NIR-predicted data of wood discs.....	109
3.6.4	NIR spectral heritability estimates	123
4	CONCLUDING REMARKS	127
4.1	Spatial variation of wood traits.....	127
4.2	Influence of MFA on wood traits.....	128
4.3	Combining techniques for assessing wood traits.....	129
4.3.1	Resonance.....	129
4.3.2	NIR spectroscopy calibrations.....	129
4.4	Genetic and environmental control of wood traits	131
4.4.1	Genetic studies from the progeny tests.....	131
4.4.2	Genetic studies from the clonal tests	132
5	PERSPECTIVES.....	135
6	ANNEXES	137
6.1	Phenotyping the air-dried scantlings of clonal tests.....	137
6.2	Correlations between wood traits of air- and kiln-dried scantlings.....	138
6.3	Environmental and radial position effect on MFA and its correlation with wood traits	140
6.4	Comparing 3- and 4-points bending tests.....	141
6.5	Genetic studies from resonance on air-dried scantlings	142
6.6	Spatial variation of heritability estimates	144
7	REFERENCES.....	147
	LIST OF TABLES	161
	LIST OF FIGURES.....	165

EXPANDED SUMMARY

The first studies on genetics of *Eucalyptus* were carried out in order to determine the suitability of species and provenances for particular environments and to estimate genotype by environment interactions in a range of trials. Afterwards, the studies on genetics of *Eucalyptus* started to concentrate on tree growth, survival, stem straightness and branch quality because the forest industry was focused mainly on achieving gains in growth and form. Thus, the continuity of forestry research on *Eucalyptus* over the past several years has allowed some companies to reach productivity notably higher than those of the first generations. As a result, plantations are producing merchantable trees at higher growth rate with trees harvested at a younger age.

However, the progress in wood production leads to two main concerns. Increasing the growth rate can favour the occurrence of growth stress while shortening the rotation causes an increase in the proportion of juvenile wood within the stem. Growth stress is a major cause of degrade and processing problems (warping and splitting of logs and boards). Juvenile wood has lower density, thinner cell walls, shorter fibres and higher microfibril angles when compared to mature wood. Lower densities and reduced fibre dimensions, higher MFA and low stiffness of juvenile *Eucalyptus* wood are expected to produce a poorer quality product. As a result, these defects affecting wood quality and product yield are the main obstacles for greater market acceptance of fast grown *Eucalyptus* wood as a higher value sawn timber product. Trees develop growth stresses as they grow and this phenomenon manifests itself when the tree is felled, cut into logs and converted into boards. Growth stress is a problem difficult to solve in *Eucalyptus* plantations since it is a natural mechanism of tree for surviving. On the other hand, any reduction of juvenile wood or genetic improvement in the quality of juvenile wood could have broad economic implications for the forest industry. For these reasons, wood traits have begun to receive more attention in *Eucalyptus* breeding programs.

So much knowledge about the wood has been gathered over the past decades and numerous studies are making valuable contributions in wood science and technology. Thus, many traits are known to be important in determining the value of *Eucalyptus* wood as sawn timber including its basic density, wood stiffness and strength, juvenile wood proportion and the microfibril angle (MFA), the preferable angle of the cellulose microfibril within its cell walls. Previous studies investigating the relationship between microfibril angle, basic density (ρ) and wood stiffness showed that MFA was the prime determinant of both the modulus of elasticity (E) and the specific modulus (E/ ρ) in *Eucalyptus* wood. These wood traits seem to be important in improving overall products quality in *Eucalyptus* wood. Thus, breeding programs for *Eucalyptus* should include them as selection criteria. While the heritability estimates for wood density have been exhaustively reported for many Eucalypt species, the genetic control over microfibril angle was neglected in breeding strategies for improving wood quality. In short, the genetic and environmental control of microfibril angle (MFA), its genetic correlations with other wood and growth traits and implications for selection are still not well established in *Eucalyptus*.

Thus, the aims of this study were: i) to establish the spatial variation of ρ , E and MFA within the trees; ii) to determine the influence of MFA on wood traits and iii) to determine genetic control over circumference at breast height (C), tree height (H) of MFA, ρ , E, Klason lignin (KL) content, syringyl to guaiacyl (S/G) ratio and growth traits, their variation from pith to cambium and their genetic correlations.

This thesis makes an effort to understanding how genetic and environmental factors control the wood properties variation and how *Eucalyptus* trees adapt their wood traits in order to continuously grow up and at the same time maintains upright even when they are constrained by bending movements in response to wind and gravity. To attend its purposes, this study falls into two parts. The first consisted on phenotyping wood traits and the second on the quantifying the genetic parameters of wood traits.

The parts of the study are valued in the form of publication, but in this thesis the main results were combined along the text in order to make a logical and coherent manuscript.

Wood traits, heritability and correlations were assessed in a progeny test represented by 340 control-pollinated progenies of 14-year-*Eucalyptus urophylla* S.T. Blake and in a clonal test represented by 150 6-year-*Eucalyptus urophylla* x *grandis* hybrids growing at contrasting sites.

In order to provide experimental data to perform such analyses, indirect methods and techniques such as sonic resonance, X-ray diffraction and near infrared (NIR) spectroscopy were combined for assessing MFA and wood stiffness in a large sampling of *Eucalyptus* wood. Traditional methods and indirect methods such as sonic resonance, X-ray diffraction were used in order to provide an experimental data set. Hence, near infrared spectroscopic models were developed based on experimental data for estimating such wood traits from NIR spectra recorded at various radial and longitudinal positions.

The relationships among wood traits investigated in 6-year-*Eucalyptus* wood from clonal test have shown that MFA variation accounted for only 44 percent of the variation in specific modulus in *Eucalyptus* wood. The basic density wood was the prime determinant of both modulus of elasticity and modulus of rupture while the MFA played a secondary role on stiffness and strength of wood from fast growing plantations.

High heritability were found for MFA ($h^2=0.65$), ρ ($h^2=0.61$), LK ($h^2=0.72$) and S/G ($h^2=0.71$) for 14-years-*Eucalyptus* from the progeny test. The genetic control of ρ and MFA and the genetic and residual correlation between chemical and growth traits varied with age. The genetic correlation C x ρ was always strongly negative ($r<-0.88$) while the correlation ρ x MFA remained constant and positive in the juvenile wood ($r=0.7$), decreasing considerably in the mature wood ($r=0.3$). This could mean that trees with a strong potential to grow fast are genetically programmed to produce low-density woods and also to decrease the microfibril angles for ensuring stiffness (the negative correlation MFA x C). Variations in MFA and KL in the mature wood are also genetically controlled. The low microfibril angle compensating low wood density and fast growth and the changes in KL content can be functionally explained by gene pleiotropic effect or statistically by linkage disequilibrium induced by sampling. From a biological point of view, the correlation MFA x density is strategic for tree survival, maintaining them ever-growing and in upright position even under winds that induces constantly bending movements. In conclusion, the genetic correlations MFA x ρ and MFA x KL acting together reveal a smart biological strategy for the survival of the tree. The underlying principles of the interaction of stiff cellulose fibrils embedded in a pliant matrix would be utilized to adjust mechanical properties. From a technological point of view, these findings allow discussing the impact on breeding strategies for pulpwood, fuelwood and timber wood production. As forestry industries are mainly searching for adequate density woods, such unfavourable correlations between growth and wood traits are of critical importance.

Low to moderate levels of broad-sense heritability (H^2) estimates were found for basic density, wood stiffness and microfibril angle of 6-year-*Eucalyptus* clones. The findings clearly revealed that heritability estimates for E and MFA exhibited opposite patterns of radial variation in the bottom of the tree, and

similar trends towards the top. For density, higher H^2 estimates were found in the higher regions of the tree, especially at the intermediate zone.

Genetic parameters were calculated directly from NIR spectra recorded on the wood. Variations in specific ranges of NIR spectra are related to variation in lignin and cellulose and hemicelluloses contents, and other wood traits. The findings clearly revealed that the variations on these specific ranges of the NIR spectra were controlled by genetic factors. The assignments of absorption bands were useful to identify which wood components presents higher broad-sense heritability estimates from NIR spectroscopic data. Some ranges of the spectra presented H^2 estimates greater than 50%. Considering that NIR spectra is countless source of information concerning many wood traits, the analysis of genetic parameters from them appears to be an efficient and promising way to evaluate the genetic control over various wood traits at once.

Most wood properties were unfavourably genetically correlated with growth, although favourable genetic correlations were observed between many *Eucalyptus* wood traits. Because of these unfavourable genetic correlations between wood and growth, selection for increasing density and stiffness or reducing MFA in the absence of selection for growth will result in a reduction (genetic loss) in volume production. Therefore, breeders, forest managers and wood producers will have to strike a balance between overall wood and growth traits, and geneticists should develop breeding strategies to deal with such negative, unfavourable genetic correlations in *Eucalyptus* plantations.

Keywords: Wood, quality, stiffness, microfibril angle, breeding, quantitative genetic, genetic control, genotype by environment interaction, clonal propagation, progeny trials

RÉSUMÉ ÉTENDU

Les premières études sur la génétique des *Eucalyptus* ont porté sur la détermination de l'aptitude en comportement et en croissance des espèces et des provenances pour des environnements particuliers, ainsi que sur l'estimation des interactions génotype environnement dans une série d'essais. Elles se sont ensuite concentrées sur la croissance des arbres, la survie, la forme des tiges et la branchaison, car les objectifs de l'industrie forestière sont basés essentiellement sur les gains en termes de volume de bois produit et de forme des arbres. Ainsi la recherche forestière sur les *Eucalyptus* au cours des dernières années, par la production de variétés améliorées, a apporté aux industriels des gains importants par rapport aux variétés des premières générations. Il en a résulté des plantations produisant plus et plus vite et permettant des récoltes à des âges plus précoces.

Toutefois, les progrès réalisés dans la production de bois conduit à deux préoccupations principales. L'augmentation de la vitesse de croissance peut favoriser l'apparition de contraintes de croissance, tandis qu'en réduisant la durée de rotation la proportion de bois juvénile dans la tige est plus élevée. Les contraintes de croissance sont une cause majeure de dévalorisation des produits et de problèmes rencontrés lors de la première transformation (déformations et fentes en bout au moment de l'abattage quand les contraintes sont libérées). Les caractéristiques du bois juvénile par rapport au bois mature sont les suivantes : faible densité, parois cellulaires plus minces, fibres plus courtes et angles de microfibrilles plus élevés. La densité plus faible, la réduction de la longueur des fibres et une rigidité moindre du bois d'*Eucalyptus* entraînent une réduction de la qualité technique et marchande. En conséquence, ces défauts affectant la qualité du bois et le rendement du produit sont les principaux obstacles à une plus grande acceptation par le marché du bois d'*Eucalyptus* à croissance rapide en bois de sciage. Les contraintes de croissance sont un problème difficile à résoudre dans les plantations d'*Eucalyptus*, car ce sont les conséquences d'un mécanisme naturel de l'arbre pour croître et s'adapter à l'environnement. D'un autre côté, la réduction de bois juvénile ou l'amélioration génétique de la qualité du bois juvénile pourrait avoir d'importantes répercussions économiques pour l'industrie forestière. Pour ces raisons, les programmes de sélection des *Eucalyptus* se mobilisent de plus en plus sur la qualité des bois.

De nombreuses connaissances sur le bois ont été recueillies au cours des dernières décennies et de nombreuses études en science des bois apportent une contribution précieuse. Ainsi, plusieurs propriétés des bois sont connues pour jouer un rôle important dans la détermination de la valeur du bois d'*Eucalyptus* : densité basale (ρ), module d'élasticité (E), proportion de bois juvénile et angle des microfibrilles (MFA) de cellulose cristalline dans les parois cellulaires. Des études antérieures sur la relation entre MFA, ρ et E ont montré que le MFA serait le principal facteur déterminant à la fois du module d'élasticité et du module spécifique (E/ρ) du bois d'*Eucalyptus*. Ces propriétés deviennent donc importantes pour l'amélioration de la qualité globale des bois d'*Eucalyptus*, et les programmes de sélection pour les *Eucalyptus* cherchent à les inclure dans les critères de sélection. Le contrôle génétique de la densité du bois est largement rapporté pour de nombreuses espèces d'*Eucalyptus*, par contre pour le MFA ce n'est pas le cas. En bref, le contrôle génétique et environnemental du MFA, ses corrélations génétiques avec les autres propriétés du bois, les caractères de croissance et les implications pour la sélection n'ont pas été encore abordés pour *Eucalyptus*.

Ainsi, les objectifs de cette étude sont les suivants: i) décrire la variabilité intra-arbre de la densité (ρ), le module (E) et l'angle des microfibrilles (MFA); ii) déterminer l'influence du MFA sur les propriétés du bois et iii) déterminer le contrôle génétique de la circonférence à hauteur de poitrine (C), la hauteur des

arbres (H), le MFA, ρ , E, la lignine de Klason (LK), le ratio syringyl sur guaiacyl (S/G) et les caractères de croissance, leur variation de la moelle au cambium et leurs corrélations génétiques.

Cette thèse s'efforce de comprendre comment les facteurs génétiques et environnementaux contrôlent la variabilité des propriétés du bois et comment les arbres d'*Eucalyptus* adaptent ces propriétés afin de croître, s'adapter à l'environnement propre aux plantations forestières intensives et résister aux contraintes telles que vent, terrain en pente, etc.

Chaque partie de l'étude est valorisée sous la forme de publications, mais le choix a été fait de rédiger ce manuscrit reprenant dans leur totalité les travaux effectués, afin de rendre compte des résultats de façon logique et cohérente.

Matériel végétal

Wood traits, les corrélations et l'héritabilité ont été évaluées à partir d'un test de descendance représenté par 340 descendants issus de pollinisation contrôlée d'*Eucalyptus urophylla* ST Blake de 14 ans (Table 4, p. 57) et à partir de trois tests clonaux échantillonnés par 150 *Eucalyptus grandis* x *urophylla* hybrides de 6 ans sur des sites contrastés (Table 5, p. 58).

Stratégie de la recherche

Pour répondre aux objectifs, cette étude se divise en deux parties. La première concerne le phénotypage des propriétés du bois et la seconde l'estimation des paramètres génétiques de ces propriétés avec la croissance. La stratégie de cette étude est décrite comme suit. Un résumé de tous les travaux menés est donné, y compris les procédures de préparation des échantillons et mesures des caractères du bois, ainsi que les principales analyses. La description détaillée de chaque élément est fournie dans Matériel et Méthodes, Résultats et discussion des différents articles.

Phénotypage des propriétés du bois

Une étude détaillée sur les propriétés du bois pour différents types d'échantillons a été réalisée en utilisant le bois de d'un essai de descendance et de tests clonaux. La Figure 12 (p. 80) résume les caractéristiques de croissance et du bois étudié dans les deux modèles expérimentaux.

Afin de fournir des données expérimentales pour effectuer les analyses génétiques, des méthodes directes et indirectes comme la résonance acoustique, la diffraction des rayons X et la spectroscopie proche infrarouge (SPIR) ont été combinées pour évaluer le MFA et la rigidité du bois pour un nombre important d'échantillon de bois d'*Eucalyptus*. Les modèles en SPIR ont été développés à partir des données de références et ont été utilisés pour estimer la qualité du bois à partir de spectres mesurés selon les positions radiales et longitudinales.

Dispositif 1 : Test de descendance du Congo

Les propriétés des bois des arbres issus d'un plan de croisement ont été étudiées à partir des disques de bois récoltés à 1,3 mètre. Tout d'abord, les disques ont été coupés en deux quartiers opposés ; 2 bandes radiales exemptes de nœuds et défauts en ont été extraits. Les spectres ont été enregistrés sur la face radiale des quartiers à trois positions radiales (1, 2 et 3) de la moelle à l'écorce. Ensuite, à partir des bandes radiales différents échantillons ont été débités selon le type de mesure, tandis que les spectres PIR ont été obtenus sur tous les échantillons (solides et poudre). Ces spectres PIR ont été utilisés pour les prédictions

(Figure 14, p. 59). Les bandes radiales ont été divisées en petits échantillons (20 x 20 x 30 mm) pour les mesures de densité du bois et en sections tangentielles (2 x 20 x 30 mm) pour les mesures du MFA. Les spectres PIR ont été mesurés sur les faces transversales, radiales et tangentielles, des petits échantillons et sur les deux côtés des sections tangentielles. Par la suite, trois valeurs T ont été enregistrées par diffraction des rayons X en trois points sur 175 sections tangentielles et la densité du bois a été mesurée sur les petits échantillons. L'article 3 présente la variation radiale du MFA et de la densité du bois, la corrélation entre eux et l'influence de l'âge de formation du bois sur ces relations dans le bois *Eucalyptus urophylla* de 14 ans.

Dispositif 2 : Tests clonaux du Brésil

150 arbres ont été récoltés à partir de 3 tests clonaux. Un billon de 2,4 mètres et 5 disques de bois ont été débités à 0, 25, 50, 75 et 100% de la hauteur commerciale pour chaque arbre. Des bandes diamétrales ont été découpées à partir des disques. Les bandes ont été poncées et les spectres PIR ont été mesurés. Ces spectres PIR ont été utilisés pour les prédictions. Les billes ont été sciées en planches centrales, et un total de 410 carrelets (45 x 60 x 2100 mm) dénommés «scantlings» ont été extraits des planches (Figure 15, p. 60). Les carrelets ont été séchés à l'air libre pendant 90 jours. Une première série de carrelets ne présentant pas de défaut a été sélectionnée avec des dimensions variables (en moyenne, 1,54 mètres de longueur, variant de 0,645 m à 2.080 m et d'épaisseur moyenne comprise entre 60 et 43 mm). Les échantillons ont été soumis à des tests de vibrations transversales et longitudinales (BING). Par la suite, les carrelets ont été séchés dans des conditions douces au séchoir à 14% d'humidité (nominale) pendant deux semaines. De nouveaux tests de vibrations transversales et longitudinales ont été effectués sur les carrelets. Enfin, des petits échantillons sans défauts (25 x 25 x 41 mm) appelés «specimens» ont été découpés à partir des carrelets et soumis à des tests de vibrations transversales et longitudinales. La masse et les dimensions de chaque spécimen ont été mesurées et la densité de poids de chaque pièce de bois a été calculée. Les propriétés dynamiques de ces bois sont discutées dans l'article 1, tandis que les approches génétiques obtenues à partir de ces résultats sont rapportés dans l'article 9.

Ensuite, ces échantillons de bois ont été testés en utilisant une machine d'essai universelle. Les essais statiques en flexion 3 et 4 points ont été effectués afin de déterminer le module de rupture (MOR). De chaque carrelet, un ou plusieurs échantillons jumeaux ont été débités : quand au moins deux spécimens jumeaux étaient obtenus, le premier était testé en flexion 4 points et le second en flexion 3 points. Cette procédure a permis de comparer les deux types d'essais de flexion sur des échantillons appariés. Ces résultats sont présentés dans la section des annexes (item 6.4, p. 141).

Par la suite, un échantillon de bois mesurant 25 mm × 25 mm × 25 mm a été découpé de ces specimens afin de mesurer la densité basale et le retrait au séchage. Les retraits ont été mesurés à partir de deux mesures, à l'humidité d'équilibre (EMC) et un état au dessus du point de saturation des fibres. Enfin, une section de 2 mm radiale a été découpée à partir de chaque petit échantillon pour les mesures de l'angle des microfibrilles. Ces différentes étapes de mesure nous ont fourni une gamme complète d'informations sur les propriétés physiques, mécaniques et anatomiques de ces échantillons de bois. L'article 2 évalue les relations entre angle des microfibrilles, densité, rigidité et résistance, module de cisaillement et retrait pour les clones d'*Eucalyptus*.

Les modèles SPIR

Cette partie de l'étude est consacrée à l'élaboration de modèles SPIR afin d'évaluer une gamme de propriétés du bois. L'objectif était également d'examiner et d'expliquer pourquoi la spectroscopie NIR

pourrait être utilisée pour prédire les propriétés dynamiques du bois et l'AMF. Le Table 3 (p. 55) présente un résumé des principales statistiques des étalonnages SPIR.

Pour les bois issus de l'essai descendance, les étalonnages SPIR ont été élaborés pour évaluer les principaux composants chimiques de bois, y compris la teneur en lignine Klason (KL), la teneur en lignine soluble dans l'acide (LAS) et le ratio syringyl et guaiacyl (S/G). Ces calibrations SPIR pour les propriétés chimiques du bois sont décrites dans **l'article 4**, où l'influence de la préparation des échantillons et son effet sur la performance du modèle sont discutés. Dans la présente étude, la lignine soluble dans l'acide n'a pas été présentée. Ensuite, les étalonnages SPIR sont élaborés pour les propriétés physiques et ultrastructurelles des échantillons de bois provenant des bandes diamétrales. **L'article 5** rapporte les modèles SPIR pour la densité basale. La démarche démontre la robustesse des modèles établis par la validation indépendante. **L'article 6** présente les modèles SPIR d'estimation de l'angle des microfibrilles et explique pourquoi la spectroscopie SPIR peut être utilisée pour prédire cette propriété ultrastructurale des parois cellulaires du bois d'*Eucalyptus*.

Pour le bois à partir des test clonaux, les étalonnages SPIR ont été élaborés pour évaluer les propriétés mécaniques du bois, tels que la densité à l'air sec et la densité du bois, le module d'élasticité dynamique, le module de cisaillement et de frottement interne, ainsi que leur première fréquence de résonance. **L'article 7** rapporte les modèles SPIR d'estimation des ces propriétés du bois. Ces modèles sont basés sur les échantillons de bois issus des billes récoltées sur chacun de 150 arbres. Ils ont été utilisés pour prédire ces propriétés à partir des spectres sur les 750 disques de bois afin de cartographier la variation des propriétés du bois dans les tiges.

Approches en génétique quantitative

Les variations génétiques et environnementales des propriétés du bois ont été évaluées. Les calibrations SPIR ont été appliqués sur le bois permettant l'estimation des propriétés sur un grand nombre d'échantillons de bois issus des essais de descendance et de clones. Ces estimations nous ont permis de déterminer les variations spatiales, les corrélations entre les propriétés et le degré du contrôle génétique et environnemental des propriétés du bois.

Dispositif 1 : Test de descendance du Congo

Les valeurs prédites par SPIR pour les caractères du bois des arbres du test de descendance (Figure 33, p. 94) ont été utilisées pour évaluer le niveau du contrôle génétique et environnemental sur une gamme de propriétés du bois, avec un accent particulier sur le MFA et sa corrélation avec d'autres traits. Par ailleurs, les corrélations génétiques et environnementales entre les propriétés du bois et la croissance ont été évaluées à des âges différents afin d'améliorer nos connaissances sur les aspects fonctionnels de la formation du bois chez *Eucalyptus*. Le degré du contrôle génétique et l'environnemental de l'AMF, de la densité, de la teneur en lignine, sa structure et les caractères de croissance a été présenté et une série d'implications pour la sélection a été discutée dans **l'article 8**.

Dispositif 2 : Tests clonaux du Brésil

Les valeurs prédites par SPIR pour les caractères du bois des arbres à partir des tests clonaux (Figure 34, p. 95) ont été utilisées pour évaluer les paramètres génétiques et la variabilité intra arbre de la densité de base, la rigidité du bois et de l'AMF en bois d'*Eucalyptus*. La variation entre les clones et les sites des propriétés élastiques mesurées sur l'échantillonnage par la technique de résonance a été présentée et discutée dans **l'article 9**. A partir de ces constatations, nous espérons être en mesure d'indiquer quels sont

les géotypes les plus appropriés pour la production de bois d'œuvre provenant des plantations d'*Eucalyptus*.

Résultats principaux

Influence de l'angle des microfibrilles pour la rigidité et retraits au séchage du bois

Les relations entre les propriétés du bois sur les clones d'*Eucalyptus* de 6 ans ont montré que la variation du MFA n'expliquait que 44 % de la variation du module spécifique (Figure 30, p. 88). La densité du bois basale est le principal déterminant du module d'élasticité et du module de rupture alors que le MFA joue un rôle secondaire sur la rigidité et la résistance du bois provenant de plantations à croissance rapide (Table 21, p. 89). L'angle des microfibrilles de cellulose dans la paroi cellulaire n'explique pas les retraits radial et tangentiel au séchage.

Contrôle génétique

Des héritabilités élevées ont été enregistrés pour le MFA ($h^2=0,65$), ρ ($h^2=0,61$), LK ($h^2=0,72$) et S/G ($h^2=0,71$) pour les *Eucalyptus* de 14 ans du test de descendance (Table 28, p. 100). Le contrôle génétique de ρ et MFA et leurs corrélations génétiques avec la composition chimique et la croissance varient avec l'âge de formation du bois (Figure 36, p. 104). La corrélation génétique C x ρ est fortement négative ($r < -0,88$), tandis que la corrélation ρ x MFA est constante et positive dans le bois juvénile ($r=0,7$), en diminuant considérablement dans le bois mature ($r=0,3$). Cela pourrait signifier que les arbres avec un fort potentiel de croissance rapide sont « génétiquement programmés » pour produire des bois de faible densité et avec de faibles angles des microfibrilles pour assurer la rigidité. Les variations du MFA et de LK dans le bois mature sont également génétiquement contrôlées. Le faible angle des microfibrilles compense la diminution de la densité, et la croissance rapide avec les changements de la teneur en KL peut s'expliquer fonctionnellement par les effets pléiotropes des gènes ou par le déséquilibre de liaison induit par l'échantillonnage. D'un point de vue biologique, la corrélation MFA x densité est stratégique pour la survie des arbres, leur maintien en position verticale et les conséquences des vents induisant constamment des mouvements de flexion. En conclusion, les corrélations génétiques MFA x densité et MFA x LK agissent de concert et révèlent une stratégie biologique liée à la survie de l'arbre. Le mécanisme sous-jacent à l'interaction de la cellulose cristalline noyée dans une matrice souple serait utilisé pour ajuster les propriétés mécaniques. D'un point de vue technologique, ces résultats permettent de discuter de l'impact sur les stratégies de sélection pour le bois de pâte à papier, le bois énergie et la production de bois massif. Comme les industriels forestiers sont à la recherche de bois selon leur besoin, la connaissance de ces corrélations entre les caractères de croissance et les propriétés du bois sont d'une importance cruciale.

Des niveaux faibles à modérés de l'héritabilité au sens large (H^2) ont été obtenus pour la densité basale, la rigidité du bois et de l'angle des microfibrilles des clones d'*Eucalyptus* de 6 ans (Figure 45, p. 119). Les résultats ont clairement révélé que l'estimation de l'héritabilité pour E et MFA présente des variations selon la position radiale et longitudinale. Pour la densité, la plus élevée des estimations de H^2 ont été trouvées dans les régions supérieures de l'arbre, en particulier dans la zone intermédiaire.

Héritabilité spectrale

Les paramètres génétiques ont été calculés directement à partir des spectres PIR mesurés sur le bois (Figure 46, p. 123). Les variations de zones spécifiques des spectres PIR sont liées aux variations de lignine, cellulose et hémicelluloses contenues et par conséquent corrélées aux propriétés du bois. Les résultats ont clairement montré que les variations sur ces zones spécifiques des spectres PIR sont

contrôlées par des facteurs génétiques. Les attributions des bandes d'absorption sont utilisées pour identifier les composantes du bois qui présentent les héritabilités au sens large les plus élevées à partir des données spectrales. Certaines zones du spectre présentent des H^2 de plus de 50%. Considérant les spectres PIR comme une source d'informations importantes liées aux propriétés du bois, l'analyse des paramètres génétiques pour les variables des spectres semble être un moyen efficace et prometteur pour évaluer le contrôle génétique de plusieurs propriétés du bois à la fois. Ceci est d'autant plus important que la prise de spectres est très rapide et donc peu coûteuse pour un grand nombre d'échantillons.

Considérations finales

Notre étude montre que la plupart des propriétés du bois sont génétiquement corrélées négativement avec la croissance, bien que les corrélations génétiques observées entre les propriétés du bois d'*Eucalyptus* soient positives. En raison de ces corrélations génétiques négatives entre le bois et la croissance, la sélection pour augmenter la densité et la rigidité ou la réduction du MFA en l'absence de sélection pour la croissance se traduira par une réduction (perte génétique) dans la production de volume. Par conséquent, les planteurs, les gestionnaires forestiers et les producteurs de bois devront trouver un équilibre entre le bois et les caractères de croissance, et les généticiens devraient élaborer des stratégies d'amélioration en tenant compte de ces résultats.

Mots-clés: qualité bois, rigidité, densité basale, angle des microfibrilles, génétique quantitative, contrôle génétique, le génotype de l'interaction environnement, la propagation clonale, test de descendance

LIST OF NOTATIONS

BING - Beam Identification by Non-destructive Grading®
BLUP - Best Linear Unbiased Prediction
LV - Latent variable
NIRS - Near Infrared Spectroscopy
PLS-R - Partial Least Squares Regression
R²_C - Coefficient of determination of calibration between lab-measured and NIR-predicted values
R²_{CV} - Coefficient of determination of cross-validation between lab-measured and NIR-predicted values
R²_P - Coefficient of determination of prediction between lab-measured and NIR-predicted values
REML - Restricted Maximum Likelihood
RMSEC - Root mean square error of calibration
RMSECV - Root mean square error of cross-validation
RMSEP - Root mean square error of prediction
RPD - Ratio of performance to deviation
SEE - Standard error of estimation
SNV - Standard Normal Variate
SPIR - Spectroscopie proche infrarouge
XRD - X-ray Diffraction

LIST OF WOOD TRAITS

D - Basic density of wood from progeny trees estimated by NIRS
E - Modulus of elasticity estimated by sonic resonance (E_F for Flexural modulus of elasticity and E_L for longitudinal modulus of elasticity)
E' - Specific modulus (E/ρ)
 f_1 - First resonance frequency
Fmax - Force at fracture point
KL - Klason lignin
MFA - Microfibril angle (MFA_C for MFA estimated by Cave's (1966) method, $MFA_{Y(RS)}$ for MFA estimated from radial strips and $MFA_{Y(S)}$ for MFA estimated from specimens)
MOR - Modulus of rupture
S to G ratio - Syringyl to Guaiacyl (S/G) ratio
tan δ - Internal friction or loss tangent
 δ - Shrinkage tangential (tg) or radial (rd)
 ρ - Basic density of wood (ρ_{14} for kiln-dried at 14% density of wood, ρ_{ad} for air-dried density of wood, ρ_s for basic density of small samples and ρ_{sp} for air-dried density of entire specimens)

LIST OF PAPERS

Papers concerning wood traits

Paper 1 - Hein PRG, Lima JT, Gril J, Rosado AM and Brancheriau L (2011) Resonance of structural timbers indicates the stiffness even of small specimens of *Eucalyptus* from plantations. **Wood Science and Technology**, Berlin (*online first*) DOI: 10.1007/s00226-011-0431-1

Paper 2 - Hein PRG (2011) Relationships between microfibril angle and wood traits in *Eucalyptus* from fast-growing plantations. **Holzforschung**, Berlin (submitted)

Paper 3 - Hein PRG and Brancheriau L (2011) Correlations between microfibril angle and wood density with age in 14-year-old *Eucalyptus urophylla* S.T. Blake wood. **BioResources**, Raleigh (submitted on July 1st 2010)

Papers concerning NIRS calibrations

Paper 4 - Hein, PRG, Lima JT and Chaix G. (2010) Effects of sample preparation on NIR spectroscopic estimation of chemical properties of *Eucalyptus urophylla* S.T. Blake wood. **Holzforschung**, Berlin, v.64, p.45-54

Paper 5 - Hein PRG, Lima JT and Chaix G (2009) Robustness of models based on near infrared spectra to predict the basic density in *Eucalyptus urophylla* wood. **Journal of Near Infrared Spectroscopy**, Chichester, v.17, n.3, p.141-150

Paper 6 - Hein PRG, Clair B, Brancheriau L and Chaix G (2010) Predicting microfibril angle in *Eucalyptus* wood from different wood faces and surface qualities using near infrared spectra. **Journal of Near Infrared Spectroscopy**, Chichester, v.18, n.6, p.455-464

Paper 7 - Hein PRG, Brancheriau L, Trugilho PF, Lima JT and Chaix G (2010) Resonance and near infrared spectroscopy for evaluating dynamic wood properties. **Journal of Near Infrared Spectroscopy**, Chichester, v.18, n.6, p.443-454

Papers concerning genetic studies of wood traits

Paper 8 - Hein PRG, Bouvet JM Mandrou E, Vigneron P and Chaix G (2011) Genetic control of growth, lignin content, microfibril angle and specific gravity in 14-years *Eucalyptus urophylla* S.T. Blake wood. **Annals of Forest Science** (submitted)

Paper 9 - Hein PRG, Brancheriau L, Lima JT, Rosado AM, Gril J and Chaix G (2010) Clonal and environmental variation of structural timbers of *Eucalyptus* for growth, density, and dynamic properties. **Cerne**, v.16, suplemento, p.74-81

1 INTRODUCTION

1.1 BACKGROUND

Wood has an important role in the world as an environmentally responsible and sustainable material. The deforestation of natural forests causes serious economic and environmental problems, not only locally but also globally while sustainable management of forests is an urgent necessity. The establishment of forest plantations to supply the raw material for pulp and paper, energy and wood products industries was a key to the reduction of deforestation of natural forests. According to Meder et al. (2010), plantation forest globally covers 140 millions ha providing a sustainable approach to ensuring the continued supply of traditional building materials and, with the advent of emerging technologies, developing novel fuels, speciality chemicals and nano-crystalline cellulose, all of which will play a vital role in shaping our future society and economy.

Worldwide, forest and forest products play a major economic role in the world with global gross domestic product (GDP) topping US\$63 trillion in 2010 and this is projected to grow by 3.2 percent per annum reaching US\$117 trillion by 2030 (FAO 2011). The Brazilian forest sector has played an important role as a source of income for the national economy, generating products for direct consumption or for export, generating taxes and jobs to people and also working in conservation and preservation of natural resources. According to Tonello et al. (2008) this sector accounts for 3% of the GDP, totalling more than \$ 30 billion. In 2008 the roundwood production of *Eucalyptus* reached an estimate of 174.6 million m³ whereas a total of 114 million m³ were consumed (ABRAF 2010). Brazilian exports of wood products from planted forests reached US\$ 6.8 billion which represents 3% of total Brazilian exports in 2008. The most representative products in the export agenda for 2008 were pulp (57.4%) and paper (28.1%) in total exports of planted forest products. The export share of other products is low compared to pulp and paper because most of its production is oriented to the domestic market.

Over last years, plantation forests expand ~2.0-2.5 million ha by year meeting an increase proportion of global demand of wood (FAO 2006). *Eucalyptus* is one of the most widely cultivated hardwood genera in tropical and subtropical regions of the world. Nowadays the total area of *Eucalyptus* plantations in world covers about 19.5 million hectares (Iglesias-Trabado and Wilstermann 2008) representing ~0.131% of the total land of the earth surface. In Brazil, the *Eucalyptus* plantation surface covers around 4,515,730 ha (ABRAF 2010). This success largely reflects the adaptability of this genus to a variety of climatic and edaphic conditions, its fast growth and the flexibility and usefulness of its wood for industrial applications (Santos et al. 2004). Originally from Australia, *Eucalyptus* was introduced in Brazil between 1865 and 1870 and in 1904 some *Eucalyptus* species were selected in order to obtain trees which would produce the highest economic return by unity area of wood for poles, railway sleeper and fuel for steam locomotives (Berti Filho 1997).

Many countries have verified significant advances in intensive clonal silviculture with remarkable differences on parameters of growth and development between species clones and hybrids of *Eucalyptus*. As a pioneer species, *Eucalyptus* grows even under shallow and poor quality soils with few nutrients. Brazil has highly favourable climate and soil conditions for development of commercial plantations of fast growing species. *Eucalyptus grandis* presents growth at high rates while the *E. urophylla* is a robust species being able to growth under a range of conditions (poor soils, low precipitation) and to resist against diseases. Thus, the most common species in Brazil are *E. grandis* and *E. urophylla* and the hybrid

known as *E. urograndis*. Massive plantations of genetically uniform monocultures have moved *Eucalyptus* silviculture into the domain of classic sustainability issues from agriculture: genetic uniformity, pests and pathogens, and environmental impacts of intensive land management (Binkley and Stape 2004).

As a fast-growing and short-rotation source of wood, *Eucalyptus* plantations are the basis for several industries, such as pulp and paper and iron and steel producers. The continuity of forestry research over the past several years has allowed Brazilian companies to reach high productivity for *Eucalyptus* ($40.5 \text{ m}^3 \text{ ha}^{-1} \text{ yr}^{-1}$), notably higher than those of Australia ($25 \text{ m}^3 \text{ ha}^{-1} \text{ yr}^{-1}$), South Africa ($18 \text{ m}^3 \text{ ha}^{-1} \text{ yr}^{-1}$) and Portugal ($12 \text{ m}^3 \text{ ha}^{-1} \text{ yr}^{-1}$) for hardwood plantations (ABRAF 2010). Some Brazilian pulp and paper industries, such as Fibria Celulose, for instance, has recorded yields superior to $70 \text{ m}^3 \text{ ha}^{-1} \text{ yr}^{-1}$ with *Eucalyptus* hybrids growing under favourable conditions.

The wood produced by these *Eucalyptus* plantations principally attends the demand of three main industrial needs: pulp and paper (37.3%), energy (37.6%) and timber production (18.8%). Table 1 presents the distribution of *Eucalyptus* and *Pinus* forest plantations in Brazil by industrial segment in 2009.

Table 1 - Distribution of *Eucalyptus* and *Pinus* forest plantations in Brazil by industrial segment in 2009

Segment	Roundwood consumption (1,000 m ³) - 2009		
	<i>Eucalyptus</i>	<i>Pinus</i>	Total
1. Pulp and Paper	52,545 (47.3%)	8,086 (15.7%)	60,631 (37.3%)
2. Industrial Fuelwood	32,363 (29.1%)	9,347 (18.2%)	41,710 (25.7%)
3. Charcoal	19,388 (17.4%)	0 (0%)	19,388 (11.9%)
4. Timber Industry	3,093 (2.8%)	27,463 (53.4%)	30,556 (18.8%)
5. Reconstituted wood panels	2,872 (2.6%)	6,520 (12.7%)	9,392 (5.8%)
6. Others	895 (0.8%)	7 (0%)	902 (0.6%)
TOTAL	111,156	51,423	162,579

(Source: ABRAF 2010)

Pulp and paper industry is the main industrial segment consumer absorbing around 47.3% of the roundwood production from the *Eucalyptus* plantations. Just over a quarter of the roundwood production (29.1%) is consumed as fuelwood while the pig iron and steel industry, in turn, consumed 17.4% (charcoal). Only a small part of roundwood production is directed toward to the timber industry (2.8%) and to the manufacture of engineering wood products (2.6%). On the other hand, 53.4% of the *Pinus* roundwood production is destined for the timber industry and 12.7% for wood panels industry. Given this scenario, it is important to think why only ~5% of the *Eucalyptus* roundwood production has been employed as raw material for furniture, flooring, structural material and engineered wood products industry.

1.2 *Eucalyptus* as a timber source

Since the concept of multiple uses of tree logs to increase the yield of the forest enterprises has been introduced (Arango and Tamayo 2008), numerous companies are changing their focus. In many parts of the world there is a move to the use of smaller logs and there has been a growing need and interest in establishing plantations for sawnwood production, as log supplies from natural hardwood forests are likely to decrease in future (Yang 2007). For example, most of *Eucalyptus* plantations in Australia are being grown for pulpwood, but increasing numbers are being managed for sawlogs (Pelletier et al. 2008). In South Africa, small pine logs (such as those with small-end diameter as small as 10 cm, from plantation

thinning), which were also previously sent to pulp mills, are now being used for solid wood products (Verryn 2008). Yang and Waugh (1996a; 1996b) have evaluated the potential of plantation-grown *Eucalyptus* for structural sawn products. The knowledge that has been established over decades for the natural forests must now be coupled with new knowledge for the plantation forest (Meder et al. 2010). In current wood processing and manufacturing operations, knowledge about wood traits, its co-variation within the stem and their relationships are essential to ensure optimal utilization.

1.2.1 Problems of *Eucalyptus* wood

Although wood from *Eucalyptus* breeding programs presents an optimal performance to pulp and energy, its performance in the timber industry is usually not satisfactory. The properties required of *Eucalyptus* wood put to traditional uses in Brazil (pulp and paper and charcoal production) are not the same as those required of solid wood, where in particular mechanical properties are of importance (Lima et al. 1999). Thus, it is widely recognized that most species have many wood quality characteristics which can have adverse impacts on effective and efficient conversion, product processing and product quality (Shield 2007). The greater proportion of juvenile wood presented in this wood, long time ago indicated by Wilkes (1988) as a critical factor, and the growth stress expression (Jacobs 1945; Boyd 1950; Archer 1986) are probably the most frequently referenced characteristics in an abundant literature detailing often severe problems arising in the course of conversion and processing. The potential of *Eucalyptus* wood for higher value products such as solid wood products, especially appearance-grade sawn timber is influenced by numerous factors. Some of these problems are discussed as following.

Growth stress

High levels of growth stress in *Eucalyptus* are undoubtedly the most serious growth phenomenon affecting wood quality, product yield and product dimensions. Growth stress is a problem difficult to solve in *Eucalyptus* plantations since it is a natural mechanism of tree for surviving and for supporting external forces, such as prevailing winds, thunderstorms and its own weight. According to Alm eras and Fournier (2009), the tensile longitudinal stress in the periphery of the stem allows the tree to stay upright and optimizes the resistance of wood against bending forces such as wind. Growth stress result from the superposition of two kinds of stress: (i) support stress, that is, an elastic response to the increasing load of wood and shoots supported by the tree, and (ii) maturation stress, which appears spontaneously inside wood during its formation (Clair et al. 2006).

Growth stress is a major cause of degrade and processing problems, especially in fast-growing *Eucalyptus* wood inducing warping and splitting of logs and boards (Panshin and De Zeeuw 1980). Bamber et al. (1982) have evaluated the effect of fast growth on *Eucalyptus* wood properties. Severe splitting develops in log ends following cross-cutting while further splitting and distortion takes place during conversion into sawn boards (Malan 1995). A reduction in stress levels in tree stems would certainly be by far the most important improvement that can be made regarding many eucalypt species, as the impact on the wood processing industry will be impressive.

Tension wood

Tension wood is a particular kind of wood formed during wood formation on the upper side of the leaning stem and associated to a large longitudinal tensile stress. It occurs frequently in plantation-grown *Eucalyptus* at the stem periphery (Washusen et al. 2005) causing high variations on wood traits within the trees. According to Wardrop (1956), this tissue is an anatomical manifestation of various regulatory processes associated with the maintenance of tree form and movements of orientation in response to

environmental changes. Tension wood is associated to the formation of a peculiar layer of the fiber wall, the gelatinous or G-layer (Clair et al. 2006) which is characterized by its large thickness and its low MFA and lignin (Chaffey 2000). Tension wood of broadleaves such as *Eucalyptus* usually presents high specific longitudinal modulus of elasticity, so that the strongly negative maturation strains (shrinkage) lead to high level of tensile stress in the new layer, without requiring necessarily a compensating material production (Thibaut et al. 2001). Tension wood occurs also in wood of intermediary regions of the stem since it is formed during the wood formation and its localization changes as the tree grows over the years. Normal or opposite wood also can have a low MFA. For instance, Washusen et al. (2001) investigated tension and normal wood in the sapwood and heartwood in 10-year-old *Eucalyptus globulus* Labill finding very low MFA in normal wood, where most tension wood was found.

Tension wood occurrence brings other problems for wood quality. The cells of the stem periphery are in state of tension while the central parts of the stem are under compressive forces (Thibaut et al. 2001). When these cumulative effects exceeds the maximum crushing strength of wood, numerous slip planes and compression failures take place generating a common problem experienced especially by hardwood saw millers known as "brittle heart" (Malan 1995). The presence of this defect has a very significant effect on the quality and yield of the end product.

Juvenile wood

Eucalyptus plantations have been harvested before their wood reach maturity for reasons of economic efficiency. Hence, an important factor in fast growing stands is the quality in the juvenile wood. *Eucalyptus* stems with high proportion of juvenile wood led to inferior performance as sawn wood. Juvenile wood is characterized by large microfibril angles, short fibres with thin walls and lower density contributing to the lower quality of juvenile wood products (Zobel and Van Buijtenen 1989).

Short rotation ages results large proportions of juvenile wood, deteriorating even further in future generations as trees are bred to grow faster. As the logs from plantations are often younger and smaller diameter, this problem can be solved by waiting the tree reach their maturity before harvesting or selecting trees with better juvenile wood traits.

Grain angle

Spiral grain is the tangential inclination angle of wood fibers from the vertical stem axis and the variation in grain angles is great among tree species and individual trees (Harris 1989) and it can be caused by winding or spiral growth of wood fibers about the bole of the tree instead of vertical growth. Trees develop spiral grain to adapt themselves to various mechanical constraints; for instance, to withstand stem under forces induced by wind (Skatter and Kucera 1997). However, this adaptive mechanism is an undesirable phenomenon since gives rise to severe problems in sawn timber. It is well known that spiral grain reduces both strength and stiffness of sawn wood (Skatter and Kucera 1997). For instance, Green et al. (1999) showed that the grain slope has strong effect on some wood traits. Moreover, a large amount of spiral grain in the wood causes shrinkage and warping along the longitudinal plane of boards and planks (Eklund and Säll 2000) and also decreases the strength of timber. Brémaud et al. (2011) have investigated the dependence on grain angle on the visco-elastic properties of wood.

Collapse shrinkage

Shrinkage and swelling may occur in wood when the moisture content is changed (Stamm 1964). Shrinkage occurs as moisture content decreases, while swelling takes place when moisture content increases. Collapse is an abnormal shrinkage encountered in wood of certain trees species in the process of

drying (Wu et al. 2005). It results from the physical flattening of fibres to above the fibre saturation point and is thus not a form of shrinkage anisotropy. Collapse can be defined as the difference between the total shrinkage of a specimen and the shrinkage in the same structural direction of an end-matched cross-section of 1 mm thickness in the fibre direction (Kauman 1961, from Ilic and Hillis 1986). Collapse shrinkage can often be recovered by reconditioning with live steam, but collapse induced checking is a permanent for of degrade (Innes 1996). Some *Eucalyptus* species are prone to collapse during drying contributing to split problems. Thus collapse shrinkage is an important issue in the context of wood drying.

Knots presence

Knots are a major defect factor in plantation grown logs, even those of excellent form and apparently sound. Knots do not only directly contribute to defect in converted products, but they are often associated with other defects such as grain deviation and decay. Decay enters through branch stubs which, in *Eucalypts*, do not become filled with protective resins as is the case with conifers. This signals a caution for pruning *Eucalypts* which is otherwise to be strongly recommended as minimising the defects associated with knots (Shield 2005).

Because of short rotations (6-7 years for pulp and paper, and energy and 12-15 years for sawntimber, in Brazil), logs from *Eucalyptus* plantations are often younger, smaller diameter and of greatly differing wood properties. For these reasons, in many regions of the world *Eucalypts* plantations do not have a good image as sawnwood provider or as their equivalents for rotary peeling. Shield (2007) claims that “the scarcity of the most fundamental requirement for success - prudent and patient investors - leads to poor silviculture, poor sawlog quality, poor sawmilling, poor lumber quality and, unsurprisingly, poor lumber prices”.

1.2.2 What is wood quality?

Savidge (2003) presents some interesting concepts about wood quality. According to him, wood quality has to do with its degree of excellence in relation to some application. Because quality assessment is multi-faceted and depends on the intended application, there is no absolute measure. Quality assessment by the woodsmen who fell and process the trees and by the mill workers who decide how logs should be used involves experienced observation and snap-judgment integration of particular features, based largely on subjective experience.

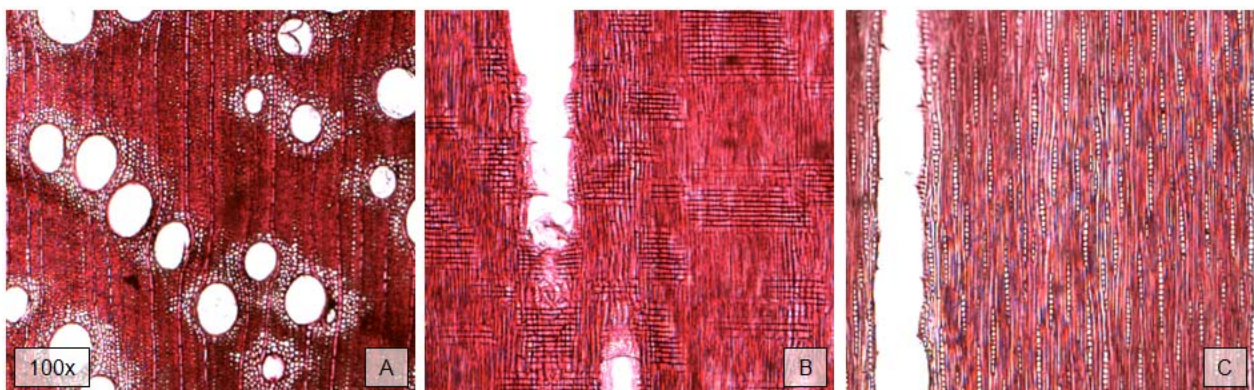


Figure 1 - Transversal (A), radial (B) and tangential (C) sections of 6-year-old *Eucalyptus* wood (source: personal image)

Savidge (2003) affirms that some aspects of the wood quality, such as its density and its amount of cellulose, lignin or extractive can be repeatedly analyzed and quantitatively expressed with high accuracy and precision (it depends of the method accuracy and technician ability). However, other measures such as fibre length, cell wall thickness, microfibril angle, and percentages of the various types of anatomical elements coexisting in a wood are more problematic. Upon repeated random sampling and measurement of the same preparation, a Gaussian distribution is predictably obtained, and the magnitude of the standard deviation may provide equally or more important information than the mean value. However, that information essentially is no more than a confirmation of what can be readily observed when viewing a wood section in the compound light microscope (Figure 1): large variation exists within wood.

1.2.3 Selecting traits for wood improvement

Many wood traits are known to be important in determining the value of *Eucalypts* wood as sawn timber including its basic density, mechanical properties, grain angle, knots and resin pockets, juvenile wood proportion and the microfibril angle (MFA), the preferable angle of the cellulose microfibril within the cell walls. Most wood properties are age related and co-vary with one another (Zobel and Van Buijtenen 1989) and the correlations between wood traits can be high, leading a positive or adverse effect for industrial applications. Selection of any favourable characteristic has benefits for a number of wood properties, with the overall gain depending on the characteristic sought for improvement (Walker and Butterfield 1995) and its effect on all wood properties.

Due to the ease of measurement and because basic density of wood present high genetic control and correlation with other properties, there are numerous statements that density is the most important characteristic in determining the properties of wood. Hence, a considerable number of studies were conducted for investigating the wood density in *Eucalyptus* breeding in the last decades (Whittock et al. 2007; Hamilton and Potts 2008; Hamilton et al. 2008; Kien et al. 2008; Pelletier et al. 2008; Volker et al. 2008; Wey and Borralho 1997; Kube et al. 2001; Greaves et al. 1997a; Poke et al. 2006; Apiolaza et al. 2005).

Although the density is a desirable characteristic for many industrial applications (Zobel and Jett 1995; Zobel and van Buijtenen 1989), selection according to density does not appear to be a very effective method for identifying better structural conifers timber (Walker and Butterfield 1995) because density is a kind of measure of the “quantity” of matter in a piece of wood. In the case of some softwood, especially in *Pinus*, the intrinsic characteristic whose improvement is likely to yield the greatest economic benefits is the microfibril angle (Walker and Butterfield 1995), because MFA is a kind of measure of the “quality” of the material in the cell wall. Lindström et al. (2004) claimed that the use of stiffness rather than wood density as a selection criterion will also benefit from the fact that modulus of elasticity is a composite function of MFA and wood density.

Specific modulus is wood trait consisting of the elastic modulus per wood density. The specific modulus is used to find varieties of woods which will produce structures with minimum weight. Wood presenting high specific modulus has wide application in which minimum structural weight is required such as large wood structures, bridges, furniture, roof structures etc. Specific modulus is an interesting property because it represents two important traits at once.

According to Verryn (2008), it is suggested that the breeder and wood specialists invest in very careful consideration of which traits are of key importance, and will still be of such importance in years to come (target deployment and harvesting time). The commercial importance of MFA for wood quality is well established for softwoods, but is less clear for hardwoods (Donaldson 2008). In *Pinus*, the MFA is known

to be the best indicator of its stiffness (Cave 1968; Barnett and Bonham 2004; Walker and Butterfield 1995). In *Eucalyptus*, few studies have examined the influence of the MFA on wood stiffness (Evans and Ilic 2001; Yang and Evans 2003; Evans 2006) and the relationship between MFA and wood stiffness remains unclear, requiring a deeper investigation.

1.2.4 MFA controls wood quality

Microfibril angle (MFA) is a structural characteristic of the cell wall of wood fibres and tracheids, which is made up of millions of strands of cellulose called microfibrils (Fang et al. 2006). This ultrastructural cell wall property represents the orientation of crystalline cellulose along the fiber axis (Andersson et al. 2000). In the secondary cell walls of xylem, the fibres or tracheids typically have three layers, an outer S_1 with transversely oriented microfibrils, a thick S_2 layer with axially oriented microfibrils, and an inner S_3 layer also with transversely oriented microfibrils, in a S-Z-S helical organization (Donaldson 2008). Figure 2 presents the arrangement of cellulose microfibrils in the secondary cell wall of a fibre.

Each layer has its own particular arrangement of cellulose microfibrils, which determine the mechanical and physical properties of the wood in that cell. These cellulose microfibrils may be aligned irregularly (as in the primary (P) cell wall), or at a particular angle to the cell axis (as in layer S_1 , S_2 , and S_3). The middle lamella (ML) ensures the adhesion between cells (Figure 2). Because S_2 layer is generally much thicker than the other layers is therefore considered to dominate the physical and chemical properties of the cell wall (Donaldson and Xu 2005).

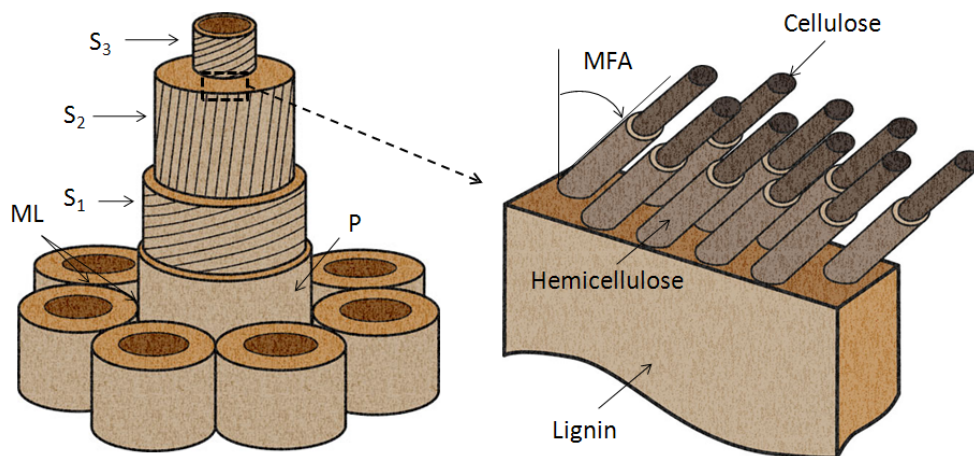


Figure 2 - Three-dimensional structure of the secondary cell wall of a fibre (personal image)

Plants are able to control the orientation of cellulose fibrils during deposition in the cell walls. Therewith they manifest a powerful tool at the nanoscale to create anisotropy of the cell wall (Burgert and Fratzl 2009). Barnett and Bonham (2004) stated the biological and mechanical role of MFA and its variation in the living trees: “Tracheids or fibres with a high MFA in the centre of the tree, which were produced when the tree was a sapling, endow the wood with a low modulus of elasticity (stiffness). This enables the sapling to bend in a high wind without breaking. As the tree enlarges, the stem has to become stiffer to support the increasing weight of the stem and crown. The lower MFA of the outer wood means that it has a higher modulus of elasticity to enable it to fulfil this role”.

The importance of MFA for wood quality is well established for softwoods, but is less clear for hardwoods (Donaldson 2008). In conifers is well known that MFA decreases with height (Megraw et al. 1998) and varies from pith to bark being large near the pith and declining gradually from pith to cambium (Walker

and Butterfield 1995). Relatively few hardwoods have been characterized, so there is a need to extend the range of species and ecotypes to be investigated (Donaldson 2008). Specifically in the genus *Eucalyptus*, the MFA variation within the trees and its effects on wood properties other than mechanical ones are rarely reported in the literature (Lima et al. 2004).

1.2.4.1 Correlation of MFA with wood traits

Over the past decade, lots of scientific contributions were dedicated on investigation of the microfibril angle of the S₂ layer of the wall in woody plants. MFA has also long been known to have major effects on two key properties of wood: its stiffness and shrinkage. Furthermore, microfibril angle has long also been known to present from moderate to strong, however sometimes none, correlation with fibre or tracheids length (Hirakawa and Fujisawa 1995; Kibblewhite et al. 2005; Tsutsumi et al. 1982), lignin content (Hori et al. 2003; Jungnikl et al. 2008), spiral grain (Cown et al. 2004), growth stress occurrence (Washusen et al. 2001), and other factors. However, the relationship of MFA with wood properties at what Kretschmann et al. (1998) have classified as “macroscopic level” is not fully understood and this is an area of active research. Some of these relationships are described above and most of studies were based on softwoods.

MFA x stiffness

The curvilinear relationship between MFA and longitudinal stiffness (modulus of elasticity or Young’s modulus) has been repeatedly demonstrated in the literature for a range of species. Cave (1968) demonstrated that a reduction in MFA from 40° in the innerwood to 10° in the outerwood correspond to the increase of the longitudinal modulus of elasticity fivefold (from 1,000 to 5,000 kg mm⁻²). This finding was confirmed by Via et al. (2009) who reported a fourfold increase in stiffness of longleaf pine when the microfibril angle dropped from 40° to 5°. Donaldson (2008) lists several studies addressing to this issue in many species and environmental conditions.

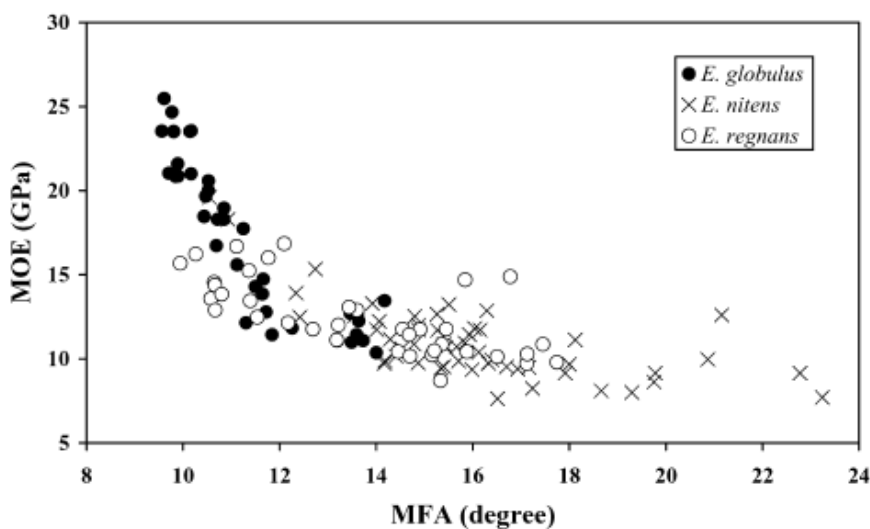


Figure 3 - Relationship between MFA and modulus of elasticity (MOE) of *E. globulus*, *E. nitens* and *E. regnans* wood between 15 and 33 years of age (from Yang and Evans 2003)

In *Eucalyptus*, Evans and Ilic (2001) and Yang and Evans (2003) have investigated the relationship between microfibril angle, basic density and wood stiffness. Figure 3 presents the relationship between MFA and wood stiffness in three *Eucalyptus* species. It is important to note that the stiffness decreased ~3.5 times while MFA increased twofold (from ~9° to 18°). Investigating these relationships in 104 *E. delegatensis* wood samples, Evans and Ilic (2001) have concluded that MFA was the major determinant of

specific modulus, while density could not be used as selection criteria for stiffness in tree improvement programs. Yang and Evans (2003) have reported that MFA alone accounted for 87 percent of the variation in E, while density alone accounted for 81 percent. Together, MFA and density (as Density/MFA) accounted for 92 percent of the variation in E. The above studies indicated that MFA was the prime determinant of both the modulus of elasticity (E) and the specific modulus (E/ρ). If their conclusions can be generalized, MFA measurements should make possible the evaluation of the wood quality.

MFA x shrinkage

The MFA has also long been known to influence dimensional changes in wood with changes in moisture content (Meylan 1968; Yamamoto et al. 2001; Barnett and Bonham 2004). Donaldson (2008) stated that MFA is one of the dominant parameters affecting shrinkage. As water bound to cellulose and hemicelloses moves out of the cell wall during drying of timber, these molecules move closer to each other and the wall shrinks (Barnett and Bonham 2004). As a result, cell walls with very low MFA tend to have greater tangential shrinkage, while cell walls with very high MFA tend to have greater longitudinal shrinkage (Donaldson 2008). Figure 4 presents a theoretical model explaining the influence of cellulose microfibril orientation on shrinkage anisotropy. Shrinkage anisotropy is responsible for some degrade on drying; especially crook (Walker and Butterfield 1995).

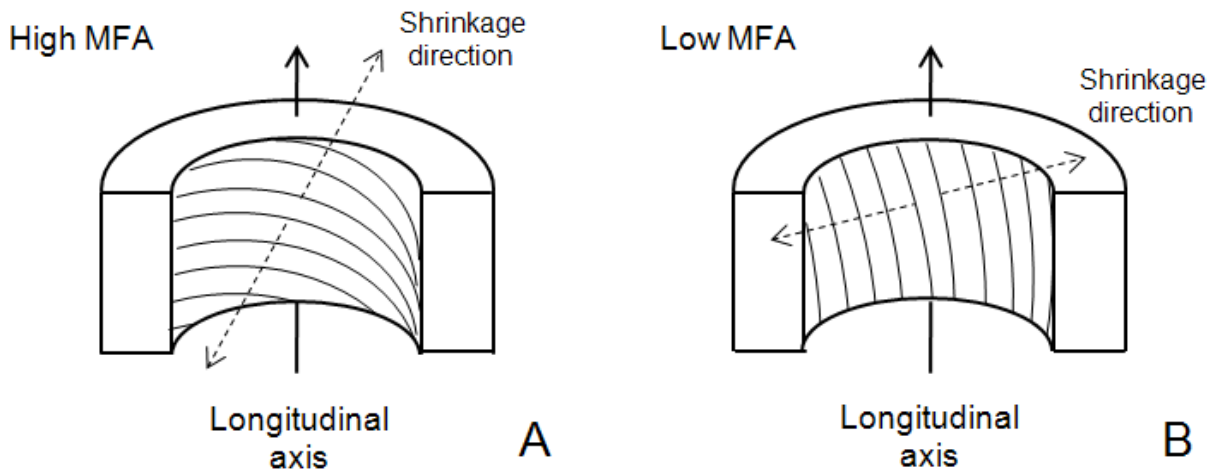


Figure 4 - Theoretical model explaining the influence of high microfibril angle (A) and low microfibril angle (B) on longitudinal and transversal components of shrinkage and swelling

In *Eucalyptus*, Wu et al. (2006) explored the relationships of the main anatomical features with shrinkage in *Eucalyptus urophylla*, *E. grandis*, and *E. urophylla* × *E. grandis*, planted in South China demonstrating that the main factors affecting unit shrinkage were cell wall proportion, microfibril angle, and cell wall thickness and that factors playing an important role in total shrinkage were cell wall proportion, ray parenchyma proportion, and MFA. Changes in moisture content may affect the cellulose crystallite width. For instance, Washusen and Evans (2001) have examined the correlations between tangential shrinkage and cellulose crystallite width in 11-year-old *Eucalyptus globulus*. Their results showed that cellulose crystallite width was closely associated with tangential shrinkage suggesting that cellulose crystallite width is an important predictor of shrinkage. As crystallite width increased, shrinkage also increased. The correlation between tangential shrinkage and crystallite width was strongest in the lower 5% of tree height.

Experimental data showing the relationship between anisotropic shrinkage and MFA is demonstrated in Figure 5. The small black squares (gray path) represent samples of *Pinus jeffreyi* wood from Meylan

(1968) while the black and white circles represent *Sugi* wood samples from Yamamoto et al. (2001) in transversal (T-direc.) and longitudinal (L-direc.) shrinkages.

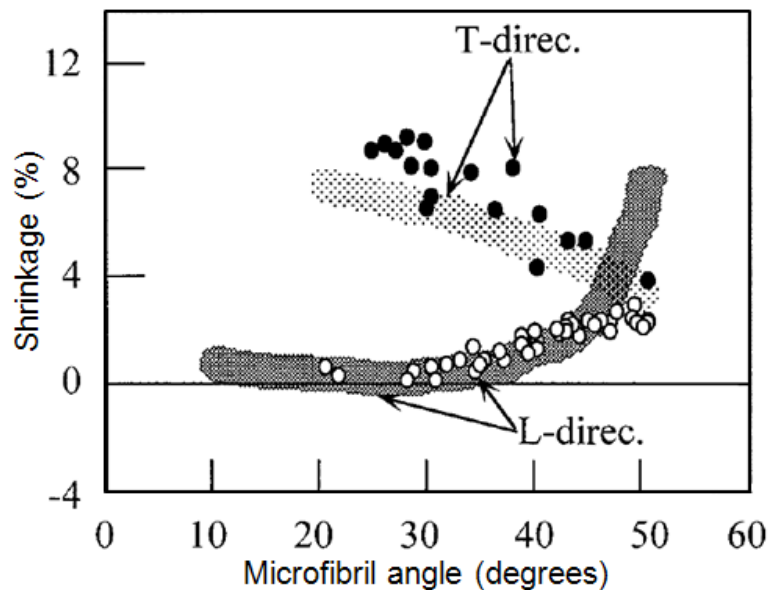


Figure 5 - Relationship between anisotropic shrinkage (from green to oven-dried) and MFA (from Yamamoto et al. 2001)

MFA x density

MFA shows a variable relationship with wood density (Donaldson 2008). Fang et al. (2004) reported significant correlation between MFA and wood density ($r=-0.45$) for *Populus*. On the other hand, Bergander et al. (2002) found no correlation between fiber morphology (i.e., average length, width, density) and mean fibril angle in wood samples of 100-year old Norway spruce (*Picea abies* L. Karst.). Similarly, Lin and Chiu (2007) studied such wood traits in 20-year-old *Taiwania cryptomerioides* trees reporting no significant relationship between microfibril angle and wood density by linear regression analysis.

In *Eucalyptus*, Evans et al. (2000) compared MFA and density of 29 *Eucalyptus nitens* wood finding good local relationships between MFA and density but the whole tree average MFA and density yielded no correlation. Washusen et al. (2001) evaluated such traits in 10-year-old *Eucalyptus globulus* reporting strong linear relationship ($r=-0.70$) between density and MFA. The findings of Washusen et al. (2001) suggest that fibre wall thickening primarily due to thickening of the S_2 (hence increasing density) is the main factor contributing to decreasing MFA. However, Donaldson (2008) pointed out that any relationship between MFA and density is entirely coincidental since MFA is not related to fibre wall thickness. However, the amount of juvenile and mature wood might be responsible for relationships in some cases since both MFA and density are related to these factors. It is important to note that these two characteristics of wood vary from pith towards the bark and this systematic trend may play a role in part of the correlation, when it exists.

1.2.4.2 MFA implication on wood uses

While orientation of cellulose microfibril seems to be an important strategy for tree development and survival, the MFA has important, but sometimes adverse impacts in industrial applications. For sawn

timber, a piece in which the MFA is large has a low stiffness and it is therefore suitable only for low-grade use, reducing its value as a raw material and its economic value. This problem was not too serious in the past when trees were allowed to reach maturity before being harvested. Increasing demand for timber, pulp and wood products is driving the forest industry towards short-rotation cropping of fast-growing species (Barnett and Bonham 2004). Thus, trees with high contents of juvenile wood are used by industry resulting in loss of quality of the end product. According to Barnett and Bonham (2004) the real industrial problem, however, arises in a piece of wood containing partly normal wood with a small MFA, and a proportion of reaction wood with a large MFA can be a problem for industrial uses. From a technological point of view, this problem always existed: such pieces will distort during drying owing to the differential shrinkage occurring as a result of the difference in MFA. Differential shrinkage in pieces of normal timber, which incorporate both juvenile and mature wood, can also lead to distortion or cracking on drying.

When using fibres for paper production, microfibril angle and fibre length significantly affect pulp and paper properties (Thamarus et al. 2004). In wood of *Pinus*, for instance, low MFAs are associated with high tensile strength in paper, while high MFAs are associated with greater stretch and tear indices (Donaldson 1993). In the present study, the implications of the variation in MFA on wood traits and products are examined in *Eucalyptus*.

1.2.4.3 Methods for MFA measurement

MFA can be determined by two types of measurement: from individual tracheids or fibres using microscopy-based techniques and from a bulk wood samples using X-ray diffraction and near infrared (NIR) spectroscopy.

Optical methods

Microscopy-based techniques are divided into those that rely on the optical properties of crystalline cellulose, employing variations on polarised light techniques, and those that directly or indirectly visualise the orientation of the microfibrils themselves. Such methods include confocal reflectance microscopy, fluorescence microscopy, micro-Raman spectroscopy, scanning electron microscopy (SEM), transmission electron microscopy (TEM), iodine precipitation and other biological, chemical or physical treatments. These techniques are detailed described in Donaldson (2008) who presented a detailed review on MFA, its measurement, variation and relationships.

X-ray diffraction

It is likely that X-ray diffraction is currently the most popular method for measuring MFA. It is a fast and reliable technique, but X-ray diffraction is an indirect method and authors should provide the measurement uncertainty. This technique is a direct estimation of cellulose microstructure in the wood, but it needs a model to obtain the microfibril angle estimation from the diffraction pattern called the T parameter. Thus, X-ray diffraction provides only a relative figure for the MFA since the estimative comes from an interpretation of the T parameter.

The relationship of T to the true angle must be determined by other techniques. Thus, numerous studies have proposed models to estimate MFA from T parameters. First, Cave (1966) proposed that microfibril angle is $0.6 T$. Then, Meylan (1967) determined microfibril angle to be $0.612T + 0.843$ for radiata pine. Yamamoto et al. (1993) proposed a formula of determining the MFA over a wide range using two gymnosperms and two angiosperms species whose normal wood shows thin fibre cell walls and tension

wood does not show G-layer. According to Yamamoto et al. (1993), their formula improved the Cave's method giving better results, especially for reaction wood. Latter, Megraw et al. (1998) showed microfibril angle to be $0.93T + 10.71$ for loblolly pine with slightly differing equations for early and latewood samples. Ruelle et al. (2007) proposed formulas for estimating MFA from T parameter using three tropical species (*Eperua falcata*, *Laetia procera* and *Simarouba amara*) in order to verify if the existing formulas could provide good estimations for microfibril angle in tropical species with G layer and/or with thick fibre cell walls. Figure 6 shows two examples of converting T parameter into MFA measured by other techniques. The blue line (Figure 6 B) represents the estimates by Cave' formula (1966) while the dotted line represents the estimates by Yamamoto' approach (1993).

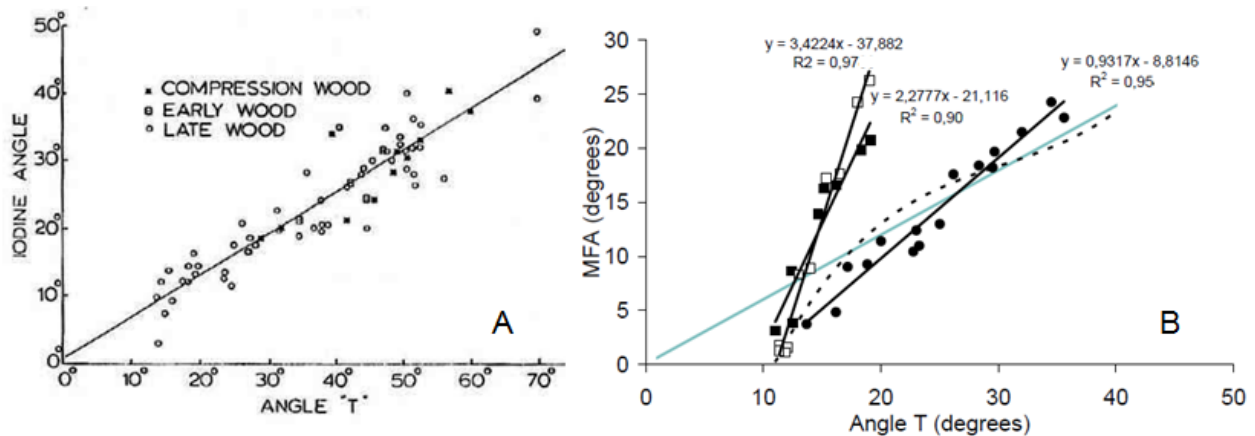


Figure 6 - The relationship between the angle T derivated from the X-ray intensity variation and the mean microfibril angle measured by iodine staining (A, from Meylan 1967) and by Field-Emission Scanning Electron Microscopy (B, from Ruelle et al. 2007)

In this study the formula proposed by Yamamoto et al. (1993) was used in most of cases because the interesting point is to know the relative value of the characteristic between trees or regions of the stem, its variation or stability within the logs. These MFA estimates can be useful for selection of candidate genotypes or commercial clones in forestry industries from a large wood sampling.

NIR spectroscopy

Near infrared spectroscopy technique relies on calibrating multivariate regressions that relates the NIR spectra recorded from wood samples to their known properties, for example lignin content. This NIR-based model is then applied on the NIR spectra of further samples in order to estimate their lignin content. This method has been mainly used for a range of chemical properties of wood. Mechanical and physical properties of wood have been also successfully evaluated by NIR spectroscopy models. Recently, many studies have been proposed NIR spectroscopy as a new tool for estimating microfibril angle in wood samples. NIR spectroscopy do not respond to MFA *per se* (only to chemical composition) but MFA can be correlated to chemistry and physical aspects and these indirect correlation makes possible to assess MFA from NIR spectra in some cases. These issues are discussed in more details within the item 1.3.4.4 (pg. 46).

1.3 *Eucalyptus* breeding programs

Forest genetics principles are central to tree improvement programs that develop genetically improved varieties for plantation systems around the world. Genetically improving the yield, health and product quality of these plantations directly enhances the economic and social value of the plantations (White et al.

2007). Advances in tree breeding and management practices are making significant gains. Forest sectors demand higher productivity and quality, and a faster adaptation of their varieties to rapid changes (Verryn 2008). Hence, the determination of the genetic factors contributing to quantitative trait variation of wood properties is essential for tree breeders (Raymond 2002; Apiolaza 2009). This thesis focuses on verifying in which extent the MFA, stiffness and wood density are controlled by genetic and environmental factors in *Eucalyptus* plantations.

Selection and mating are key activities in breeding programs. The objective of breeding is to produce new generations or varieties of trees by mating trees with good characteristics in order to adequately meet the requirements of the industry and society. Thus, selecting potential trees from large populations and mating them with each other is expected to produce offspring that potentially will have superior (or inferior) mean phenotypes for the target features. According to Hardwood et al. (2001), selection and mating activities accumulate genes, which influence yield and adaptation, increasing over successive generations the frequency of superior trees. Mating can be done by open pollination or controlled pollination, carefully minimising the potential of inbreeding, which has been shown to be strongly deleterious in *Eucalyptus*.

Figure 7 illustrates an ideal situation where trees having traits of interest were selected from the initial population and artificially mated with each other. Thus, in this new generation (improved population) the frequency of the phenotypic value of interest is increased producing an improved population for such characteristic. The mean of the phenotype value increased from 62 to 72 in the second generation population. The genetic gain is indicated by the gray arrow. However, parents pass on their genes and not their genotypes on their progeny (Falconer 1993). It is therefore the averaged affects of the parent's genes that determine the mean genotypic value of their progeny. The value of an individual, judged by mean value of its progeny, is called *breeding value* of the individual (Falconer 1993).

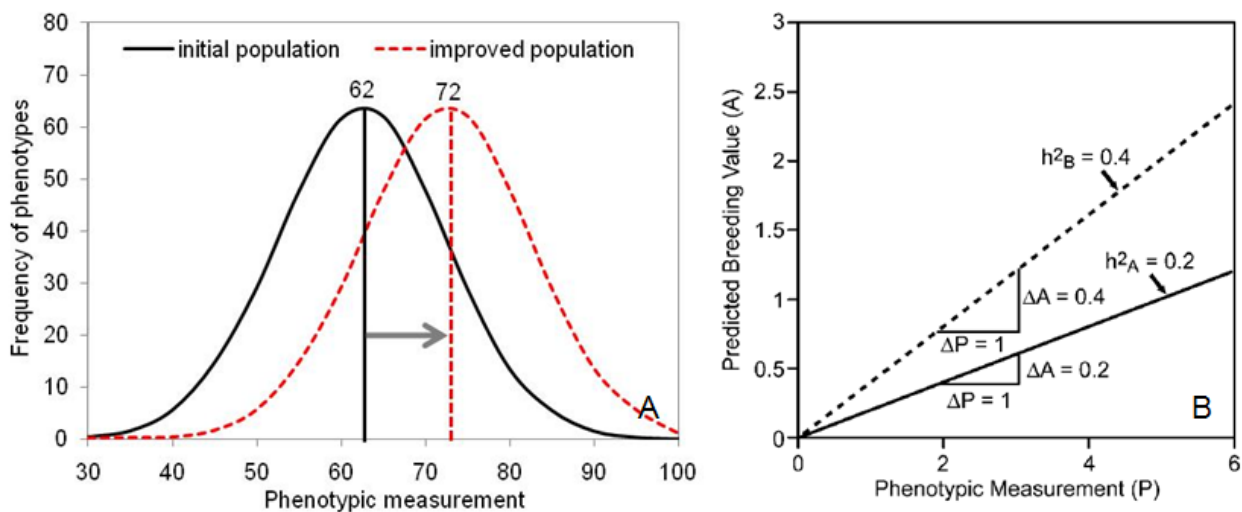


Figure 7 - Genetic gain from tree breeding programs (A, personal source) and graphs of the regression lines of breeding values on phenotypic values for two hypothetical traits, A and B, with $h^2_A=0.2$ and $h^2_B=0.4$ (B, from White et al. 2007)

Every successful breeding strategy, therefore, requires efficient methods of selecting superior material including the progeny tests in which the selection is carried out, appropriate measurement techniques and selection technology (Hardwood et al. 2001). In summary, to improve a characteristic of wood, we should be able to accurately measure it by means of a reliable and repeatable method or technique, and such wood property needs to be variable and genetically controlled (inherited). Most wood properties exhibit

continuous variation and as such are viewed as quantitative traits influenced by multiple genetic factors and the environment (Zobel and Jett 1995).

1.3.1 Quantitative genetic of wood

Resemblance between relatives with respect to a given wood trait is a basic genetic phenomenon; the degree of resemblance determines the amount of additive genetic variance (Falconer 1993). The causes of resemblance in trees and their wood properties are related to genetics and environment factors (Zobel and Jett 1995). Therefore, the phenotypic value of the growth or wood trait is the sum of genetic and environmental effects.

The genetic of a wood properties centres round the study of its variation, for it is in terms of variation that primary genetic questions are formulated. The basic idea in the study of variation is its partitioning into components attributable to different causes. The relative magnitude of these components determines the genetic properties of the population, in particular the degree of resemblance between relatives.

In genetic approaches, the amount of variations in wood properties are measured and expressed as the variance. According to Falconer (1993) the components into which the variances are partitioned are the genotypic variance (the variance of the genotypic values) and the environmental variance (the variance of the environmental deviations). The total variance of each wood property is the phenotypic variance, or the variance of the phenotypic (measured) values, and is the sum of the separate components. Table 2 lists the components of variance and the values whose variance they measure.

Table 2 - Components of variance of growth and wood traits (from Falconer (1993))

Variance component	Symbol	Value whose variance is measured
Phenotypic	σ^2_P	Phenotypic value
Genotypic	σ^2_G	Genotypic value
Additive	σ^2_A	Breeding value
Dominance	σ^2_D	Dominance deviation
Interaction	σ^2_I	Interaction deviation
Environmental	σ^2_E	Environmental deviation

According to Falconer (1993) the total variance is then, with certain qualification, the sum of the components, thus:

$$\sigma^2_P = \sigma^2_G + \sigma^2_E \quad \text{Eq. (1)}$$

$$\sigma^2_P = \sigma^2_A + \sigma^2_D + \sigma^2_I + \sigma^2_E \quad \text{Eq. (2)}$$

The qualifications are, first, that genotypic values and environmental deviation may be correlated, in which case σ^2_P will increase by twice the covariance of G with E; and, second, there may be interaction between genotypes and environments, in which case there will be an additional component of variance attributable to the interaction.

Most wood characteristics controlling wood quality, such as density, stiffness, lignin etc. are influenced by genetic and environment factors (Zobel and Jett 1995) and can be modified or improved by means of tree breeding programs (Raymond 2002).

Figure 7 contains a hypothetical situation where the offspring from selected parents have improved the target wood property. However, the successful of the genetic gain mainly depends on the heritability level of such trait. The contribution of the genetic variation on the genetic gain (the amount of increase in performance that is achieved through breeding programs) is also of particular importance. When the characteristic present high heritability estimates (h^2 , hereafter called as genetic control) high genetic gains can be achieved. Falconer (1993) states a clear definition of heritability, as well as their applications:

“Heritability of a wood trait is one of its most important properties. It expresses the proportion of the total variance that is attributable to differences of breeding values, and this is what determines the degree of resemblance between relatives. The most important function of heritability in breeding programs is its predictive role, expressing the reliability of the phenotypic values as a guide to the breeding value. Only the phenotypic values of wood traits can be assessed, but it is the breeding value that determines their influence on the next generation. Therefore if the breeder or experimenter chooses individuals to be parents according to their phenotypic values, his success in changing the characteristics of the population can be predicted only from acknowledge of the degree of correspondence between phenotypic values and breeding values. This degree of correspondence is measured by the heritability”.

Heritability estimates of two hypothetical traits, A and B, are presented in Figure 7 B. Note that phenotypic values are closer in magnitude to the underlying breeding value for trait B with its higher heritability. Two trees that are different by one unit in their phenotypic value are expected to have breeding values that differ by 0.2 and 0.4 units for traits A and B, respectively. Selection of outstanding phenotypes for trait B is more likely to result in trees that have higher breeding values and therefore, produce better-performing offspring (White et al. 2007).

Therefore, the relative importance of heredity in determining phenotypic values is called the heritability of the wood property. There are, however, two distinctly different meanings of ‘heredity’ and heritability, according to whether they refer to genotypic values or to breeding values Falconer (1993). Broad-sense heritability estimates (H^2), is the ratio of the entire genetic variance to the total phenotypic variance while narrow-sense heritability estimates (h^2) is the ratio of additive genetic variance to total phenotypic variance (White et al. 2007). In short, the heritability expresses the reliability of the phenotypic values as a guide to the breeding value, or the degree of correspondence between phenotypic values and breeding values (Falconer 1993).

Progeny tests allow the determination of genetic additive variance σ^2_A providing the narrow-sense heritability estimates (h^2) while the Clonal tests allow the determination of the genotypic variance (σ^2_G) providing the broad-sense heritability estimates (H^2). Therefore, it is valuable to have estimates of genetic parameters, such as heritability estimates of the important properties when developing breeding strategies. In the present study, a progeny test and a clonal test were assessed in order to estimate genetic parameters.

1.3.2 *Eucalyptus* breeding programs

The first studies on genetics of *Eucalypts* were carried out to determine the suitability of species and provenances for particular environments (Turner et al. 1983). Thus progeny trials were established in order to evaluate the potential of many progenitors, to estimate genetic parameters and to detect genotype by environment interactions (Wang et al. 1984; Malan 1988). In the past, wood processors tended to demand absolutely straight logs for sawnwood and any deviation from straight logs would translate into lost timber production. Then, the studies on genetics of *Eucalyptus* started to concentrate on tree growth, survival, stem straightness and branch quality because the forest industry was focused mainly on achieving gains in growth and form (Raymond 2002; Dungey et al. 2006). In modern times, the sawing

and drying technologies have advanced to the point where stem straightness may not be as important any more (Verryn and Hettasch 2006).

Currently, the purpose of growing plantations is to produce wood, not only in quantity but also in quality, in order to provide a range of wood processing sectors with materials possessing physical, mechanical and chemical properties that match their required qualities. Thus, the need for technological interventions goes beyond productivity gains. In addition to volume, it is important to increase raw materials (wood and fiber) quality and optimize chemical composition contents, pulp yield (for pulpwood), caloric power (for fuelwood), wood density, stiffness and other characteristics of interest of each wood processing sector.

Most of breeding programs of *Eucalyptus* are focusing on important traits to pulp and paper and bioenergy production. The improvements achieved in the last years by the tree breeders for wood quality traits have showed the importance of research in wood anatomy and technology along the genetic improvement program (ABRAF 2010).

Genetic control over growth and wood traits

Numerous studies have addressed to the genetic control of growth traits (Greaves et al. 1997; Wei and Borralho 1997; Kube et al. 2001; Costa e Silva et al. 2004; Volker et al. 2008; Kien et al. 2009; Costa e Silva et al. 2009) reporting variable heritability estimates for these traits in *Eucalyptus* trees. The genetic control for growth traits are lower than those for wood traits, because growth is a polygenic trait strongly influenced by the environment.

Many wood traits have been found to have moderate to high heritability estimates in a range of genera including *Eucalyptus* (Raymond 2002), *Picea* (Rozemberg and Cahalan 1997) and *Pinus* (Apiolaza and Garrick 2001). Thus, breeding for wood quality traits alone would be effective because heritability for wood quality traits such as wood density, microfibril angle and modulus of elasticity were usually high and there are broad genetic variations (Baltunis et al. 2007). Identification of the genetic factors contributing to quantitative trait variation is an important step in many tree breeding programs.

Genetic control for wood density has been exhaustively reported for many Eucalypt species. It ranges from $h^2=0.6$ (Kien et al. 2008) to $h^2=0.71$ (Wey and Borralho 1997) in *E. urophylla*; from $h^2=0.51$ (Kube et al. 2001) to $h^2=0.73$ (Greaves et al. 1997) in *E. nitens*, from $h^2=0.24$ (Poke et al. 2006) to $h^2=0.44$ (Apiolaza et al. 2005) in *E. globulus* and of $h^2=0.17$ (Raymond et al. 1998) in *E. regnans*. These examples show that the heritability estimates of such trait exhibit variable magnitudes. Hamilton and Potts (2008) presented a review of the genetic parameters of *Eucalyptus nitens*, reporting that heritability estimates of 12 independent studies ranged from 0.11 to 0.96 presenting mean value of 0.51 for the same species. Despite the large number of studies on this issue, there is no global trend concerning the genetic control over wood density.

The genetic control of the chemical components of wood has been relatively less studied. Gominho et al. (1997) reported high heritability estimates ($h^2=0.83$) for lignin content in *E. globulus* clones. Poke et al. (2006) evaluated open-pollinated families of *E. globulus* reporting narrow-sense heritability estimates of $h^2=0.13\pm 0.2$ and family means of $h^2=0.42\pm 0.19$. Apiolaza et al. (2005) examined 188 open-pollinated progenies of 11-year-old *E. globulus* reporting high narrow-sense heritability estimates for cellulose content ($h^2=0.84\pm 0.27$) and moderate ones for pulp yield ($h^2=0.44\pm 0.24$). Costa e Silva et al. (2009) evaluated *E. globulus* progenies finding moderate heritability estimates ($h^2=0.42\pm 0.14$) for pulp yield.

Few studies have reported genetic parameters for shrinkage and anatomical features, but these traits are known to be partially under genetic control. For instance, Pelletier et al. (2008) have investigated the

genetic variation in linear shrinkage of 152 open-pollinated families of *Eucalyptus pilularis* reporting moderate heritability estimates ($h^2=0.36\pm 0.1$) for tangential shrinkage but not significant for radial shrinkage ($h^2=0.1\pm 0.09$) or the ratios of the two. Raymond et al. (1998) examined the genetic control fibre length and coarseness in 10-year-old *E. regnans* finding low estimates of heritability for fibre coarseness ($h^2=0.15$) and moderate for fibre length ($h^2=0.36$). Apiolaza et al. (2005) reported low (and not significant) heritability estimates for fibre length ($h^2=0.16\pm 0.17$) in 11-year-old *E. globulus*.

The genetic control over microfibril angle was seldom reported for *Eucalyptus*. Apiolaza et al. (2005) used increment cores from 188 open-pollinated progenies of 11-year-old *E. globulus* reporting $h^2_{MFA}=0.27\pm 0.24$ while Lima et al. (2004) reported broad-sense heritability estimates ranging from 0.13 to 0.36 in 8-year-old clones of *E. grandis* x *E. urophylla*.

Genetic and residual correlations

An observed phenotypic correlation between two wood traits may be due to genetic or environmental causes, their interaction and also to ontogenic factors (age etc) inside the tree. Just as with phenotypic variances, there is a need to understand these underlying components that give rise to a phenotypic correlation (White et al. 2007). Genetic correlation can be defined as the ratio of genetic covariance and the product of the genetic standard deviations of two traits and can be thought of as the correlation of the breeding values (Falconer and Mackay 1996).

Two mechanisms can play a major role on genetic correlations: (i) pleiotropic (manifolds) effects of genes and (ii) linkage disequilibrium (non-random associations of alleles) between loci affecting different characters (Falconer 1993). When pleiotropy occurs this implies that a given gene locus influences the expression of more than one trait (Mode and Robinson 1959). When linkage disequilibrium occurs this means that the genes controlling these traits can be statistically associated, but there is no functional relationship between them.

An observed phenotypic correlation between two traits may also be caused by an underlying environmental (or residual) correlation (r_E) if environmental effects that influence one trait also influence the second trait (White et al. 2007). For example, consider a hypothetical conifer stand in which favorable microsites in the stand (e.g. locations with moister, deeper soils) lead to faster spring stem diameter growth. That is, the amount of spring wood is increased on favorable sites, but growth later in the season is unaffected (and therefore, the amount of late wood is similar on all microsites). Trees on these favorable microsites tend to have faster diameter growth and lower wood specific gravity, since they have a larger fraction of spring wood, which has lower specific gravity than late wood. In this case, there is a negative environmental correlation between diameter growth and wood specific gravity (faster diameter growth associated with lower specific gravity). This does not imply any relationship between the gene loci affecting the two traits, and there may or may not be a genetic correlation.

Genetic and environmental correlations are equally important in estimating the correlated response to selection in breeding programs (Falconer and Mackay 1996). Adverse genetic correlations can curtail breeding progress as, for example, a negative genetic correlation between growth and wood density would make it more difficult to select concurrently for improvement in both traits. Thus, estimating genetic correlations between traits of interest is necessary in proposing the basis for setting up breeding populations and selecting environmentally stable genotypes (Kien et al. 2009).

Genotype by environment interactions

According to White et al (2007) the essence of genotype x environment interaction is a lack of consistency in the relative performance of genotypes when they are grown in different environments. This may mean that the relative rankings of genotypes change in the different environments (called rank change interaction) or that, even in the absence of rank changes, differences in performance are not constant in all environments (called scale effect interaction). Lima et al. (2000) states that “following a study of interactions it may be possible to identify genotypes with high general adaptability (for example, genotypes which produce wood with high basic density on a range of sites) and others which perform better on particular sites”.

According to Muneri and Raymond (2000), genotype by environment interaction may be caused by two factors: different variances between the sites, or changes in the ranking of genotypes across sites. Thus, determining the size and practical importance of genotype by environment interactions is critical for designing tree breeding programs and making decisions about plantation establishment (Muneri and Raymond 2000).

Many *Eucalyptus* forests are planted over a wide range of climatic and edaphic conditions because the pulpwood producers may have extremely large surfaces of plantations for supplying wood to attend their ever-increasing demand for pulp and paper. While some clones have wide amplitudes in terms of the areas where they grow and perform well, other varieties have narrower limits. This is an important concern for wood industry.

Which traits to breed for?

Currently, tree breeders are faced with a growing “shopping list” of traits for which to breed, and in a shorter time period. This is a perilous situation, because, as the list of selection criteria increases, so too does the size of the breeding effort increase, or alternatively, the breeder may have to reduce the level of improvement in the traits (Verry 2008). A range of key traits to breed for each industrial need was suggested by Raymond (2002). According to her, for pulp and paper industry, the main characteristics are basic density, pulp yield, and cellulose content and fibre length. For sawn timber production, the traits of importance probably are basic density and gradient, microfibril angle, strength and stiffness, dimensional stability, shrinkage and collapse, tension wood, knot size, incidence of decay, spiral grain and end splits. The wood colour is also an important characteristic. For composites manufacturing, the key traits are suggested to be basic density and lignin, extractive and cellulose contents. For bio-energy purposes, wood may have high basic density and lignin content and superior mechanical properties (Brito and Barrichelo 1977).

Breeding strategies for different industrial application are not the same because the processing technologies require different, changing, and sometimes opposing, wood properties. For instance, lignins are undesirable compounds for pulp and paper production, because the delignification process requires energy and reagent consumption (Chang and Sarkanen 1973). Thus varieties of trees growing for pulpwood production should present lignin content as low as possible. On the other hand, the wood for bio-energy applications (charcoal production) may contain high lignin content (Brito and Barrichelo 1977) since wood with high lignin content is known to provide charcoal with high caloric power (Chen et al. 1997).

1.3.3 Challenges

The great difficulty for improving wood by means of breeding programs is the high cost involved on wood phenotyping. Indeed, the difficulty and cost of measuring such wood traits in large samplings have limited the efforts from wood specialists in understanding the genetic and environmental contribution on wood variation. As genetic studies require large dataset, producing them is very expensive and can make the implementation of the project impracticable.

A challenge for tree breeders and wood quality researchers of today is to respond appropriately to a complex environment demanding more productivity, higher quality, and a quicker adaptation of their crops to rapid changes (Verryn 2008). In this context, it is essential to know the variability, the inheritance, the genetic and environmental control of the wood traits (in particular, the orientation of the microfibrils in the S₂ layer of cell wall) of *Eucalyptus* wood and its implications with others properties. Hence, the use of new available methods and tools, model plant systems, molecular biological and genetic techniques can make a significant contribution to understand how and why microfibril angle changes in wooden plants (Donaldson 2008).

Considering the great silvicultural advantages of *Eucalyptus* and the low volume of wood managed towards to sawmills in Brazil, researches on *Eucalyptus* wood quality are required in order to verify if this wood specie can be an alternative for sawn timber industry.

1.3.4 Strategies for wood phenotyping

In tree breeding programs, knowledge of wood traits and their measurement are essentials to generate reliable findings. The development of rapid, accurate and industrially feasible methods becomes therefore necessary for characterization and classification of raw material in the forestry-related industry, including pulp and paper or steel production (charcoal), since these companies require methods that will cover a large number of samples. In order to accurately measure the wood traits, there is the need to have systems capable of evaluating the wood properties rapidly, precisely, without altering its end-use capabilities and at low cost. Among the current techniques, sonic resonance, X-ray diffraction and near infrared (NIR) spectroscopy are emerging technologies that could provide large data set of wood measurements.

According to Ross and Pellerin (1994), the techniques and methods for evaluating wood differ greatly from those for homogeneous, isotropic materials such as metals, plastics, and ceramics. In such non wood-based materials, whose mechanical properties are known and tightly controlled by manufacturing processes, the techniques for evaluation are used only to detect the presence of discontinuities, voids, or inclusions. However, in wood, these irregularities occur naturally and may be further induced by degradative agents in the environment. Therefore, sonic resonance, x-ray diffraction and near infrared (NIR) spectroscopy could be applied in wood to measure how genetic and environmental factors induces variation in a woods.

1.3.4.1 *Methods for assessing standing trees*

Nowadays a range of techniques has been proposed for generating a large data set in order to evaluate phenotypic, genetic and environmental parameters for a range of wood properties. Some non-destructive techniques, such as Resistograph (Rinn 1994; Rinn et al. 1996) and Pilodyn wood tester (Rozenberg and Van de Sype 1996; Raymond and MacDonald 1998) have been extensively used because they make possible the evaluation of trees in field. Figure 8 shows the two portable devices for evaluating living *Eucalyptus* trees in field conditions.

The Pilodyn instrument consists of a spring-loaded pin device that drives a hardened steel pin into the wood (Ross and Pellerin 1994). Originally, it was developed to measure the degree of degradation by means the depth of pin penetration (Hoffmeyer 1978), but nowadays this parameter is used as criteria for selection of trees by the density of their wood. For instance, Greaves et al. (1996) used Pilodyn for the indirect selection of basic density in *E. nitens* in field conditions. Then, a range of similar studies were done in order to evaluate genetic parameters in *Eucalyptus* (Rosado et al. 1983; MacDonald et al. 1997; Kien et al. 2008; Volker et al. (2008), *Pinus* (Klein 1995; Wang et al. 1999; Koch and Fins 2000) and *Picea* plantations (Rozenberg and Van de Sype 1996; Hansen and Roulund 1996).

Resistograph was originally developed to evaluate the health condition of trees and wooden poles (Costello and Quarles 1999); however, it has been suggested as a promising technique for estimating wood density and its genetic parameters in many wooden species. Many studies have used this portable instrument for generating data set for genetic studies on *Eucalyptus* (Lima et al. 2007; Rodrigues et al. 2008), *Pinus* (Gantz 2002; Isik and Li 2003) and *Pseudotsuga* (Chantre and Rozenberg 1997) genera, among other.



Figure 8 - Evaluating standing trees with Resistograph (A) and Pilodyn (B). Dotted lines shows in detail the pine penetration (source: personal image)

Indeed, these field portable equipments are able to estimate wood density in standing trees producing large data base in situ. Their advantage is their relatively low cost for purchasing and maintenance. Whilst they are attractive for real-time assessment of forests, their performance has had contradictory acceptance. While some studies reports clear correlation between density and pine penetration, other studies had shown indicative results. Pilodyn, for instance, is able to assess only the wood of the external portion of the stem providing a local inspection. It is not possible to assess how the wood density varies inside the tree or stem. According to Raymond (2002), the use of a pilodyn is not recommended for indirect assessment of basic density in breeding programs due to the low heritability of pine penetration. The resistograph results are strongly affected by wind because the tree swings altering the tension on the outer stem. Moreover, there may be mechanical problems resulting from intensive use of equipment.

Ultrasonic tomography has been used for evaluating the internal condition and decay on living trees using sound waves (Nicolotti et al. 2003; Gilbert and Smiley 2004; Deflorio et al. 2008). In short, a series of sensors are installed around the tree for sending or receiving sound waves. The distances between the measuring points are measured and recorded. Then, sound waves are generated by a hammer tapping on one of the sensors and the time of flights of sound waves between the sending point and the other receivers are measured. Finally, the apparent sonic velocities (distance/time) are calculated and a

"velocity" or "density" map of the tree is plotted by combining the measured tree geometry with sonic data recorded during the assessment (Figure 9). The sonic velocity can be correlated with wood densities and therefore with the soundness of the wood. Bucur (2003) lists a range of methods and techniques for non-destructive characterization and imaging of wood and standing trees.

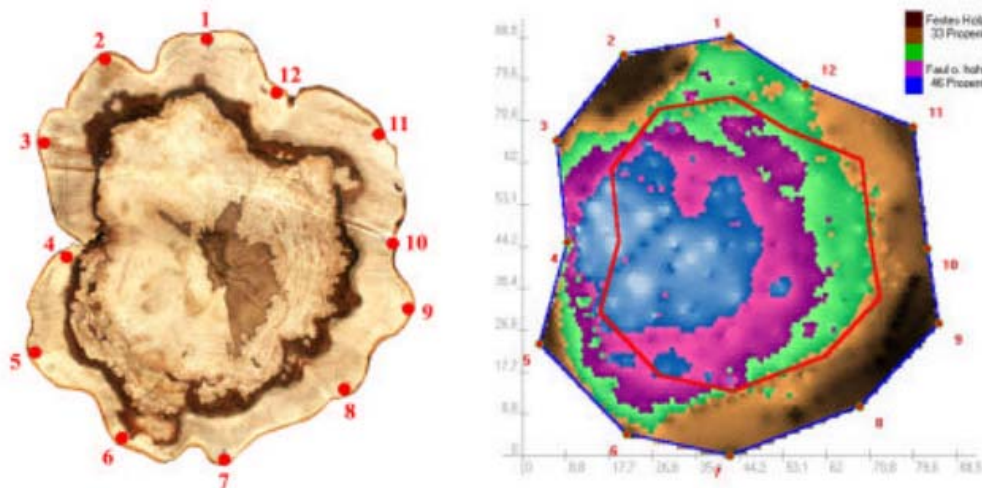


Figure 9 - Example of tomography analysis; a photograph of the disc (diameter: 90 cm) and the corresponding acoustic tomogram showing the decay (blue parts) in a wood disc (from Rabe et al. (2004))

1.3.4.2 X-ray densitometry

Radiation densitometry is a commonly used technique for assessing density characteristics of wood samples. Most of applications have used variations of the Polge (1963) method, i.e., production of a negative image of a wood sample by exposure of the wood and a film to X-rays generated electrically. The films must be developed under carefully controlled conditions and analysed in some form of optical densitometer to give analog or digital output of wood density variations (Cown and Clement 1983). The X-ray system gained widespread acceptance for evaluating variations of wood density (Walker and Dodd 1988). Decoux et al. (2004) have compared optical anatomical measurements to wood density variations assessed by X-ray densitometry within annual rings in softwoods. In *Eucalyptus*, Tomazello et al. (2008) have shown the application of X-rays for evaluating wood density changes across radial samples.

1.3.4.3 Sonic Resonance

Natural vibration analysis is a simple and efficient way of characterizing the mechanical properties of many materials, including wood (Bucur 1995; Brancheriau and Baillères 2002). Using various species of wood, sample dimensions and growth conditions, several studies have shown a strong linear correlation between dynamic and static modulus of elasticity (Ross et al. 1991; Wang et al. 2001; Green et al. 2004; Biblis and Carino 1999; Biblis et al. 2004). For instance, Ilic (2001) obtained strong correlations between static test and longitudinal ($r=0.95$) or flexural ($r=0.99$) elastic modulus using short specimens (20 mm x 20 mm x 300 mm) of *Eucalyptus delegatensis* R. Baker. Using larger pieces, Brancheriau and Baillères (2002) reported good correlation between Young's modulus in four-point bending and the flexural vibration modulus of elasticity on 76 beams of *Dicorynia guianensis* Amsy.

Dynamic tests based on the resonance frequency have been applied successfully in order to assess the dynamic modulus of elasticity of small, clean specimens (or clearwood) at the laboratory scale (Haines et

al. 1996; Ilic 2003; Brancheriau and Baillères 2003; Ohsaki et al. 2007), as well as of structural timber (Haines et al. 1996; Burdziak and Nkwera 2002; Liang and Fu 2007; Jiang et al. 2010) and logs (Ouis 1999; Wang et al. 2002; Grabianowski et al. 2006).

BING (Beam Identification by Non-destructive Grading) is a portable, simple and low-cost system developed at CIRAD (<http://www.xylo-metry.org/fr/bing.html>) allowing precise, reliable material characterization (Figure 10). Based on resonance frequency of vibrating beams measured by this system, it is possible to calculate the modulus of elasticity, shear modulus and internal damping in a range of materials, with various cross-sections, such as wood, metals, plastic, and ceramics.

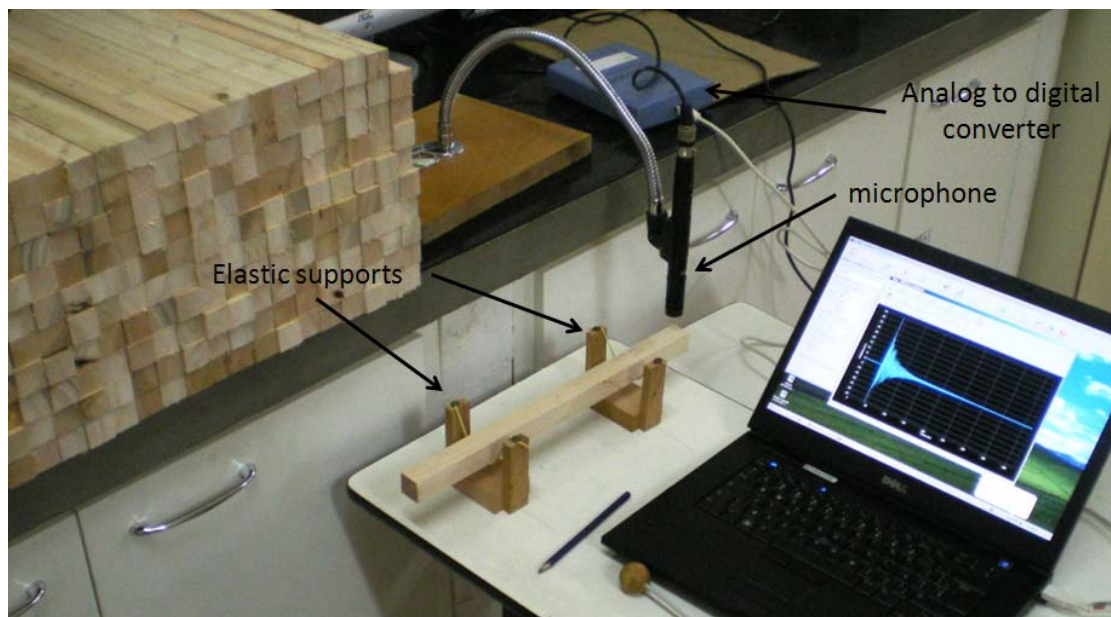


Figure 10 - Portable device for estimating dynamic elastic properties of wood based on sonic resonance frequency (source: personal image)

1.3.4.4 Near infrared spectroscopy

Near infrared spectroscopy (NIRS) is a fast, non-destructive technique (one minute or less) applicable to any biological material, including on-line processes, demanding little or no sample preparation (Pasquini 2003). It is based on vibrational spectroscopy which measures the interaction between light and the material (Næs et al. 2002). Bokobza (1998) and Pasquini (2003) reviewed the basic theory of NIR spectroscopy and its applications presenting the concepts that make a near infrared spectrum understandable. The simple physical principles of the spectrometer are presented in Figure 11. This NIR spectrometer device that operates in transmittance mode, however, there are also spectrometers equipped with sensors that measure the amount of light absorbed or reflected by the material.

In resume, the technique relies on developing a calibration that relates the NIR spectra of a large number of wood samples to their known chemical constitution, for example pulp yield or cellulose content (Raymond 2002). This NIR-based calibration is then used to predict, for instance, the pulp yield or cellulose content of further samples.

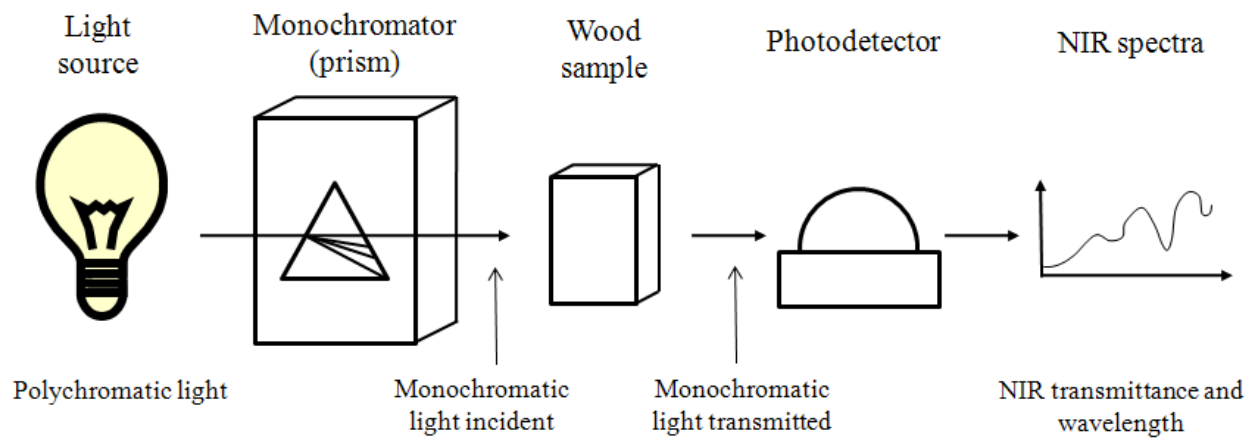


Figure 11 - Schematic of NIR spectrometer readings

The first works that used the NIR spectroscopy technique to assess wood concentrated on properties directly related to wood chemistry and were based on milled chips obtained from composite whole-tree samples. Birkett and Gambino (1989), Easty et al. (1990), Wright et al. (1990) and Wallbacks et al. (1991) presented the first results concerning NIR spectra and chemical properties of the wood, especially its cellulose content. Later, NIR spectroscopy approach has been also extended to assess non-chemical characteristics of solid wood samples showing that NIRS is capable to also estimate physical, mechanical, and anatomical features. The first study involving NIR spectra and wood density probably was presented by Thygesen (1994). She used shavings and solid wood of Norway spruce *Picea abies* (L.) Karst. demonstrating that the technique could be used to estimate the dry matter content and density of wood. Afterward, Hoffmeyer and Pedersen (1995) used NIR spectroscopy in solid wood samples of the same specie to evaluate dry density (dry weight per dry volume). They stated that NIRS could be used to predict wood density, compression and bending strength of dry wood. Since then, NIR spectroscopy has been widely used to evaluate many wood traits covering a wide range of applications. Tsuchikawa (2007) presented a complete review article where recent technical and scientific reports concerning the main NIR spectroscopy application in the wood are discussed. NIR spectroscopy models are especially attractive for tree breeders and genetic programs because it is possible to quickly provide estimates of many wood traits from a single NIR spectrum, if a NIR-based calibration is available. Since measuring NIR spectra is a simple operation, large data set can be rapidly produced at relatively low cost.

1.4 Scientific strategy

To understand the processes that govern the growth of the tree and to optimize the use of wood as a raw material in many industrial applications, numerous research activities are directed to cover different aspects of the structure and properties of wood (Peura 2007). Hence, much knowledge about wood structure, its properties and its performance in industrial applications has been accumulated over the years. However, many questions concerning wood properties, the methods of their measurement, and the analyses made from them remains still unclear. Moreover, the strategy that trees uses to change the MFA, stiffness and density of their wood in order to survive and to respond to specific needs (wood more or less dense, stiff etc) and the interactions between the growing tree and its environment is not well established.

1.4.1 Lacks of knowledge

Knowledge concerning wood, its properties, its variability and its performance in various applications are continuously increasing. However, a series of questions concerning these issues are raised.

1.4.1.1 *Wood traits, its variation and relationships*

Eucalyptus is the main genera for forestry in Brazil, where the plantations were target for pulp and paper production and bio-energy applications. The forest companies plant their genetically improved varieties of *Eucalyptus* trees on lands of all type, from drastic conditions (sloped terrain, hydric stress, strong winds, poor fertility etc) to optimal conditions (plan fields, light winds, adequate fertility etc) and they have the hard goal of producing homogeneous products from variable raw material. In this regard, the tree breeder and wood processors have to be aware of some important aspects.

How do wood traits vary within trees?

From an evolutive point of view, the variation of wood traits is vital for tree survival. Trees change their wood in order to respond to specific needs. For instance, if prevailing winds occur, the tree produces a kind of flexible wood (high MFA and low E/ρ) to resist to the bending forces induces by winds. Thus, the microfibril angles and lignin content drastically decrease while cellulose content increases when trees produce tension wood. This wood is stiffer making the tree able to withstand wind action. Such mechanism is well known in the literature; however, the genetic control of this phenomenon is unknown.

On the other hand, knowing how the key traits vary longitudinally and radially within the stem is of key importance for processors. Information about how the wood traits change within the stem in *Eucalyptus* clones planted on contrasting sites are unknown and would be useful in order to increase its economic value. The spatial variation of microfibril angle, elastic modulus and density, as well their relationships along the stem are not well known in *Eucalyptus* trees and are issues that deserve further studies. This kind of knowledge would be valuable to determining the best position for sampling, for instance.

What are the traits of key importance?

Breeders and processors should work on the traits of key importance for controlling the wood and end-product quality. While the importance of the microfibril angle for wood quality is well established for softwoods (Donaldson 2008), the relationship between MFA and wood quality traits remains unclear in *Eucalyptus* wood reserving further studies. Moreover, the effects of some environmental conditions (such as plantations on sloped terrains) on growth rate and wood quality are not well established for fast-

growing plantations. This issue is of particular concern, at least in Brazil, where plantations are grown in variable conditions and regions.

Besides increasing volume production and kraft pulp or calorific value yield, breeders and growers should be alert to biological and mechanical requirements for trees survival. Trees may be stiff enough to support the bending movements in response to wind without breaking and maintaining its erect habit. Hence, MFA and its relationships with density, wood stiffness and strength of woods from fast-growing plantation can be a critical subject deserving deeper investigation.

How to manipulate wood quality

Wood specialists may know in which extent key traits control the wood quality. The extent in which the microfibril angle controls the stiffness in *Eucalyptus* wood is not well established. Indeed, the papers by Evans and Ilic (2001) and Yang and Evans (2003) who exploring the relationship between MFA, ρ and E in *Eucalyptus* wood have demonstrated that MFA was the prime determinant of both the E and the specific modulus (E/ρ). However, their data come from Silviscan device (aparattus developed and presented by Evans 1999), which is a powerful instrument for MFA measurement for the one who can access to one of the three apparatus in the world. Indeed, the relationships between MFA and wood stiffness were still not verified in *Eucalyptus* by studies based on non-Silviscan data. If their conclusions can be generalized, selection of trees by MFA should make possible the improvement of the wood quality.

1.4.1.2 Questions concerning techniques for assessing wood traits

In order to phenotyping wood, there is a need to have systems able to precisely, rapidly, and at low cost evaluate them. The techniques employed in this thesis (sonic resonance, near infrared spectroscopy and x-ray diffraction) are used for wood characterization since long time ago. For instance, the relationship between modulus of elasticity and vibration frequency is known to nearly 150 years. Specifically for wood, early studies involving the resonance technique started more than 50 years (Jayne 1959). NIR spectra were used to investigate relationships between water and gelatine (Ellis and Bath 1938) more than 70 years ago. In wood, it is likely that Birkett and Gambino (1989) were the first to report findings involving NIR spectra and wood characteristics. X-rays were discovered in 1895 and used as a technique for producing interesting images of all kind. Then, X-ray diffraction patterns has been used to determine the preferred angle of the cellulose microfibrils of cell walls after the initial studies reported by Preston (1934) who analyzed single tracheids of *Sequoia* and *Abies nobilis*. Nowadays, these techniques are currently used in science and technology of wood and a sizable body of literature exploring such techniques are available; however, many methodological aspects still need to be better clarified. Some of these specific aspects are raised below.

What is the relationship between the characteristics obtained from laboratory tests and those of the material working in real situations?

In wood science and technology, much knowledge about the wood strength and flexibility has been accumulated over the years. In this regard, the dynamic tests based on the resonance frequency has played a major role since the technique have been applied successfully in order to analyze the dynamic modulus of elasticity of wood samples of any dimensions, from small specimens at the laboratory scale to logs.

Most studies have been done in order to evaluate the mechanical properties of pieces of wood with variable dimensions from large to small specimens. Few studies have been compared the mechanical properties obtained on large pieces of wood and on small specimens sampled from them. The relationships

between the mechanical properties of large and small wood samples are not still well established, especially for *Eucalyptus* wood. These findings would be useful in explaining the scale effect observed on mechanical behaviours of small clear specimens (as they are tested at the laboratory) and structural size material (as they would be really employed). This issue deserves deeper investigation since *Eucalyptus* wood is becoming a potential source as building material.

In order to provide the best estimates of chemical traits of wood, the NIR spectra should be measured in which conditions of sample preparation?

Numerous studies have reported the effects of varying wood surfaces on the NIR spectra (Tsuchikawa et al. 1992; Gierlinger et al. 2004) and their influence on model performance (Thumm and Meder 2001; Schimleck et al. 2003; Jones et al. 2006). However, the influence of the milling procedure, particle size, and solid wood surface quality on NIR-based calibrations for chemical traits is unknown, especially in *Eucalyptus* wood. Thus, wood specialists do not know precisely how they should prepare their samples in order to extract the maximum of information from them. This issue deserves further investigation.

Why NIR spectroscopy is able to estimate non-chemical wood traits, such as wood density, elastic properties and anatomical features?

Although the feasibility of NIR spectroscopy has been shown for numerous wood traits, it is still unclear how this technique can evaluate physical, mechanical traits and anatomical features of wood on the basis of vibrational spectroscopic analysis. In this context, many aspects need to be clarified by validating NIR-models, and analysing and interpreting coefficient regressions.

The association of near infrared spectroscopy, sonic resonance (for estimating elastic properties), x-ray diffraction (for estimating microfibril angles) and multivariate analysis would be a useful, rapid and reliable tool for phenotyping wood. NIR calibrations for dynamic elastic properties based on resonance technique were rarely reported. It is likely that Fujimoto et al. (2008) were the first team to report findings in regard to this issue.

Concerning MFA prediction by NIR spectroscopy, most of studies have been based on reference data provided by SilviScan measurements. NIR calibrations for MFA based on polyvalent X-ray diffractometer and NIRS devices are rarely reported. Schimleck et al. (2007), Kelley et al. (2004) and Huang et al. (2008) used softwoods to build their NIRS calibrations for MFA based on measurements made on polyvalent XRD apparatus. There is no report that the association of XRD and NIR would yield good calibrations for more complex wood, such the hardwoods species.

How accurate NIR-based models can predict wood traits in unknown samples?

Several works have used independent test sets to validate their NIR-based calibration for wood traits (Fujimoto et al. 2008; Schimleck et al. 2001; Via et al. 2003; Via et al. 2005; Cogdill et al. 2004; Gierlinger et al. 2002; Mora et al. 2008). These studies were carried out on a sampling systematically divided in two groups and the regressions were performed with one group and validated with the other. These approaches do not adequately simulate a real situation where the properties of unknown samples may be predicted by established NIR models. Few studies have been addressed to verify the robustness of the predictive models using external and independent sample sets (Souza-Correia et al. 2007; Rodrigues et al. 2006). The NIR spectroscopy ability of predicting wood traits on unknown samples from pre-established models is still not fully demonstrated and then, this issue requires further simulations.

1.4.1.3 Lack of information on Genetics of *Eucalyptus* wood

A number of wood traits, including wood density, stiffness and microfibril angle were identified as worthy of attention for *Eucalyptus* tree improvement (Raymond 2002). Recent studies have centered on the heritability of stiffness and MFA in softwoods (Dungey et al. 2006; Baltunis et al. 2007; Wu et al. 2007), but the degree to which stiffness and MFA are heritable and their genetic relationship with other traits in *Eucalyptus* has been poorly reported. It is likely that there is only one study reporting narrow-sense heritability (Apiolaza et al. 2005) and one study providing broad-sense heritability (Lima et al. 2004) of MFA in *Eucalyptus*. Moreover, genetic and environmental correlations among MFA, elasticity, density, lignin, S/G ratio and growth traits are unknown in *Eucalyptus*. Hence, the extent in which the microfibril angle, stiffness and density are regulated by additive genetic and environmental effects; how are the relationship of MFA and E with the other physico-chemical and growth traits, and how these relationships vary within the tree are still not well established in *Eucalyptus*. Finally, the means through which trees control changes in MFA, density, wood stiffness in response to developmental and environmental influences are poorly understood.

Indeed, the difficulty and cost of measuring such wood traits in large samplings have limited the efforts from wood specialists in understanding the genetic and environmental contribution on wood variation. If high throughput phenotyping tools exist, and make possible obtaining large dataset from a range of experimental dispositive, these issues are able to be answered, at least partially.

1.4.2 Hypothesis of this study

The present study has tested three hypotheses:

- 1) MFA controls the wood stiffness even in juvenile wood of *Eucalyptus*;
- 2) MFA and wood stiffness are heritable traits and could be tampered by mating in *Eucalyptus* breeding programs by combining the most favourable genes (allelic forms) and
- 3) MFA and wood stiffness, in addition to the commonly used wood traits (growth traits and wood density), could be used as target properties in current breeding programs for *Eucalyptus* in order to produce phenotypes exploitable for a wide range of processing needs, allowing effective response to the rapidly changing market, technological, and natural environments.

1.4.3 Purposes of this study

This study was undertaken in order to meet three main objectives, namely:

- [i] to establish the radial and longitudinal variation of the microfibril angles, wood stiffness and basic density within *Eucalyptus* trees;
- [ii] to provide information about the effective influence of MFA on *Eucalyptus* wood traits;
- [iii] to generate a better understanding about the genetic and environmental control over MFA, wood stiffness, basic density and chemical properties of *Eucalyptus* wood.

To attend the main goals of this study, two experimental designs were investigated, namely:

Progeny test: factorial design represented by 35 full-sib families of 14-year-*Eucalyptus urophylla* coming from mating between 16 parents (8 mothers and 8 fathers) conducted by the “Centre de Recherche sur la Durabilité et la Productivité des Plantations Industrielles” (CRDPI) in Pointe Noire, Republic of Congo;

Clonal test: experimental design represented by 10 clones of 6-year-*Eucalyptus* hybrids (*E. urophylla* and *E. grandis*) from tests managed for pulp and paper production by “Celulose Nipo-Brasileira S.A” (CENIBRA), in Belo Oriente, Minas Gerais State, Brazil.

Specific objectives

The specific objectives concerning wood and its variation of this study were: **(i)** to understand the effect of environmental factors on the variation patterns of microfibril angle, wood stiffness and wood density and **(ii)** to establish the correlation between the stiffness of scantlings and small specimens of *Eucalyptus* wood. These findings would be useful in explaining the scale effect observed on mechanical behaviours of wood of different dimensions.

Concerning the methods and techniques for phenotyping wood, polyvalent techniques such as X-ray diffraction and sonic resonance were combined with near infrared spectroscopy in order to obtain precise information from the wood. Then, multivariate data analyses were applied for extracting information about physical, mechanical, and chemical characteristics and also anatomical features of the wood. The specific objectives concerning the NIR spectroscopic models were: **(i)** to evaluate the influence of the milling procedure, particle size, and solid wood surface quality on the predictive power of NIR spectroscopy models for chemical properties of *Eucalyptus* wood; **(ii)** to evaluate the robustness of the predictive models based for wood basic density in *Eucalyptus* wood using two totally independent sample sets; **(iii)** to build NIR spectroscopy models for estimating modulus of elasticity and visco-elastic traits in *Eucalyptus* wood using reference values obtained from dynamic tests; **(iv)** to develop NIR spectroscopy models for estimating MFA traits in *Eucalyptus* wood using reference values obtained by X-ray diffraction.

The genetic studies of the present thesis were performed from two distinct trials, the clonal and the progeny test. Genetic approaches of the clonal test were made using dataset obtained from dynamic tests of large pieces of wood, and from NIR-based estimates of MFA, wood stiffness and density across the discs. Thus, the specific objectives concerning the genetic studies of the clonal test were: **(i)** to investigate the clonal and environmental variation of the elastic properties on large pieces of 6-year-old *Eucalyptus grandis* x *urophylla* wood by means of sonic resonance technique and **(ii)** to explore the variations of the genetic control over basic density, stiffness and microfibril angle of wood within clones of 6-year-old *Eucalyptus grandis* x *urophylla* stem. The genetic approaches of the progeny test were done using dataset obtained from NIR-based estimates of chemical component contents, wood density and MFA values along the discs. Therefore, the specific objectives of the study of progeny test were: **(i)** to determine the level of genetic control over MFA in control-pollinated progeny families of 14-year-old *Eucalyptus urophylla* wood; **(ii)** to determine the genetic and environmental correlations among microfibril angle, wood density, lignin content, syringyl to guaiacyl ratio and growth traits and **(iii)** to investigate the age trends of these genetic parameters.

Knowledge about the variations in wood density, modulus of elasticity and microfibril angle of commonly deployed clones can better describe genetic gains made by each clonal variety. Thus, this thesis hopes to be able to respond/indicate how variable are the wood traits in *Eucalyptus* plantations; if the woods from these trials can be improved and how much; and which are the most appropriate genotypes for timber production to future *Eucalyptus* plantations in Brazil.

1.4.4 Strategy of this study

To attend its purposes, this study falls into two parts. The first consisted on phenotyping wood traits and the second on the quantifying the genetic parameters of wood traits. The strategy of this study is described below. It presents a resume of all activities of this study, including procedures for sample preparation and measurements of wood traits, as well the main analysis. The detailed description of each item is provided within Material and Methods, and Results and Discussion sections.

1.4.4.1 *Phenotyping wood traits*

A detailed investigation about wood characteristics of many kinds of samples (from larger samples to small specimens) was carried out using the wood from the progeny and clonal tests. Figure 12 sums up the growth and wood traits under examination in the two experimental designs.

Progeny test

The wood of the trees of the progeny test were investigated from wood discs. First, the discs were cut into two opposite wedges and radial strips (free of knots and defects). NIR spectra were recorded on the radial surface of the wedges on three radial positions (1, 2 and 3) from pith to bark. Then, the wedges were grounded and NIR spectra were obtained from the wood powders. These NIR spectra were used for predictions. The radial strips were divided in small samples (20 x 20 x 30 mm) for wood density measurements and tangential sections (2 x 20 x 30 mm) for MFA measurements. NIR spectra were recorded on transversal, radial and tangential surfaces of small samples and on two sides of tangential sections. Afterwards, three *T* values were recorded by X-ray diffraction at three points on 175 tangential sections and basic density of wood was measured on the off-cut small samples. **Paper 3** reports the radial variation of MFA and wood density, the correlation between them and the influence of age on such relationships in the 14-year-*Eucalyptus urophylla* wood.

Clonal test

One-hundred fifty trees were harvested from Clonal tests. A log of 2.4 meters and 5 wood discs were cut at 0, 25, 50, 75 and 100% of the commercial height were cut from each tree. Diametrical strips were cut from the discs. The diametrical bands were sanded and NIR spectra were recorded. These NIR spectra were used for further predictions. The logs were cut into central boards, and a total of 410 pieces of wood with nominal sizes of 45 x 60 x 2,100 mm (hereafter referred to as scantlings) were taken from the central boards. Subsequently, a pile of scantlings was set up for air-drying under protected exterior conditions (shed of the wood processing sector at UFLA, Brazil) during 90 days. After air-drying process the scantlings presented defects such as small cracks, checks and splits in their ends and, therefore, were trimmed to variable dimensions, depending of the extension of their defects. The clean scantlings had, on average, 1.54 meters of length, varying from 0.645 m to 2.080 m and the averaged width and thickness were 60 and 43 mm, respectively. The scantlings were submitted to flexural and longitudinal vibration tests. Subsequently, the air-dried (unseasoned) scantlings were kiln-dried at 14% (nominal) of moisture content under soft condition during two weeks. Thus, new flexural and longitudinal vibration tests were performed on the kiln-dried scantlings. Finally, small, clean specimens measuring 25 x 25 x 41 mm were cut from the scantlings and submitted to transversal and longitudinal vibration tests. The mass and dimension of the scantlings and the small, clear specimens were measured and the air-dried density of each piece of wood was calculated. The dynamic properties of these woods are discussed in the **paper 1** while the genetic approaches obtained from these results are reported in **paper 9**.



Progeny test (14 years)

Eucalyptus urophylla x E. urophylla

Density of plantation: 4 m x 4 m

Origin: Republic of Congo

Sampling: 348 wood discs (9-10 by family)

Traits: circumference and height, klason lignin, Syringyl to guaiacyl ratio, basic density and microfibril angle

Clonal test (6 years)

Eucalyptus urophylla x E. grandis

Density of plantation: 3 m x 2 m

Origin: Brazil

Sampling: 750 wood discs (10 clones x 3 sites x 5 repetitions x 5 longitudinal positions)

Traits: circumference and height, wood density, modulus of elasticity, specific modulus, modulus of rupture, shear modulus, loss tangent, shrinkage and MFA

Figure 12 - Wood discs from the the progeny and clonal tests and the growth and wood traits under examination in this study (source: personal image)

Subsequently, these wood specimens were tested using a universal testing machine. Static tests in 4-point and 3-point bending tests were performed to determine the modulus of rupture (MOR). From each beam one or more twin specimens were cut, so when two twin specimens were removed from the same scantling, the first was tested in a 4-point bending while the second was tested in a 3-point bending. Similarly, when three or more specimens were removed from the same beam, the first and third specimens were tested in a 4-point bending, and the second (and the fourth, if exists) was performed in a 3-point bending. This procedure was used to compare the two types of bending tests on twin specimens. These findings are presented in the Annexes section (item 6.4, pg. 141).

Afterward, a small wood sample measuring 25 mm × 25 mm × 25 mm was removed from the intact wood in order to measure the basic density and the linear shrinkage of wood. The shrinkage of wood was measured in two situations: from over-dried to equilibrium moisture content (EMC) condition and from EMC to above of saturation point, or green condition. Finally, a 2 mm radial section was cut from each small sample for microfibril angle measurements. This procedure provided a complete range of information about the physical, mechanical and anatomical features of these wood samples. **Paper 2** have evaluated the relationships between microfibril angle, density, wood stiffness and strength, modulus of shear and shrinkage in *Eucalyptus* clones.

NIR-based models

This part of the study was dedicated to developing NIR-based models in order to estimate a range of wood traits and improving the methodology. The objective was also to examine and explain why NIR

spectroscopy could be used for predicting dynamic wood traits and microfibril angles. Table 3 lists a summary of the main statistics of the NIR-based calibration.

Table 3 - Resume of the main statistics of the NIR-based calibration for estimating wood traits of progeny and clonal tests and the corresponding paper

Test	Trait	R ² p	RMSEP	LV	Outliers	RPD	Paper
Progeny	KL	0.85	0.53	6	5.00%	2.58	4
	S/G	0.86	0.13	7	5.00%	2.68	4
	ρ	0.85	30	3	2.10%	2.70	5
	MFA	0.59	1.36	6	-	1.57	6
Clonal	ρ_{sp}	0.67	34.78	4	0.90%	1.75	7
	ρ_s	0.8	22.88	3	2.60%	2.32	-
	MFA	0.75	1.31	5	6.60%	2.10	-
	E_L	0.81	1149	5	1.20%	2.34	7
	E'_L	0.76	1.62	5	-	1.41	7
	f_1	0.72	215.3	6	-	1.92	7
	E_F	0.74	1219	4	0.60%	2.01	7
	E'_F	0.7	1.69	6	0.30%	1.88	7
$\tan\delta_L$	0.38	0.81	5	1.40%	1.84	7	

For wood from the progeny test, NIR-based calibrations were developed for assessing the main chemical components of wood, including klason lignin content (KL), acid-soluble lignin content (ASL) and syringyl and guaiacyl ratio (S/G). These NIR-based calibrations for wet-chemistry wood traits were reported in **paper 4**, where different procedures for sample preparation and its effect on model performance were discussed. In the present study, the acid-soluble lignin was not presented. Afterwards, NIR-based calibrations were developed for physical and ultrastructural features for wood samples from diametrical bands. **Paper 5** reports the NIR-based models for basic density estimates demonstrating the robustness of the established models by validating them with different sets of samplings, bringing insight to the real external, independent validation approach. **Paper 6** presents the NIR-based models to estimate microfibril angle and explains why NIR spectroscopy could be used to predict this complicated ultrastructural feature of the cell walls in *Eucalyptus* wood.

For wood from Clonal tests, NIR-based calibrations were developed for assessing the mechanical properties of wood, such as air-dry density and basic density of wood, dynamic modulus of elasticity, shear modulus, and internal friction of the specimens, as well as their first resonance frequency. **Paper 7** reports the NIR-based models for estimating such wood properties. These models were based on the wood of the first log of the trees: the samples came from the scantlings, which came from the central boards. These models were applied on the NIR spectra measured on the 750 wood discs in order to predict a range of wood traits making possible to propose the cartography of wood variation within the stem.

1.4.4.2 *Quantitative genetic approaches*

The genetic and environmental variations of wood traits were assessed. The NIR-based calibrations were applied on the woods enabling the assessment of many wood traits in the progeny and clonal tests. These predictions permitted the determination the patterns of spatial variation, the correlations between traits and degree of genetic and environmental control of wood traits. These findings provided new elements for generating a comprehensive knowledge about patterns of variation in heritability estimates and on the traits themselves within the *Eucalyptus* trees.

Progeny test

The NIR-predicted values of the wood traits of the trees from the progeny test were used to assess the level of genetic and environmental control over a range of wood traits, with special focus on MFA and its correlation with other traits. Moreover, genetic and like-environmental correlations among those traits were assessed at different ages improving our knowledge on the functional aspects of wood formation in *Eucalyptus*. The degree of genetic and environmental control over MFA, ρ , lignin content and its structure and growth traits were presented and a series of implications for selection were discussed in **Paper 8**.

Clonal test

The NIR-predicted values of the wood traits of the trees from the clonal tests were used to assess the genetic parameters and the spatial variation of basic density, wood stiffness and MFA in *Eucalyptus* wood. **Paper 10** reports such results. The variation between clones and sites of elastic properties measured on the scantlings by resonance technique were presented and discussed in **paper 9**. From these findings, we hope to be able to indicate what are the most suitable and environmentally stable genotypes for future timber production from *Eucalyptus* plantations.

As a final point, I hope the findings of this PhD thesis helps us to obtain a deeper understanding about the genetic and environmental control, and the clonal variation of a range of wood traits in *Eucalyptus* wood from plantations. The correlations between growth and wood traits in *Eucalyptus* plantations were also investigated. I expected to bring new element to understand how trees adapt their wood traits in order to maintain their erect habit even when they are constrained by bending movements in response to wind and gravity.

2 MATERIAL AND METHODS

2.1 Origin of the material

2.1.1 Progeny test

348 disks taken at breast height of 14-year-old *Eucalyptus urophylla* S.T. Blake trees coming from progeny test established in the Republic of the Congo in the experimental area of research centre UR2PI “Unité de Recherche sur les plantations Industrielles du Congo” (04°45’ S, 12°00’ E, alt 50 m) were used in this study. The climate is tropical humid with a mean annual temperature of 24°C, a mean annual rainfall of 1,200 mm and a dry season from May to October. This progeny trial was composed by 35 full-sib families produced by controlled pollination (Table 4). These families provided from an un-complete factorial mating design (8 x 8) with *E. urophylla* (16 genitors originated from two provenances). The families were planted in a randomized design and density of plantation was 625 trees/ha (4 x 4 m spacing).

Seeds obtained by controlled pollination were sown in the nursery in the Republic of the Congo from July to September of each year in poly-bags (20 cm high, 10 cm diameter) containing adequate media (one third sand, one third forest soil and one third compost). Five to six months after sowing, the seedlings were planted in a field trial. The full-sib families were planted in a 4x4 m spacing (625 trees/ha). Within each field trial, the experiment was a complete block design with a 16-tree square plot in four replicates. To minimize the impact of borders, two border lines were planted around the field trials.

Table 4 - Arrays of parents in the incomplete factorial mating design under controlled crosses

BRG project		<i>E. urophylla</i> (male)							
		14-130	14-135	14-137	14-142	14-132	14-146	14-147	14-148
<i>E. urophylla</i> (female)	14-128		F9	F8	F10		F12		
	14-133	F15	F14				F16	F17	
	14-138	F5		F35	F6	F36			F7
	14-144	F2	F1		F3			F4	F33
	14-136						F20	F21	F22
	14-140		F24	F23		F25	F26	F27	
	14-149				F39	F32			F37
	14-152	F28				F29		F30	F31

Nine to ten trees were harvested from each family, resulting in a total of 348 trees. Breast height wood disk (~30 mm thick) was obtained from each tree and transported to the CIRAD in Montpellier, France. Circumference at breast height (C) and commercial height (H) were measured before harvesting.

2.1.2 Clonat test

One hundred and fifty (150) *Eucalyptus grandis* x *urophylla* hybrids with 6 years-old from clonal tests managed for pulp and paper industry (Cenibra Nipo-Brasileira S.A.) established in Brazil (19°17’ S, 42°23’ W, alt 230-500 m) were used in this study. Ten (10) hybrids coming from three clonally replicated trials established in contrasting site (Table 5) were investigated.

Table 5 - Description of the environmental information of the clonal tests

Clonal test	Location	Slope of terrain	Type of soil	Mean Temp. (°C)	RH (%)	Precip (mm)	Hidric deficit (mm)	Vapor pressure deficit (hPa)	Global radiation (MJ m ⁻² day ⁻¹)	Effectiv radiation (mmol m ⁻² s ⁻¹)	Wind speed (m s ⁻¹)
303	Brejo	0°	LVd1	24.5	70.5	1,230	299	4.8	17.7	33,442	0.9
301	Guanhães	20°	CXbd9	21.3	65.7	1,182	150	4.0	15.8	33,158	3.2
302	Coruja	40°	RUbd5	24.5	70.5	1,230	299	4.8	17.7	33,442	0.9

The type of climate is Aw (Tropical Savanna Climate), according to the classification of Köppen (Peel et al. 2007), with mean annual rainfall of around 1,200 mm, mean annual temperature of around 23°C and the average annual humidity is around 70%. Sites 302 and 302 present similar meteorological conditions, but the terrain slope was very contrasting. The location of these two clonal tests is close. The Clonal test 301 is around 100 kilometers distant from others and their weather condition is different, especially the wind speed.



Figure 13 - Differences of field conditions between clonal tests (source: personal image)

Table 6 - Information about the clones' origin describing their relatives and species

Clone	Mother	Species	Father	Species
4426	89	<i>E. grandis</i>	6	<i>E. urophylla</i>
4494	7	<i>E. grandis</i>	5	<i>E. urophylla</i>
4514	9	<i>E. grandis</i>	12	<i>E. urophylla</i>
4515	3	<i>E. grandis</i>	5	<i>E. urophylla</i>
4535	48	<i>E. grandis</i>	2	<i>E. urophylla</i>
4541	53	<i>E. grandis</i>	13	<i>E. urophylla</i>
4557	24	<i>E. grandis</i>	8	<i>E. urophylla</i>
4579	89	<i>E. grandis</i>	6	<i>E. urophylla</i>
4588	97	<i>E. grandis</i>	10	<i>E. urophylla</i>
4609	10	<i>E. urophylla</i>	26	<i>E. grandis</i>

Five individuals per clone were sampled in each clonal test, totalizing 150 trees (10 clones x 3 sites x 5 individuals). Trees were selected among those upright, healthy, without fork and out of embroidery and harvested at 72 months (6 years). Circumference at breast height (C) and commercial height (H) were measured before harvesting. Figure 13 illustrates the difference in slope of terrain between sites. The

clones were planted at 2003 in a randomized design and density of plantation was 1,667 trees/ha (3 m x 2 m spacing).

2.2 Sampling preparation

2.2.1 Progeny test

A pith to bark radial strip and a clean wedge (knot-free) were cut by a vertical bandsaw machine from each disc. These wood strips had variable height and length (depending of the circumference and thickness of each wood disc), but their width was fixed at 30 mm.

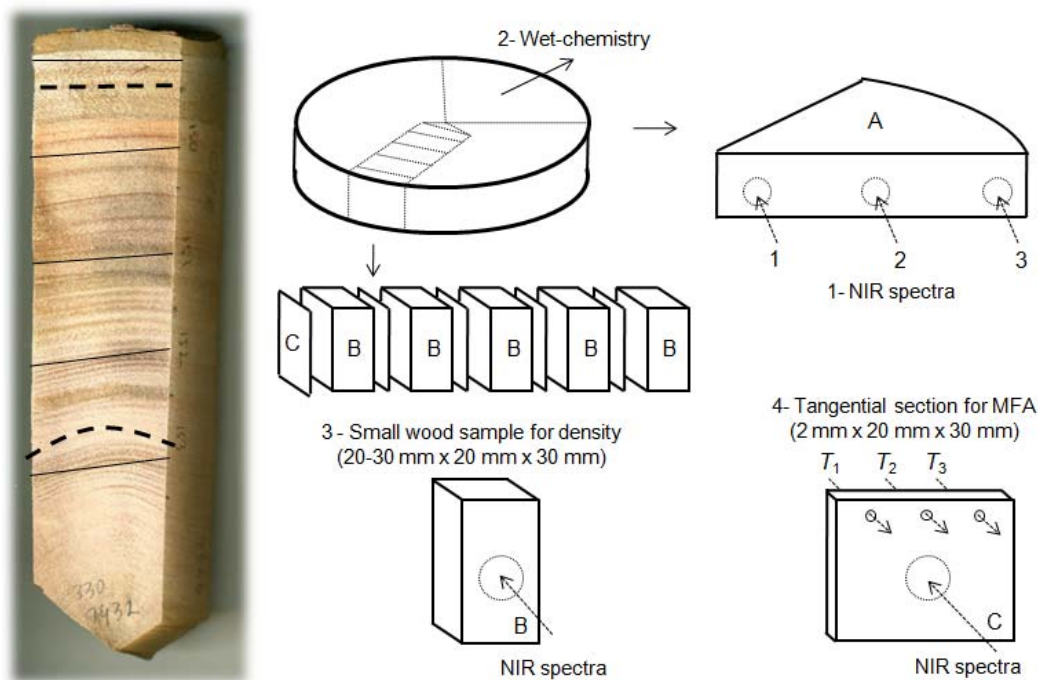


Figure 14 - Strategy of wood sampling and wood measurements of the progeny test

The radial surfaces of the radial strip were sanded with 300-grit sandpaper for approximately 30 seconds. Tangential sections (2 mm x 20 mm x 30 mm), as parallel as possible, to the growth rings boundaries and wood samples (~20-30 mm x 20 mm x 30 mm) were cut for microfibril angle and wood density measurements, respectively.

Wood powder was produced from wedges which were ground in a Retsh ultra-centrifugal mill (ZM 200). The particle sizes of wood meals obtained were less than 0.5 mm and were designated “0.5 mm” for NIRS. 60 wood meals samples were selected according to their NIR spectra from principal component analyses and were submitted to chemical analysis. Figure 14 sums up the strategy of sampling and measurements of the wood from progeny test.

All samples (solid samples and the milled samples) were kept in a conditioned room with 60% relative humidity and temperature of 20°C before analysis. Under these conditions, the equilibrium moisture content was 12%.

2.2.2 Clonal test

2.2.2.1 Wood from logs

Scantlings

A total of 410 pieces of wood (Figure 15 C) with nominal sizes of 45 mm x 60 mm x 2,100 mm (hereafter referred to as ‘scantlings’) were taken from 150 central boards (Figure 15 B). As the scantlings were removed systematically at each 45 mm of the boards (60 mm in thick), naturally, some parts of the scantlings contained pith, knots and other features inherent to wood. Subsequently, a pile of scantlings was set up for air-drying under protected exterior conditions during 90 days.

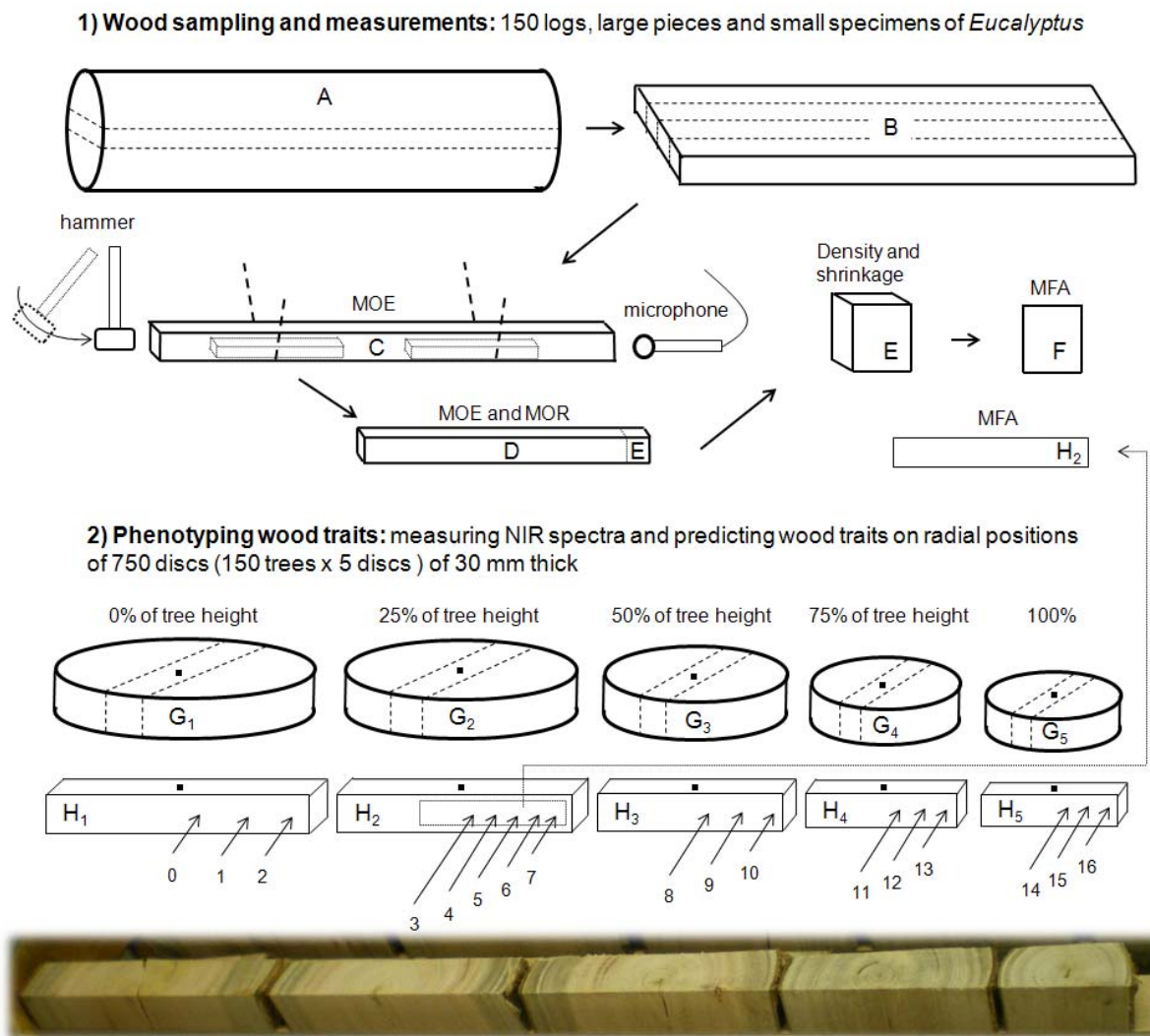


Figure 15 - Strategy of wood sampling and wood measurements of the clonal test and reference of codes relative to radial and longitudinal positions for NIR spectroscopic and genetic analysis

After air-drying process the scantlings presented defects such as small cracks, checks and splits in their ends and, therefore, were trimmed to variable dimensions, depending of the extension of their defects. The clean scantlings had, on average, 1.54 meters of length, varying from 0.645 m to 2.080 m (COV=16.9%) and the averaged width and thickness were, 60 mm and 43 mm, respectively, fluctuating slightly (COV=5.7% for width and COV=2.8% for thickness). Thus, all pieces were free of large fissures,

biological affections, defects produced in the saw mill as severe reduction of width or thickness, but they presented knots and small cracks as well. In the second step, the unseasoned scantlings were kiln-dried at 14% (nominal) under soft condition during two weeks. Therefore, new transversal and longitudinal vibration tests were performed on the kiln-dried scantlings. Figure 15 presents the strategy for preparing wood samples.

Specimens and small wood samples

160 scantlings were selected among the best (i.e. annual rings well oriented, free of large cracks etc) and surfaced on the plane machine; beams were cut from them and trimmed to nominal cross-section of 25 mm x 25 mm using a circular saw machine. Finally, clearwood specimens measuring 25 mm x 25 mm x 41 mm (Figure 15 D) were cut from the beams, according to the standard D 143-94 (ASTM 2007). Twin small wood samples (25 mm × 25 mm × 25 mm) were removed from the intact clearwood specimens (Figure 15 E) for wood density and shrinkage measurements;

Wood sections and radial strips

Radial sections (50 mm x 20 mm x 2 mm) were cut from the small wood samples (Figure 15 F) for microfibril angle measurement. Radial strips (50-150 mm x 30 mm x 2 mm) were cut from the discs at 25% of the height (Figure 15 H2) for microfibril angle measurement.

2.2.2.2 Wood from discs

Diametrical strips around 30 mm of width were cut from wood discs. The strips of the trees coming from sloping grounds were removed in the sense of the inclination of sites. Thus, the upslope portion of the strip possibly contains tension wood and those from down slope portions probably contains opposite wood. This procedure was done in most of discs; however, there were some samples presenting cracks and slits and the strip was cut perpendicular to slope to obtain “normal wood”. In these regions (Site 301 and 302) the prevailing wind can neutralize the supposed tension wood occurrence due to the sloping grounds. The company's field technicians reported that when high winds occurs breaking trees, the trees topple on top of the hill, in the wind direction.

Table 7 - Reference of codes relative to radial and longitudinal positions

Code	Relative height	Radial position	Code	Relative height	Radial position
0		inner HW ⁰	8		HW ⁸
1	0%	outer HW ¹	9	50%	inner SW ⁹
2		SW ²	10		outer SW ¹⁰
3		inner HW ³	11		inner SW ¹¹
4		middle HW ⁴	12	75%	middle SW ¹²
5	25%	outer HW ⁵	13		outer SW ¹³
6		inner SW ⁶	14		outer SW ¹⁴
7		outer SW ⁷	15	100%	outer SW ¹⁵
HW means heartwood while SW means sapwood.			16		outer SW ¹⁶

The radial surface of each diametrical strip were sanded using a sanding machine in order to produce a homogeneous surface quality. Figure 15 presents the strategy for preparing the radial bands and measuring

NIR spectra from discs, including the reference of codes relative to radial and longitudinal positions for NIR spectroscopic analysis. Table 7 lists the reference of codes relative to radial and longitudinal positions. The main results on genetics of clonal test are presented using these reference codes.

The author is aware that 6-year-old trees still do not produce mature wood or heartwood. This nomenclature has been proposed to facilitate data interpretation and explanation of findings.

2.3 Methods for phenotyping

2.3.1 Sonic resonance

The dynamic tests used to evaluate the elastic properties of wood samples were based on sonic resonance (Brancheriau and Baillères 2002; 2003). The scantlings and clear wood specimens were placed on elastic supports so as to generate free vibrations. An exciting impulse was produced by lightly striking the scantlings with a hammer at the opposite side of the output transducer (acoustic microphone). The transverse vibration was induced by an edgewise impact and the longitudinal vibration by an impact along the bound. The output signals were transmitted via a low-pass filter to an acquisition card on a computer and recorded as described by Brancheriau and Baillères (2003).

2.3.1.1 Equations of motion

The theoretical model used to describe the motion of a uniform prismatic beam that transversally vibrates freely was proposed by Timoshenko (1921) as follow:

$$E_F I_{Gz} \frac{\partial^4 v}{\partial x^4} - \rho I_{Gz} \left(1 + \frac{E_F}{K G_{XY}} \right) \frac{\partial^4 v}{\partial x^2 \partial t^2} + \frac{\rho^2 I_{Gz}}{K G_{XY}} \frac{\partial^4 v}{\partial t^4} + \rho A \frac{\partial^2 v}{\partial t^2} = 0 \quad \text{Eq. (3)}$$

where E_F is the modulus of elasticity; I_{Gz} is the moment of inertia; v is the transversal displacement; ρ is the density; G_{XY} is the shear modulus; K is a constant which depends of the geometry of the section (For rectangular section, $K=5/6$); x is the distance along the axis of the beam; A , cross-sectional area of the beam; t is the time. Using the Bordonné's (1989) solution for this differential equation, the shear effect is taken it account, but the support effects are ignored. The elastic (E_X) and shear modulus (G_{XY}) were calculated according to the follow equation, described by Brancheriau and Baillères (2002):

$$\frac{E_F}{\rho} - \frac{E_F}{K G_{XY}} \left[Q F_2(m) 4\pi^2 \frac{A L^4}{I_{Gz}} \frac{f_n^2}{P_n} \right] = 4\pi^2 \frac{A L^4}{I_{Gz}} \frac{f_n^2}{P_n} [1 + Q F_1(m)] \quad \text{Eq. (4)}$$

where f_i is the resonance frequency of the order i and P_n is the coefficient associated with the solution of Bernoulli (rank n). Parameters Q , F_1 , F_2 , m and θ are calculated as follows:

$$Q = \frac{I_{Gz}}{A L^2} \quad \text{Eq. (5)}$$

$$F_1(m) = \theta^2(m) + 6\theta(m) \quad \text{Eq. (6)}$$

$$F_2(m) = \theta^2(m) - 2\theta(m) \quad \text{Eq. (7)}$$

$$\theta(m) = m \frac{\tan(m) \tanh(m)}{\tan(m) - \tanh(m)} \quad \text{Eq. (8)}$$

$$m = \sqrt[4]{P_n} = (2n+1) \frac{\pi}{2}, \quad n \in N^* \quad \text{Eq. (9)}$$

Parameters m , P_n , $F_1(m)$ and $F_2(m)$ are calculated on the basis of index n , and are used in practical applications to calculate the value of the modulus E_X and that of the shear modulus G_{XY} .

In practice, the first frequencies are those that are least influenced by the viscosity of the material; these are theoretically those that give the modulus nearest to the static modulus conventionally obtained by a static bending test (Cilas et al. 2006).

In longitudinal vibrations, the theoretical model used to describe the motion of a uniform prismatic beam that vibrates freely was given in Brancheriau and Baillères (2002) as follow:

$$E_L \frac{\partial^2 u}{\partial x^2} - \rho \frac{\partial^2 u}{\partial t^2} = 0 \quad \text{Eq. (10)}$$

where u is the longitudinal displacement. The first vibration mode can be used in order to estimate its dynamic longitudinal modulus of elasticity (E_L), which represents its stiffness under compressive stress, by means the formula:

$$E_L = 4L^2 \rho f_1^2 \quad \text{Eq. (11)}$$

A deep discussion about different theoretical models of motion, their approximate solutions and their respective hypotheses in longitudinal and transversal vibrations; and the effects of the elastic support was provided in Brancheriau and Baillères (2002).

To extract relevant parameters from acoustic sounds, the concept of additive synthesis was applied (Brancheriau et al. 2006). Each temporal signal $s(t)$ was then considered as a sum of exponentially damped sinusoids as follow:

$$s(t) = \sum_{i=1}^{\infty} \beta_i \exp(-\alpha_i t) \sin(2\pi f_i t + \varphi_i) \quad \text{Eq. (12)}$$

Where s is the radiated signal as a function of time t and φ_i is the phase shift. The parametric method of Steiglitz and McBride (1965) was used to simultaneously determine the first resonance frequency f_1 , the amplitude β_1 , and the temporal damping α_1 associated with f_1 . Only the first frequency was considered because of its high energy.

Vibrations are damped by internal friction ($\text{tg } \delta$), a property of solid materials that transforms mechanical energy to heat when subjected to cyclical stress (Brancheriau et al. 2010). The internal friction was calculated associated with the complex modulus concept with respect to transverse vibrations (Aramaki et al. 2007) according to the equation given by Brancheriau et al. (2006):

$$\text{tg } \delta = \frac{\alpha_1}{\pi f_1} \quad \text{Eq. (13)}$$

2.3.1.2 Parameters of vibration tests

The analysis of the signal, the selection of the natural frequencies of vibration and the estimates of the E_F , G , E_L and $\text{tg } \delta$ were performed using the software BING ® (CIRAD, Montpellier, France, version 9.1.3). The sampling frequencies of the signal were 78,125 Hz and 39,062 Hz for longitudinal and flexural vibration, respectively. The spectral acquisition was carried out by using 32,768 points for each test.

2.3.2 Static bending test

The modulus of rupture (MOR) of the clearwood specimens were tested using an electromechanical universal testing machine (Adamel Lhomargy, model DY 36), of 100 kN capacity in traction-compression.

For 4-point bending test, the specimens were tested according to an adaptation of the procedure ASTM D143-94 of the (ASTM 2007) standard. The span between lower supports was 320 mm; the distance between two loading points was 160 mm (1 free and 1 fixed); the diameter of roller bearings was 60 mm; and the test was conducted at a rate of 0.08 mm/s. Figure 16 presents the schema for four-point statistic bending test. The proportional limit, ultimate load, and deflection were obtained from load-deflection curves; and the MOR was calculated as follows:

$$MOR_{4p} = \frac{3 \times F \times (L - a)}{2 \times b \times d^2} \quad (\text{Eq. 14})$$

where F is the load (force) at the fracture point, L is the length of the support span, a is the distance between the 2 loading points, b is the width and d is the thickness of the wood specimen.

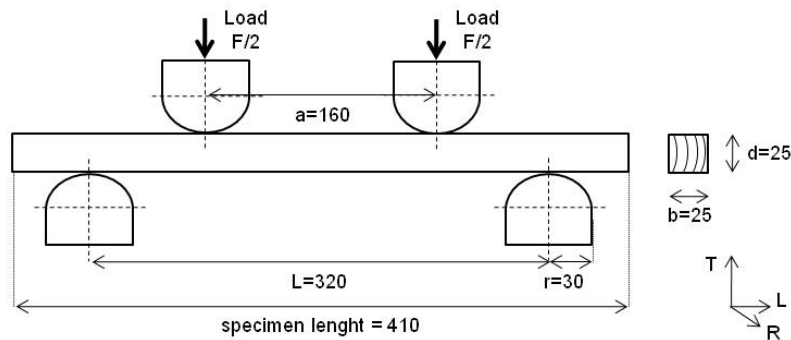


Figure 16 - Schema for four-point static bending test

For 3-point bending test, the specimens were tested according to an adaptation of the procedure ASTM D143-94 of the (ASTM 2007) standard. The proportional limit, ultimate load, and deflection were obtained from load-deflection curves; and the MOR was calculated as follows:

$$MOR_{3p} = \frac{3 \times F \times L}{2 \times b \times d^2} \quad (\text{Eq. 15})$$

where F is the load (force) at the fracture point, L is the length of the support span, b is the width and d is the thickness of the wood specimen. Figure 17 presents the schema for three-point static bending test.

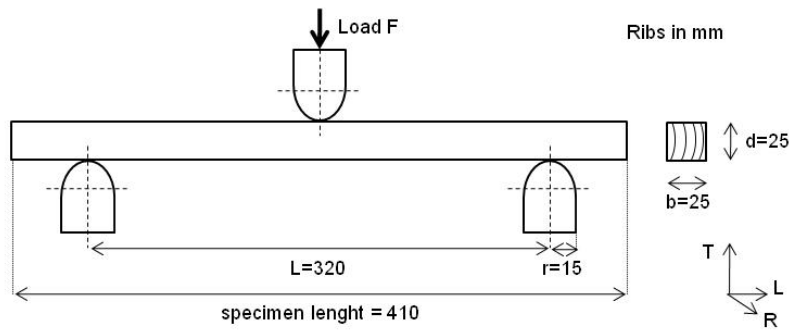


Figure 17 - Schema for three-point static bending test

2.3.3 Basic density and shrinkage of wood

The basic density and the shrinkage of the wood samples were measured simultaneously. The small wood samples (in most of cases measuring 25 mm × 25 mm × 25 mm) were removed from the intact wood of the specimens used in bending tests. These small wood samples were used for basic density (ρ) and shrinkage (δ_{rd}) measurements, which was determined by the ASTM D2395 (ASTM 2002) procedures. The formulas for calculating the basic density and shrinkage are given as follows:

$$\rho = \frac{\text{oven - dried weight}}{\text{green volume}} \quad (\text{Eq. 16})$$

$$\delta = \frac{\text{initial length} - \text{final length}}{\text{final length}} \times 100 \quad (\text{Eq. 17})$$

The green volume of a piece of wood was determined by water displacement according to the principle of Archimedes. The samples were first soaked in water to ensure that water is not taken up during the immersion process. An experimental dispositive was used for measuring the green volume of the samples (Figure 18 A).



Figure 18 - Experimental dispositive for measuring the green volume of the samples (A) and the sample dimensions (B) (source: personal image)

Then, a digital dispositive (Figure 18 B) was used for precisely measuring the sample dimensions of the saturated samples immediately after measuring the green volume. After determining the green volume, the samples were oven-dried at 103°C. The time necessary for drying depends on the size of the samples and also on the capacity of the oven. The digital dispositive was used again for precisely measuring the sample

dimensions of the oven-dried samples immediately before measuring their dry weight. Radial (δ_{rd}) and tangential (δ_{tg}) shrinkage was determined in three conditions: (i) from the oven-dry (0%) condition to equilibrium moisture content - EMC (~14%); (ii) from the EMC to the green (100%) condition and (iii) from oven-dried to green condition.

2.3.4 X-ray diffraction

All X-ray diffraction data were collected on a diffractometer (Gemini-S, Agilent Technologies, Yarnton, UK) with CuK α radiation (Figure 19). Images were integrated between $2\theta = 21.5^\circ$ and 23.5° along the whole 360° azimuthal interval to plot the intensity diagram of the (200) plane. An automatic procedure allowed the detection of the 200 peaks and their inflexion points. The T parameter, as defined by Cave (1966), was measured as the half distance between intersections of tangents at inflexion points with the baseline. The results are given as the mean of values obtained for the two 200 peaks. As shown by Cave (1966), T parameter is affected by the cross-sectional shape of the cells. Thus, as also reported by Yamamoto et al. (1993) and latter Ruelle et al. (2007), the corrective factor proposed by Cave (1966) cannot be used for all species but need to be calibrated specie by specie; However, their works show that the T parameter allows comparison within a specie which is the purpose of our study. In this thesis, the cross-sectional shape of the cells was considered to remain constant enough from pith to bark allowing comparison with a single T parameter within the species.



Figure 19 - X-ray diffractometer device with CuK α radiation used for measuring XRD patterns (A), detail of the specimen holder (B) and the mini-circular machine used for cutting samples (C) (source: personal image)

Two methods were applied in order to estimate the MFA's based on their X-ray diffraction pattern, namely: (i) MFA_C for the values estimated by the Cave (1966) formula and (ii) MFA_Y for estimations using formula proposed by Yamamoto et al. (1993) These formulas give an estimation of the mean MFA of woods based on their T value and are given by:

$$(i) MFA_C = 0.6 \times T \quad (Eq. 18)$$

$$(ii) MFA_Y = 1.575 \times 10^{-3} \times T^3 - 1.431 \times 10^{-1} \times T^2 + 4.693 \times T - 36.19 \quad (Eq. 19)$$

Three X-ray diffraction profiles were recorded on three points of each sample (Figure 14). The MFA estimates using these two formulas had a correlation of 0.97. The error of the measure of T parameter was estimated at 3%.

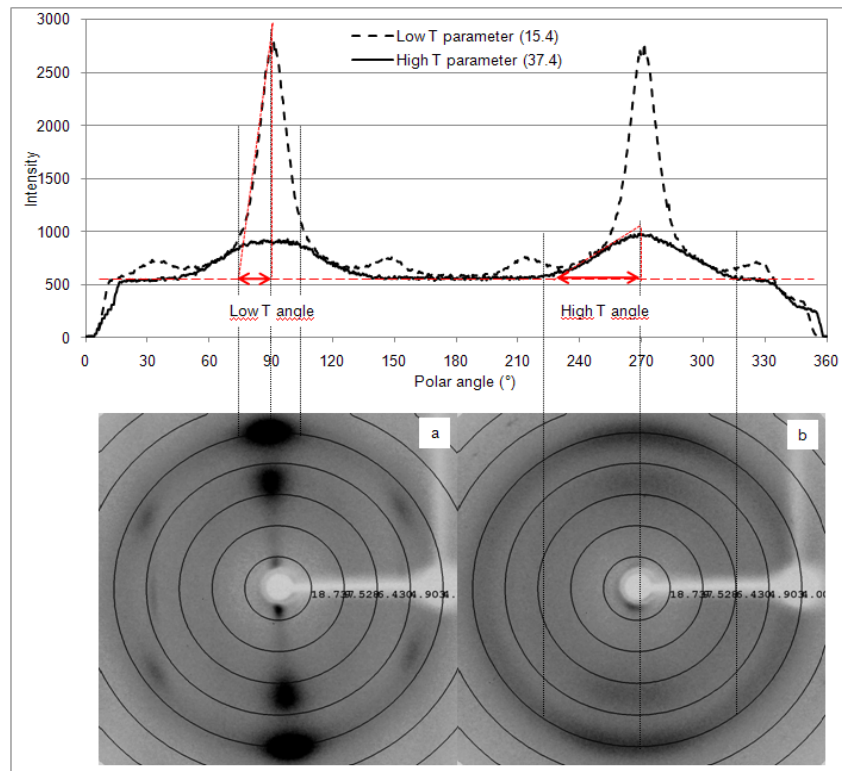


Figure 20 - X-ray scattering patterns recorded in 2 mm tangential sections of *Eucalyptus* samples with low (a) and high (b) T parameter

2.3.5 Wet-lab chemistry

The chemical analyses were conducted by the Biological Chemistry Laboratory at INRA-Agro ParisTech. All the samples were subjected to an exhaustive extraction in a soxhlet apparatus with toluene:ethanol (2/1, v/v) ethanol, and then water in order to eliminate all the extractives that could interfere with the lignin analyses. The Klason lignin (KL) and acid-soluble lignin (ASL) were determined from the extractive-free dried material (300 mg of “fine” powder which particle size less than 0.5 mm) according to the standard method (Dence 1992). The ratio between syringyl (S) and guaiacyl (G) units was performed on the extractive-free dried material by thioacidolysis, whereupon the method previously described by (Lapierre et al. 1995). Chemical analyses were performed in duplicate for the 60 samples.

2.3.6 NIR spectroscopy

Bruker spectrophotometer (model Vector 22/N, Bruker Optik GmbH, Ettlingen, Germany) was used in the diffuse reflectance mode (Figure 21). This Fourier transform spectrometer is designed for reflectance analysis of solids with an integrating sphere which measures the diffuse reflected light on a 150 mm² spot. This integrating sphere collects light from all angles; thus, the effects of wood texture and other non-homogeneities are minimized. It also practical that the sphere is "upward looking", with a window on top of the sphere. A sintered gold standard was used as background. NIR spectral analysis was performed within the 12,500-3,500 cm⁻¹ range at 8 cm⁻¹ resolution (each spectrum consisted of 2,335 absorption values).

Each spectrum was obtained with 32 or 64 scans and then means were calculated and compared to the standard in order to obtain the absorption spectrum of each sample. Thus, one spectrum is the mean of 32 or 64 scanning. In some cases, more than one spectrum was measured per sample and they were averaged into a single NIR spectrum. For solid woods, NIR spectra were recorded directly on the transversal and/or longitudinal wood surfaces while for wood meals, NIR spectra were also collected using a 50 mm spinning cup module (Figure 21 B).

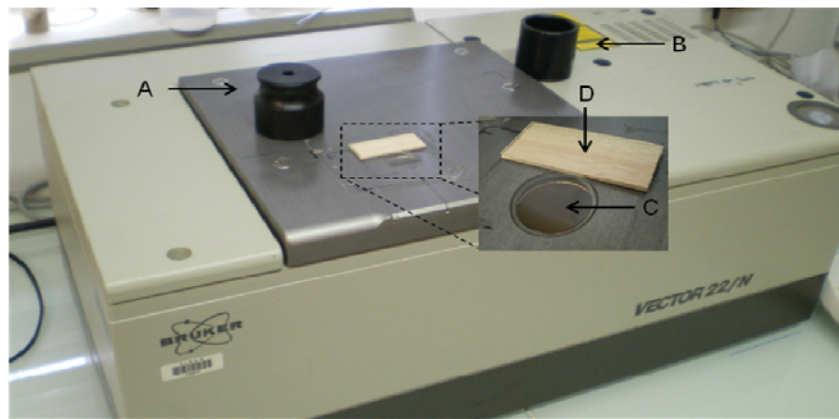


Figure 21 - NIR spectrophotometer used for measuring diffuse reflectance of wood samples showing the sintered gold standard (A), cup module for measuring NIR spectra from grounded wood (B), window for NIR spectra scanning - 10 mm of diameter (C) and 2-mm radial section of wood (D) (source: personal image)

2.3.7 Resume of wood traits measurements

Table 8 and Table 9 list the growth and wood traits measurements, the methods used for determine them, the dimension of the samples and the number of observations for each trait of the trees and wood samples.

Table 8 - Resume of growth and wood traits measurements, methods, sample dimension and number of observations of the trees from Clonal test

Trait	Method	Samples	N
C	Tape-measure in field	Tree (at 1.3 m)	150
H	Tape-measure in field	Tree	150
ρ_{sp}	Caliper / balance	Specimen (410 mm x 25 mm x 25 mm)	327
f_{Lsp}	Resonance	Specimen (410 mm x 25 mm x 25 mm)	334
E_{Lsp}	Resonance	Specimen (410 mm x 25 mm x 25 mm)	334
E'_{Lsp}	Resonance	Specimen (410 mm x 25 mm x 25 mm)	334
$tg \delta_{Fsp}$	Resonance	Specimen (410 mm x 25 mm x 25 mm)	141
f_{IFsp}	Resonance	Specimen (410 mm x 25 mm x 25 mm)	334
E_{Fsp}	Resonance	Specimen (410 mm x 25 mm x 25 mm)	334
E'_{Fsp}	Resonance	Specimen (410 mm x 25 mm x 25 mm)	334
G_{Fsp}	Resonance	Specimen (410 mm x 25 mm x 25 mm)	334
MOR4p	Static test	Specimen (410 mm x 25 mm x 25 mm)	224
MOR3p	Static test	Specimen (410 mm x 25 mm x 25 mm)	137
ρ_s	Balance (immersion)	Small sample (25 mm x 25 mm x 25 mm)	225
Shrinkage	Caliper	Small sample (25 mm x 25 mm x 25 mm)	225
MFA	X-ray diffraction	Radial section (25 mm x 25 mm x 2 mm)	165 + 225

Table 9 - Resume of growth and wood traits measurements, methods, sample dimension and number of observations of the trees from Progeny test. Chemical properties were done in duplicate

Trait	Method	Samples	N
C	Tape-measure in field	Tree (at 1.3 m)	348
H	Tape-measure in field	Tree	348
KL	Klason lignin	Wood powder 0.5 mm	60 (x 2)
S/G	Thioacidolysis	Wood powder 0.5 mm	60 (x 2)
D (ρ)	Balance (immersion)	Wood sample (15 mm x 20 mm x 20 mm)	190
MFA	X-ray diffraction	Tangential section (30 mm x 20 mm x 2 mm)	175

2.4 STATISTICAL ANALYSIS

2.4.1 Descriptive statistics and correlations

The descriptive statistic, bivariate correlations, analysis of variance and the comparison between means were performed using SPSS statistics software (SPSS Inc., version 17.0, Chicago, IL). The parameters of each analysis are given in the corresponding Tables.

2.4.2 Developing NIR spectroscopy models

Principal component analysis (PCA) and Partial least squares (PLS) regression analyses were performed using the Unscrambler software (CAMO AS, version 9.7, Norway).

The main advantage of PLS method is their ability to compress the relevant spectral information into a few latent variables; the orthogonality between these variables ensures the stability of the obtained model (Jouan-Rimbaud et al. 1996). In order to analyze NIR spectra information, PLS regression is of particular interest because it can analyze the data strongly collinear (correlated), with noise, with many X-variables (NIR spectra), and also, simultaneously, several variables can shape-response Y (Wold et al. 2001). PLS-R analyses were used to describe the relationship between the data sets obtained from NIR spectra and wood properties. First derivatives (13-point filter and a second order polynomial) and second derivatives (25-point filter and a third order polynomial) were applied on the NIR spectral data by the Savitsky and Golay (1964) algorithm to enhance the quality of the calibrations. In many cases, the NIR spectra were treated using standard normal variate (SNV) transformations. The PLS-R calibrations were performed in full cross-validation mode with a maximum of twelve latent variables (LV). The final number of LVs adopted for each model corresponded to the first minimal residual variance and the outlier samples were identified from the Student residuals and leverage value plot analyses. The Martens' uncertainty test (Westad and Martens 2000) was used to select the wavenumbers with regression coefficients significantly different of zero in order to develop more robust and reliable PLS models. To compare calibration and validation, the following statistics were examined: (i) Coefficient of determination of calibration set (R^2c), cross-validation set (R^2cv) or prediction set (R^2p); (ii) Root mean square error of calibration (RMSEC), cross-validation (RMSECV) or prediction (RMSEP); (iii) Ratio of performance to deviation (RPD) and (iv) Number of latent variables (LV). The general formulas for RMSEC, RMSECV and RMSEP are given in Burns and Ciurczak (2008) and can be calculated as follows:

$$RMSEC = \sqrt{\frac{\sum_{i=1}^N (\hat{y}_i - \hat{y}_i^2)}{N - A - 1}} \quad \text{Eq. (20)}$$

$$RMSECV = \sqrt{\frac{\sum_{i=1}^N (\hat{y}_{CV_i} - \hat{y}_i^2)}{N}} \quad \text{Eq. (21)}$$

$$RMSEP = \sqrt{\frac{\sum_{i=1}^{N_p} (\hat{y}_i - \hat{y}_i^2)}{N_p}} \quad \text{Eq. (22)}$$

where the y_i 's are obtained by testing the calibration equation directly on the calibration (or cross-validation - y_{cv}) data, A is the number of latent variable, N is the number of samples of calibration set, N_p is the number of samples of the prediction set. RMSEC, RMSECV or RMSEP should be as low as possible whereas coefficient of determination should be high. The RMSEC statistic is a useful estimate of the optimal accuracy obtainable for a given set of wavelengths used to develop a calibration equation, while the calculation of RMSECV is a method useful for determining the “best” number of latent variables to use in building a calibration equation by cross-validation and it is an estimate of the RMSEP. The cross-validation (CV) method is based on an iterative (repetitive) algorithm that selects samples from a sample set population to develop the calibration equation and then predicts on the remaining unselected samples (Workman and Weyerwer 2007). RMSEP allows the comparison between NIR-observed predicted values and laboratory values (reference values) during the validation test with independent sample set.

The RPD value is the ratio of the RMSECV or RMSEP to the standard deviation (Sd) of the cross-validation or validation sample set and can be calculated as follows:

$$RPD = \frac{Sd}{RMSE} \quad \text{Eq. (23)}$$

This statistic provides a basis for standardizing the RMSECV (Williams and Sobering 1993) and makes possible a comparison of different calibration parameters such as spectral information obtained from different wood faces. According to Fujimoto et al. (2008), the higher the RPD index the more reliable is the model.

2.4.3 Genetic parameter estimation

2.4.3.1 Progeny test

Quantitative genetic analysis was performed with ASReml version 2.0 (Gilmour et al. 2005). Growth, lignin content, syringyl to guaiacyl ratio, wood density and microfibril angle were normally distributed. Each trait was analyzed independently (univariate analysis) to estimate the variance components by using an individual (animal) model proposed by Mrode (2005). The following mixed linear model was considered:

$$y = X.b + Z.a + e \quad (\text{Eq. 24})$$

where y is the vector of observations, b is the vector of fixed effects (in our case the mean value of the trait in the population), a is the vector of genetic effects (individual additive genetic values), e is the vector of residuals and X and Z are the incidence matrices linking observations to the effects.

The random effect fits a normal distribution whose parameters were

$$E \begin{bmatrix} a \\ e \end{bmatrix} = \begin{bmatrix} 0 \\ 0 \end{bmatrix} \quad \text{and} \quad \text{Var} \begin{bmatrix} a \\ e \end{bmatrix} = \begin{bmatrix} G & 0 \\ 0 & R \end{bmatrix} \quad (\text{Eq. 25})$$

The variance-covariance matrices were defined as follows:

$$G = A.\sigma^2_A \quad (\text{Eq. 26})$$

$$R = I.\sigma^2_e \quad (\text{Eq. 27})$$

where A is the additive genetic relationship matrix computed from a pedigree file that takes into account all the relationships between the individuals, I is the identity matrix, σ^2_A the additive genetic variance and σ^2_e the residual variance. The variances associated to random effects were estimated by restricted maximum likelihood (REML method) using ASReml (Gilmour et al. 2005). As the variances are assumed to be independent, the total phenotypic variance σ^2_P was calculated as follows:

$$\sigma^2_P = \sigma^2_A + \sigma^2_E \quad (\text{Eq. 28})$$

Because, full-sib families were not replicated in the experimental design (the measurements were done in a single block), dominance and micro-environmental effects were confounded and cannot be properly estimated with this experimental design.

The narrow-sense heritability estimates were calculated as follows:

$$h^2 = \frac{\sigma^2_A}{\sigma^2_P} \quad (\text{Eq. 29})$$

Variances are not independent of the scale and the mean of the respective traits (Sokal and Rohlf 1995). Therefore, to compare the genetic and phenotypic variances of the different traits, a parameter measuring the genetic (CV_A) and phenotypic (CV_P) coefficient of variation was calculated as:

$$CV_{A_j} = \frac{100 \times \sigma_{A_j}}{\bar{x}} \text{ and } CV_{P_j} = \frac{100 \times \sigma_{P_j}}{\bar{x}} \quad (\text{Eq. 30})$$

where CV_{A_j} is the coefficient of additive genetic variation; σ_{A_j} is the square root of the additive genetic variance for the trait; CV_{P_j} is the coefficient of phenotypic variation; σ_{P_j} is the square root of the phenotypic variance for the trait and \bar{x} is the population mean for trait.

CV_{A_j} or CV_{P_j} expresses the genetic or phenotypic variance relative to the mean of the trait of interest and gives a standardized measure of the variance relative to the mean of the trait. The higher the coefficient of variation for a trait, the higher is its relative variation.

To estimate phenotypic (r_P), residual (r_E) and genetic additive (r_A) correlations between two traits (X and Y), were performed from a bi-variate analysis using the same individual model as for univariate analysis. r_P , r_E and r_A were estimated as follows:

$$r_P = \frac{Cov_P(x, y)}{\sqrt{\sigma_{Px}^2 \cdot \sigma_{Py}^2}} \quad (\text{Eq. 31})$$

$$r_E = \frac{Cov_E(x, y)}{\sqrt{\sigma_{Ex}^2 \cdot \sigma_{Ey}^2}} \quad (\text{Eq. 32})$$

$$r_A = \frac{Cov_A(x, y)}{\sqrt{\sigma_{Ax}^2 \cdot \sigma_{Ay}^2}} \quad (\text{Eq. 33})$$

Standard errors of h^2 , σ^2_A , σ^2_P , r_P , r_E and r_A were calculated with ASReml using a standard Taylor series approximation (Gilmour et al. 2005).

2.4.3.2 Clonal test

Quantitative genetic analysis was performed with R statistical software version 2.8.1 (R Development Core Team 2008). Circumference and height, wood density, modulus of elasticity and microfibril angle values were normally distributed. Each trait was analyzed independently (univariate analysis) to estimate the variance components by using an individual mixed linear model as following:

$$y = \mu + Clone + Site + Clone \times Site + \varepsilon \quad (\text{Eq. 34})$$

where μ is the mean value, *Clone* is the random genetic effect, *Site* is the fixed environmental effect, *Clone* × *Site* is random interaction effect and ε is the residual. The variances associated to random and fixed effects were estimated by restricted maximum likelihood (REML) analysis using the “nlme” package of R software (R Development Core Team 2008). As the variances are assumed to be independent, the total phenotypic variance was calculated as follows:

$$\sigma^2_P = \sigma^2_G + \sigma^2_{GxE} + \sigma^2_E \quad (\text{Eq. 35})$$

$$\sigma^2_P = \sigma^2_G + \sigma^2_E \quad (\text{Eq. 36})$$

where σ^2_P is the phenotypic variance, σ^2_G is the clonal variance, σ^2_{GE} is the clone by site interaction variance and σ^2_E is the environmental (error) variance. The broad-sense heritability estimates were calculated as follows:

$$H^2 = \frac{\sigma^2_G}{\sigma^2_G + \sigma^2_{G \times E} + \sigma^2_E} \quad (\text{Eq. 37})$$

$$H^2 = \frac{\sigma^2_G}{\sigma^2_G + \sigma^2_E} \quad (\text{Eq. 38})$$

The choice of model (Eq. 27 or Eq. 28) was based on BIC values (Burnham and Anderson 2004). The model which yielded the lower BIC value was chose. In short, the wood traits were analyzed by the Equation 27 while the growth traits by the Equation 28.

NIR spectral heritability

NIR spectra were recorded from 12,500 to 3,500 cm^{-1} range at 8 cm^{-1} resolution. The NIR range from 8,910 from 5,350 containing 1,400 absorption values was selected. Each NIR spectrum was reduced along its wavenumber by a reduction factor of 5 producing a NIR spectrum containing 280 absorption values. As the NIR spectrum consisted of 280 wavenumbers, the same number of broad-sense NIR spectral heritability estimates was performed using the equation 37.

Surface plots

The 2-D plots presenting the spatial variation of wood traits and heritability estimates (Figure 39, Figure 40, Figure 41, Figure 45, Figure 46 and Figure 47) were developed using the library “grayplot” of the Scilab software (v.5.3.1). As NIR spectroscopic models were used to estimate wood traits on specific points along the tree stem. Thus, data were interpolated in order to create estimates in a whole tree making possible to build the cartography of wood traits.

Scripts for calculating genetic parameters using R

```
Data <- read.table("CNB150predNIR.csv", dec=".", sep="," , header=T)
Data$Site <- as.factor(Data$Site)
Data$Clone <- as.factor(Data$Clone)

## Estimating variance components
Resume <- NULL
Resumel <- NULL
for (i in 4:124){
Y <- Data[,i]
lme <- lme(Y~ 1 + Site, random=~1|Clone, data=Data, method="REML")
lme1 <- lme(Y~ 1 + Site, random=~1|Clone/Site, data=Data,
method="REML")
Resume <- c(Resume, list(lme))
Resumel <- c(Resumel, list(lme1))
Resume
Resumel

## For calculating BIC
Selection <- NULL
Selection1 <- NULL
for (i in 4:124){
Y <- Data[,i]
lme <- lme(Y~ 1 + Site, random=~1|Clone, data=Data, method="ML")
lme1 <- lme(Y~ 1 + Site, random=~1|Clone/Site, data=Data,
method="ML")
Selection <- c(Selection, list(lme))
Selection1 <- c(Selection1, list(lme1))
Selection
Selection1

## To display BIC results
Resultat <- NULL
for (i in 1:121){ lme0 <- Selection[[i]]
lme1 <- Selection1[[i]]
Resultat <- c(Resultat, list(anova(lme0, lme1)))}
Resultat
```

3 RESULTS AND DISCUSSION

3.1 Growth traits

Circumference at breast height (C) and commercial height (H) were measured before harvesting the trees. Table 10 shows the descriptive statistics of growth traits in 14-year-old *Eucalyptus urophylla* from progeny trial (BRG) in the Republic of Congo and in 6-year-old *Eucalyptus grandis* x *urophylla* from three clonal tests (CNB) established in Brazil.

Table 10 - Descriptive statistics of growth traits in 14-year-old *Eucalyptus urophylla* from progeny test and in 6-year-old *E. urophylla* x *grandis* from clonal test, including circumference at 1.3 meter height (C) and total height (H) by site and considering all samples

	Progeny test		Clonal test							
			Site 303 (0°)		Site 301 (20°)		Site 302 (40°)		Overall	
	C (cm)	H (m)	C (cm)	H (m)	C (cm)	H (m)	C (cm)	H (m)	C (cm)	H (m)
Mean	52.8	21.2	67.3	23.1	60.8	23.6	57.4	20.4	61.8	22.4
Sd	11.26	3.67	11.63	3.25	5.87	1.87	8.71	3.28	9.89	3.2
Min	24.0	7.8	45.0	16.1	49.5	17.3	42.0	14.8	42.0	14.8
Max	84.0	29.6	96.0	28.3	75.0	27	81.0	28.5	96.0	28.5
CV (%)	21.3	17.3	17.3	14.0	9.7	7.9	15.2	16.1	16.0	14.3
N	340	340	50	50	50	50	50	50	150	150

The range of variation for growth traits of the trees from progeny test (CV=21.3%) was higher than those from clonal tests (CV=16%). This result was expected because the genetic variation of a progeny test (where offspring of a range of progenitors are evaluated) is larger than the genetic variation of a clonal test (where the best offspring are vegetatively propagated). The environment effect on the growth rate of the trees from the clonal tests is presented in Figure 22.

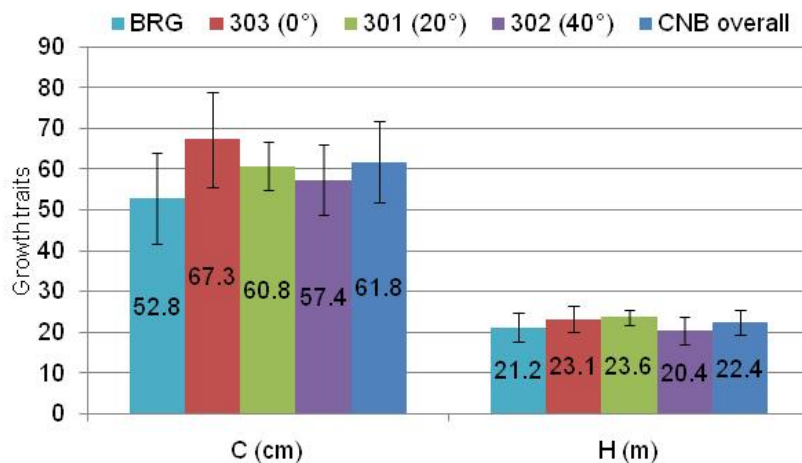


Figure 22 - Mean and standard deviation of circumference at breast height (C) and commercial height (H) for each site and considering all samples

While trees growing under optimal conditions (in this case, no terrain slope) produce biomass at high growth rates, trees grow up relatively slower at sites with high inclination (40°). The site 301, with 20° of inclination, presented the lower standard deviation while the site 303 (0°) had the higher variability in the growth traits. Multiple range tests for mean circumference and height by clone and by site are presented and discussed in the genetic studies section (Table 31, pg. 107).

On average, the *E. urophylla* trees from progeny trial (BRG) presented a mean circumference at 1.3 meters of 52.8 cm and 21.2 meters of height. The circumference of these trees were much lower than those reported by Cruz (2006) who evaluated 16-year-old *Eucalyptus urophylla* from Paraopeba (Brazil) with a mean circumference of around 110 cm and mean height of around 32 meters.

3.2 Wood phenotyping of progeny tests

3.2.1 Wood chemical composition

Table 11 shows the statistical summary of wet-chemistry analysis including the mean, minimum (Min) and maximum (Max) values of the results, and the coefficient of variation (CV) of wood of sixty *Eucalyptus urophylla* from progeny test. Analyses were performed in duplicate and had good reproductive values. The duplicates never showed differences at the 5% significance level.

Table 11 - Descriptive statistic for Klason lignin (KL); acid-soluble lignin (ASL) and total lignin content (TL); syringyl to guaiacyl ratio (S/G); and extractive content (EXT) in 14-year-old *Eucalyptus urophylla* wood

	KL (%)	ASL (%)	TL (%)	S/G	EXT (%)
Mean	28.5	1.63	30.1	2.4	14.6
Sd	1.37	0.22	1.33	0.35	2.15
Min	25.1	1.14	26.95	1.7	11.2
Max	31.95	2.12	33.25	3.04	19.6
CV (%)	4.8	13.2	4.4	14.5	14.7
N	60	60	60	60	60

Because the delignification process requires energy and reagent consumption, trees presenting high lignin content are undesirable in plantations for pulp and paper. On the other hand, wood may have high lignin content for bioenergy purposes. Here, Klason lignin content varied from 25.1 to 31.95 percent but the coefficient of variation was small (4.8%). Acid-soluble lignin content varied in higher magnitude presenting CV of 13.2 percent and the S to G ratio ranged from 1.7 to 3.04. These results are compatible with those reported in similar studies on *Eucalyptus* genus. For instance, Brito and Barrichello (1977) investigated 7-year-old *E. urophylla* in Rio Claro (Brazil) with Klason lignin content of 23.6% and 11-year-old *E. urophylla* in Timor with 29.8 percent of Klason lignin content. Carvalho and Nahuz (2001) studying hybrids of 7-year-old *E. grandis* and *E. urophylla* reported woods with an averaged KL content of 22.4%. Alencar et al. (2002) found averaged levels of KL of 27.38% in 7-year-old *E. grandis* x *E. urophylla* hybrids. Gomide et al. (2005) reported total lignin content ranging from 27.5 to 30.5 percent, and acid-soluble lignin from 3.1 to 5.1% in *E. grandis* and *E. urophylla* clones.

The S/G ratio is an important parameter for tree breeders. High S/G is advantageous for pulping (Rodrigues et al. 1999) since every unit increase in the lignin S/G ratio would roughly double the rate of lignin removal (Chang and Sarkanen 1973). Here, the mean S/G was of 2.42 ranging from 1.67 to 3.13

(Table 11). The variation range is in agreement with those reported in the literature. For instance, Gomide et al. (2005) studied 7-year-old *Eucalyptus* reporting S to G ratio ranging from 2.1 to 2.8. Silva (2006) studied *E. grandis* and *E. urograndis* reporting averaged S/G values of 2.1 and 2.5, respectively and Yamada et al. (2004) investigated transgenic trees presenting mean S/G ratio of 2.8.

3.2.2 Microfibril angle and wood density

Microfibril angle and wood density were investigated. Tangential sections (2 mm of thickness) of wood were cut to evaluate the MFA by X-ray diffraction technique (Cave 1966) and the offcut small samples were used for wood density measurements. Figure 14 sums up the procedure of sample preparation and measurements. The samples taken close to the pith presents a “curvature effect” while the tangential sections taken near the bark, parallel to the growth ring, showed little or no “curvature effect”. The curvature effects are illustrated by dotted lines in Figure 23. This procedure was used to verify the influence of the curvature effect on the repeatability of the XRD measurements. The findings concerning these issues were presented and discussed in Hein and Brancheriau (2011) (**paper 3**).

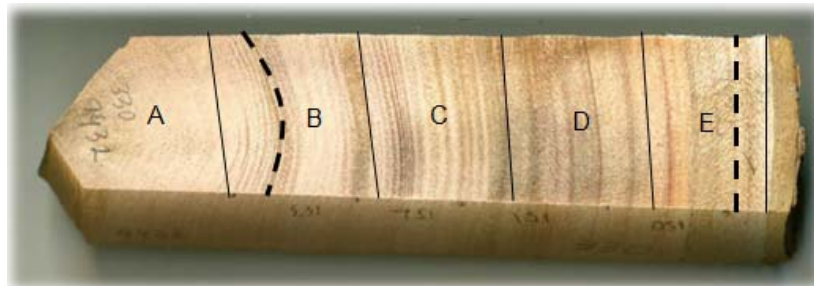


Figure 23 - Radial strips showing curvature effect by dotted lines and classes by continuous lines

The approach for conversion of the X-ray diffractometer pattern to microfibril angle was based on the *T* parameter and on Yamamoto’s formula (Yamamoto et al. 1993). Table 12 presents the descriptive statistics for wood basic density, *T* parameter and microfibril angle determinations in *Eucalyptus* wood. The variation range of wood density (CV of ~14%) and microfibril angle (CV of ~17%) are crucial for *Eucalyptus* breeding programs whereas the tree breeders are interested in selecting progenies or clones presenting the most appropriate phenotype.

Table 12 - Descriptive statistics, including average, standard deviation (Sd), minimum (Min), maximum (Max) and coefficient of variation (CV) for basic density (ρ), *T* parameter and microfibril angle (MFA) measurements in 14-year-old *Eucalyptus urophylla* wood

	Average	Sd	Min	Max	CV (%)	N
ρ (kg m ⁻³)	547	79	372	742	14.4	175
<i>T</i> parameter (°)	19.7	2.87	14.6	28.7	14.6	175
MFA (°)	12.5	2.14	7.7	19.7	17.1	175

The samples were sorted by radial position in ascending order of their relative radial position. The variation on MFA and density as a function of the relative distance from the pith to bark for 14 radial strips is given in Figure 24. The samples from class B (from 20 to 40% of radial distance) represent the wood formed at the 4th to 6th years while samples from class E (from 80 to 100%) correspond to the wood developed at approximately the 12th, 13th and 14th years. Due to the small dimension of some radial strips, only two or three tangential sections for MFA, and small wood samples for density were removed and these data were not presented in Figure 24.

The patterns of radial variation of these wood traits are in accordance with those reported in the literature, ie, MFA decrease from juvenile wood to mature wood in *Eucalyptus*. For instance, Evans et al. (2000), reported variation in MFA from 20° near the pith to 14° near the bark in 15-year-old *Eucalyptus nitens*. Lima et al. (2004) investigated 8-year-old *E. grandis* × *E. urophylla* clones reporting that its MFA decreased slightly from pith to bark. The radial variation of these wood traits is important, because such properties are targeted in breeding programs to distinguish improved varieties according to their variance; however, frequently, the within-tree variability is higher than the between-trees variability.

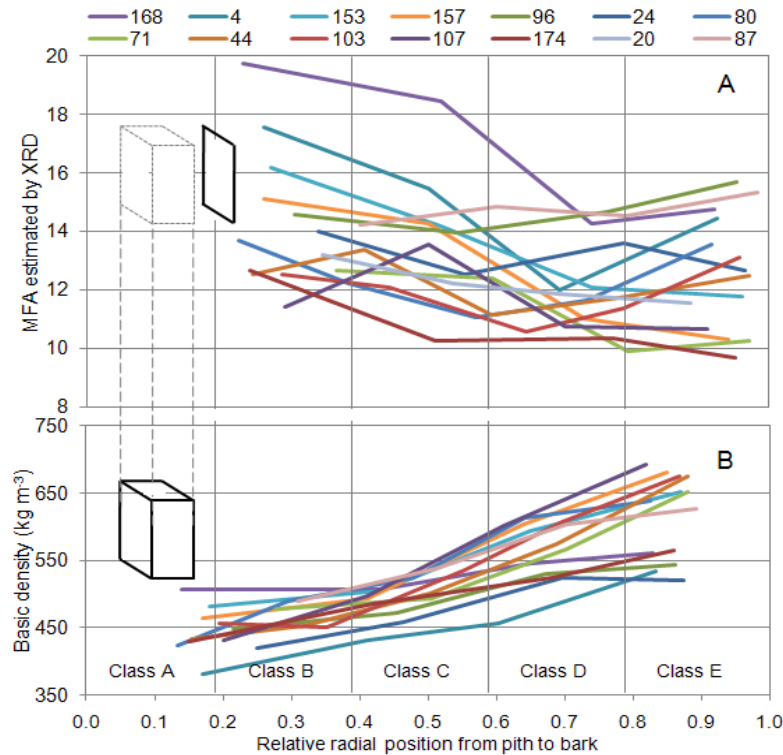


Figure 24 - Radial variation of MFA (A) and basic density (B) in 14-year-*Eucalyptus urophylla* wood for radial strips (N=14)

The mean MFA values of each class (B to E) were not statistically different by the Tukey test at $p > 0.01$ while the mean basic density of wood significantly increased in a linear way from pith to bark (Table 13). Thus, the radial variation of MFA in *Eucalyptus* wood is not statistically evident, because the large MFA variability between trees results in a large standard deviation within each class (for instance, in class B the MFA ranged from ~11° to ~19°).

The trends in radial variation of MFA and density (Table 13) are in accordance to those of Lima et al. (2004), who reported that the microfibril angle of 8-year *Eucalyptus* seemed to decrease slightly from pith to bark in a non-linear fashion, but not statistically significant. However, a decrease of MFA values from pith to bark can be clearly observed when each radial strip was analysed. Figure 24 reveals that, on average, the microfibril angles appears to be higher near the pith of the discs (Class B), decreasing radially towards to the bark (Class E). Such pattern of MFA variation occurred most frequently, but among the various strips we used (40), different trends could be observed. For instance, the MFA of samples 80, 87, 96, 103 and 153 slightly increased near to the bark. For basic density of wood, a linear increase from pith to bark was found (Figure 24), even if the variability of density between trees was taken into account.

Table 13 - Description of tangential sections from the radial wood strips, their influence on the T parameter measurements and the radial variation of MFA and basic density in 14-year-old *Eucalyptus urophylla* wood. The relative radial position is presented within squared brackets while the range of variation of traits is presented within parentheses

Classes	A [0-20]	B [21-40]	C [41-60]	D [61-80]	E [81-100]
Curvature effect	very strong	strong	moderate	weak	none
T_1	-	20.3 ^a (16-27)	19.0 ^a (16-24)	19.1 ^a (15-26)	19.3 ^a (15-25)
T_2	-	20.3 ^a (16-26)	19.5 ^a (16-25)	19.3 ^a (15-28)	19.4 ^a (15-24)
T_3	-	19.5 ^a (16-22)	19.4 ^a (16-27)	19.6 ^a (15-29)	19.4 ^a (15-25)
ρ	-	450 ^a (370-520)	507 ^b (430-620)	564 ^c (420-740)	622 ^d (520-700)
% of samples	-	16.6	26.9	26.3	30.3

Means followed by the same letter are not significantly different at 1% level by the Tukey test.

3.2.3 Effect of wood chemical components on MFA

Based on studies on hardwood and softwood tissue reaction, which possess special features in cell wall composition, one may assume that cellulose MFA and lignin content in the S_2 layer could be generally related to each other (Jungnikl et al. 2008). In softwoods, Via et al. (2009) showed that MFA and lignin content are associated, at least in some way. In hardwoods, this relationship has been observed in a range of wood species (Barnett and Bonham 2004) both in reaction and normal wood, but some studies have reported no correlations between MFA and chemical components. For instance, Baillères et al. (1995) investigated hybrids of *Eucalyptus* clones from Congo demonstrating clearly that decreases in microfibril angles of cellulose are linked to the decrease in lignin content and increase in syringyl to guaiacyl ratio. On the other hand, Jungnikl et al. (2008) examined this correlation in *Picea abies* tissues finding any correlation, neither for the individual tissue types nor for the compiled data of all tissues.

In the present study, MFA showed a low coefficient of correlation with lignin content predicted by NIR-based model. We applied our NIR-based model for klason lignin content (Hein et al. 2010d, **paper 4**) in the 175 tangential sections. The correlation between the NIR-based estimates of lignin content and XRD measured microfibril angle values was 0.4. It is important to note that this klason lignin model was calibrated from NIR spectra measured on the transverse face of the wood discs (such discs were surfaced using a plane). Phenotypic, residual and genetic relationships between Klason lignin and microfibril angle are presented and discussed within the item 3.5.3 at page 103.

3.3 Phenotyping the wood of clonal tests

3.3.1 Kiln-dried scantlings

The air-dried scantlings were kiln-dried at 14% (nominal) under soft condition during two weeks. Table 14 lists the descriptive statistics of the kiln-dried density and dynamic properties of the kiln-dried at 14% scantlings of *Eucalyptus* wood.

For kiln-dried scantlings there was no statistically significant difference between averaged values of longitudinal and flexural elastic modulus (Table 14). Flexural vibrations are assumed to be more sensitive to the presence of knots and small cracks in the scantlings than longitudinal vibrations, especially for air-

dried scantlings. Some key factors affecting the transverse vibration were reported by Murphy (2000) and possibly influenced our results. In addition to these factors, according to Burdzik and Nkwera (2002) no elasticity measurement method leads to the calculation of pure modulus of elasticity in bending, due to the presence of a shear component in the deflection of the specimen, except for the region of the specimen between the two loading points of 4-points bending tests. However, in this study, the differences between E_L and E_F did not come about from shear effects on flexural vibration, which could bias the estimation, because the model we used to estimate the elastic modulus takes into account the shear effect. Here, we applied the solution proposed by Bordonné (1989) to the Timoshenko (1921) motion equation to the first four vibration modes of the scantlings.

Table 14 - Descriptive statistics of dynamic properties of the kiln-dried scantlings of 6-year-old *Eucalyptus grandis* x *E. urophylla*, including kiln-dried density (ρ_{14} , kg m⁻³), first resonant frequency (f_{i14} , Hz), elastic modulus (E_{14} , MPa), specific modulus (E'_{14} , E/ ρ), loss tangent ($\text{tg } \delta_{14}$, 10⁻³) and shear modulus (G_{14} , MPa) estimated by longitudinal (L) and flexural (F) vibration tests

	ρ_{14}	f_{iL14}	E_{L14}	E'_{L14}	$\text{tg } \delta_{L14}$	f_{iF14}	E_{F14}	E'_{F14}	G_{F14}
Mean	548	1,618	12,825	23.43	7.74	98.27	13,278	24.3	693.69
Sd	65.8	346	2,565	2.98	1.74	49.04	2740	3.32	207.6
Min	383	1,027	7,432	15.6	4.45	42.9	6,555	13.8	123
Max	776	3,414	21,236	32.5	18.7	441.1	23,941	35.5	1,833
CV (%)	12	21.4	20	12.7	22.4	49.9	20.6	13.7	29.9
N	410	410	410	410	328	410	410	410	378

The wood density of the kiln-dried scantlings varied from 518 to 573 kg m⁻³ according to the site where they come from. As trees from site 303 (no inclination) grew up faster than those from site 302 (40 degrees of inclination), the results presented in Figure 25 lead us to suppose that trees developing at low growth rates produce high wood densities while trees growing at high growth rates will result in low dense woods, at least, from a phenotypic point of view. Thus, the differences in mean wood density between sites reflect the effect of growth conditions on biomass production.

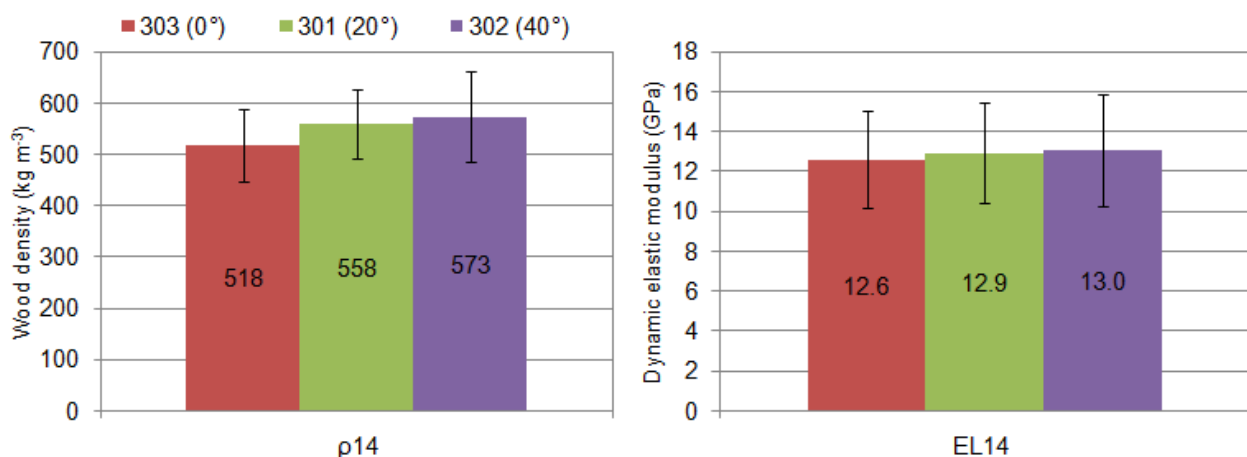


Figure 25 - Mean and standard deviation values of kiln-dried wood density and dynamic elastic modulus in kiln-dried scantlings for each site

The environmental effect on the dynamic elastic modulus on longitudinal vibration test is not clear (Figure 25). Because the elastic properties greatly varied between clones, the standard deviations were high and there were no significant differences between sites according to Tukey test.

Further details are described within the genetic studies section (Table 49, pg. 143) where multiple range tests for density of wood and for dynamic elastic modulus on longitudinal vibration by clone and by site are presented and discussed.

3.3.2 Wood specimens from scantlings

From the 410 scantlings, 160 were selected among the best ones (i.e. annual rings well oriented, free of large cracks etc) and surfaced on the plane machine; beams were cut from them and trimmed to nominal cross-section of 25 mm x 25 mm using a circular saw machine. Then, clean, small specimens measuring 25 mm x 25 mm x 410 mm were cut from the beams. Table 15 lists the descriptive statistics of the dynamic properties and densities of the 334 specimens (sp) of *Eucalyptus* wood. The loss tangent values of the scantlings were calculated from longitudinal test while the loss tangent of the specimens derived from flexural vibrations. As the software alerts us about imprecise estimations, only 141 values for $\text{tg } \delta_{\text{Fsp}}$ were used.

Table 15 - Descriptive statistics of dynamic properties of the clearwood specimens of 6-year-old *Eucalyptus grandis* x *urophylla*, including air-dried density (ρ_{sp} , kg m^{-3}), resonant frequency (f_{Lsp} , Hz), elastic modulus (E_{sp} , MPa), specific modulus (E'_{sp} , E/ρ), loss tangent ($\text{tg } \delta_{\text{Fsp}}$, 10^3) and shear modulus (G_{sp} , MPa) estimated by longitudinal (L) and flexural (F) vibration tests

	ρ_{sp}	f_{Lsp}	E_{Lsp}	E'_{Lsp}	$\text{tg } \delta_{\text{Fsp}}$	f_{Fsp}	E_{Fsp}	E'_{Fsp}	G_{Fsp}
Mean	518	6,174	13,391	25.66	7.33	721.69	12,495	24.02	693.68
Sd	59.05	395	2,540	3.52	1.01	42.52	2,356	3.082	168.5
Min	362.4	4,918	6,522	16.27	5.71	567.4	5,930	14.05	344
Max	708.3	6,945	20,785	32.43	10.5	805.9	18,732	30.61	1,499
CV (%)	11.4	6.41	18.97	12.53	13.8	5.89	18.8	12.81	24.3
N	334	334	334	334	141	334	334	334	334

Wood traits of 6-year *Eucalyptus* specimens from Clonal tests strongly varied: coefficient of variation ranging from ~6 (for resonance frequencies) to ~20% (for moduli of elasticity). The air-dried density of the wood specimens ranged from ~350 to ~700 kg m^{-3} . Figure 27 presents the air-dried density of the wood specimens (ρ_{sp}) and the basic density of the small wood samples taken from specimens (ρ_{s}) by site, highlighting the environmental effect on this trait. It appears that trees growing under plan sites produce low density woods, but this pattern of wood density variation seems to be more linked to the growth rate. The results indicate that trees grow up faster in plan sites and their densities are lower. The correlations between these wood traits are presented within the section 3.3.4 (pg. 87).

3.3.2.1 Air-dry density

The effect of growth rate on wood properties, especially on wood density, has been studied intensively (Zobel and Van Buijtenen 1989; Zobel and Jett 1995). According to Zobel and Jett (1995) the growth rate and wood density show little or no meaningful relationship in most of the conifers with dense wood, especially hard pines and in most diffuse-porous hardwoods. However, there were contradictory reports about the relationship between growth rate and wood properties in the hardwoods. A negative relationship between growth rate and wood density has been reported in several softwood genera such as *Picea* (Herman et al. 1998; Dutilleulet al. 1998; Petty et al. 1990) and *Pinus* (Zamudio et al. 2002; Kärenlampi and Riekkinen 2004). Examining the relationships of wood density with growth rate in 16 timber species

(including soft- and hardwoods), Zhang (1995) pointed out that compared to softwoods, density of hardwoods is remarkably less influenced by growth rate.

For tree breeding programs and industrial applications, the correlation between growth rate and density is of great importance. If increased growth rate results in low-density wood, it also means poor wood quality which limits the suitability of raw material for high quality products. On the other hand, it may also be possible to select trees with both high growth rate and high wood density for breeding.

3.3.2.2 Modulus of elasticity

The flexural vibrations are influenced by the shear effect while the longitudinal ones are affected by the Poisson effect when the length to thickness ratio of the beams is small (Rayleigh 1877). Early studies on dynamic tests of wood (Hearmon 1961; Ilic 2001) showed important differences between E_L and E_F ; however, when Ilic (2001) applied the Timoshenko correction, the difference between E_L and E_F varied from 13% (for uncorrected E_F) to 1.1% (for corrected E_F). Table 15 show that average value of E_{Lsp} (13,391 MPa) was higher than E_{Fsp} (12,495 MPa). In this study, the differences between E_L and E_F did not come about from shear effects on flexural vibration because the model we used to estimate the E_F takes into account the shear effect. Here, the solution proposed by Bordonné (1989) to the Timoshenko (1921) motion equation was applied to the first four vibration modes of the wood beams. The Poisson effect in longitudinal vibrations is negligible because the length to thickness ratio of the scantlings and small specimens was superior to 30 and 15, respectively. Additional factors affecting the flexural vibrations were reported by Murphy (2000).

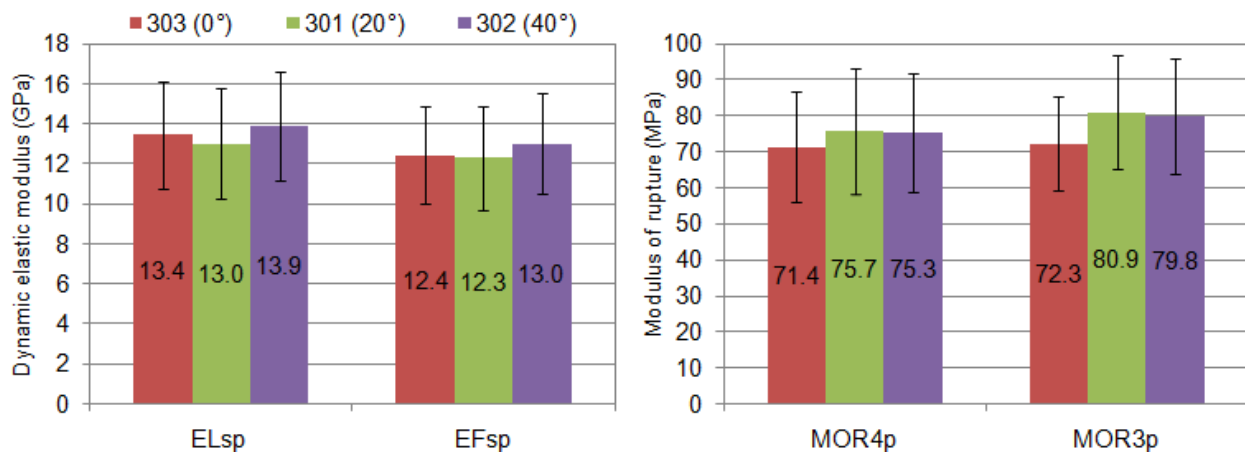


Figure 26 - Mean and standard deviation values of longitudinal and flexural dynamic elastic modulus and modulus of rupture obtained in 4- and 3-points bending test in small samples of *Eucalyptus* for each site

Figure 26 shows the statistics of longitudinal and flexural dynamic elastic modulus by site. Although the wood stiffness is related with its density, the pattern of variation of elastic modulus according to the site is different from that presented for wood density (Figure 27). Since the standard deviations were high, there were no differences between sites for wood stiffness; however there was significant effect for clones. These findings (Figure 26) are discussed within the genetic studies section (Table 39, pg. 116) where multiple range tests for wood stiffness by radial position, by clone and by site are presented.

3.3.2.3 *Modulus of rupture*

After the dynamic tests, the twin wood specimens were tested in a 4- and 3-points bending test using a universal testing machine. Table 16 lists the modulus of rupture (MOR) and force at rupture point (Fmax) in 4- and 3-points bending test using 224 and 137 specimens, respectively.

Table 16 - Descriptive statistics of the 4- and 3-points bending test of the specimens of 6-year-old *Eucalyptus grandis* x *urophylla* wood, including force at rupture point (Fmax, N) and modulus of rupture (MOR, MPa)

	Fmax _{4p}	MOR _{4p}	Fmax _{3p}	MOR _{3p}
Mean	3,404	73.7	2,129	77.2
Sd	757	16.3	419	15.3
Min	1,207	25.4	1,149	42.3
Max	5,557	119.1	3,528	122.5
CV (%)	22.2	22.1	19.7	19.8
N	224	224	137	137

According to Brancheriau et al. (2002), contrary to 3-points bending, a 4-points loading does not induce a shear effect between the loading points. Moreover the indentation of the supports and the loading head does not influence the deflection measurement.

The results using the twin specimens shows no significant differences between MOR obtained by 4- and 3-points bending tests; However, force at rupture point (Fmax) were significantly higher in 4-points (3,404 N) than in 3-points (2,129 N) bending tests. Figure 26 shows the modulus of rupture in 3- and 4-points bending test by site. Similarly to wood stiffness, there were no differences between sites for modulus of rupture.

3.3.3 Small wood samples

3.3.3.1 *Dimensional Stability*

Wood is dimensionally stable when moisture content is greater than the fibre saturation point (FSP). Below FSP wood changes dimension as it gains moisture (swells) or loses moisture (shrinks), because volume of the cell wall depends on the amount of bound water (Glass and Zelinka 2010). As an anisotropic material, wood shrinks (swells) most in the direction of the annual growth rings (tangentially) and about half as much across the rings (radially). Here, the radial and tangential shrinkage of wood samples is presented under three conditions: (i) from the oven-dried (0%) to the equilibrium moisture content (EMC) condition [0-EMC]; (ii) from the EMC to the green (100%) condition [EMC-100] and (iii) from oven-dried to green condition [0-100%]. Table 17 shows the descriptive statistics of the basic density and radial and tangential shrinkage of the small wood samples, taken from the wood specimens.

From the oven-dried condition to EMC, the wood samples swell around 1.2% and 1.8% radially and tangentially, respectively (Table 17). From EMC to the green condition, the wood samples swell around 3.5 and 5.9% in radial and tangential sense, respectively. In short, wood swell 4.8% (radially) and 7.8% (tangentially) from oven-dried to above FSP condition. Figure 27 shows the mean and standard deviation values of radial and tangential shrinkage from oven-dried to green conditions for each site. It seems that shrinkage is affected by growth rate or by density (since growth rate and density are correlated and

affected by site); however, the analysis of variance (GLM procedure) shows no difference of shrinkage between sites.

Table 17 - Descriptive statistics of basic density (ρ_s , kg m⁻³) and radial and tangential shrinkage (%) of the small samples of 6-year-old *Eucalyptus grandis* x *urophylla*

	ρ_s	radial shrinkage			tangential shrinkage		
		0-EMC	EMC-100	0-100	0-EMC	EMC-100	0-100
Mean	420	1.21	3.54	4.80	1.79	5.90	7.80
Sd	52.2	0.56	1.18	1.40	0.79	1.54	1.58
Min	288	0.10	1.23	1.75	0.04	1.94	3.24
Max	617	4.02	7.55	10.39	5.76	12.26	13.35
CV (%)	12.4	46.6	33.4	29.2	43.8	26.2	20.3
N	225	225	225	225	225	225	225

The combined effects of radial and tangential shrinkage can distort the shape of wood pieces because of the difference in shrinkage and the curvature of annual rings (Glass and Zelinka 2010). Thus, these dimensional changes are important because can result in warping, checking, and splitting of the wood decreasing utilization and economic value of wood products.

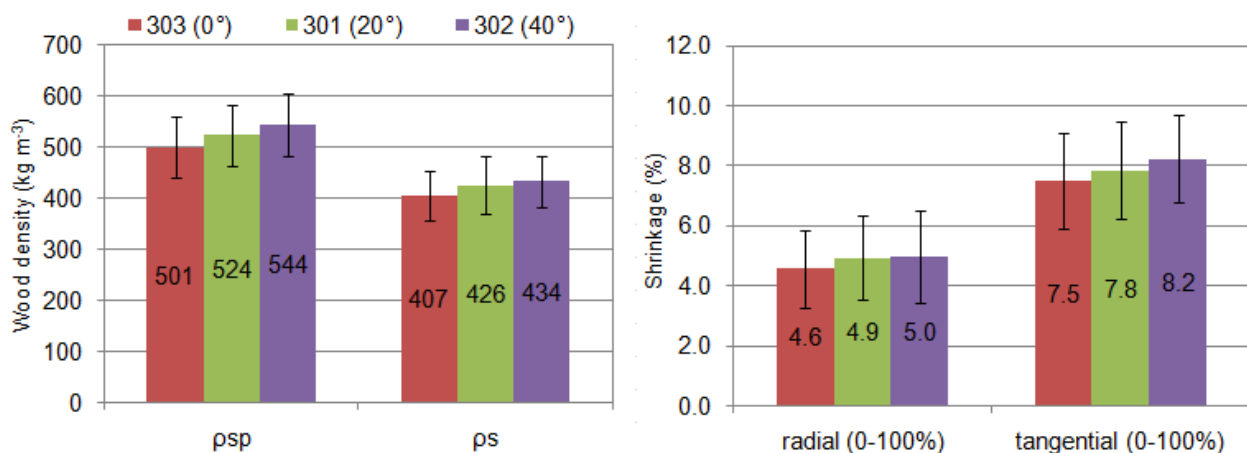


Figure 27 - Mean and standard deviation values of air-dried density of the specimens (psp) and of the basic density of the small wood samples (ps) and radial and tangential shrinkage from oven-dried to green conditions for each

3.3.3.2 Microfibril angle

Microfibril angle of the secondary cell wall were analysed by X-ray diffraction using 2-mm radial sections taken from the specimens and from radial strips. Table 18 lists the descriptive statistics of the T parameter obtained by X-ray diffraction and microfibril angle estimated by Cave (MFA_C) and Yamamoto (MFA_Y) formulas from the small wood samples and radial strips of 6-year-old *Eucalyptus grandis* x *urophylla*. Figure 28 exhibits the microfibril angles estimated from X-ray diffraction patterns measured on 2-mm radial sections while Figure 29 shows the MFA's measured on 2-mm radial strips of *Eucalyptus* by clone and by site presenting the radial variation of the microfibril angle in 6-year-old *Eucalyptus* wood. Table 19 lists the statistics of microfibril angle measured on the radial strips according to the year of wood formation by site. The variation in MFA between clones appears to be uniform in the Site 303 (Figure 29 A2) presenting standard deviation of similar magnitude over the radial range (Sd \approx 1.6°) while the MFA of

samples from Site 301 (Figure 29 B2) clearly varied in higher magnitude in the first years ($Sd \approx 3^\circ$) decreasing their variance magnitude towards the cambium ($Sd \approx 0.7^\circ$).

Table 18 - Descriptive statistics of the T parameter obtained by X-ray diffraction and microfibril angle estimates by Cave (MFA_C) and Yamamoto (MFA_Y) formulas from the small samples of 6-year-old *Eucalyptus grandis x urophylla*. Samples were taken from the small wood samples (MFA_{YS} or MFA_{CS}) and from radial strips (MFA_{YRS} or MFA_{CRS})

	XRD measures from small wood samples			XRD measures from radial strips		
	T ($^\circ$)	MFA_{CS} ($^\circ$)	MFA_{YS} ($^\circ$)	T ($^\circ$)	MFA_{CRS} ($^\circ$)	MFA_{YRS} ($^\circ$)
Mean	19.57	11.68	12.11	17.72	10.63	10.33
Sd	3.91	2.25	2.55	3.06	1.83	2.76
Min	15.43	9.37	8.21	12.98	7.79	4.06
Max	41.09	24.66	24.31	33.05	19.83	19.47
CV (%)	20	19.2	21	17.2	17.2	26.7
N	225	225	225	165	165	165

Trees from site 301 (20°) presented, in average, the higher MFA. It is important to note that wind velocity (see Table 5, pg. 58) of this site is higher (3.2 m/s) than other (0.9 m/s) and this factor also can explain why MFA is higher. The radial strips of sites 301 (20°) and 302 (40°) were taken from the region presenting (hypothetically) tension wood because the terrain slope. In *Eucalyptus*, as in many other hardwood species, tension wood is associated to the formation of the gelatinous layer where the microfibril angle is very small (Clair et al. 2006). For this reason, the averaged MFA values of XRD measurements from radial strips ($MFA_{YRS}=10.3$) are lower than those for small specimens ($MFA_{YS}=12.1$) in which samples were taken containing opposite, normal, and tension wood. Because these data comes from two independent set of samples (logs and discs), it was not possible to perform multiple range tests to verify if the mean values were significantly different. However, the analysis of variance shows no difference in MFA between sites. In short, as the standard error bars overlap (Figure 28) this implies that the two means were not significantly different. Table 19 shows the radial variation of the MFA mean values measured on the radial strips.

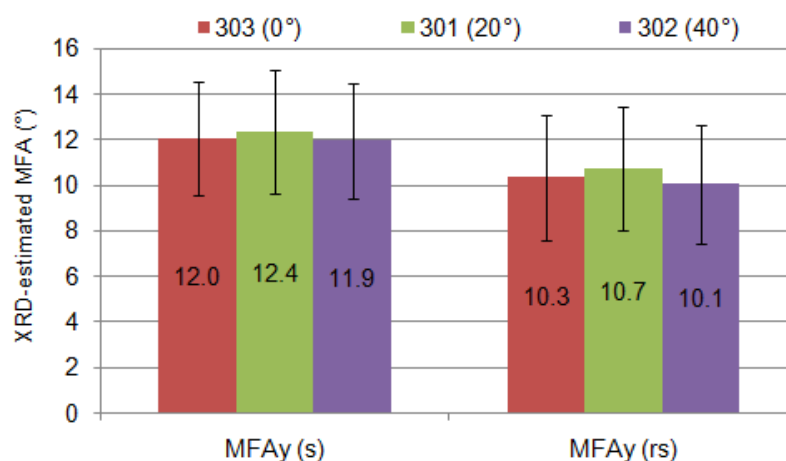


Figure 28 - Mean and standard deviation values of MFA in small wood samples (MFA_{YS}) and radial strips (MFA_{YRS}) of *Eucalyptus* wood for each site and for all samples

X-ray diffraction is fast and reliable technique, but gives only a relative figure for the microfibril angle since the estimative comes from an interpretation of the diffraction pattern called the T parameter.

Numerous studies have proposed models to estimate MFA from T parameters (Cave 1966; Meylan 1967; Yamamoto et al. 1993; Ruelle et al. 2007). In this study the formula proposed by Yamamoto et al. (1993) was used in most of cases. We did not propose a formula for transforming T values into MFA estimates specifically for *Eucalyptus* because the absolute value of the property is of no matter in this study. The interesting point is to know the relative value of the characteristic between trees or regions of the stem, its variation or stability within the logs. These MFA estimates can be useful for selection of candidate genotypes or commercial clones in forestry industries from a large wood sampling. For instance, clones 4557 and 4515 appear to produce the lower microfibril angles.

Table 19 - Mean and standard deviation (in parentheses) of microfibril angle according to the year of wood formation estimated by Yamamoto (MFA_{YRS} in degrees) formulas from radial strips of 6-year-old *Eucalyptus* clones from sites 301, 302 and 303

Site	1 st year	2 nd year	3 th year	4 th year	5 th year
303 (0°)	14.2 (1.9)	12.0 (1.6)	10.4 (1.3)	8.7 (1.8)	8.4 (1.3)
301 (20°)	13.3 (3.0)	11.3 (2.1)	9.5 (0.8)	8.4 (0.6)	7.9 (0.7)
302 (40°)	14.6 (1.7)	11.3 (1.8)	9.2 (1.9)	8.3 (0.8)	7.9 (1.7)

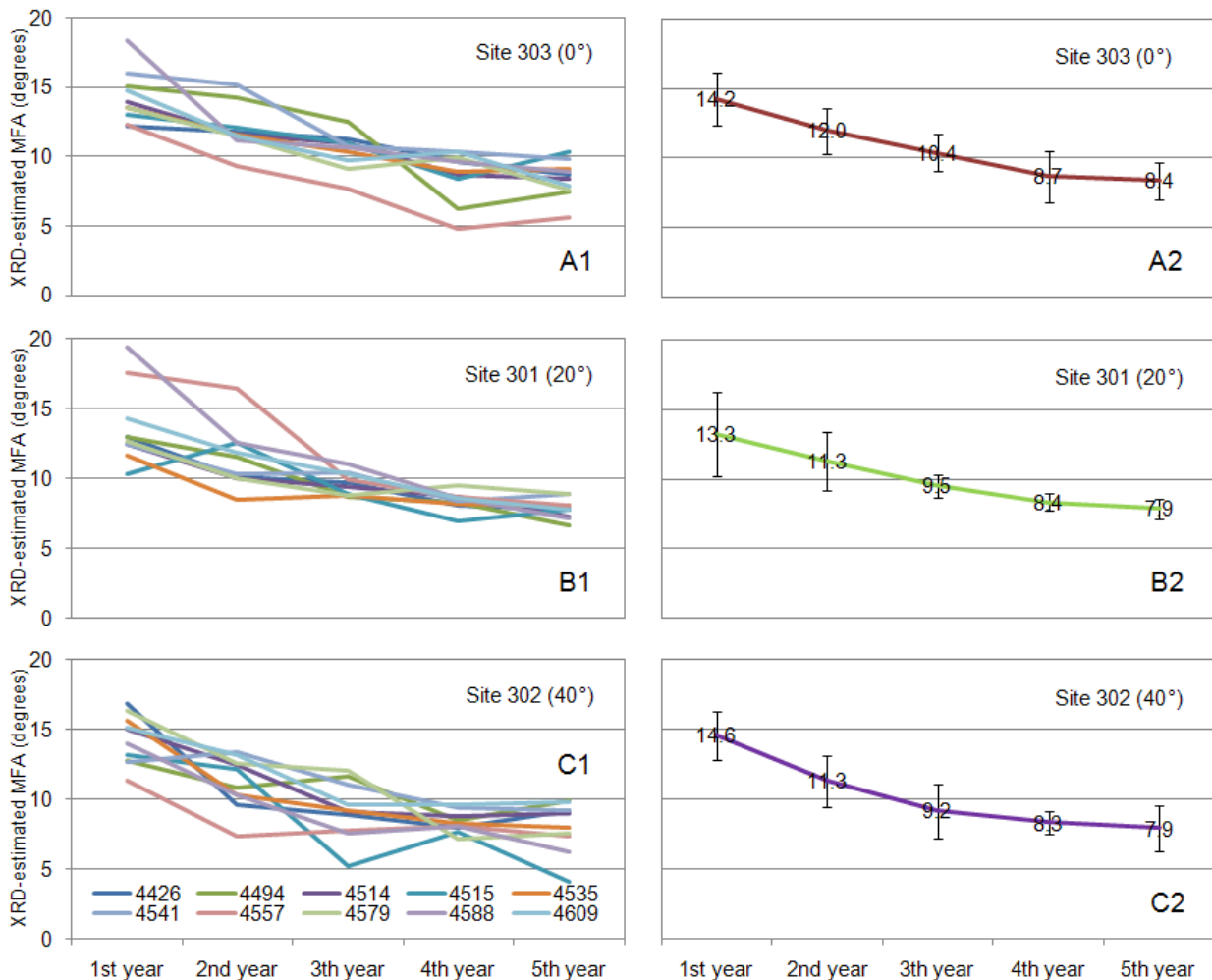


Figure 29 - Radial variation of MFA (estimated by Yamamoto's formula) for wood samples taken from radial strips of 6-year-old *Eucalyptus* clones

The X-ray diffraction data from radial strips were used to develop NIR calibrations while the XRD data from small wood samples provided information about the relationships concerning MFA and other wood traits.

3.3.4 Correlations between wood traits of *Eucalyptus* from clonal test

The correlations among MFA, wood stiffness and strength, density and shrinkage are presented in Table 20. As expected, wood density was found to be well correlated with stiffness ($r=0.82$) and strength ($r=0.68$ for MOR_{4p} and $r=0.71$ for MOR_{3p}) in these *Eucalyptus urophylla* x *grandis*. Early studies have reported correlation between these traits in higher magnitudes. For instance, Evans and Ilic (2001) found higher relationship between density and modulus of elasticity ($R^2=0.70$) in *Eucalyptus delegatensis*. Yang and Evans (2003) reported strong correlations between wood density and modulus of rupture ($R^2=0.80$) in wood samples of *Eucalyptus globulus*, *E. nitens* and *E. regnans*.

MFA was negatively correlated to radial ($r=-0.24$) and tangential ($r=-0.33$) shrinkage (Table 20). Because the variation ranges of MFA are greater in softwoods, these correlations are lower than those presented by Meylan (1968) for *Pinus* and Yamamoto et al. (2001) for *Sugi*.

Although the range of variation in MFA is narrow in *Eucalyptus* some studies have been demonstrated the influence of microfibril orientation on anisotropic shrinkage. Washusen and Evans (2001) examined the correlations between tangential shrinkage and cellulose crystallite width in 11-year-old *Eucalyptus globulus* showing that cellulose crystallite width was closely associated with tangential shrinkage. According to their results, shrinkage increases as crystallite width increased. Wu et al. (2006) explored the relationships of the main anatomical features with shrinkage in *Eucalyptus* wood demonstrating that the main factors affecting shrinkage were microfibril angle and cell wall thickness.

Table 20 - Correlations between wood traits including wood density (ρ), elastic modulus (E), specific modulus (E'), shear modulus (G), radial (δ_{rd}) and tangential shrinkage (δ_{tg}), microfibril angle, ρ /MFA parameter and modulus of rupture (MOR). The correlations were statistically significant at $p<0.01$

	ρ	E_L	E'_L	G	δ_{rd}	δ_{tg}	MFA	ρ /MFA	MOR_{4p}	MOR_{3p}
E_L	0.82									
E'_L	-	0.83								
G	0.28	-	-0.23							
δ_{rd}	0.39	0.40	0.28	0.18						
δ_{tg}	0.43	0.44	0.29	-	-					
MFA	-0.40	-0.61	-0.65	0.20	-0.24	-0.33				
ρ /MFA	-	0.82	0.60	-	0.36	0.43	-0.84			
MOR_{4p}	0.68	0.81	0.66	-	0.29	0.29	-0.47	0.61		
MOR_{3p}	0.71	0.79	0.53	-	0.31	0.29	-0.46	0.60	0.86	

Wood density also shows a negative relationship with MFA and positive relationship with shrinkage. According to Donaldson (2008) MFA shows a variable relationship with wood density. Here, we found a moderate, but significant negative correlation between MFA and density ($r=-0.40$) in *Eucalyptus urophylla* x *grandis* wood from clonal tests. However, this finding is contrary to that reported in this study for the woods from progeny test, where no correlation between density and MFA were found. Evans et al. (2000) also reported no correlation between MFA and density in *Eucalyptus nitens* wood samples.

Figure 30 shows the correlations of MFA with specific modulus (A), tangential shrinkage (B), and the correlations of ρ /MFA with modulus of elasticity (C) and modulus of rupture (D) in *Eucalyptus* wood. The specific modulus decreased as microfibril angle increased (Figure 30 A) as expected (Evans and Ilic 2001; Yang and Evans 2003; Donaldson 2008). However, MFA variation accounted for only 44 percent of the variation in specific modulus. Thus, microfibril angle controls in low magnitude the wood stiffness in 6-year-old *Eucalyptus*. The correlation (r) between MFA and modulus of elasticity was -0.61. These relationships were lower than those reported in previous studies. For instance, Evans and Ilic (2001) showed that various combinations of MFA and density accounted for up to 96 percent of the variability in modulus of elasticity. Similarly, Yang and Evans (2003) reported that MFA alone accounted for 87 percent of the variation in E , while density alone accounted for 81 percent. Thus, MFA and density accounted together for 92 percent of the variation in wood stiffness. MFA was also negatively correlated to MOR_{4p} ($r=-0.47$) and MOR_{3p} ($r=-0.46$) in these wood samples (Table 20). The relationships of modulus of elasticity and modulus of rupture were high ($r=0.81$ for 4-point and $r=0.79$ for 3-point bending test).

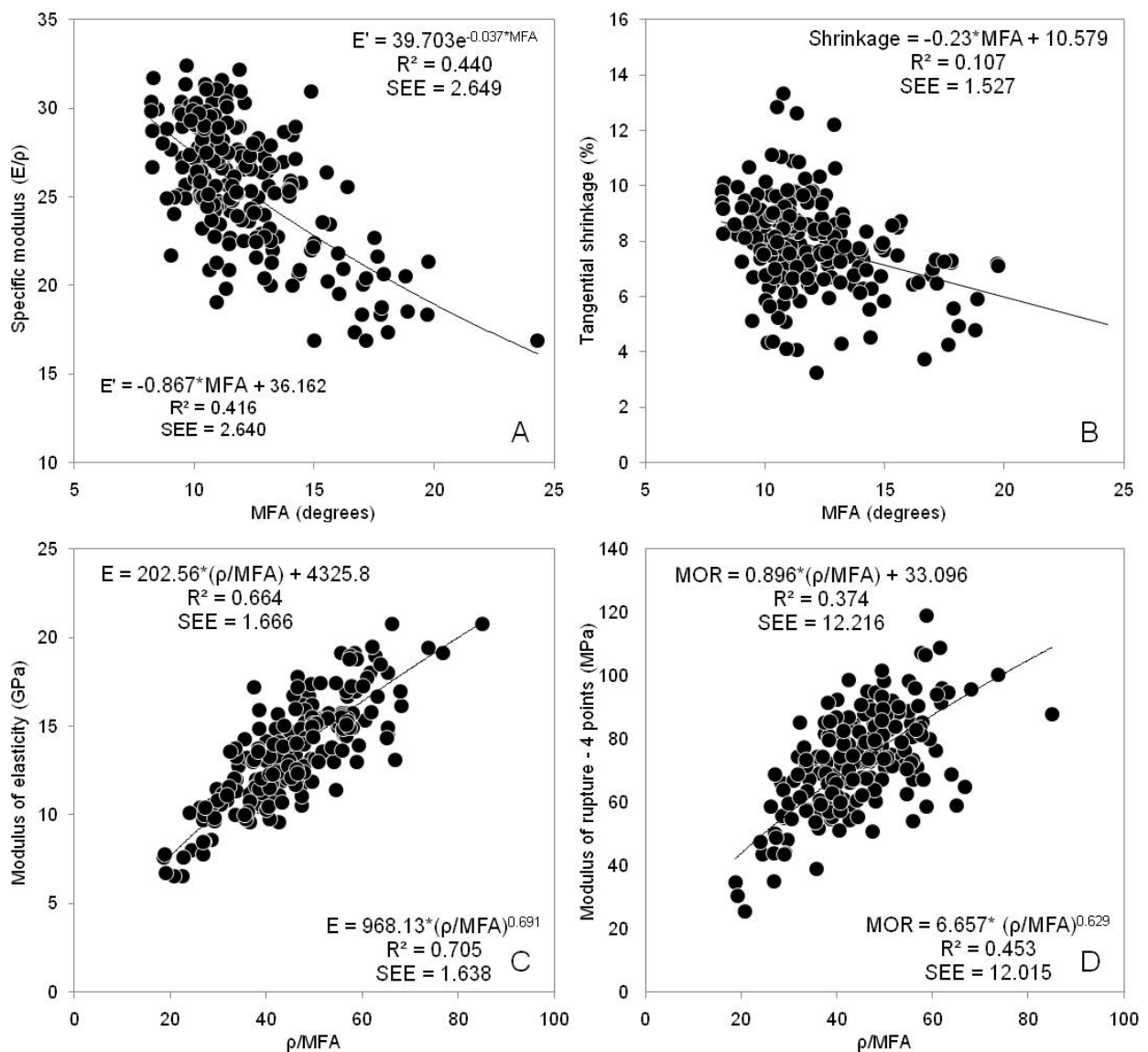


Figure 30 - Relationship between wood traits in *Eucalyptus* wood. SEE is the standard error of estimation

3.3.4.1 Relationships of density and MFA with stiffness and strength

The influence of MFA and/or density on stiffness and strength of these wood samples were better examined. Table 21 presents regression models for predicting modulus of elasticity and modulus of rupture with MFA, density, ρ /MFA and MFA and density together. These findings are particularly useful for understanding the relationships between MFA and stiffness, and strength with and without considering wood density. Because fewer samples were tested in 3-point bending test, only MOR_{4p} was examined in this part of the study.

Evans and Ilic (2001) reported that density variation alone accounted for 70% of the variation in E, while MFA alone accounted for 86% using *Eucalyptus delegatensis* R.T. Baker samples. Thus, the influence of MFA on wood stiffness was significantly greater than that of density for their samples. Afterward, Yang and Evans (2003) found that MFA alone accounted for 87% of the variation in modulus of elasticity. They also reported a strong coefficient of determination ($R^2=0.92$) between ρ /MFA and E in *Eucalyptus globulus*, *E. nitens* and *E. regnans*.

Table 21 - Regression models for predicting modulus of elasticity in longitudinal (E_L) and flexural (E_F) vibrations and modulus of rupture (MOR_{4p}) with MFA, density, and ρ /MFA

Trait	Intercept	MFA	ρ	ρ /MFA	R ²	SEE
E_L	21427.2	-680.43			0.37	2,281
	-5287.1		35.976		0.68	1,609
	4325.7			202.567	0.67	1,651
	1995.6	-367.61	30.557		0.78	1,349
E_F	20208.6	-634.28			0.38	2,082
	-4606.6		32.940		0.67	1,509
	4170.2			186.068	0.67	1,521
	2441.4	-352.01	27.612		0.77	1,253
MOR _{4p}	110.97	-3.166			0.22	14.10
	-22.17		0.184		0.46	11.72
	33.096			0.896	0.37	12.20
	11.42	-1.660	0.158		0.51	11.12

After the previous studies presented by Evans and Ilic (2001) and Yang and Evans (2003), the parameter ρ /MFA has been used for explaining the stiffness in a range of wood. This parameter (ρ /MFA) is able to predict the modulus of stiffness better than MFA explains variation in specific modulus of wood of a range of genera. For instance, McLean et al. (2010) recently demonstrated that 76% of the variation in E was explained by the factor ρ /MFA in wood samples of Sitka spruce.

Despite these relationships (Figure 30 A and C) involve the same variables (E, ρ and MFA), many studies have systematically reported equivalent findings (Evans and Ilic 2001, Yang and Evans 2003, McLean et al 2010). The arisen hypothesis is that the coefficient of variation of MFA (21.2), E (21.2) and ρ (12.5) played a critical role to explain this trend. In the correlation concerning the parameter ρ /MFA, the numerator represents a quantity varying 12.5 percent while the denominator varies twice as. On the other hand, the correlation concerning specific modulus (E/ρ), the CV of the denominator is 2 times greater than the numerator's CV. There may be also a scale effect since the E values were calculated from entire specimens whereas the ρ and MFA represented only a small portion of them.

Here, the coefficient regressions for longitudinal and flexural elastic modulus are very close (Table 21). These two dependent variables are much correlated and models were performed using the two variables to serve as a sort of validation. Density was the prime factor controlling wood stiffness. The models relating wood density to its stiffness yield coefficient of determination (R^2) of 0.68 (using E_L) and 0.67 (using E_L). MFA variations accounted for around 0.38 percent of the variation in modulus of elasticity. When density and MFA are considered together, variations in modulus of elasticity are better explained ($R^2=0.78$). The parameter ρ/MFA was also a good predictor of wood stiffness. The relationships of MOR_{4p} with MFA and wood density presented similar patterns. Again, density was the primary factor controlling wood strength ($R^2=0.46$) but MOR_{4p} is better predicted when density and MFA are considered together ($R^2=0.51$). The coefficient of determination was high and the standard error of prediction was lower when E or MOR_{4p} were modeled from density and MFA together. These findings are similar to those presented by Lachenbruch et al. (2010) who evaluate these relationships in Douglas fir. **Paper 2** presents and discusses these issues.

3.4 Near infrared spectroscopic models

3.4.1 NIR spectra

Wood is a complex three-dimensional biopolymer material composed of an interconnected network of cellulose, hemicelluloses, and lignin with minor amounts of extractives and inorganics (Kollmann and Côté 1968). Hence, NIR spectra reflect the energy absorbed by chemical bonds from different wood components, their contents and interactions. Figure 31 illustrates the untreated NIR spectra measured directly in two contrasting specimens (A and B) of 14-year-old *Eucalyptus urophylla* wood from progeny test. The specimen labeled as “A” exhibits the NIR spectra of the denser or stiffer sample while B represents to the less dense or stiff sample.

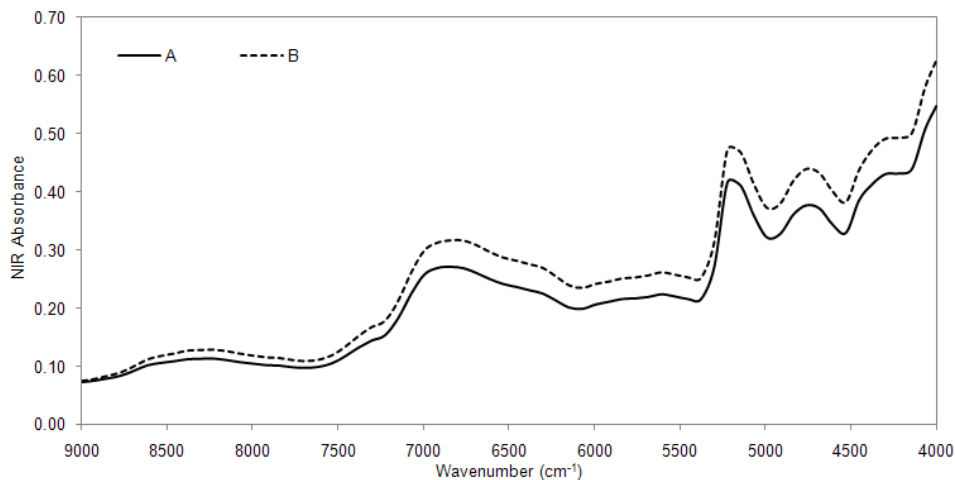


Figure 31 - NIR absorbance versus wavenumber plot for raw (untreated) NIR spectra from 9,000 to 4,000 cm^{-1} range.

Figure 32 shows minutely the NIR absorbance versus wavenumber plot for first and second derivative of the NIR spectra from 8,000 to 5,500 cm^{-1} range spectra of two contrasting specimens (A and B) of 6-year-*Eucalyptus* wood from clonal test. The scaling factor for first derivatives was of 10^2 and for second derivatives was of 10^3 . Bands assigned to chemical compounds are represented by numbers and listed in Table 26. This wavenumber range is important because the differences between the stiffest and the weaker samples can be clearly visualized. The band at 7,092-7,057 cm^{-1} (index 3) is assigned to lignin.

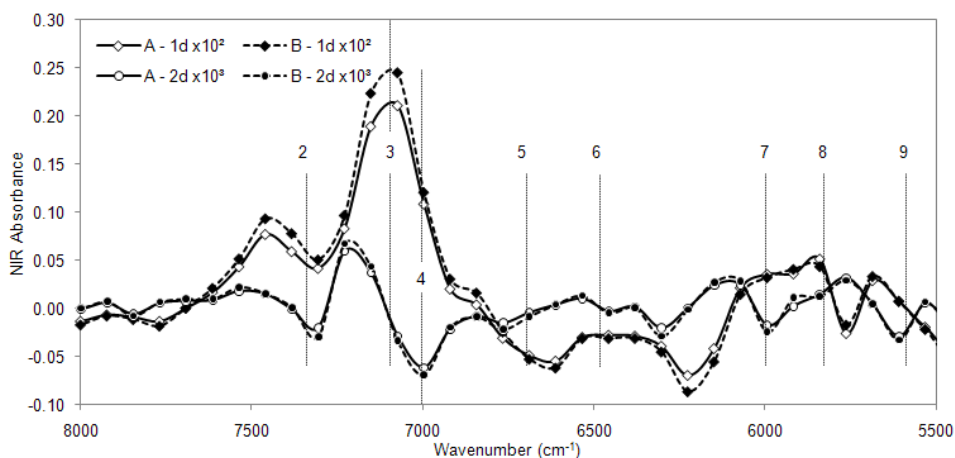


Figure 32 - Absorbance versus wavenumber plot for first and second derivative of the NIR spectra

3.4.2 Reference data

Table 22 and Table 23 list the mean, minimum and maximum values, coefficient of variation and number of samples of the calibration and test sets for a range of *Eucalyptus* wood traits from progeny and clonal tests, respectively. According to Mora and Schimleck (2008) the predictive models must include all possible sources of variation that can be encountered later in real applications because the goal is to estimate values in new samples.

Table 22 - Descriptive statistics of Klason lignin (KL), S to G ratio (S/G), basic density (ρ) and microfibril angle (MFA) of 14-year-old *Eucalyptus urophylla* woods from progeny test

Traits	Average	SD	Min	Max	CV (%)	N
Klason lignin (%)	28.5	1.37	25.4	31.9	4.8	60
S/G ratio*	2.4	0.34	1.7	3.0	14.5	60
ρ (kg m ⁻³)	525	82	338	746	15.6	190
MFA (degrees)	12.5	2.14	7.7	19.7	17.1	175

* syringyl to guaiacyl ratio obtained by thioacidolysis

Cross-validation models were performed for KL and S/G because only 60 samples were analysed by wet-chemistry. On the other hand, independent test sets could be used to validate the PLS-R models for density (ρ), MFA and dynamic elastic properties. A range of PLS-R models were developed from calibrations set and validated from the validation set. The subsets were manually selected in order to guarantee that the test set of such wood traits had as extreme values as possible. The extreme samples of the validation set were comprehended within the variation interval of the calibrations set.

Table 23 - Statistical summary of the overall, calibration and validation sets for air-dry density and basic density (kg m⁻³), microfibril angle (degrees), longitudinal and flexural modulus of elasticity (E, MPa), specific modulus (E', MPa/ ρ), first resonance frequency (f_1 , MHz) and loss tangent ($\tan\delta_L$, 10³) of the small, clean specimens of *Eucalyptus* wood from clonal test

	ρ_{sp}	ρ_s	MFA	E_L	E'_L	f_1	E_F	E'_F	$\tan\delta_L$
Mean	517.4	419.8	10.33	13361	25.7	6170	12468	24.0	7.51
min	362.5	287.7	4.06	6522	16.3	4919	5930	14.1	5.18
max	708.4	617.4	19.47	20785	32.4	6945	18732	30.6	15.60
CV	11.3	12.4	26.7	18.9	12.6	6.4	18.7	12.8	20.3
N	327	225	165	326	326	326	327	327	147
Calibration set									
Mean	517.1	418.5	10.20	13333	25.6	6170	12455	24.0	7.52
min	362.5	313.8	4.20	6522	17.9	4919	5930	14.1	5.18
max	708.4	548.9	18.10	20785	29.8	6916	18732	30.6	15.60
COV	11.0	11.0	22.2	18.2	8.2	6.2	18.1	12.5	20.9
N	196	129	98	195	195	195	196	196	80
Validation set									
Mean	517.8	419.6	10.60	13403	25.6	6171	12488	24.1	7.51
min	375.2	331.4	6.24	6715	18.0	5014	6035	15.3	5.66
max	697.1	537.4	19.20	19475	29.7	6945	18176	29.8	13.70
COV	11.8	10.2	28.3	20.0	9.0	6.7	19.6	13.2	19.7
N	131	90	63	131	131	131	131	131	67

3.4.3 NIRs-based calibrations and validations

3.4.3.1 Progeny test

Statistical summaries of the predictive PLS-R models for klason lignin, S to G ratio, density and microfibril angle of the wood from progeny test are presented in the Table 24. The PLS-R models for chemical properties, especially KL and S/G, were previously presented in Hein et al. (2010) (**paper 4**). In regard to the non-chemical wood traits, the PLS-R models for wood density were presented, validated and discussed in Hein et al. (2009) (**paper 5**) while the models for MFA in Hein et al. (2010b) (**paper 6**).

Table 24 - PLS-R models for Klason lignin (KL, %), syringyl to guaiacyl ratio (S/G, no unit), wood basic density (ρ , kg m⁻³) and microfibril angle (MFA, degrees) used for estimating phenotypic values for 14-year-old *Eucalyptus urophylla*

Trait	Treat	R ² c	RMSEC	R ² p	RMSEP	LV	Outliers	RPD
KL	none	0.88	0.44	0.85	0.53	6	5.0%	2.58
S/G	2 nd der.	0.92	0.01	0.86	0.13	7	5.0%	2.68
ρ	2 nd der.	0.89	27.0	0.85	30.0	3	2.1%	2.70
MFA	2 nd der.	0.66	1.24	0.59	1.36	6	0.0%	1.57

NIR-predicted versus laboratory-determined values plots for klason lignin (A), syringyl to guaiacyl ratio (B), basic density (C) and microfibril angle (D) of the wood from progeny test are given in Figure 33. The PLS-R models for KL and S/G were based on NIR spectra measured from milled wood at 0.5 mm while the predictive models for density and MFA were developed with NIR spectra measured from radial surface of the wood samples.

3.4.3.2 Clonal test

PLS-R models validated by independent test set

The PLS-R models were built from the untreated and treated NIR spectra data from 9,000 to 4,000 cm⁻¹ for ρ , E_L , E'_L , f_{1L} , E_F , E'_F and $\tan\delta_F$ of *Eucalyptus* wood specimens. The statistics associated to the PLS-R models validated by test sets are presented in the Table 25.

Table 25 - PLS-R models for air-dry density (ρ_{sp} , kg m⁻³), wood basic density (ρ_s , kg m⁻³), microfibril angle (MFA, degrees), longitudinal and flexural modulus of elasticity (E, MPa), longitudinal and flexural specific modulus (E' , MPa/ ρ), first resonance frequency (f_1 , MHz) and loss tangent ($\tan\delta_L$, 10³) used for estimating phenotypic values for 6-year-old *Eucalyptus* clones

Trait	Treat	R ² c	RMSEC	R ² p	RMSEP	LV	Outliers	RPD
ρ_{sp}	2 nd der.	0.66	31.44	0.67	34.78	4	0.9%	1.75
ρ_s	snv+1 st der.	0.82	21.75	0.80	22.88	3	2.6%	2.32
MFA	snv+1 st der.	0.77	1.11	0.75	1.31	5	6.6%	2.10
E_L	1 st der.	0.78	1128	0.81	1149	5	1.2%	2.34
E'_L	2 nd der.	0.74	1.59	0.76	1.62	5	0.0%	1.41
f_1	2 nd der.	0.77	185.6	0.72	215.3	6	0.0%	1.92
E_F	1 st der.	0.71	1211	0.74	1219	4	0.6%	2.01
E'_F	1 st der.	0.62	1.82	0.70	1.69	6	0.3%	1.88
$\tan\delta_L$	1 st der.	0.49	0.71	0.38	0.81	5	1.4%	1.84

While promissory model statistics ($r^2_p \geq 0.70$) were obtained for ρ , MFA, E_L , E'_L , E_F , E'_F and f_{1L} , the PLS-R models for air-dry density (ρ_{sp}) and loss tangent ($\tan\delta_T$) provided low to moderate coefficients of determination ($r^2_p=0.67$ and $r^2_p=0.38$, respectively) but still acceptable “ratio of performance to deviation” values (RPD=1.75 and RPD=1.84, respectively) for screenings. Specific modulus (E') yielded models with good r^2_p , but low RPD values.

NIR-predicted versus laboratory-determined values plot for air-dry density (A), basic density (B), microfibril angle (C), longitudinal elastic modulus (D), first resonance frequency (E) and loss tangent (F) of the woos from clonal test are given in Figure 34.

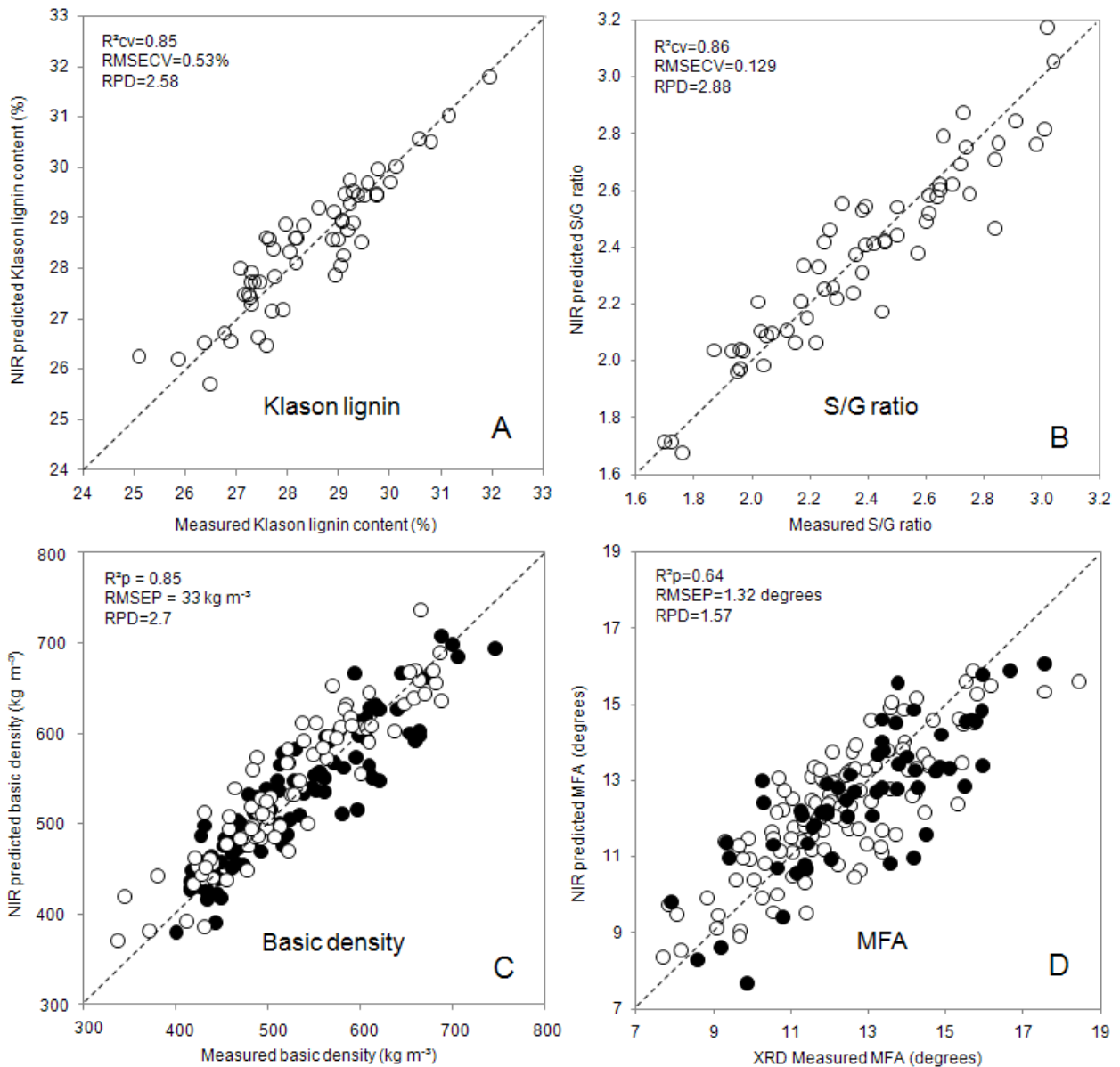


Figure 33 - NIR predicted versus measured values plot for Klason lignin (A), S/G ratio (B), basic density (C) and microfibril angle (D) of wood. The calibration set samples are represented by white circles and the validation set samples are represented by black circles

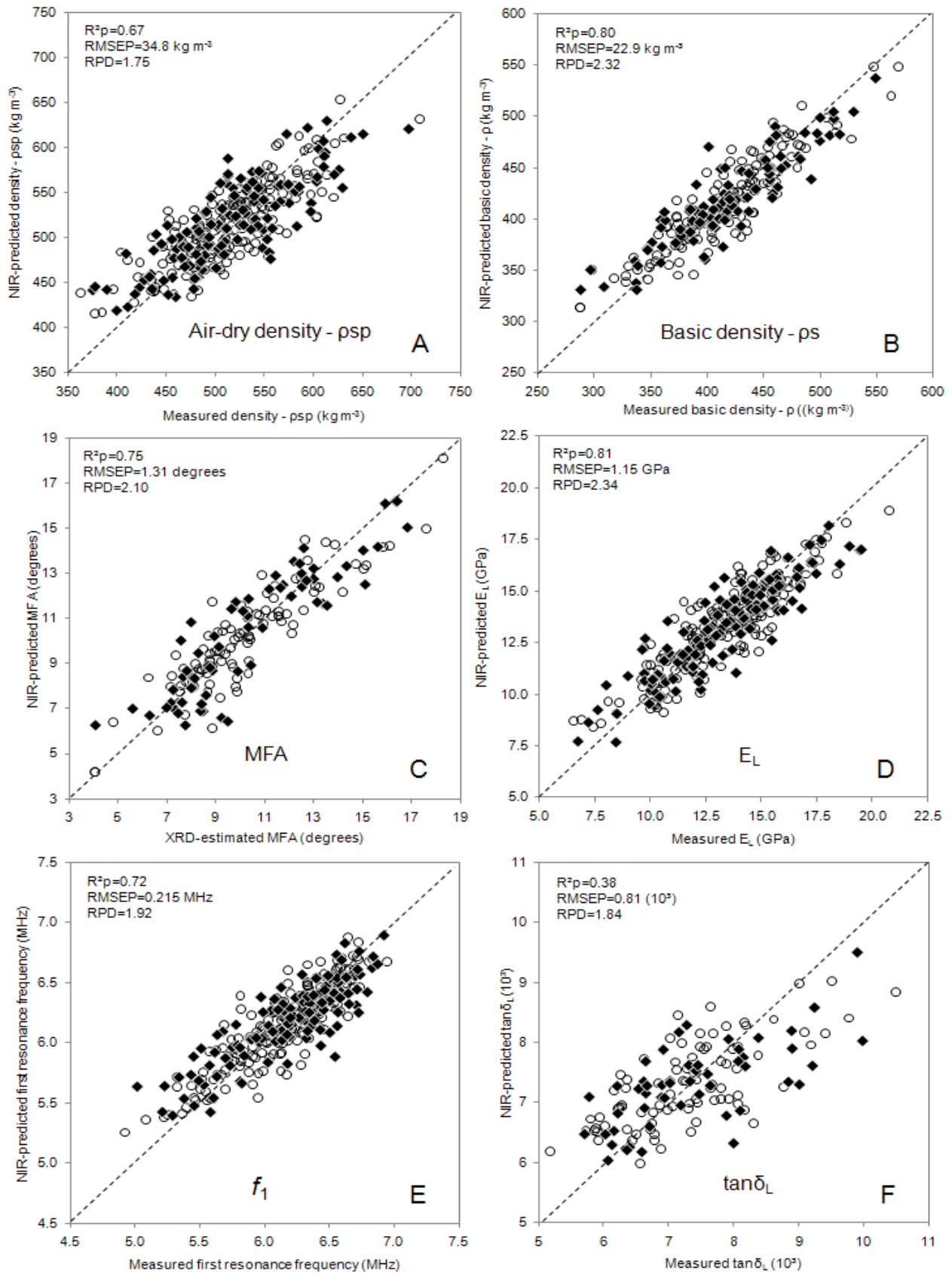


Figure 34 - NIR predicted versus measured values plot for air-dry density (A), basic density (B), MFA (C), dynamic elastic modulus (D), first resonance frequency (E) and loss tangent (F) based on NIR spectra for both training (open circles) and test sets (filled rhombs)

3.4.3.3 PLS-Regression coefficients

The underlying factors controlling wood properties are essentially the result of its chemical composition at three levels: i) chemical features of the molecules that constitute the cell walls (structural components) and those contained within the cellular structure (extractive components); ii) distribution of the chemical components in the cell structure and iii) the relative proportions of the different chemical components in the wood cells and tissues. The specific properties of wood may be traced back to a combination of these aspects, and wood utilization and end-product related quality should thereby link directly to its chemical characteristics (Pereira et al. 2003). For this reason, mechanical, physical, and chemical wood traits are often correlated. For instance, it is known that the influence of density on strength and elasticity of wood is strong (Kollmann and Côté 1968).

Table 26 - NIR absorption bands normally associated to the main wood components (cellulose, hemicelluloses, lignin, and water) contained in the wood specimens

Index	cm ⁻¹	Bond vibration	Structure	Ref.
1	8547	2nd overtone asymmetric stretching CH, HC=CH	Lignin	a
2	7353	CH deformation + CH stretching 2nd overtone	CH ₃	b
3	7092	OH stretching 1st OT lignin or first overtone of an O-H stretching vibration of phenolic hydroxyl groups	Lignin	c
3	7057	C-H combination, aromatic associated C-H	Lignin	a
4	7003	1st overtone OH stretching (amorphous region in cellulose)	Cellulose	e
5	6711	1st overtone OH stretching	Cellulose	a,d
6	6460	1st overtone OH stretching (crystalline regions in cellulose)	Cellulose	c
7	5981	1st overtone CH stretching	Lignin	e
7	5934	1st overtone CH stretching (aromatic associated CH)	Lignin	a,d
8	5800	1st overtone CH stretching	Hemicellulose	e
9	5618	1st overtone CH ₂ stretching	Cellulose	a,d
10	5250	not assigned	-	
11	5050	OH stretching + OH deformation combination band	Water	e,a
12	4800	Asymmetric NH stretching + amide III	-	a
13	4750	not assigned	-	
14	4545	CH stretching and C=O combination	Lignin	a
15	4490	not assigned	-	
16	4375	not assigned	-	
17	4282	CH stretching + CH ₂ deformation combination band (and 2nd overtone of CH ₂ stretching)	Cellulose	a,c
17	4261	CH (1st overtone CH ₂ symmetric stretching and δ CH ₂) combination	Cellulose	a,c
17	4252	CH bending and stretching combination band	Cellulose	a
18	4063	CH stretching + CC stretching	Cellulose	a

a: Workman and Weyer (2007); b: Schimleck and Evans (2004); c: Shenk et al. (2001); d: Schimleck et al. (2004) and e: Fujimoto et al. (2008)

The analysis of the loading plots for each calibration is useful to investigate the underlying relationships that have made the estimation of air-dry density and dynamic elastic properties of wood possible by NIR spectroscopy. The assignments of absorption bands indicated in Figure 35 are useful to identify which wood components were important for the PLS-R models. It helps to understanding how NIR spectroscopy

can evaluate wood traits based on resonance analysis. Table 26 lists the NIR absorption bands normally associated to the main wood components (cellulose, hemicellulose lignin, and water) contained in the wood specimens. Numbers assigned to the specific bands and regression coefficients are presented in Figure 35

The lignin content of wood was important for air-dry density PLS-R models, as bands at 7,092-7,057 cm^{-1} (index 3) and 5,081-5,934 cm^{-1} (index 7) yielded high regression coefficients and were assigned to lignin. The high regression coefficient at 4,282 cm^{-1} (Index 18) indicates that cellulose content also played an important role on PLS-R models for air-dry density. Band at 4,490 cm^{-1} (index 15) seems to be important for air-dry density calibration. For dynamic elastic models, the bands at 5,800 cm^{-1} (index 8), associated to the hemicellulose contents; at 4,800 cm^{-1} (index 12) and 4,750 cm^{-1} (index 13) had a strong coefficient regression, but the bands at 4,375 cm^{-1} (index 16) and 4,282 cm^{-1} (index 18) appears to be the most important for stiffness. Schimleck et al. (2002) also reported similar loading plots for air-dry density and for stiffness.

The bands with higher coefficient of regression for first frequency resonance were those associated to hemicellulose (4,750 cm^{-1}) and cellulose (4,282 cm^{-1}) contents, and also the bands at 5,250 (index 10) and 4,750 cm^{-1} (index 13). Cellulose and hemicellulose contents were also important for PLS-R models for loss tangent. High absorptions occurred at 5,800 cm^{-1} (index 8), at 4,750 cm^{-1} (index 13), at 4,375 cm^{-1} (index 16) and at 4,282 cm^{-1} (index 18). In short, combinations of lignin, hemicelluloses and cellulose contents in wood control the elastic properties of wood. The absorptions correspondent to lignin (index 3, 7 and 14), to hemicelluloses (index 8) and to cellulose (index 4, 5, 6, 9, 17 and 18) content were significant to the Martens' uncertainty test (Westad and Martens 2000) for the wood traits, and other important bands (index 10, 13 and 16) seems to be associated or combined to the specific absorptions of the known wood components.

Figure 35 is useful for brings new elements to understand the underlying relationships between wood traits. For instance, density and stiffness are wood traits well correlated. Figure 35 A and D reveals that these properties presented high peaks at the same bands (index 14 and 18), confirming that both cellulose and lignin content variations are closely associated. Similarly, the regression coefficients for MFA and modulus of elasticity have high peaks at bands indicated by index 14 and 16.

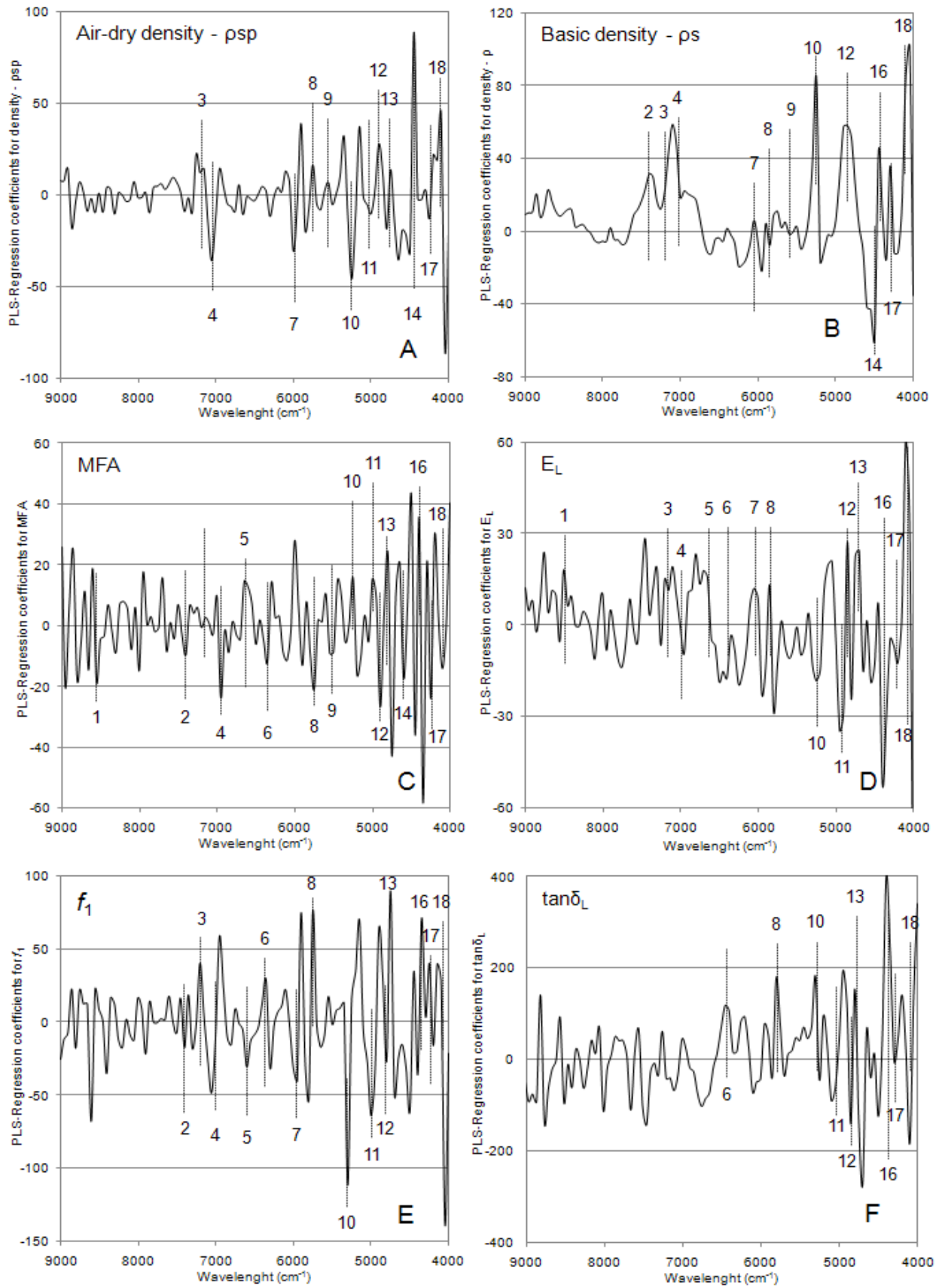


Figure 35 - PLS-regression coefficients for NIR-based model for estimating air-dry density (A), basic density (B), microfibril angle (C), dynamic elastic modulus (D), first resonance frequency (E) and loss tangent (F)

3.5 Genetic studies from progeny test

The descriptive statistics of the wood traits of the 14-year-old *Eucalyptus urophylla* population are listed in Table 27. This phenotypic database was produced from NIR-based estimates for Klason lignin, S to G ratio, basic density of wood and microfibril angle of the cell walls. To take into account the within-tree variation, MFA and D were evaluated at the inner heartwood (point 1), at the outer heartwood (point 2), and at the sapwood (point 3). In this part, the NIR-predicted basic density is designed as “D”, in order to avoid confusion with lab-measured values or NIR-predicted densities of wood from clonal tests.

Table 27 - Mean, minimum and maximum values, coefficient of variation and number of observations (N) for measured circumference (C, centimeters) and height (H, meters), and NIR-estimated Klason lignin (KL, %), syringyl to guaiacyl ratio (S/G, no unit), wood density (D, kg m⁻³) and microfibril angle (MFA, degrees) of the 14-year-old *Eucalyptus urophylla* population

Trait	Mean	Minimum	Maximum	CV (%)	N
C	52.68	24	84	21.17	340
H	21.15	7.8	29.6	17.26	340
KL	28.03	25.1	31.75	4.42	321
S/G	2.29	1.54	3.51	13.54	321
D ₁	443	330	607	10.23	274
D ₂	522	391	698	8.43	274
D ₃	615	480	761	8.11	274
D	526	423	654	7.09	274
MFA ₁	18.05	12.7	23.9	10.08	274
MFA ₂	15.34	10.0	21.1	12.39	274
MFA ₃	13.32	7.22	19.5	13.89	274
MFA	15.57	11	20	9.76	274

The wood chemical properties (KL and S/G) are comparable to those found in similar studies which have investigated mature *Eucalyptus* wood (Brito and Barrichelo 1977; Poke et al. 2006) and higher than those reported for juvenile wood (Baillères et al. 2002; Gomide et al. 2005).

Patterns in pith to bark variation of these traits have been known for many years; wood density generally increases while MFA decreases from pith to bark (Kollmann and Côté 1968). Here, the microfibril angles were, on average, higher near the pith decreasing radially towards the cambium whereas an opposite trend was observed for the basic density of wood (Table 27). The software alerted us about some estimates presenting high deviations. Thus we removed these outliers from the original dataset.

The coefficients of variation were similar to those observed in previous studies on *Eucalyptus* in the Congo (Bouvet et al. 1999). They were higher for growth traits than for wood property traits. Their magnitude showed that the sampling used in this study was representative of a breeding population involved in genetic improvement programs in the Congo (Bouvet et al. 2009).

3.5.1 Heritability of growth and wood traits

While many papers have reported heritability estimates and correlations among growth and density (or pilodyn penetration) in *Eucalyptus* wood, few studies have addressed to genetic parameters of chemical,

mechanical and anatomical properties (Kube et al. 2001; Apiolaza et al. 2005; Poke et al. 2006; Mandrou et al. 2011). This study presents the genetic control for microfibril angle, wood density, klason lignin content, syringyl to guaiacyl ratio of the wood and for circumference and height of the trees and should contribute to the knowledge on the role on genetic and non-genetic factors on the variation of these kind of traits.

Table 28 presents the additive genetic and residual variance components, genetic (CV_A) and residual (CV_E) coefficient of variance and narrow-sense heritability estimates for various traits, including circumference (C), height (H), microfibril angle (MFA), basic density (D), Klason lignin (KL) and syringyl to guaiacyl ratio (S/G).

Genetic and residual variation was higher for growth traits than for wood property traits as shown by CV_A and CV_E . As expected, the narrow-sense (h^2) estimates were lower for growth traits: $h^2=0.30$ for height and $h^2=0.14$ for circumference while moderate to high levels of heritability (from 0.37 to 0.72) were reported for wood traits. The low heritability estimates for growth traits confirms the trends described in previous studies addressing the heritability of growth traits for other *Eucalyptus* breeding programs (Kube et al. 2001; Costa e Silva et al. 2004; Volker et al. 2008; Kien et al. 2009; Costa e Silva et al. 2009) and more specifically in the Congo (Bouvet et al. 2003, Bouvet et al. 2009).

Table 28 - Additive genetic and residual variance components, genetic and residual coefficient of variance and narrow-sense heritability estimates for various traits

Trait	Additive genetic variance			Residual variance			Genetic control	
	σ^2_A	SE σ^2_A	CV_A	σ^2_E	SE σ^2_E	CV_E	h^2	SE h^2
C	13.62	9.44	7.0	85.61	8.59	17.6	0.14	0.09
H	3.27	1.69	8.6	7.63	6.37	13.1	0.30	0.14
KL	1.11	0.47	3.8	0.43	1.72	2.3	0.72	0.20
SG	0.068	0.069	11.4	0.027	1.770	7.2	0.71	0.20
D ₁	8.16	4.11	6.4	13.54	4.95	8.3	0.37	0.16
D ₂	8.90	4.02	5.7	11.40	4.40	6.5	0.44	0.17
D ₃	13.44	6.12	6.0	12.89	3.67	5.8	0.51	0.18
D	9.22	3.69	5.8	5.51	2.35	4.5	0.61	0.17
MFA ₁	1.47	0.68	6.7	1.96	4.75	7.7	0.43	0.16
MFA ₂	1.88	0.82	8.9	1.88	3.70	8.9	0.50	0.14
MFA ₃	1.58	0.74	9.5	1.96	4.27	10.5	0.44	0.17
MFA	1.57	0.60	8.0	0.84	2.25	5.9	0.65	0.15

σ^2_A - additive genetic variance component; σ^2_E - residual variance component; h^2 - narrow-sense heritability estimates and SE - standard errors. For the estimates of variance components for wood density, the phenotypic values were divided by 10.

Narrow-sense heritability estimate of elevated magnitude was found for MFA ($h^2=0.65\pm 0.17$) when calculated from the mean values per disc (Table 28). These h^2 estimates were higher than those reported in two previous studies. Apiolaza et al. (2005) used increment cores from 188 open-pollinated progenies of 11-year-old *E. globulus* reporting $h^2_{MFA}=0.27\pm 0.24$ while Lima et al. (2004) reported mean broad-sense heritability (H^2) of 0.29 in 8-year-old *Eucalyptus* wood. Normally, broad-sense heritability estimates are higher than narrow-sense estimates. The low H^2 estimate by Lima et al. (2004) was expected since they evaluated clones of *E. grandis* x *E. urophylla* for pulpwood so genetic base was narrow. On the other hand, the relatively lower narrow-sense h^2 estimates of Apiolaza et al. (2005) can be attributed to larger environmental variation since their CV_A (8.36%) is close to the CV_A of Table 3 (8%).

Just as the phenotypic values, the genetic control also varied with age. The heritability estimates of the MFA in the inner heartwood ($h^2_{MFA1}=0.43\pm 0.16$) increased towards the outer heartwood ($h^2_{MFA2}=0.50\pm 0.14$), decreasing again in the sapwood ($h^2_{MFA3}=0.44\pm 0.17$). This variation trend with age (Table 28) was similar to the variation pattern reported by Lima et al. (2004) in *Eucalyptus* clones (h^2_{MFA} departing from 0.13, increasing to 0.36 and decreasing to 0.16 towards the cambium). However, the biological significance of these two results is not compatible since the peaks in heritability estimates occurred at different ages.

Comparing these findings requires prudence because the experimental dispositive were different (open and controlled-pollinated and clonally propagated tests) and the methods for wood phenotyping were distinct: Apiolaza et al. (2005) estimated the phenotypic MFA values of their study by means of the SilviScan device (based on X-ray diffraction); Lima et al. (2004) used polarised light microscopy technique and, here, X-ray-diffraction patterns were associated with NIR spectroscopy to estimate the MFA).

Moderate genetic control was found for mean wood density ($h^2=0.62\pm 0.17$) and for local wood density measurements. The heritability estimates linearly increased from 0.37 ± 0.16 to 0.51 ± 0.18 towards the sapwood; however this linear trend should be considered with caution since the standard errors (SE) were elevated (~ 0.17).

Due its relatively easy and simple measurement, the wood density has been extensively investigated in *Eucalyptus* and the heritability of such trait exhibits variable magnitudes: from $h^2\approx 0.6\pm 0.12$ (Kien et al. 2008) to $h^2=0.71\pm 0.2$ (Wey and Borralho 1997) in *E. urophylla*; from $H^2=0.51\pm 0.13$ (Kube et al. 2001, for all sites) to $h^2=0.73$ (Greaves et al. 1997, for whole-disk density at 1.3 m across sites) in *E. nitens*; from $h^2=0.24\pm 0.26$ (Poke et al. 2006) to $h^2=0.44\pm 0.22$ (Apiolaza et al. 2005) in *E. globulus* and of $h^2=0.17$ (Raymond et al. 1998) in *E. regnans*. Most of these studies have shown the high heritability of this trait mainly explained by the low environmental rather than by marked genetic variation (see CV's in table 3); our study reinforces these previous results.

Lignin content and S/G ratio were traits shown to be under strong genetic control (Table 28). The high narrow-sense heritability estimates of these chemical traits ($h^2>0.7\pm 0.2$) indicates that genetic improvement is possible through breeding. The heritability for lignin ($h^2=0.72\pm 0.2$) were lower than those reported by Gominho et al. (1997) in *E. globulus* clones ($h^2=0.83$) and higher than those reported by Poke et al. (2006) in *E. globulus* families (narrow-sense $h^2=0.13\pm 0.2$ and family means $h^2=0.42\pm 0.19$). As lignin content and its composition are key traits of *Eucalyptus* breeding programs, especially for pulp, paper and bioenergy production the high genetic control of lignin content and syringyl to guaiacyl ratio reported here (Table 28) are of major importance for tree breeders.

Although these estimates are population- and site-specific parameters, these findings are coherent with previous studies and useful for tree breeders since they show that MFA, density, lignin and S to G ratio present a high heritability being susceptible to improvement.

3.5.2 Genetic and residual correlations

Genetic correlation is the ratio of genetic covariance and the product of the genetic standard deviations of two traits and can be thought as the correlation of the breeding values (Falconer and Mackay 1996). According to Baltunis et al. (2007) a strong genetic correlation may imply that the same genes may be responsible for the two traits (pleiotropy). In tree improvement, genetic correlations are important in describing the extent to which one trait can indirectly be improved by selecting for another trait (Zobel

and Talbert 2003). For instance, strong negative genetic correlation indicates that selection for reducing one trait would lead to gain in another one, and vice-versa.

Estimates of genetic and residual correlations among growth, Klason lignin content, S/G ratio and mean MFA and wood density are shown in Table 29. Here, few relationships (C x H; KL x MFA and KL x SG) presented additive and residual correlation with the same sign. These correlations presenting the same sign indicates pleiotropic gene effect (Falconer 1993). This becomes a problem when selection on one trait favours one specific version of the gene (allele), while the selection on the other trait favours another allele.

Most of correlations (Table 29) presented opposite sign indicating that linkage disequilibrium (non-random associations of alleles) between loci may affect the relationship among different wood traits (Falconer 1993). This means that the genes controlling these traits can be statistically associated, but there is no functional relationship between them. Sampling procedure used in this study could have played a role on linkage disequilibrium, since the 9 or 10 trees of each family were selected among the best ones in growth and stem straightness. According to Villanueva and Kennedy (1990) selection not only produces changes in the genetic variance of the trait directly selected, but genetic variances of and co-variances between other correlated traits are also affected. Moreover, Lande (1984) states that “when two characters under separate genetic control are selected to be highly correlated, in a large randomly mating population with no linkage between loci influencing different characters the genetic correlation maintained is small in magnitude”.

Table 29 - Estimated additive genetic (r_A , below the diagonal) and residual (r_E , above the diagonal) correlations for various traits, including circumference (C), height (H), microfibril angle (MFA), basic density (D), Klason lignin (KL) and syringyl to guaiacyl ratio (S/G). Standard errors are shown in parentheses

	C	H	MFA	D	KL	SG
C		0.80 (0.05)	0.07 (0.15)	0.48 (0.27)	0.30 (0.18)	-0.20 (0.17)
H	0.46 (0.32)		0.16 (0.22)	0.41 (0.24)	0.35 (0.29)	-0.41 (0.27)
MFA	-0.50 (0.33)	-0.70 (0.21)		-0.87 (0.00)	0.22 (0.34)	0.63 (0.49)
D	-0.99 (0.18)	-0.56 (0.26)	0.48 (0.16)		-0.35 (0.44)	0.10 (0.43)
KL	-0.16 (0.39)	-0.61 (0.24)	0.58 (0.20)	0.28 (0.28)		-0.24 (0.39)
SG	0.18 (0.39)	0.37 (0.30)	-0.27 (0.28)	-0.65 (0.18)	-0.16 (0.29)	

Our results bring new element to understand the correlation between wood and growth traits. However these results should be considered with caution due to the low accuracy of our estimation (see Table 29). A sizable body of literature exists about genetic correlations between growth traits and wood density; however the findings concerning this issue are inconsistent. Zobel and Van Buijtenen (1989) reviewed a number of studies prior to 1986, reporting contradictory findings for a range of wood species. Recently, Hamilton and Potts (2008) reviewed the studies on genetic parameters in *Eucalyptus nitens* showing genetic correlations between growth and density between -0.79 to 0.08, with a mean correlation of -0.27 for density-diameter from more than 10 studies. In regard to the *Eucalyptus* genus, this issue is still not clear. While numerous papers have reported low genetic correlations between growth traits and wood density ($r=-0.20$, Greaves et al. 1997; $r=-0.11$, Kube and Raymond 2005), a range of studies has reported a moderate negative genetic correlations ($r=-0.36$, and Borralho 1999; $r=-0.57$, Kube et al. 2001). Moreover, numerous papers have shown contrasting results of correlations between the same traits but

from different sites (Wei and Borralho 1999; Muneri and Raymond 2000; Osorio et al. 2003; Hamilton et al. 2009) outlining the environmental x genotype interaction effect on these correlations.

As expected, the genetic and residual correlation between growth traits was positive. The correlations between growth and wood traits (MFA, D and KL) were negative. Positive residual correlations were obtained for this same group of correlations. Such patterns are different for S to G ratio. The correlations concerning S/G are of low magnitude considering the standard errors (Table 29).

The strong genetic correlation between C and D was investigated by means of the residual scattering analysis (not shown). The point's dispersion revealed that there was no aberrant point, which could favour (stretching) the correlation. The correlation estimates had large standard errors probably due to the small sample size.

3.5.3 Age trends of additive genetic, residual and phenotypic correlations

Age trends of genetic, residual and phenotypic correlations, respectively, between density and circumference (D x C), and between microfibril angle and circumference (MFA x C), klason lignin (MFA x KL) and, density (MFA x D) are shown in Table 30 and Figure 36. The correlation between circumference and wood density remained high during all phases of wood formation, from the first to the last years of development. On the other hand, the correlation between circumference and MFA seems to decrease towards the bark. This kind of linear increase of correlation is also found between MFA and lignin in which there is an increase with age. The correlation between MFA and wood density decreased from juvenile to mature wood.

Table 30 - Variation with age of additive genetic, residual and phenotypic correlations of density with C, and MFA with C, KL and density. Standard errors are in parenthesis

	Inner heartwood (1)	Outer heartwood (2)	Sapwood (3)
Additive genetic correlation			
D-C	-0.89 (0.24)	-0.99 (0.00)	-0.88 (0.23)
MFA-C	-0.67 (0.28)	-0.53 (0.32)	-0.27 (0.40)
MFA-KL	0.40 (0.27)	0.52 (0.23)	0.74 (0.15)
MFA-D	0.69 (0.22)	0.70 (0.21)	0.30 (0.30)
Residual correlation			
D-C	0.20 (0.12)	0.34 (0.07)	0.39 (0.16)
MFA-C	-0.06 (0.11)	-0.06 (0.12)	0.24 (0.11)
MFA-KL	0.11 (0.24)	0.16 (0.27)	0.19 (0.25)
MFA-D	-0.79 (0.24)	-0.92 (0.33)	-0.52 (0.22)
Phenotypic correlation			
D-C	-0.06 (0.07)	0.00 (0.05)	0.01 (0.08)
MFA-C	-0.20 (0.07)	-0.17 (0.07)	0.11 (0.07)
MFA-KL	0.27 (0.09)	0.37 (0.08)	0.50 (0.07)
MFA-D	-0.17 (0.10)	-0.13 (0.11)	-0.13 (0.10)

The residual correlation is of low magnitude, except for the correlation between MFA and D. The phenotypic and additive genetic correlation between C and MFA, and LK and MFA presented the same

trends slightly differing in their magnitude. The phenotypic correlation between circumference and wood density is null while the genetic is strong. Similarly, the phenotypic correlation between MFA x D is of low magnitude while the residual and genetic are considerable. These findings indicate that the phenotypic correlation is not a good predictor of genetic correlation.

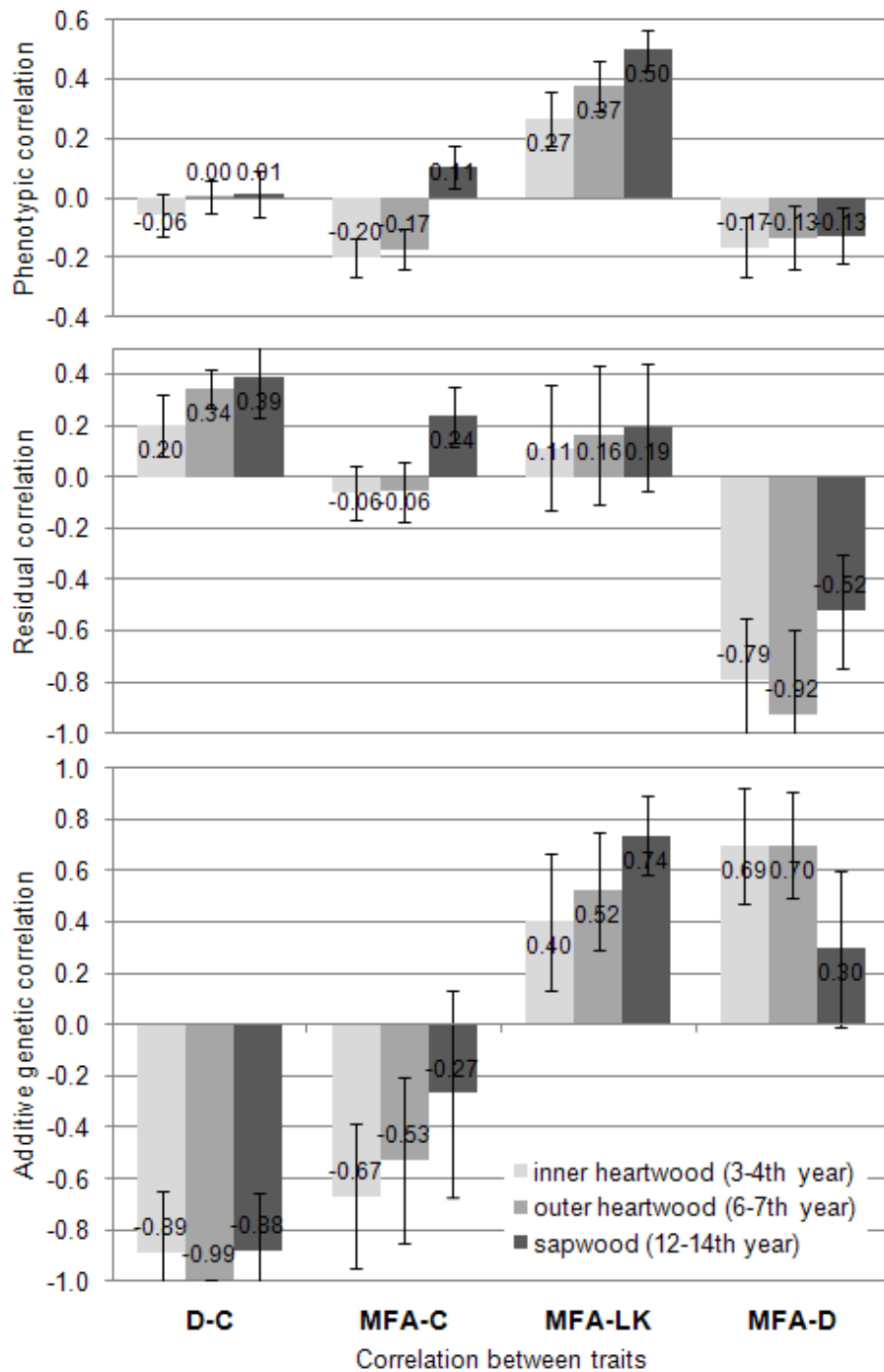


Figure 36 - Age trends of phenotypic, residual and additive genetic correlations of density with C, and MFA with C, KL and density

In general, additive genetic correlations presented higher magnitudes when compared with the residual correlations. Moreover, the radial variations of the values of the genetic relationships were stronger than those for residual or phenotypic correlations.

As the tree grows up, new layers of wood are produced and overlapped in order to withstand the ever-increasing mass of the tree. The variations of the genetic and residual correlations with age may be useful to understanding how one tree adapt the characteristics of its wood to support gravity and bending movements caused by winds. A theoretical view of this issue was provided in Alm eras and Fournier (2009).

The narrow-sense heritability estimates for wood density and MFA varied with age (Table 28), as well as their phenotypic values (Table 27). This means that trees adapt both their density, lignin content and MFA to answer to the specific needs of the stems (such as its ever-increasing mass or its vulnerability to wind) and such adaptations are somewhat regulated by genetic factors.

The genetic correlation C x D is always strongly negative while the correlation D x MFA remained constant in the juvenile wood, decreasing considerably in the mature wood (Figure 36). This means that trees with a strong potential to grow fast are genetically programmed to produce low-density woods and also to decrease the microfibril angles for ensuring stiffness. Wood stiffness is partially controlled by the MFA in most wood species, including *Eucalyptus* (Evans and Ilic 2001). Hence, it appears that the trees try to compensate the weakness of its low-density by reducing its MFA, and consequently by increasing the specific modulus of the wood ($r_{A(MFA1 \times D1)}$ and $r_{A(MFA2 \times D2)} \approx 0.7$), especially in the juvenile stage.

When the tree reaches maturity, the stem becomes especially susceptible to prevailing winds because the higher heights and inertia moments. It is known that a reaction wood is typically formed as the tissues of the periphery are held in “tension” (Clair et al. 2006) and in many wood species, tension wood is characterised by the presence of a thick, inner cell-wall layer that consists of highly crystalline cellulose, in which the MFA is close to zero (Thibaut et al. 2001). Moreover, this particular layer (G-layer) is almost invariably unligified (Du and Yamamoto 2007). Thus, the low lignin content and MFA of the sapwood could be associated to tension wood occurrence and our results indicate that variations in these wood traits are also genetically controlled: the genetic correlation between MFA and KL increases from 0.4 to 0.74 towards the cambium (Figure 36). In conclusion, the genetic correlations MFA x D and MFA x KL acting together reveal a smart biological strategy for the survival of the tree.

It is important to note that the tension wood is distributed tangentially and not radially whereas the lignin content slightly varies with age. Regrettably, there was only a mean, single estimative of Klason lignin content by tree in this study because the NIR calibration was based on powder of the wedge. Here, the hypothesis is that NIR-based models for MFA and KL are sensible to the variations in wood characteristics. Thus the decrease in lignin content should be more important than that of MFA due to tension wood presence. Moreover, another source of co-variation should play a role on these findings, such as the changes in S to G ratio with age within the wood.

3.5.4 Implications for selection

The phenotypic and genetic correlations show opposite patterns for wood traits. While phenotypic correlation between C and D exhibit null magnitudes, the genetic associations between these traits can be prominent. For the correlation MFA x D, the phenotypic values yield no relationships while their genetic or residual estimates indicates that these traits are linked (Figure 36). These findings suggest that the phenotypic value of the trait is not a good predictor of its genetic potential or its consequences. When trees are selected on the base of only their phenotypic values, the characteristics of their offspring can be surprising since the consequences of mixing different allelic forms are unpredictable. Our study allows considering the consequences that these results can have on the genetic improvement strategies.

In the frame of pulpwood production, the objective is to produce tree with important biomass production and reduced lignin content. The negative r_A between growth traits and lignin content (-0.61 for height and $r_A=-0.16$ for circumference) and MFA and S/G ($r_A=-0.27$) and the positive correlation between MFA and lignin content ($0.4 < r_A < 0.74$) are favourable for pulp and paper production since the improvement in all of these traits would be simultaneously possible (Table 30). Lignins are undesirable compounds for pulp and paper production, because the delignification process requires energy and reagent consumption. In regard to its structure, high syringyl to guaiacyl ratio is advantageous for pulping (Rodrigues et al. 1999) since every unit increase in the lignin S/G ratio would roughly double the rate of lignin removal (Chang and Sarkanen 1973).

In the frame of bio-energy production, the positive genetic correlation between lignin and density (0.28) is favourable, despite the low magnitude. However, positive additive correlations between MFA and lignin (Table 30) are unfavourable for bioenergy purposes since decreasing MFA, may result in decreasing lignin content. The problem is that, for energy production, the wood may simultaneously have high lignin content and adequate mechanical properties. Charcoal is used in blast furnace for iron-steel production and has to support the weight charge of the iron feedstock during the steps of oxydo-reduction reactions at elevated temperature (higher to 1500°C) without breaking. As lignin content and its composition are key traits of *Eucalyptus* breeding programs, especially for pulp, paper and bioenergy production the high genetic control of lignin content and syringyl to guaiacyl ratio reported here (Table 28) are of major importance for tree breeders. These issues are presented and discussed in the **paper 8**.

3.6 Genetic studies from clonal test

3.6.1 Growth traits

Understanding the interaction between the genotype and the environment is increasingly becoming a key modelling element for the management of forests (Verryn 2008). Generalized linear model (GLM) was performed to analyze the clonal and environmental variance of growth traits. Results of the analyses of variance for circumference at breast height (C) and commercial height (H) for the trees from the clonal tests (not presented) showed significant ($p < 0.0001$) effect for clone, site and clone x site interaction for these growth traits ($R^2_C=0.68$ and $R^2_H=0.51$).

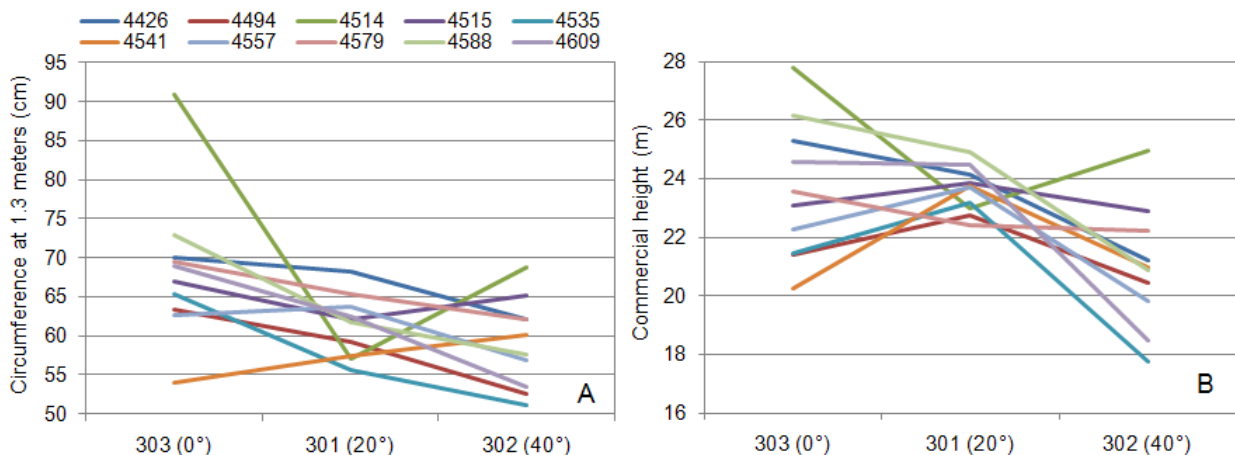


Figure 37 - Clone x site interaction for mean circumference at 1.3 meters (A) and commercial height (B) of the trees from Clonal test

Thus, multiple range tests for circumference at breast height (C) and commercial height (H) by clone and by site where performed (Table 31) in order to classify the clones and sites according to their growth traits. Clone 4514 presented the higher circumference at breast height (77.8 cm) and commercial height (26 meters) while clones 4494, 4535, 4541 and 4557 presented relatively low, but even satisfactory growth rates. The trees grow up faster on site 303 (no slope ground) presenting a circumference of 72 centimeters, on average, an elevated growth rate for trees with only six-years old.

Genotype by environmental interaction for growth traits is of particular concern to tree breeders since it determines critical decisions in developing optimal breeding strategies and realizing genetic gains. Figure 37 presents the clone x site interaction for mean circumference at 1.3 meters (A) and commercial height (B) of the 6-year-old *Eucalyptus urophylla* x *grandis* trees.

Table 31 - Tukey (HSD) multiple range tests for growth traits by clone and by site in 6-year-old *Eucalyptus urophylla* x *grandis* clones

Clone	C (cm)	H (m)
4426	66.8 ^B	23.6 ^{BC}
4494	59.2 ^D	21.7 ^{DE}
4514	77.8 ^A	26.0 ^A
4515	64.7 ^{BC}	23.3 ^{BCD}
4535	58.3 ^D	21.1 ^E
4541	57.7 ^D	21.8 ^{DE}
4557	61.5 ^{CD}	22.2 ^{CDE}
4579	66.1 ^{BC}	22.8 ^{BCD}
4588	64.5 ^{BC}	24.1 ^B
4609	62.3 ^{BCD}	22.9 ^{BCD}
Site	C (cm)	H (m)
301	61.6 ^B	23.7 ^A
302	59.8 ^B	21.2 ^B
303	72.0 ^A	24.3 ^A

Means with the same letter are not significantly different at $\alpha = 0.05$ threshold, using Tukey multiple range tests

Clone 4514 presented the higher genotype by environmental interaction for circumference. This clone presented optimal performance in growth in the Sites 303 (0 degrees) and 302 (40 degrees) but its circumference is low in site 301. This trend can be explained by possible sampling error. In general, all clones had better performance in the plane site (303), decreasing their growth rate in sloped Sites. The higher the terrain slope, the lower the growth rate, except for clone 4541 that shows an opposite trend.

Taking into account only the growth traits, clones 4514, 4426, 4579 and 4588 are the best ones, presenting superior circumference at 1.3 meters and commercial height. On the other hand, clones 4535, 4494 and 4541 showed the worst performances for growth.

3.6.2 Genetic studies from the kiln-dried scantlings

Table 32 shows the analysis of variance (GLM) for density and dynamic traits in kiln-dried scantlings. Similarly to air-dried scantlings (Table 48), there were significant differences among clones for all traits, and among clones and sites for density and shear modulus.

Table 33 lists the classification of clones and sites for density and dynamic traits of kiln-dried scantlings. Clones 4494, 4515, 4535, 4557 and 4609 presented the higher mean density values and the lower growth rates. On the other hand, clones 4426 and 4588 presented the lower densities, but their growth rates are high. In regards to the elastic modulus of scantlings, clone 4515 produced the stiffest wood while clones 4426 and 4579 produced the less rigid wood (this clones presented the higher growth rates).

Table 32 - Analysis of variance for density and dynamic traits in kiln-dried at 14% scantlings of 6-year-old *Eucalyptus urophylla* x *grandis* clones

	ρ_{14}	E_L14	$tg\delta_{14}$	E_F14	G14
Clone	$p < 0.0001$	$p < 0.0001$	$p < 0.001$	$p < 0.0001$	$p < 0.005$
Site	$p < 0.0001$	ns	$p < 0.001$	ns	$p < 0.03$
interaction	$p < 0.0001$	ns	ns	ns	$p < 0.04$
R^2	0.41	0.22	0.18	0.21	0.16

Table 33 - Tukey (HSD) multiple range tests for density and dynamic traits by clone and by site in kiln-dried at 14% scantlings of 6-year-old *Eucalyptus urophylla* x *grandis* clones

Clone	ρ_{14} (kg m ⁻³)	E_L14 (MPa)	$tg\delta_{14}$ (10 ³)	E_F14 (MPa)	G14 (MPa)
4426	496.6 ^{EF}	11,254 ^D	7.25 ^{ABC}	11,801 ^D	625.6 ^B
4494	560.2 ^{ABCD}	13,636 ^{ABC}	8.16 ^{ABC}	14,906 ^A	599.3 ^B
4514	546.9 ^{BCDE}	12,934 ^{ABCD}	7.82 ^{ABC}	13,301 ^{BCD}	680.0 ^{AB}
4515	564.7 ^{ABCD}	14,272 ^A	7.96 ^{ABC}	14,639 ^{AB}	728.5 ^{AB}
4535	578.4 ^{AB}	13,877 ^{AB}	7.07 ^{BC}	14,269 ^{BC}	778.1 ^A
4541	528.8 ^{DEF}	11,959 ^{CD}	8.37 ^{AB}	12,421 ^C	742.8 ^{AB}
4557	586.5 ^A	14,131 ^{AB}	7.88 ^{ABC}	14,515 ^{AB}	741.5 ^{AB}
4579	540.2 ^{CDE}	11,638 ^D	8.55 ^A	12,114 ^D	689.6 ^{AB}
4588	518.3 ^{EF}	12,451 ^{BCD}	6.95 ^C	12,593 ^C	678.2 ^{AB}
4609	568.5 ^{ABC}	12,490 ^{BCD}	7.58 ^{ABC}	12,833 ^{BC}	705.2 ^{AB}
Site	ρ_{14} (kg m ⁻³)	E_L14 (MPa)	$tg\delta_{14}$ (10 ³)	E_F14 (MPa)	G14 (MPa)
301	558.5 ^A	12,930 ^A	7.56 ^B	13,528 ^A	700.1 ^{AB}
302	573.4 ^A	13,044 ^A	8.38 ^A	13,355 ^A	742.2 ^A
303	518 ^B	12,610 ^A	7.45 ^B	13,042 ^A	653.3 ^B

Means with the same letter are not significantly different at $p = 0.05$ threshold, using Tukey multiple range tests

According to Muneri and Raymond (2000), as wood properties are generally under much stronger genetic control than tree growth it may be expected that the magnitude and patterns of genetic by environment interaction for wood traits (Figure 38) may differ from those observed for growth traits (Figure 37). Clone by site interaction for wood density (A) and longitudinal elastic modulus (B) of the kiln-dried scantlings is presented in Figure 38. The more inclined the terrain, the lower the growth rate. Clones 4426 and 4588 grow at fast rates but presented the lower wood density in all sites while the clones 4535 and 4557 grow slowly producing the denser woods. The lower growth rate implies an increase in wood density and

stiffness. This trend can be observed for most clones, except for the 4494, that produced the higher density in the site 303 (0 degrees) compared to densities in site 301 (20 degrees). The higher wind velocity (3.2 m/s) striking the trees from the site 301 (20°) (see Table 5, pg. 58) also can contribute to changes in wood traits.

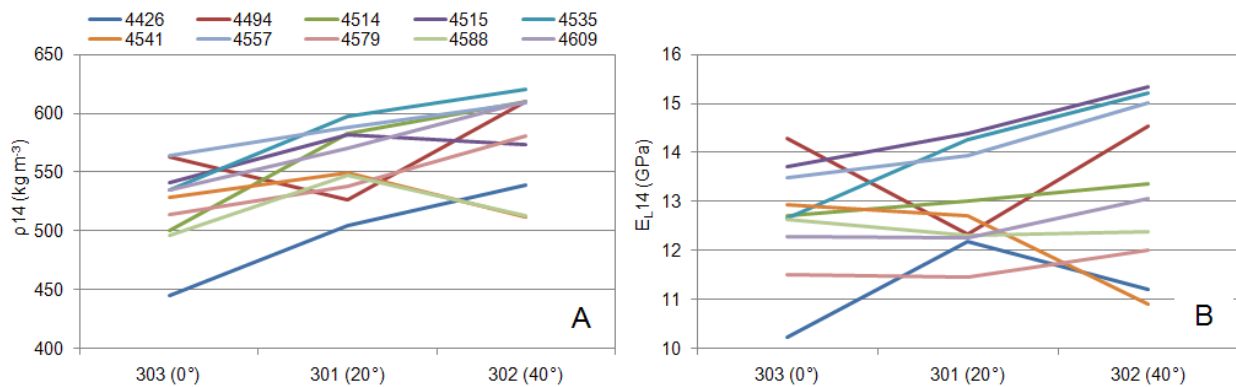


Figure 38 - Clone x site interaction for wood density (A) and longitudinal elastic modulus (B) of the kiln-dried scantlings

Resonance technique was able to simply, rapidly and at such low cost characterize the mechanical properties of these scantlings. The method permitted to rapidly estimate key wood properties (such as the modulus of elasticity, the shear modulus and the loss tangent) of the scantlings even in pieces containing knots, small cracks and also slightly damaged areas. In short, the BING system rapidly provided a large, reliable data set of mechanical wood properties as required for high-throughput phenotyping tool of genetic approaches. These results can be useful for initial classifications, screenings or preliminary selections in breeding programs of *Eucalyptus*. As reported by Burdzik and Nkwera (2002), this method proved to be fast, highly repeatable and does not require heavy equipment, making it the ideal method for on-site determining of wood stiffness at the sawmill, for instance.

3.6.3 Genetic studies from NIR-predicted data of wood discs

This study is of particular interest since very few clonal tests exist across contrasting sites and no study is known to establish the variations of basic density, stiffness and MFA of wood along the tree and to compare these variations among contrasting sites.

3.6.3.1 Spatial variation of wood traits within the tree

NIR-based models develop and presented in the NIR section were used to estimate a large data base (N= 2,550 estimates for each wood trait) of woods from clonal tests. The spatial variation of basic density, modulus of elasticity and microfibril angle along the *Eucalyptus* trees at three contrasting sites are presented in the following Tables and Figures. The codes of radial and longitudinal positions used for presenting these results are listed in Table 7 (pg. 61). Seventeen points of measure within the tree were available and to build the cartography maps, data were linearly interpolated. It is important to note that, at the base of the tree; the comparison is made using wood developed at the first years and at the sixth year while the comparison between wood traits in the top of the tree is based on wood formed exclusively at the sixth and last year of development. Furthermore, as the cylinder of juvenile wood extends from the base (0%) to the top (100%) the proportion of juvenile wood within the stem increases.

Table 34 - Radial and longitudinal variation for wood basic density (kg m^{-3}) in *Eucalyptus* clones at three contrasting sites. The means were compared by the Tukey test at $p=0.01$ threshold. Small letters are comparisons between radial positions while capital compares sites. Values in brackets are coefficients of variation in percentage

Height	Radial	303 (0°)	301 (20°)	302 (40°)	Overall
100%	outer SW ¹⁴	514.7 ^{aA}	531.2 ^{bA}	526.9 ^{bA}	524.3 ^b
100%	outer SW ¹⁵	521.6 ^{aB}	545.9 ^{abA}	530.6 ^{abAB}	532.7 ^{ab}
100%	outer SW ¹⁶	527.1 ^{aB}	548.8 ^{aA}	551.6 ^{aA}	542.5 ^a
75%	inner SW ¹¹	511.4 ^{cB}	541.7 ^{bA}	536 ^{bA}	529.7 ^c
75%	middle SW ¹²	537.8 ^{bA}	554.8 ^{bA}	548.3 ^{bA}	547.0 ^b
75%	outer SW ¹³	558.1 ^{aB}	598.9 ^{aA}	582.7 ^{aA}	579.9 ^a
50%	HW ⁸	482.0 ^{cB}	511.6 ^{cA}	503.6 ^{cA}	499.1 ^c
50%	inner SW ⁹	537.4 ^{bB}	571.1 ^{bA}	559.5 ^{bA}	556.0 ^b
50%	outer SW ¹⁰	570.7 ^{aB}	624.0 ^{aA}	616.0 ^{aA}	603.5 ^a
25%	inner HW ³	467.5 ^{cB}	496.5 ^{dA}	461.6 ^{dB}	475.2 ^d
25%	middle HW ⁴	485.5 ^{cA}	488.3 ^{dA}	489.9 ^{cA}	487.9 ^d
25%	outer HW ⁵	521.8 ^{bB}	554.5 ^{cA}	545.0 ^{bA}	540.4 ^c
25%	inner SW ⁶	563.1 ^{aB}	598.4 ^{bA}	603.0 ^{aA}	588.2 ^b
25%	outer SW ⁷	571.9 ^{aB}	629.4 ^{aA}	618.8 ^{aA}	606.7 ^a
0%	inner HW ⁰	438.7 ^{cB}	473.8 ^{cA}	470.2 ^{cA}	460.9 ^c
0%	outer HW ¹	521.6 ^{bB}	579.5 ^{bA}	557.1 ^{bA}	552.7 ^b
0%	SW ²	566.2 ^{aB}	615.3 ^{aA}	614.6 ^{aA}	598.7 ^a

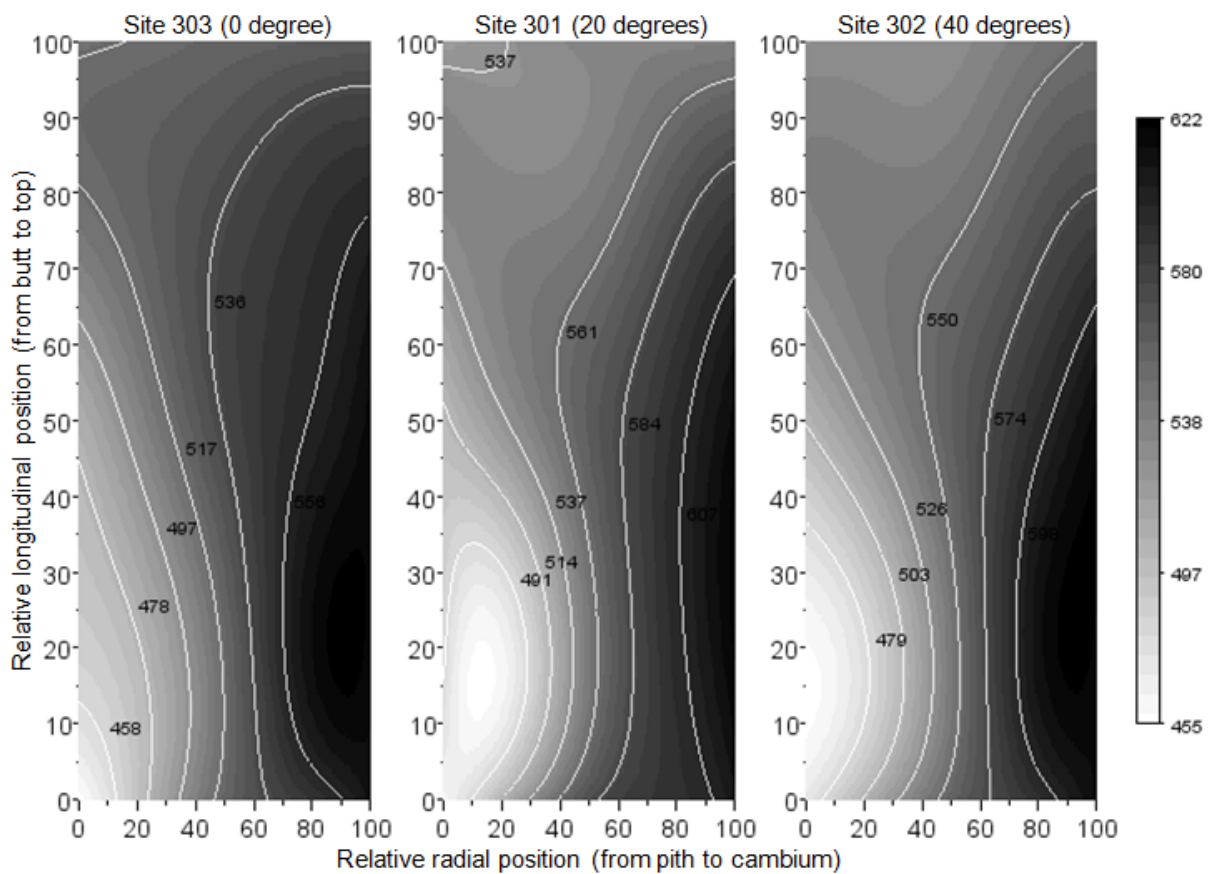


Figure 39 - Spatial variation of wood basic density (kg m^{-3}) in *Eucalyptus urophylla* x *grandis* trees

Table 35 - Radial and longitudinal variation for modulus of elasticity (MPa) in clones of *Eucalyptus* wood at three contrasting sites. The means were compared by the Tukey test at $p = 0.01$ threshold. Small letters are comparisons between radial positions while capital compares sites. Values in brackets are coefficients of variation in percentage

Height	Radial	303 (0°)	301 (20°)	302 (40°)	Overall
100%	outer SW ¹⁴	11,514 ^{bA}	11,058 ^{cAB}	10,439 ^{bB}	11,003 ^c
100%	outer SW ¹⁵	12,051 ^{abAB}	12,189 ^{bA}	11,178 ^{bB}	11,806 ^b
100%	outer SW ¹⁶	12,550 ^{ab}	13,510 ^{aA}	12,522 ^{ab}	12,861 ^a
75%	inner SW ¹¹	11,301 ^{bA}	11,268 ^{cA}	10,695 ^{cA}	11,088 ^c
75%	middle SW ¹²	13,211 ^{aA}	13,858 ^{bA}	12,416 ^{bB}	13,162 ^b
75%	outer SW ¹³	14,097 ^{ab}	16,120 ^{aA}	14,654 ^{ab}	14,957 ^a
50%	HW ⁸	10,642 ^{cA}	10,904 ^{cA}	10,522 ^{cA}	10,689 ^c
50%	inner SW ⁹	13,753 ^{bAB}	14,427 ^{bA}	13,524 ^{bB}	13,901 ^b
50%	outer SW ¹⁰	15,442 ^{ab}	17,075 ^{aA}	16,428 ^{aA}	16,315 ^a
25%	inner HW ³	10,115 ^{dA}	10,170 ^{cA}	9,333 ^{bB}	9,873 ^e
25%	middle HW ⁴	11,677 ^{cA}	11,816 ^{dA}	10,644 ^{dB}	11,379 ^d
25%	outer HW ⁵	13,656 ^{bAB}	14,358 ^{cA}	13,346 ^{CB}	13,787 ^c
25%	inner SW ⁶	15,292 ^{ab}	16,235 ^{bA}	15,692 ^{bAB}	15,740 ^b
25%	outer SW ⁷	15,876 ^{ab}	17,687 ^{aA}	16,835 ^{aAB}	16,800 ^a
0%	inner HW ⁰	6,599 ^{cB}	8,098 ^{cA}	7,832 ^{cA}	7,509 ^c
0%	outer HW ¹	10,716 ^{bA}	11,809 ^{bA}	10,998 ^{bA}	11,174 ^b
0%	SW ²	13,198 ^{aA}	14,006 ^{aA}	14,214 ^{aA}	13,806 ^a

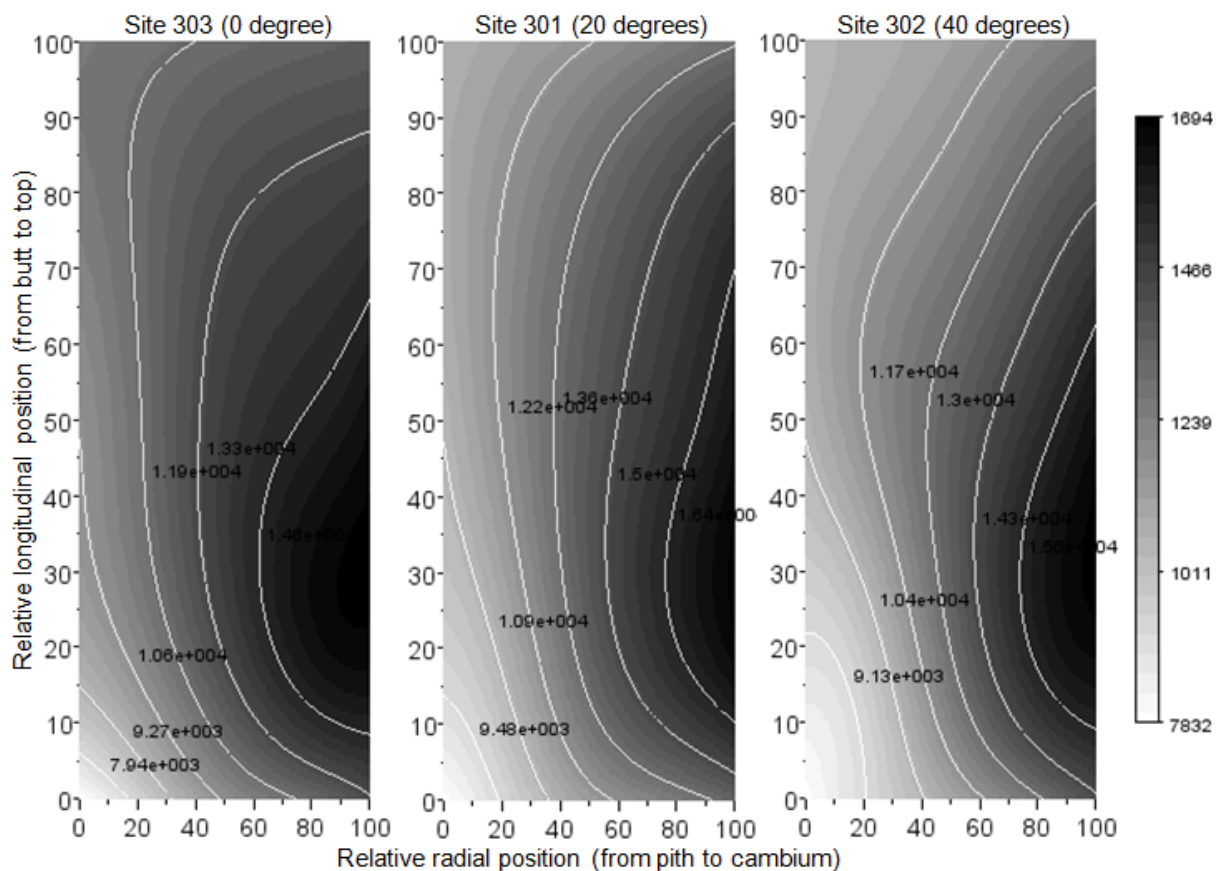


Figure 40 - Spatial variation of modulus of elasticity (MPa) in *Eucalyptus urophylla* x *grandis* trees

Table 36 - Radial and longitudinal variation for microfibril angle (degrees) in clones of *Eucalyptus* wood at three contrasting sites. The means were compared by the Tukey test at $p = 0.01$ threshold. Small letters are comparisons between radial positions while capital compares sites. Values in brackets are coefficients of variation in percentage

Height	Radial	303 (0°)	301 (20°)	302 (40°)	Overall
100%	outer SW ¹⁴	12.71 ^{aB}	13.10 ^{aAB}	13.33 ^{aA}	13.05 ^a
100%	outer SW ¹⁵	12.16 ^{bAB}	11.93 ^{bB}	12.54 ^{bA}	12.21 ^b
100%	outer SW ¹⁶	11.45 ^{cA}	10.67 ^{cB}	11.59 ^{cA}	11.24 ^c
75%	inner SW ¹¹	12.31 ^{aB}	12.71 ^{aAB}	12.88 ^{aA}	12.63 ^a
75%	middle SW ¹²	10.66 ^{bB}	10.38 ^{bB}	11.21 ^{bA}	10.75 ^b
75%	outer SW ¹³	10.03 ^{cA}	8.97 ^{cB}	9.98 ^{cA}	9.66 ^c
50%	HW ⁸	12.55 ^{aA}	12.29 ^{aA}	12.33 ^{aA}	12.39 ^a
50%	inner SW ⁹	10.15 ^{bA}	9.87 ^{bA}	10.26 ^{bA}	10.09 ^b
50%	outer SW ¹⁰	9.05 ^{cA}	8.18 ^{cB}	8.92 ^{cA}	8.72 ^c
25%	inner HW ³	12.53 ^{aA}	12.96 ^{aA}	12.53 ^{aA}	12.67 ^a
25%	middle HW ⁴	11.13 ^{bA}	11.09 ^{bA}	11.43 ^{bA}	11.22 ^b
25%	outer HW ⁵	9.88 ^{cA}	9.60 ^{cA}	9.92 ^{cA}	9.80 ^c
25%	inner SW ⁶	8.92 ^{dAB}	8.50 ^{dB}	9.06 ^{dA}	8.83 ^d
25%	outer SW ⁷	8.65 ^{dA}	7.74 ^{eB}	8.56 ^{dA}	8.31 ^e
0%	inner HW ⁰	13.18 ^{aA}	12.93 ^{aA}	12.84 ^{aA}	12.98 ^a
0%	outer HW ¹	10.78 ^{bA}	10.50 ^{bA}	10.82 ^{bA}	10.70 ^b
0%	SW ²	9.54 ^{cA}	9.12 ^{cA}	9.31 ^{cA}	9.32 ^c

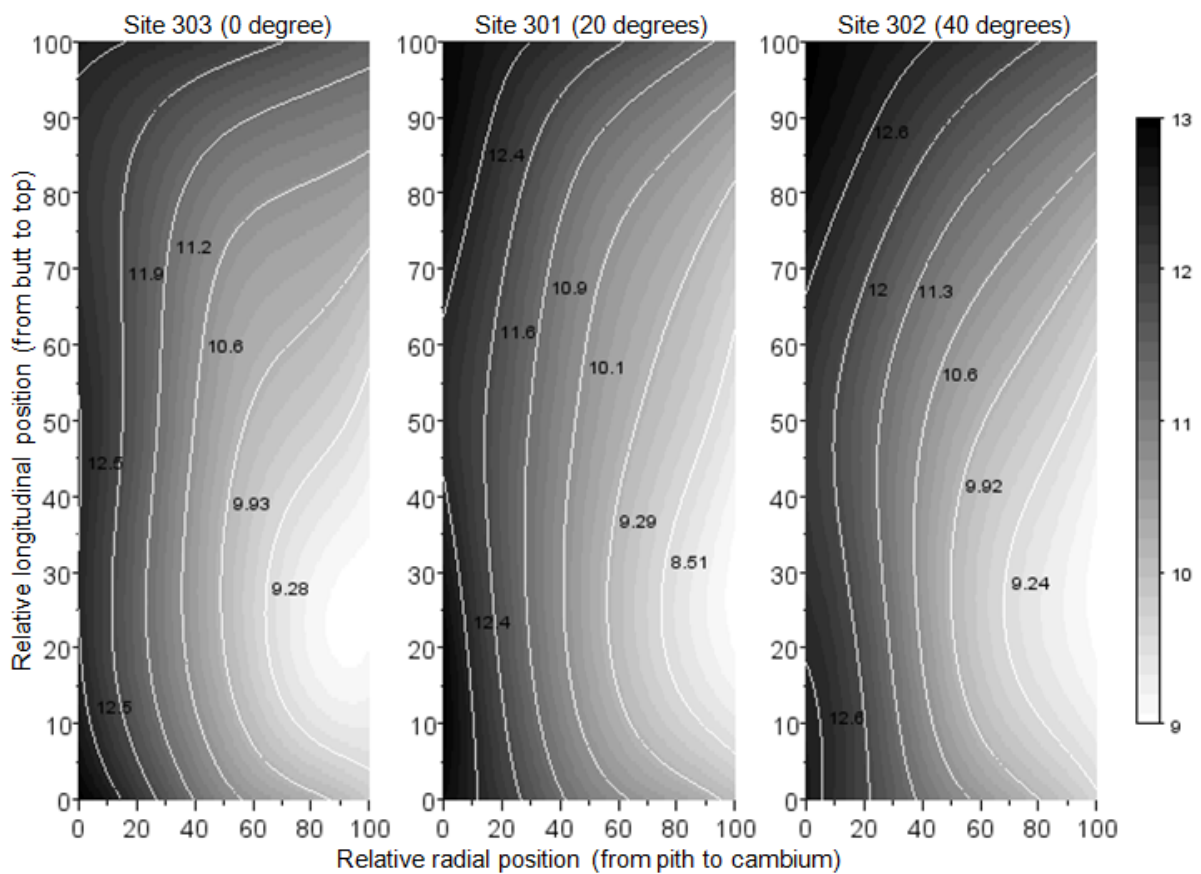


Figure 41 - Spatial variation of microfibril angle (degrees) in *Eucalyptus urophylla* x *grandis* trees.

Table 34 shows the patterns of radial and longitudinal variation in basic density of wood along the *Eucalyptus* trees. Variations in basic density of wood along the stem are less consistent than those in the radial direction (Figure 39), especially in the bottom. Overall, the wood density strongly varied from pith to cambium at the base ($\sim 140 \text{ kg m}^{-3}$) and at 25% of stem height ($\sim 130 \text{ kg m}^{-3}$). At 50% of height the trait also increased ($\sim 104 \text{ kg m}^{-3}$), but in relative low magnitude. The density slightly increased from pith to bark at 75% of height ($\sim 50 \text{ kg m}^{-3}$) and at the top of the tree the variation was of lower magnitude ($\sim 20 \text{ kg m}^{-3}$).

Figure 39 shows that the pith to cambium variation in wood density was higher in trees from the Site 302 (40°). For instance, at 25%, the radial variation was 104 kg m^{-3} in the site 303 (0°), 133 kg m^{-3} in the site 301 (20°) and 157 kg m^{-3} in the site 302 (40°). The higher the slope of the terrain, the greater the magnitude of variation in wood density.

The spatial variation of the modulus of elasticity within the *Eucalyptus* trees at the three contrasting sites is presented in Table 35 and Figure 40. The patterns of variation in modulus of elasticity and wood density were similar. Again, variations in basic modulus of elasticity along the stem are less consistent than those in the radial direction (Figure 40), especially in the bottom. Overall, the modulus of elasticity strongly increased from pith to bark at the base ($\sim 6,300 \text{ MPa}$), at 25% of height ($\sim 6,900 \text{ MPa}$), at 50% of height ($\sim 5,600 \text{ MPa}$) and at 75% of height ($\sim 3,900 \text{ MPa}$). At the top of the tree there was a significant increase ($1,800 \text{ MPa}$) but of low magnitude (Table 35). Interestingly, the stiffness at the base and at 25% of height increased in the same magnitude ($\sim 6,500 \text{ MPa}$) towards the bark, but the absolute E values at 25% of height were, on average, $2,500 \text{ MPa}$ higher. Similarly to the wood density, the variation in the top of the tree was low because these woods were produced recently, some months before the tree be harvested. The trends in spatial variation for modulus of elasticity over the contrasting sites were similar to those for density of wood.

The pith to cambium variation in wood stiffness was lower in trees from the Site 303 (0°) and higher in trees from site 301 (20°) (Table 35). For instance, at 25%, the radial variation was 7.5 GPa in the sites 301 (20°) and 302 (40°) and 5.7 GPa in the site 303 (0°). At 50% and 75% of height, the magnitude of radial variation was higher in trees from site 301 (20°) (Figure 40). These findings are interesting for sawn timber breeders because it is stiffness that is desirable rather than its constituent traits, density and MFA.

Table 36 and Figure 41 show the patterns of spatial variation in MFA of *Eucalyptus* trees. The trends in MFA were inversely similar to those for density and stiffness. The microfibril angle strongly decreased from pith to bark at 25% of height (~ 4.4 degrees). Similar decrease in MFA was observed at the base and at 50% of height (~ 3.7 degrees). A decrease in MFA of low magnitude, but significant was obtained at 75% of height (~ 3 degrees) and at the top of the tree (~ 2 degrees). In most of the positions, there was no difference between sites in MFA.

The magnitude of radial variations in MFA was higher in trees from Site 301 (20°) while the radial variation of trees from site 303 (0°) was in lower magnitude. This trend was also observed for stiffness and could be partially attributed to the higher wind velocities of Site 301. In short, for wood density, the higher the slope of the terrain, the greater the magnitude of variation in wood density and for stiffness and MFA, trees from site 301 (20°) presented the higher radial variations. These patterns of spatial variation are in accordance of those reported in numerous studies. Patterns in pith to bark variation of the traits themselves have been known for many years; wood density and stiffness generally increases while MFA decreases from pith to bark (Kollmann and Côté 1968). These variations result in wood traits becoming more advantageous for sawn timber production as trees become older.

Here, the patterns of spatial variation for basic density, stiffness and microfibril angle along the *Eucalyptus* stems indicates that variability in stems wood is not negligible, even at six years old. The interesting point of this part of the study is the establishment of the spatial variations of basic density, stiffness and MFA along the *Eucalyptus* tree and the comparison of these variations among contrasting sites.

Analyzing these results requires an important consideration: the aging of the meristematic cells that produces the cambium. At the base, the first growth ring is totally juvenile (meristem and cambium had the same age). On the other hand, the meristem had 6 years while the cambium had some months when the wood was produced in the top of these trees. The cambial juvenility is frequently less pronounced in the top. These issues are discussed in Thibaut et al. (2001). Table 37 presents the pith to cambium variation of wood density (kg m^{-3}), stiffness (GPa) and microfibril angle (degrees) at various relative heights.

Table 37 - Pith to cambium variation of wood density (kg m^{-3}), stiffness (GPa) and microfibril angle (degrees) at various relative heights.

Trait	Height	303 (0°)	301 (20°)	302 (40°)
ρ	100%	12.4	17.6	24.7
	75%	46.7	57.2	46.7
	50%	88.7	112.4	112.4
	25%	104.4	132.9	157.2
	0%	127.5	141.5	144.4
E	100%	1.04	2.45	2.08
	75%	2.80	4.85	3.96
	50%	4.80	6.17	5.91
	25%	5.76	7.52	7.50
	0%	6.60	5.91	6.38
MFA	100%	1.26	2.43	1.74
	75%	2.28	3.74	2.90
	50%	3.50	4.11	3.41
	25%	3.88	5.22	3.97
	0%	3.64	3.81	3.53

Variations in ρ along the stem were less consistent than those in the radial direction, especially in the bottom. The wood density varied 127-144 kg m^{-3} from pith to bark at the base (increasing from ~460 to ~600 kg m^{-3}) and at the top of the tree the variation were of lower magnitude (from 12 to 24 m^{-3}). The higher the slope of the terrain, the greater the magnitude of variation in wood density. Variations in E of wood along the stem were again less consistent than those in the radial direction especially at the base. E varied 5.9-6.6 GPa from pith to bark at the base (increasing from ~7.5 to ~13.8 GPa). The trends in spatial variation for E were similar to those for ρ . The pith to cambium variation in wood stiffness was lower in trees from the Site 303 (0°). However, pith to cambium variations were higher in trees from site 301 (20°) for all heights, except at the base. The MFA decreased 3.5-3.8 degrees from pith to bark at the base and 1.3-2.4 degrees at the top of the tree. The magnitude of radial variations in MFA was higher in trees from Site 301 (20°) while the radial variation of trees from site 303 (0°) was in lower magnitude. This trend was also observed for stiffness.

3.6.3.2 Clonal by environmental interaction of the wood traits

Knowledge of possible genotype by environment (G x E) interaction is vital to tree improvement if genotypes are to be planted across different environments (Zobel and Talbert, 2003). For ease of deployment, clonal performance and ranking should be predictable and stable across a range of sites, as G x E interaction can add complexity and cost to a tree improvement program (McKeand et al., 1990). Clone by site interaction for basic density, modulus of elasticity and microfibril angle in the inner heartwood (near to pith) and of the outer sapwood (near to cambium) at 25% of height are presented and discussed. The wood from this region (at 25% of tree height) was chosen because is the zone more interesting from a merchantable point of view. The radial variation of basic density of the wood at 25% of height was analyzed between clones and sites. This longitudinal position (at 25% of the tree height) was chosen because represents the most commercially valuable part of the stem. The means were compared between clones, sites and radial positions by Tukey test and the results are presented in Table 38.

Table 38 - Radial variation at 25% of the stem height for wood basic density (kg m^{-3}) for clones of *Eucalyptus* wood and sites. The means were compared by the Tukey test at $p=0.05$ threshold. Small letters are comparisons between clones or sites while capital ones compares the radial positions

Clone	inner HW ³	middle HW ⁴	outer HW ⁵	inner SW ⁶	outer SW ⁷
4426	424.1 ^{dC}	442.5 ^{dC}	482.5 ^{dB}	521.8 ^{cA}	543.6 ^{bA}
4494	474.3 ^{bcC}	493.1 ^{bcC}	548.9 ^{abcB}	625.7 ^{aA}	617.0 ^{aA}
4514	487.0 ^{abcC}	488.1 ^{bcC}	537.2 ^{bcB}	580.1 ^{abA}	600.3 ^{abA}
4515	483.3 ^{abcC}	490.9 ^{bcC}	541.8 ^{abcB}	590.6 ^{abA}	621.3 ^{aA}
4535	514.6 ^{aB}	514.7 ^{abB}	581.9 ^{abA}	605.5 ^{abA}	623.9 ^{aA}
4541	466.7 ^{cB}	474.3 ^{cB}	516.3 ^{cdB}	571.8 ^{bA}	586.3 ^{abA}
4557	505.9 ^{abcC}	531.2 ^{aC}	587.7 ^{aB}	608.4 ^{abB}	641.4 ^{aA}
4579	454.3 ^{cdC}	473.9 ^{cC}	526.0 ^{cdB}	608.7 ^{abA}	620.1 ^{aA}
4588	466.8 ^{dD}	480.7 ^{cdD}	525.7 ^{cdC}	564.7 ^{bcB}	591.7 ^{abA}
4609	474.9 ^{cdC}	489.6 ^{bcC}	556.2 ^{abcB}	604.3 ^{abA}	621.0 ^{aA}
Site	inner HW ³	middle HW ⁴	outer HW ⁵	inner SW ⁶	outer SW ⁷
301	496.5 ^{aD}	488.3 ^{aD}	554.5 ^{aC}	598.4 ^{aB}	629.4 ^{aA}
302	461.6 ^{bD}	489.9 ^{aC}	545.0 ^{aB}	603.0 ^{aA}	618.8 ^{aA}
303	467.5 ^{bc}	485.5 ^{aC}	521.8 ^{bB}	563.1 ^{bA}	571.9 ^{bA}

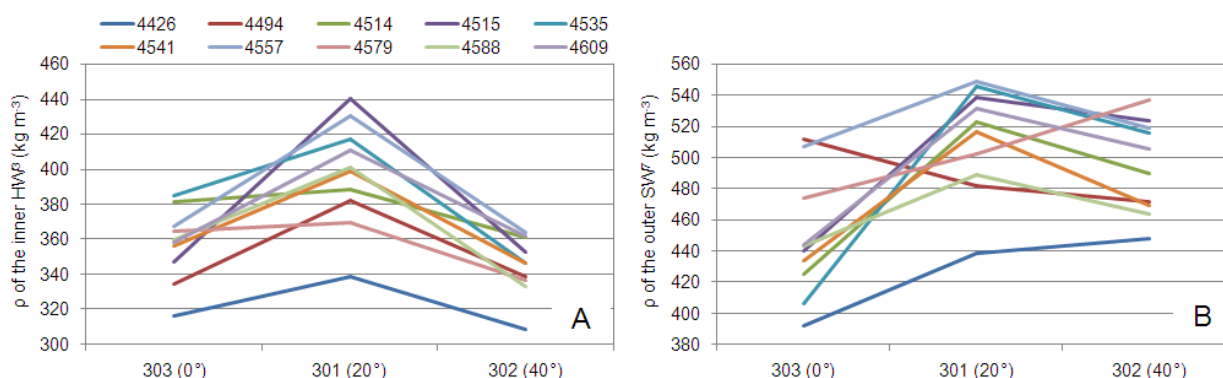


Figure 42 - Clone by site interaction for basic density of the inner heartwood (A) and of the outer sapwood (B) at 25% of height

Estimating genotype by environment interaction is necessary in proposing the basis for setting up breeding populations and selecting environmentally stable genotypes (Kien et al. 2009). Clone by site interaction for basic density of the inner heartwood and of the outer sapwood at 25% of height is presented in Figure 42. Comparing variations in genotype by environment interaction the inner heartwood and of the outer sapwood allows examining how wood traits and ranking clones varies over the years.

First, it is possible to note that, in the most of clones, site 301 (20°) produces the denser wood either at the first year (inner heartwood) or at the sixty year (outer sapwood). Site 302 (40°) produces the wood with lower densities in the inner heartwood. This finding is contrary to those reported for wood scantlings (Figure 38, pg. 109). However, the wood density of the clones from the site 302 (40°) strongly increased at the sapwood. Despite the increase of wood density near to cambium, the patterns observed from the scantlings results are still different. From the NIR-predicted data, clones planted in site 302 produced the denser woods.

The information from NIR-predicted data is more realistic and reliable because the experimental design was equilibrated, ie, each clone had its density estimated by the same NIR-based models, in the same points whereas the scantlings were sampled in a non-uniform way. 411 scantlings were taken from 150 central boards, then, the number of scantlings by site and by clone were not equivalent because of the difficulty of producing “beautiful” pieces of some clones of site 302 (40°), for example.

Second, it is important to note that clones producing the denser woods at the first year continue producing the denser woods at the sixty year (the contrary is also true). For instance, clones 4515, 4557, 4535 produces the wood with the higher densities while the clone 4426 produces lower wood density both at the first and at the last year of development. From this point of view, the findings from scantlings (Figure 38, pg. 109) and NIR-predicted wood density (Figure 42) are similar: the best (4535 and 4557) and the worst (4426) clones are the same.

Table 39 - Radial variation at 25% of the stem height for elastic modulus (MPa) for clones of *Eucalyptus* wood and sites. The means were compared by the Tukey test at $p=0.05$ threshold. Small letters are comparisons between clones or sites while capital ones compares the radial positions

Clone	inner HW ³	middle HW ⁴	outer HW ⁵	inner SW ⁶	outer SW ⁷
4426	8,279 ^{cd}	9,621 ^{cC}	11,635 ^{cB}	13,073 ^{bA}	13,776 ^{bA}
4494	9,025 ^{bcC}	10,597 ^{bcC}	13,808 ^{abB}	16,728 ^{aA}	17,593 ^{aA}
4514	10,302 ^{abC}	11,599 ^{bcC}	13,488 ^{bcB}	15,210 ^{aA}	16,287 ^{abA}
4515	10,875 ^{aC}	12,051 ^{abC}	14,573 ^{abB}	16,419 ^{aA}	17,559 ^{aA}
4535	10,829 ^{aC}	12,095 ^{abC}	14,105 ^{abB}	15,943 ^{aA}	17,151 ^{aA}
4541	9,932 ^{abD}	10,661 ^{bcCD}	12,780 ^{bcBC}	15,220 ^{aAB}	15,822 ^{abA}
4557	11,332 ^{aD}	13,533 ^{aC}	15,675 ^{aB}	16,859 ^{aAB}	18,057 ^{aA}
4579	9,022 ^{bcC}	10,741 ^{bcC}	13,677 ^{bB}	16,272 ^{aA}	17,387 ^{aA}
4588	9,023 ^{bcE}	11,207 ^{bcD}	13,535 ^{bcC}	15,229 ^{aB}	16,751 ^{aA}
4609	10,107 ^{abD}	11,686 ^{bcC}	14,589 ^{abB}	16,444 ^{aA}	17,613 ^{aA}
Site	inner HW ³	middle HW ⁴	outer HW ⁵	inner SW ⁶	outer SW ⁷
301	10,170 ^{aE}	11,816 ^{aD}	14,358 ^{aC}	16,235 ^{aB}	17,687 ^{aA}
302	9,333 ^{bE}	10,644 ^{bD}	13,346 ^{bC}	15,692 ^{abB}	16,835 ^{abA}
303	10,115 ^{aD}	11,677 ^{aC}	13,656 ^{abB}	15,292 ^{bA}	15,876 ^{bA}

The radial variation of wood stiffness at 25% of the tree height between clones and sites was examined and the means between clones, sites and radial positions were compared by Tukey test (Table 39). As the tree ages, it produces stiffer wood. Table 39 shows significant increase in wood stiffness according to the radial positions. Modulus of elasticity ranged from 8 to 12 GPa in the wood near to the pith and from 13 to 20 GPa near to the cambium.

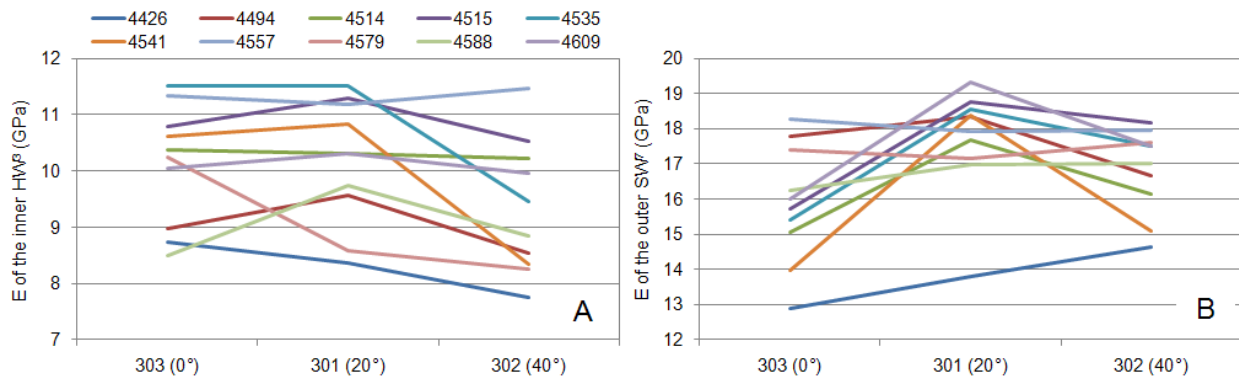


Figure 43 - Clone by site interaction for longitudinal elastic modulus of the inner heartwood (A) and of the outer sapwood (B) at 25% of height

Figure 43 presents the genotype by environment interaction for wood stiffness of the inner heartwood and outer sapwood at 25% of height. Some of the clones (4557, 4609, and 4514) present stable values of elastic modulus independently of the environment where they grow, but the ranking of the most of clones is very confusing at the first year (inner heartwood). Again, the wood of clone 4426 presented the lowest stiffness (and wood density) in the first and last years of development (but grows at fast rates). It is clear that site 301 (20°) favors the production of stiffer (and denser) woods for most of clones. The clones producing the stiffer woods at the first year continues producing the stiffer woods at the sixty year. Similarly to trends in wood density, the results obtained from the scantlings (Figure 38, pg. 109) and NIR-predicted wood density (Figure 43) indicated the same clone ranking: clones 4515, 4535 and 4557 are among the top ones while clone 4426 is again the less stiff. Both resonance and NIR spectroscopy indicates the same classification of clones, however, the ranking indicated by NIR spectroscopy analyses is more consistent.

Table 40 presents the radial variation between clones and sites of microfibril angle at 25% of the tree height. The means between clones, sites and radial positions were compared by Tukey test. As the tree ages, the microfibril angle of the cell wall of its wood significantly decrease towards the bark. For some clones, notably the 4426, 4494, 4514 and 4535, the decrease from pith to bark of microfibril angles is less accentuated.

The genotype by environment interaction for microfibril angle of the inner heartwood and of the outer sapwood at 25% of height is presented in Figure 44. Interestingly, site 302 favors the highest MFA when the trees were young and the lowest MFA when the trees reached six years old. In short, the wood of the clones growing at site 302 presented the highest variability.

This part of the study showed the size and importance of genotype by environment interactions for wood density, stiffness and microfibril angle. As stated by Muneri and Raymond (2000), this is a critical issue for designing tree breeding programs and making decisions about plantation establishment.

Table 40 - Radial variation at 25% of the stem height for microfibril angle (degrees) for clones of *Eucalyptus* wood and sites. The means were compared by the Tukey test at $p=0.05$ threshold. Small letters are comparisons between clones or sites while capital ones compares the radial positions

Clone	inner HW ³	middle HW ⁴	outer HW ⁵	inner SW ⁶	outer SW ⁷
4426	12.36 ^{abA}	11.09 ^{abB}	9.79 ^{abcC}	9.24 ^{aC}	9.09 ^{aC}
4494	12.73 ^{abA}	11.78 ^{aA}	9.83 ^{abcB}	8.56 ^{abC}	7.95 ^{abcC}
4514	13.39 ^{aA}	11.52 ^{abB}	10.57 ^{abB}	9.53 ^{aC}	9.05 ^{aC}
4515	12.47 ^{abA}	11.25 ^{abB}	9.48 ^{bcC}	8.22 ^{bD}	7.85 ^{abcD}
4535	12.55 ^{abA}	11.20 ^{abB}	10.35 ^{abB}	9.27 ^{aC}	8.43 ^{abcC}
4541	12.54 ^{abA}	11.27 ^{abB}	10.16 ^{abBC}	9.02 ^{abCD}	8.90 ^{abD}
4557	12.06 ^{bA}	10.10 ^{bB}	9.06 ^{cC}	8.10 ^{bD}	7.49 ^{cdD}
4579	12.62 ^{abA}	11.01 ^{abB}	8.96 ^{cC}	8.13 ^{bCD}	7.77 ^{bcD}
4588	13.35 ^{aA}	11.87 ^{abB}	10.26 ^{abC}	9.54 ^{aC}	8.61 ^{abcD}
4609	12.66 ^{abA}	11.09 ^{abB}	9.54 ^{abcC}	8.67 ^{abD}	8.02 ^{abcD}
Site	inner HW ³	middle HW ⁴	outer HW ⁵	inner SW ⁶	outer SW ⁷
301	12.96 ^{aA}	11.09 ^{abB}	9.60 ^{aC}	8.50 ^{bD}	7.74 ^{bE}
302	12.53 ^{aA}	11.43 ^{abB}	9.92 ^{aC}	9.06 ^{aD}	8.56 ^{aD}
303	12.53 ^{aA}	11.13 ^{abB}	9.88 ^{aC}	8.92 ^{abD}	8.65 ^{aD}

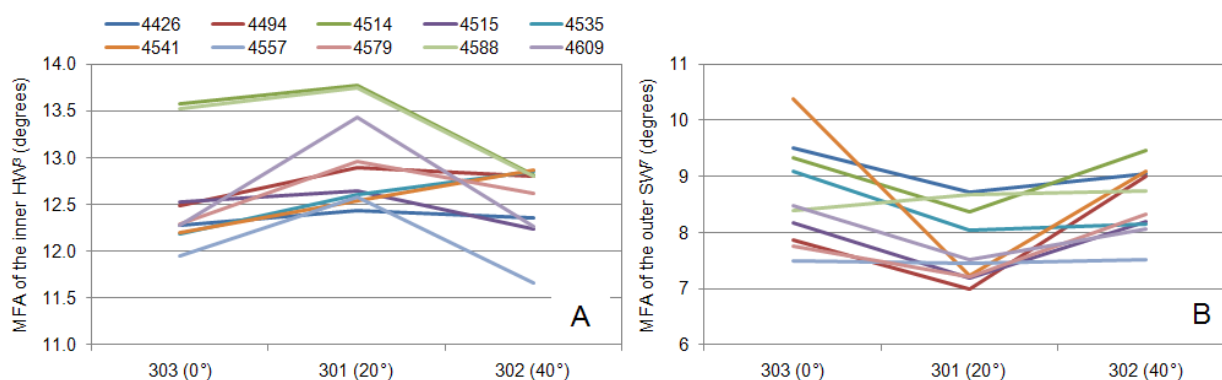


Figure 44 - Clone by site interaction for microfibril angle of the inner heartwood (A) and of the outer sapwood (B) at 25% of height

3.6.3.3 Genetic control over growth and wood traits in *Eucalyptus*

From the NIR-estimated dataset, the genetic (σ^2_G), residual (σ^2_E) and genetic by residual interaction ($\sigma^2_{G \times E}$) variance components were estimated by Restricted Maximum Likelihood (REML) method. Thus, broad-sense heritability estimates (H^2) for growth traits and basic density of wood, elastic modulus and microfibril angle at various relative heights and radial positions were calculated. For growth traits, the BIC values of the model with GxE interaction (Eq. 37) were much lower than those from models with interaction indicating that genetic control over growth traits may be evaluated by this Equation although the lower estimates. The heritability estimates of wood traits were calculated with the Equation 38, without the variance due to interaction effects. The coefficient of phenotypic variation, the genetic, residual and interaction variance components and broad-sense heritability estimates for growth traits are given in Table 41. Growth traits are under low genetic control in this clonal test

Table 41 - Genetic parameters for growth traits in 6-year-old *Eucalyptus urophylla* x *grandis* clones

Model	Trait	CV (%)	σ^2_G	$\sigma^2_{G \times E}$	σ^2_E	H ²	SE H ²
Y = μ + G + G*E + E Eq. 37	C	16.0	2.349	5.428	7.053	0.065	0.082
	H	14.3	0.691	1.335	2.489	0.056	0.071
Y = μ + G + E Eq. 38	C	16.0	3.749	-	8.304	0.169	0.087
	H	14.3	0.997	-	2.712	0.119	0.073

Y - trait; μ - mean; G - genetic effect; E - environmental (residual) effect and G*E - interaction effect

Estimates of broad-sense heritability (H²) for basic density of wood, elastic modulus and microfibril angle in various relative heights and radial positions are presented below. The patterns spatial variation in the genetic control over basic density, wood stiffness and microfibril angle within the *Eucalyptus* trees are represented in Figure 45. These plots present the heritability estimates taking into account the genetic by environmental interaction (Eq. 37). The coefficient of phenotypic variation, the genetic, residual and interaction variance components and broad-sense heritability estimates (Eq. 37, with GxE interaction) for basic density, wood stiffness and microfibril angle at various relative heights and radial positions are listed in following Tables.

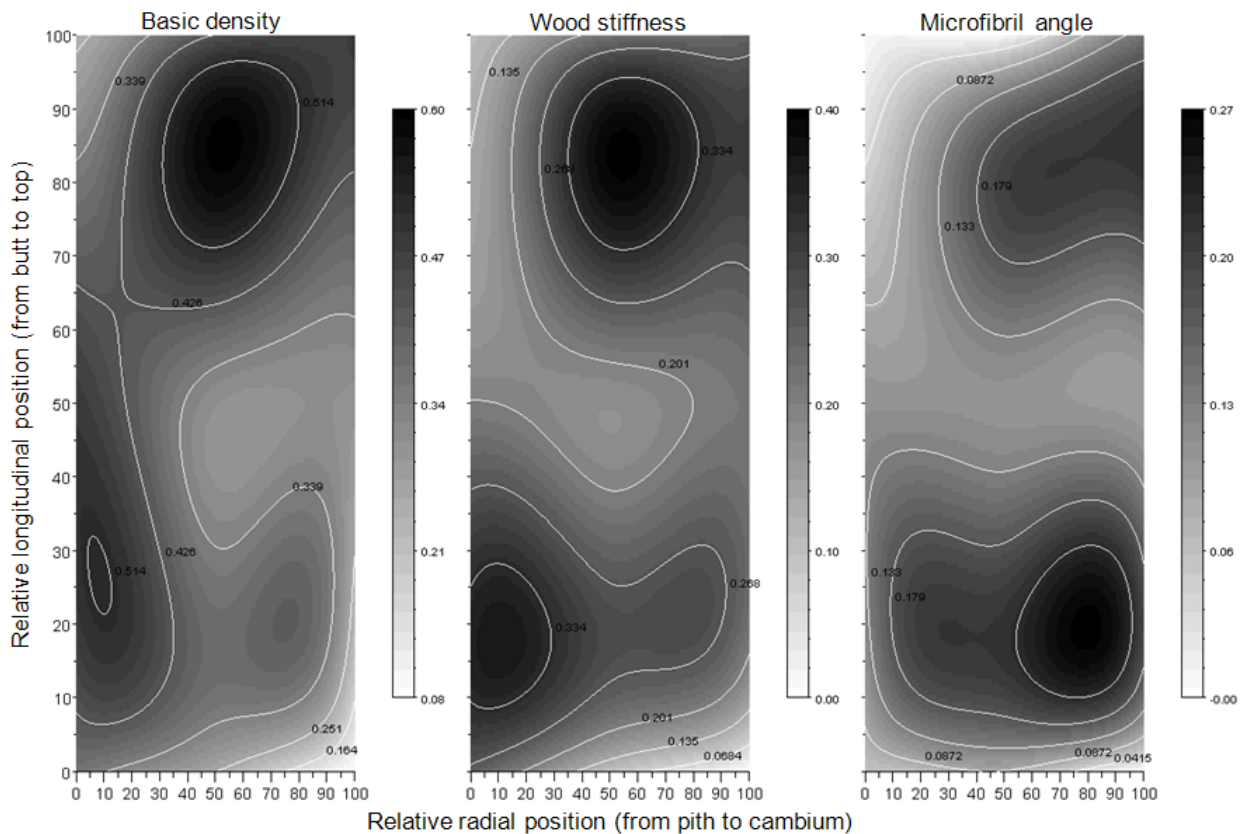


Figure 45 - Spatial variation of heritability estimates over basic density of wood, wood stiffness and microfibril angle within *Eucalyptus* trees

Table 42 - Genetic parameters for basic density of the wood in 6-year-old *Eucalyptus urophylla* x *grandis*

Height	Radial position	CV (%)	σ^2_G	$\sigma^2_{G \times E}$	σ^2_E	H ²	SE H ²
100%	inner HW ¹⁴	12.5	20.09	11.51	34.13	0.237	0.116
	outer HW ¹⁵	11.9	26.69	14.07	27.38	0.429	0.139
	SW ¹⁶	10.8	26.04	0.01	27.11	0.480	0.128
75%	inner HW ¹¹	12.8	27.71	4.93	34.80	0.383	0.130
	outer HW ¹²	10.8	28.78	1.74	25.90	0.551	0.129
	SW ¹³	10.3	24.88	12.86	27.78	0.398	0.134
50%	inner HW ⁸	10.8	28.13	14.51	25.19	0.484	0.146
	outer HW ⁹	9.7	23.23	15.34	31.39	0.307	0.121
	SW ¹⁰	12.2	23.94	9.89	35.56	0.296	0.119
25%	inner HW ³	11.2	24.19	10.49	22.07	0.495	0.138
	middle HW ⁴	8.8	22.66	7.76	22.89	0.468	0.139
	outer HW ⁵	11.3	28.96	9.52	37.16	0.363	0.126
	inner SW ⁶	11.3	28.59	3.32	34.70	0.402	0.137
	outer SW ⁷	12.6	24.05	15.32	39.91	0.240	0.110
0%	inner HW ⁰	10.2	25.52	14.78	30.11	0.367	0.131
	outer HW ¹	12.7	32.86	19.20	53.12	0.253	0.112
	SW ²	11.7	12.51	20.98	38.18	0.076	0.074

Table 43 - Genetic parameters for dynamic longitudinal modulus of elasticity of the wood in 6-year-old *Eucalyptus urophylla* x *grandis*

Height	Radial position	CV (%)	σ^2_G	$\sigma^2_{G \times E}$	σ^2_E	H ²	SE H ²
100%	inner HW ¹⁴	19.3	682.5	238.6	1974.9	0.105	0.077
	outer HW ¹⁵	17.1	947.1	849.2	1567.6	0.220	0.112
	SW ¹⁶	15.4	973.2	624.0	1586.4	0.246	0.121
75%	inner HW ¹¹	17.3	736.5	623.8	1676.2	0.145	0.078
	outer HW ¹²	13.1	1001.8	600.8	1182.6	0.363	0.131
	SW ¹³	15.0	1145.9	842.0	1573.6	0.292	0.117
50%	inner HW ⁸	15.1	734.0	447.8	1385.2	0.203	0.103
	outer HW ⁹	12.5	724.3	702.3	1397.5	0.177	0.098
	SW ¹⁰	13.1	959.1	584.0	1735.9	0.215	0.097
25%	inner HW ³	16.5	934.2	201.1	1304.5	0.334	0.117
	middle HW ⁴	15.7	1000.3	260.1	1412.2	0.327	0.121
	outer HW ⁵	14.0	995.0	303.5	1608.1	0.270	0.110
	inner SW ⁶	12.5	1042.7	0.6	1658.3	0.283	0.119
	outer SW ⁷	14.4	1128.7	330.3	2035.3	0.231	0.108
0%	inner HW ⁰	27.0	995.7	685.4	1549.9	0.257	0.121
	outer HW ¹	21.8	771.3	806.0	2163.1	0.100	0.073
	SW ²	16.0	93.8	1086.1	1911.4	0.002	0.055

Table 44 - Genetic parameters for microfibril angle of cell wall of wood in 6-year-old *Eucalyptus urophylla* x *grandis* clones

Height	Radial position	CV (%)	σ^2_G	$\sigma^2_{G \times E}$	σ^2_E	H ²	SE H ²
100%	inner HW ¹⁴	9.5	0.001	0.107	1.213	0.000	0.000
	outer HW ¹⁵	8.4	0.059	0.477	0.891	0.003	0.048
	SW ¹⁶	9.4	0.378	0.331	0.861	0.144	0.096
75%	inner HW ¹¹	7.8	0.239	0.289	0.897	0.060	0.059
	outer HW ¹²	8.7	0.390	0.350	0.709	0.196	0.102
	SW ¹³	12.7	0.507	0.517	0.895	0.194	0.125
50%	inner HW ⁸	7.7	0.323	0.178	0.888	0.113	0.079
	outer HW ⁹	8.2	0.277	0.183	0.757	0.112	0.072
	SW ¹⁰	12.2	0.322	0.271	0.918	0.101	0.077
25%	inner HW ³	7.6	0.341	0.000	0.895	0.127	0.080
	middle HW ⁴	8.5	0.435	0.101	0.849	0.205	0.104
	outer HW ⁵	10.3	0.461	0.326	0.850	0.204	0.096
	inner SW ⁶	11.2	0.495	0.323	0.786	0.253	0.112
0%	outer SW ⁷	14.0	0.480	0.370	0.926	0.188	0.106
	inner HW ⁰	8.7	0.283	0.231	1.072	0.062	0.063
	outer HW ¹	12.3	0.388	0.445	1.189	0.086	0.067
	SW ²	11.0	0.000	0.521	0.886	0.000	0.000

It is important to note that in the base of stem it is possible to compare genetic effects on wood developed at the first, third and sixth year of development. Then, the temporal difference between each H² estimate at the base of the stem is approximately of two years whereas the three H² estimates of the top of the tree refer to wood developed at the same year differing only some months.

Low to moderate levels of broad-sense heritability estimates (from 0.07 to 0.55) were found for basic density of wood within the stem of 6-year-old *Eucalyptus* clones (Table 42). The longitudinal variations in H² estimates were more consistent than those in radial direction (Figure 45), especially in the highest parts of the stem. The darker the graph, the higher the H² estimates. At 25% of tree height heritability estimates is higher near to pith and in the top, but no clear trends of spatial variation could be defined. For instance, the H² estimates linearly decreased from 0.37 near the pith to 0.08 near to the cambium in the base of the stem (0% of the commercial height) while the H² estimates increased from 0.24 to 0.48 on the top of the tree (Table 42). The higher H² estimate was found at 75% of tree height in the intermediate radial position.

The broad-sense heritability estimates for modulus of elasticity strongly varied within the stem (Table 43). Null heritability was found in the sapwood of the base while H² of 0.36 was estimated in the outer heartwood at 75% of height. Figure 45 shows that genetic control over stiffness is larger in two regions of the stem: (i) in the inner heartwood region (0-25% of relative radial position) of the lower zones of the tree (10-30% of the relative longitudinal position) (dark and round spot at the bottom of the chart) and (ii) at the top of the tree, a zone localized at 40-80% of relative radial position and at 70-90% of the relative longitudinal position (dark and round spot at the top of the chart). Again, no clear patterns of radial variation were established for H² estimates of E_L along the tree. For instance, the heritability of E_L increased from zero to 0.26 towards the cambium at the base of the stem and from 0.10 to 0.24 at the top while the H² estimates remains constant at 50% of height (Table 43). A linear decrease (from 0.33 to 0.23) was observed at 25% of height.

Genetic control over MFA exhibits variable patterns of variation presenting values from 0 to 0.25 (Table 44). The heritability estimates is low in the base and in the top of the tree and at 50% of the tree height ($H^2=0.11$). Figure 45 shows that genetic control over microfibril angle is superior in the sapwood region (60-100% of relative radial position) of the lower zones of the tree (10-30% of the relative longitudinal position) (dark and round spot at the bottom of the chart) and at the higher zones of the stem near to the cambium (dark spot at the top of the chart).

In short, Figure 45 clearly reveals that heritability estimates for D and E_L exhibited similar patterns of radial variation in the bottom of the tree, and similar trends towards the top. MFA shows opposite trends of spatial variation (mirror effect at radial direction). For density and stiffness, higher H^2 estimates were found in the higher regions of the tree, especially at the intermediate zone (dark spot at the top of the chart).

The results of heritability estimates for these wood traits from the Equation 38 (without the genotype by site interaction) are presents in the annexes section (item 6.6, pg.144).

Biological significance

The results have shown that the genetic control of MFA, stiffness and density also changes from pith to bark and from the base to top of the tree. The variation patterns of the genetic parameters in *Eucalyptus* traits have not been often reported. The estimation of genetic parameters at different ages and heights allows observation of variation of genetic control over wood traits with age. This kind of results can also be helpful when defining the optimal selection age for each species of interest.

In the base of stem, heritability estimates of wood density decreased towards the bark. These findings appear to indicate that there is more genetic control in determining the wood density in the first years, whereas the sapwood seems more likely to be controlled by external factors. Despite the low magnitude of the values, this makes biological sense. At the beginning of its development, the trees can easily find water, light and mineral nutrients and the genetic factors are the most important determinant for the tree development. As trees become older, the competition between them for light, water and space begun to take place and thus the environmental conditions increases their influence on the growth of trees at the base of the stem. On the other hand, Figure 45 clearly shows that there is more genetic control in determining the wood density from 50% of the tree height (at six years).

The heritability estimates of wood stiffness decreased towards the cambium in lower zones of the stem (Figure 45) indicating that there is more genetic control in determining the wood stiffness in the beginning of tree growth whereas the sapwood seems more likely to be controlled by external factors. When the tree reaches 5 to 6 years, there is more genetic control in determining the wood stiffness in the top of the tree. As discussed above, the genetic control over microfibril angle show opposite trends in radial variation, indicating that tree genetically controls variations in wood density, wood stiffness and microfibril angle in specific regions of the stem and at different periods (during wood development) in order to adapt the properties of its wood to support the ever-increasing weight of the stem, gravity, and wind forces.

That there exists mechanisms for controlling MFA is evidenced by the beautifully ordered structure of the secondary wall in fibers, the purposeful change from a large MFA conferring flexibility on the young stem to a small MFA conferring stiffness on the older stem, the frequent inverse relationship between cell length and MFA and the ability of the tree to over-ride this relationship in producing reaction wood (Barnett and Bonham 2004). At the same time, trees produce stiffer and denser woods at the stem periphery in order to support the external forces. The trends presented in this study revealed that part of these variations in wood density; wood stiffness and MFA are governed by genetic factors.

3.6.4 NIR spectral heritability estimates

NIR spectra contain a lot of information about wood, this complex three-dimensional biopolymer material composed of an interconnected network of cellulose, hemicelluloses, lignins and extractives. Considering a NIR spectrum as a source of information concerning many wood traits (it is based on chemical content), genetic parameters were calculated from them. The genetic (σ^2_G), residual (σ^2_E) and genetic by residual interaction ($\sigma^2_{G \times E}$) variance components were estimated by Restricted Maximum Likelihood (REML) method from the NIR spectra data. Thus, broad-sense heritability estimates (H^2) for NIR spectra in radial and longitudinal positions were calculated using the model described within the item.2.4.3.2 (pg. 72). Figure 46 presents the broad-sense NIR spectral heritability estimates at the base (A) and at 25% of the tree height (B) while Figure 47 presents the NIR spectral H^2 estimates at 50% (A), 75% (B) and at 100% (C) of the commercial height. The radial variation of broad-sense heritability estimates of the NIR spectra at the base and at 25% of the tree height is presented by the gradient colors (Figure 46).

The analysis of the NIR spectra heritability estimates by wavenumber plot is useful to investigate the underlying relationships that have made the estimation of genetic parameters possible by NIR spectroscopy. The assignments of absorption bands (Table 26, pg. 96) are useful to identify which wood components presents higher broad-sense heritability estimates from NIR spectroscopic data. It helps to understanding how NIR spectroscopy can evaluate genetic control over wood traits.

Some ranges of the NIR spectra presented heritability estimate greater than 50%. This means that NIR spectra are able to capture the potential genetic of some chemical components and wood traits indirectly. The bands normally associated with cellulosic or lignin type biomolecules may be observed in the near-infrared (NIR) spectra of wood.

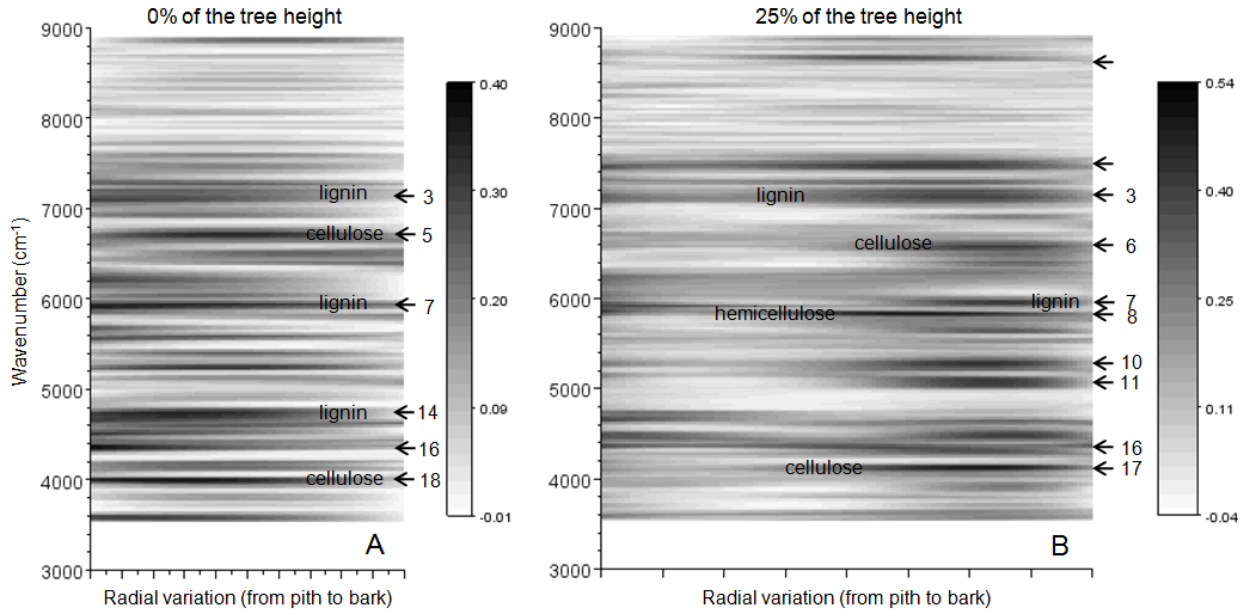


Figure 46 - Spatial variation of NIR spectral broad-sense heritability estimates at the base and at 25% of the tree height. The bands normally associated to cellulose, hemicelluloses and lignin are indicated by numbered narrows (these index are presented in Table 26, pg. 96)

In the base of the stem (Figure 46), variation in the bands around 4,060 (index 18), 4,540 (index 14), 5,950 (index 7) and at 7,085 cm⁻¹ (index 3) can be mainly attributed to genetic factors because the high values of H^2 estimates. At 25% of height, bands corresponding to index 3, 6, 7, 8 and 17 yielded high NIR spectra

heritability estimates. These bands are normally associated to cellulose and lignin contents, as indicated by numbered arrows within the plot. The bands were assigned to chemical compounds of the wood based on the Table 26 (pg. 96) and these information are also listed in Workman and Weyer (2007). At 50, 75 and 100% of the tree height (Figure 47), NIR spectral heritability estimates are systematically strong at bands around 5,000-5,600 (including index 9, 10 and 11) and 7,000-7,600 (including index 2, 3 and 4).

The band at 6831cm⁻¹ (close to the index 5) is associated to O-H polymeric (2νO-H) and is assigned to cellulose type I. The NIR spectral heritability estimates also were high at 5,669 cm⁻¹ (close to index 9) and this band is associated to functional grouping CH₂: stretching (2ν) being related to cellulose content (Workman and Weyer 2007). The band 5,553 cm⁻¹ is associated to O-H stretching plus 2x C-O stretching combination, and the band at 4,313 cm⁻¹ (close to index 16) belongs to functional grouping CH stretching plus CH₂ deformation combination, both related to the cellulose content of the wood.

According to Workman and Weyer (2007) lignin is representative of aromatic natural product compounds. The band at 7,180 cm⁻¹ (close to index 3) is associated to C-H (2νCH₂ and δCH₂) and is interrelated to lignin content. The band at 5,940 cm⁻¹ (close to index 7) belongs to functional grouping C-H (2ν), ArcC-H: C-H aromatic associated to C-H, also related to lignin content. The NIR spectral heritability estimates also were high at 4,585 cm⁻¹ and this band (close to index 14) is associated to C-H stretching and C=O combination related to lignin content of wood (Workman and Weyer 2007).

It appears that variations in the indicated bands (index 5, 6, 9, 17 and 18) can be attributed to variations in genetic control over cellulose content of wood while variations in the indicated bands (index 3, 14 and 17) are attributed to variations in heritability estimates of lignin content of the wood within the stem.

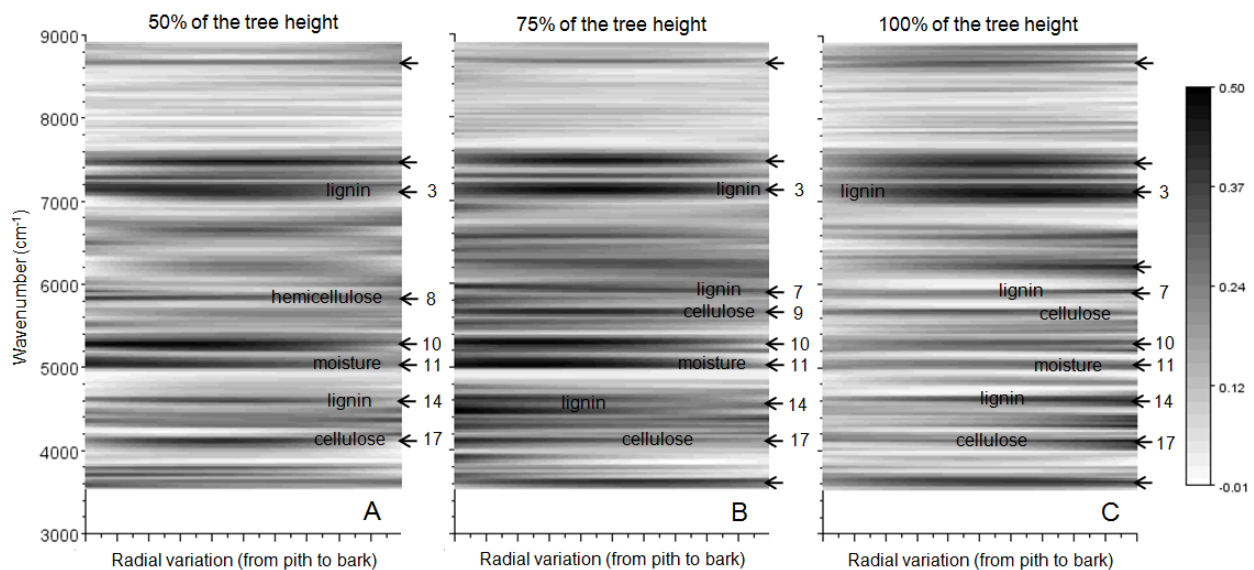


Figure 47 - Spatial variation of NIR spectral broad-sense heritability estimates at 50, 75 and 100% of the tree height. The bands normally associated to cellulose, hemicelluloses and lignin are indicated by numbered narrows (these index are presented in Table 26, pg. 96)

Indeed, Figure 46 and Figure 47 clearly reveal that the variations of some specific ranges of the NIR spectra are controlled by genetic factors. These variations in NIR spectra are supposed to be related to variation in lignin and cellulose and hemicelluloses contents. Complex combination in these specific bands may be related to variation in basic density, modulus of elasticity, MFA and other wood traits, but establishing assumption about the genetic control over these non-chemical wood traits from these NIR spectral heritability estimates is a complicated issue.

However, as NIR spectra is a countless source of information concerning chemical, mechanical, physical and ultrastructural properties of wood indirectly, the analysis of genetic parameters from NIR spectra of wood appears to be an efficient and promising way to indirectly evaluate the genetic control over many wood traits at once.

4 CONCLUDING REMARKS

4.1 Spatial variation of wood traits

In the *Eucalyptus* from **progeny tests**, the basic density of wood increased while MFA decreased towards the bark. The MFA decreased from ~18 degrees near to the pith to 13.3 degrees near to the bark. The basic density of the wood increased from ~440 kg m⁻³ near to the pith to ~615 kg m⁻³ near to the bark. These variations were observed at 1.3 meter of the tree height.

This study established spatial variations of basic density, stiffness and MFA of wood along the tree and compared these variations within trees across contrasting sites in the *Eucalyptus* from **clonal plantations**. The patterns of spatial variation for basic density, stiffness and microfibril angle along the *Eucalyptus* stems indicates that variability in stems wood is not negligible, even at six years old. In general, the basic density and stiffness of wood increased while MFA decreased towards the bark.

In short, for wood density, the higher the slope of the terrain, the greater the magnitude of variation in wood density and for stiffness and MFA, trees from site 301 (20°) presented the higher radial variations. There were significant differences between clones, but general trends could be described as follows:

Wood density: variations in basic density of wood along the stem are less consistent than those in the radial direction, especially in the bottom. The wood density strongly varied from pith to bark at the base (from ~460 to ~600 kg m⁻³) and at 25% of stem height (from ~450 to ~605 kg m⁻³). At 50% of height the trait also increased (~500 to ~600 kg m⁻³), but in relative low magnitude. The density slightly increased from pith to bark at 75% of height (from ~530 to ~580 kg m⁻³) and at the top of the tree the variation was of lower magnitude (from ~525 to ~540 kg m⁻³). The terrain slope influenced the variations in wood density. The higher the slope of the terrain, the greater the magnitude of variation in wood density.

Wood stiffness: again, variations in modulus of elasticity of wood along the stem are less consistent than those in the radial direction (Figure 40), especially in the bottom. The elastic modulus strongly increased from pith to bark at the base (from ~7.5 to 13.8 GPa), at 25% of height (from ~9.9 to ~16.8 GPa), at 50% of height (from ~10.7 to ~16.3 GPa) and at 75% of height (from ~11.1 to ~14.9 GPa). At the top of the tree there was a significant increase (from 11 to 12.8 GPa) but of low magnitude. Interestingly, the stiffness at the base and at 25% of height increased in the same magnitude (~6.5 GPa) towards the bark, but the absolute E values at 25% of height were, on average, 2.5 GPa higher. The trends in spatial variation for modulus of elasticity were similar to those for density of wood. The pith to cambium variations in wood stiffness were lower in trees from the Site 303 (0°). However, pith to cambium variations were higher in trees from site 301 (20°) for all heights, except at the base. The higher pith to bark variation at the base was found in trees from the Site 303 (0°).

Microfibril angle: The MFA decreased from pith to bark at the base (from ~13 to ~9.3 degrees), at 25% of height (from ~12.7 to ~8.3 degrees) and at 50% of height (from ~12.4 to ~8.7 degrees). A decrease in MFA of low magnitude, but significant was obtained at 75% of height (from ~12.6 to ~9.7 degrees) and at the top of the tree (from ~13 to ~11.2 degrees). In most of the positions, there was no difference between sites in MFA. The magnitude of radial variations in MFA was higher in trees from Site 301 (20°) while the radial variation of trees from site 303 (0°) was in lower magnitude. This trend was also observed for stiffness.

It is important to note that, at the base of the tree, the comparison is made using wood developed at the first year and wood produced at the sixty year while the comparison between densities in the top of the tree is based on wood formed exclusively at the sixty and last year of development. As the cylinder of juvenile wood extends from the base (0%) to the top (100%) the proportion of juvenile wood over the cross-section of the stem increases.

4.2 Influence of MFA on wood traits

The relationships among wood traits were investigated in *Eucalyptus* wood. In the trees from the **progeny tests**, there was no significant correlation between microfibril angle and basic density of wood.

For the trees from the **clonal tests**, there were weak to strong linear relationships between microfibril angle, density, wood stiffness and strength, modulus of shear and shrinkage. For instance, a strong relationship between stiffness and wood density ($r=0.82$) was found. There were significant relationship of MOR with stiffness ($r=0.81$), basic density ($r=0.68$) and MFA ($r=-0.47$). The parameter D/MFA was well correlated with stiffness ($r=0.82$) and MOR ($r=0.61$), but a slight correlation was found with tangential and radial ($r=0.29$) shrinkage. Basic density was moderately correlated with tangential ($r=0.43$) and radial ($r=0.39$) shrinkage while MFA was slightly negatively correlated to tangential ($r=-0.33$) and radial ($r=-0.24$) shrinkage. Significant, but of low magnitude relationship was found between shear modulus and wood density ($r=0.28$) and shear modulus and MFA ($r=0.2$). This study shows that MFA variation accounted for only 44 percent of the variation in specific modulus in *Eucalyptus* wood from fast growing plantations.

The influence of MFA and /or density on wood stiffness and modulus of rupture (MOR) of wood samples was better examined. Multiple regression analyses showed that wood density was the prime determinant of both modulus of elasticity and modulus of rupture. In this study, MFA variation accounted for only 37% of the variation in E while the basic density variation alone accounted for 68 percent. Acting together, basic density and MFA accounted for 78 percent of the variation in modulus of elasticity. For modulus of rupture, basic density variation accounted for 46%, and MFA for 22% of the variation in wood strength. Basic density and MFA combined accounted for 51% of the variation in modulus of rupture. The parameter “density/MFA” was fine correlated with both modulus of elasticity ($R^2=0.7$) and modulus of rupture ($R^2=0.45$) by power models.

In this study, wood density was the prime determinant of both modulus of elasticity and modulus of rupture while the MFA played a secondary role on stiffness and strength of wood from **clonal tests**.

Influence of terrain slope on correlations

In this study, the relationships between MFA and mechanical traits were examined in details for each radial position (internal, near to the pith or external, near to the bark) and contrasting sites (at 0, 20 and 40 degrees of inclination) of the **clonal tests**.

The correlations relating MFA and mechanical traits were lower for outer wood likely due the occurrence of growth stresses, tension wood and grain angle, which are more evident on stem periphery. For instance, MFA were significantly correlated ($0.7 < R^2 < 0.8$) with E for specimens sampled from central zones of stem (near to the pith) while weak E x MFA correlations ($0.2 < R^2 < 0.3$) were found for specimens sampled from external zones of the trunk.

In regard to the effect of terrain slope on wood traits, we found the same trends for the three evaluated sites. The correlation of MFA with ρ , E, E/ρ and MOR were slightly similar for the contrasting sites.

These findings indicate that environmental conditions, at least the terrain slope, did not play a major role on a cellulose microfibril orientation in the secondary cell wall of *Eucalyptus* wood.

Our results are especially useful for forest-based industries which produce their own raw material, such as pulp and paper or pig iron producers. *Eucalyptus* forests planted in sloped zones, for instance, will produce woods with similar mechanic resistance; however, differences in growth rate will be remarkable between trees from different site conditions.

4.3 Combining techniques for assessing wood traits

4.3.1 Resonance

The relationships between the mechanical properties obtained on large pieces of wood (scantlings measuring ~45 mm x ~60 mm x 645-2,080 mm) and on small specimens (measuring 25 mm x 25 mm x 410 mm) of the wood from **clonal test** were investigated. Correlations from 0.68 to 0.75 between the E of scantlings and small specimens of *Eucalyptus* wood were found when the E of the scantling with the averaged E values of the specimens per scantling were compared. When the E_F value of each single specimen was compared with its respective scantling, the coefficient of correlation decreased to 0.64 in the longitudinal tests and to 0.61 in the flexural tests. A roughly linear correlation ($r=0.59$) between specific modulus and loss tangent was obtained for the small specimens of *Eucalyptus*.

The findings demonstrate that resonance technique is potentially able to characterize the mechanical properties of wood in a simple and rapid way and at low cost. The dynamic tests enabled rapid estimates of the key mechanical properties (such as the Young, the shear modulus and the loss tangent) of the wood even in lumbers containing knots, small cracks and also slightly damaged areas.

Moreover, scantlings of different lengths were used in this study. At the outset, we think that this condition would be a limitation, but the tightness of the correlations confirms that the vibrations tests are suitable for phenotyping wood of any dimensions, with high accuracy and repeatability.

In short, the resonance technique rapidly provided a large accurate data set of mechanical wood properties as required for high-throughput phenotyping in recent genetic studies.

4.3.2 NIR spectroscopy calibrations

NIR models for chemical properties

Satisfactory NIR calibrations were obtained for estimating Klason lignin and acid-soluble lignin contents and syringyl to guaiacyl ratio in *Eucalyptus urophylla* wood from **progeny tests**. The best calibrations were developed using NIR spectra measured on wood powder (RPD from 2.0 to 2.9), but satisfactory calibrations were still developed from NIR spectra measured on solid samples (RPD from 1.7 to 2.2). Accordingly, it was demonstrated that the sample preparation influences strongly the statistics associated with the predictive models. For these *Eucalyptus urophylla* woods, the effect of the sample presentation (solid or milled wood) was stronger than the effect of the particle size (fine and coarse powder). The NIR spectral information acquired from solid wood are sufficient to provide acceptable calibrations to estimate quickly the Klason and acid-soluble lignin contents and the S/G ratio. However, the time-consuming milling operation is strongly recommended for optimum accuracy. In this study, acid-soluble lignin could be predicted from surfaced wood NIR spectra with the same statistical performance when compared to wood powder calibrations. In short, the NIR spectra acquired from coarse wood powder provided

calibrations with strong correlations for Klason lignin ($R^2_{cv}=0.86$, $SECV=0.48\%$ and $RPD=2.85$) and S/G ratio ($R^2_{cv}=0.86$, $SECV=0.12$ and $RPD=2.88$ for) and so that the extra effort required to produce 0.5 mm wood powder is not warranted.

NIR models for wood density

Promising NIR calibrations were obtained for assessing basic density of wood in *Eucalyptus* trees. The NIR spectra measured on radial surface provided the best regression statistics. These NIR calibrations yielded good estimates for basic density of woods from the **progeny** ($R^2_p=0.85$; $RMSEP=30 \text{ kg m}^{-3}$ and $RPD=2.7$) and **clonal tests** ($R^2_p=0.80$; $RMSEP=22.9 \text{ kg m}^{-3}$ and $RPD=2.3$). The procedure for validating the NIR models ensures the reliability of the application of this tool in routine analysis for the determination of basic density of wood in breeding programs and *Eucalyptus* plantations.

NIR models for visco-elastic traits

Good NIR models were established for estimating dynamic properties of the wood from **clonal test** using as reference data provided by resonance tests. The NIR models for modulus of elasticity presented good performance and acceptable statistics ($R^2=0.81$, $RMSEP=1.15 \text{ GPa}$ and $RPD=2.3$), showing the robustness of the association NIR-resonance. Models for first resonance frequency ($R^2=0.72$ and $RPD=1.9$) and loss tangent ($R^2=0.38$ and $RPD=1.8$) were also developed but the estimated values were not used for genetic studies.

NIR models for MFA

NIR calibrations for microfibril angle in *Eucalyptus* wood were developed based on reference values recorded by the X-ray diffraction technique. The NIR model for 100/MFA based on NIR spectra measured on tangential surface presented the best statistics ($R^2_p=0.72$, $RMSEP=0.89$ degrees and $RPD=1.65$) while the model based on NIR spectra measured on radial surface was the best for MFA ($R^2_p=0.64$, $RMSEP=1.32$ degrees and $RPD=1.63$) in the trees from **progeny test**. Relatively best NIR models for MFA ($R^2_p=0.75$, $RMSEP=1.31$ degrees and $RPD=2.1$) were developed for the trees from **clonal test**. With respect to these models for MFA, the reference data based on Yamamoto formula generated better statistics than those based on Cave formula. NIR spectroscopy tool was able to predict MFA of *Eucalyptus* wood, using both different wood faces, and wood quality surfaces.

Associating polyvalent techniques for assessing wood traits

The association NIR spectroscopy with resonance and X-ray diffraction techniques to evaluate wood traits has three substantial advantages: speed, accuracy and low-cost. Considering the small area scanned by X-ray beam or NIR spectra and the high correlations with MFA of wood sections and elastic properties of entire wood specimens, the scale effect was not a source of substantial error.

The association of NIR spectroscopy with resonance and X-ray diffraction techniques seems to be an adequate, low-cost tool for phenotyping woods. This technique associated to motor-driven coring system, allows predicting a range of wood traits, at the same time, in a large (dry) sample set as required by genetic studies. As NIR spectra measured on radial surface of wood are expected to be more informative, the recommendation is to cut the core sample parallel to the fiber orientation allowing the radial face to be measured by the spectrometer.

The idea behind of combining polyvalent techniques is to provide large datasets of key wood properties, sufficiently representative of the properties in parts of the stem, and sufficiently precise in order to be useful for genetic studies. Indeed, the absolute value of the property is of no matter for genetic approaches.

The interesting point is to know the relative value of the characteristic between trees or regions of the stem and its variation or stability within the logs. This thesis supports the premise that the NIR is currently the most powerful high throughput phenotyping tools for tree breeders, making possible the selection of candidate genotypes or commercial clones in forestry industries from large samplings. According to Meder et al. (2010) one often overlooked advantage of NIR is that a single spectrum has the potential to provide predictions for numerous properties once the calibrations are established. This has significant benefit to tree breeders who can potentially access chemical composition, wood density, stiffness, microfibril angle and other traits from a single NIR spectrum. For genetic screening purposes this has immense power, given that traditional methods are specific in nature and only determine a single property at a time.

4.4 Genetic and environmental control of wood traits

Genetic parameters were assessed from two independent trials of *Eucalyptus*. Progeny and clonal test are experiments that allow obtaining useful information for tree breeders. Indeed, each type of test had its advantages and inconvenient. For instance, because the full-sibs of the **progeny test** were not replicated in the experimental design, dominance and micro-environmental effects were confounded, thus family effect was not considered in the model. However, this design allows the prediction of additive genetic values of trees making possible the calculus of narrow-sense heritability estimates and the genetic and environmental correlations. The **clonal tests** were replicated in three contrasting sites allowing the examination of the genetic x environmental interaction for a range of wood and growth traits. However, this design allows the calculus of broad-sense heritability estimates, which is less informative since the additive and non-additive effects are taken into account.

4.4.1 Genetic studies from the progeny tests

MFA was found to be under strong genetic control in *E. urophylla*. While the mean MFA value per tree presented narrow-sense heritability of 0.65 the h^2 estimates increased from 0.43 in the inner heartwood to 0.50 in the outer heartwood but decreasing again to 0.44 in the sapwood. For density, the h^2 was 0.62 for the mean value, increasing from 0.37 (inner heart wood) to 0.51 towards the sapwood. Lignin content and S/G ratio were found to be under strong genetic control ($h^2 > 0.7$). These high narrow-sense heritability estimates indicate that genetic improvement is possible through selective breeding.

The genetic correlation between height and lignin ($r = -0.61$) and between MFA and lignin (r from 0.4 to 0.74 towards the bark) are favourable for pulp and paper production since they indicate that increase of one trait leads to decrease of another and vice-versa. On the other hand, these correlations are undesirable for bio-energy purposes.

We found strong negative genetic correlations for circumference and density and for density and S/G ratio and positive genetic correlation between MFA and density. The genetic correlation between wood density and MFA remained constant ($r = 0.7$) in the heartwood, decreasing considerably towards the sapwood. As forestry industries are mainly searching for adequate density woods, such correlations are unfavourable for pulpwood, sawnwood and bio-energy applications.

The genetic correlation among growth and wood traits bring new elements to understanding how trees adapt their wood traits in order to maintain their erect habit even when they are constrained by bending movements in response to wind and gravity. Trees with a strong potential to grow fast are genetically programmed to produce low-density woods, but at the same time they are pre-planned to decrease its microfibril angles in order to ensure stiffness and compensate (by increasing the specific modulus) the

weakness of its low-density. Genetic correlations between MFA and lignin increased with age showing that the decrease in these traits, usually attributed to the occurrence of reaction wood, are genetically controlled.

4.4.2 Genetic studies from the clonal tests

Growth traits

Growth traits of 6-year-old *Eucalyptus* trees are under low genetic control ($H^2_C=0.17$ and $H^2_H=0.12$) in this clonal test. There were significant differences between clones and sites for height and circumference of the trees. Taking into account only the growth traits, clones 4514, 4426, 4579 and 4588 are the best ones, presenting superior circumference at 1.3 meters and commercial height while clones 4535, 4494 and 4541 showed the worst performances for growth.

Genetic approaches from large wood pieces

Using the dynamic elastic estimates, significant differences were detected between clones for all traits. No significant differences between sites were detected for dynamic modulus of elasticity. There were significant effect of interaction clone x site for circumference, height, density and shear modulus.

Clones 4494, 4515, 4535, 4557 and 4609 presented the higher mean density values and the lower growth rates. On the other hand, clones 4426 and 4588 presented the lower densities, but their growth rates are high. In regards to the elastic modulus of scantlings, clone 4515 produced the stiffest woods while clones 4426 and 4579 produced the less rigid and more flexible woods (this clones presented the higher growth rates).

In short, the sonic resonance method rapidly provided a large accurate data set of mechanical wood properties as required for high-throughput phenotyping of genetic approaches. These results can be useful for initial classifications, screenings or preliminary selections in breeding programs of *Eucalyptus*. As reported by Burdzik and Nkwera (2002), this method proved to be fast, highly repeatable and does not require heavy equipment, making it the ideal method for on-site determining of modulus of elasticity at the sawmill.

Genetic control over wood traits

This study has established in which extend the radial and longitudinal variations in wood density; wood stiffness and MFA within trees are governed by genetic factors.

Low to moderate levels of broad-sense heritability estimates were found for basic density, wood stiffness and microfibril angle of 6-year-old *Eucalyptus* clones. For wood density, the longitudinal variations in H^2 estimates were more consistent than those in radial direction, especially in the highest parts of the stem. No clear trends of radial variation could be defined.

The findings show that genetic control over density and stiffness is larger in two regions of the stem: (i) in the inner heartwood region (0-25% of relative radial position) of the lower zones of the tree (10-30% of the relative longitudinal position) and (ii) at the top of the tree, a zone localized at 40-80% of relative radial position and at 70-90% of the relative longitudinal position. Again, no clear patterns of radial variation were established for H^2 estimates of E_L along the tree.

Genetic control over MFA exhibits variable patterns of variation. It was shown that H^2 of MFA is superior in the sapwood region (60-100% of relative radial position) of the lower zones of the tree (10-30% of the relative longitudinal position) and at the higher zones of the stem near to the cambium.

The results clearly reveal that heritability estimates for E_L and MFA exhibited opposite patterns of radial variation in the bottom of the tree, and similar trends towards the top. For density, higher H^2 estimates were found in the higher regions of the tree, especially at the intermediate zone.

NIR spectral heritability

This study shows that NIR spectra are able to capture the potential genetic of some chemical components and wood traits. Genetic parameters were obtained directly from NIR spectra. The bands normally associated with cellulosic or lignin type biomolecules may be observed in the near-infrared (NIR) spectra of wood. Thus, variations in specific ranges NIR spectra are related to variation in lignin and cellulose and hemicelluloses contents, and other wood traits. The findings clearly revealed that the variations on these specific ranges of the NIR spectra were controlled by genetic factors. The assignments of absorption bands were useful to identify which wood components presents higher broad-sense heritability estimates from NIR spectroscopic data. It helps to understanding how NIR spectroscopy can evaluate genetic control over wood traits.

Some ranges of the spectra presented heritability estimate greater than 50%. Considering NIR spectra is countless source of information concerning many wood traits, the analysis of genetic parameters from them appears to be an efficient and promising way to evaluate the genetic control over various wood traits at once.

Validity of these findings

As there are only 5 individuals per clone per site involved in the study of clonal tests, and only nine to ten individuals per family involved in the study of progeny tests presented here, these findings should be viewed with caution. Sampling is one of the most expensive steps of the genetic studies. As large samplings are, as accurate results are provided. Here, we could sample a limited number of individuals however it was possible to provide reliable indications of genetic control and genetic correlations. The similarity of the results from the two experimental designs, despite the data sets being so different in structure and representation, suggests that the results may be more generally applicable.

5 PERSPECTIVES

Wood and biomass are now regarded as renewable resources that can partially alleviate reliance on petrochemical for every day needs and at the same time sequester carbon from the atmosphere to reduce atmospheric CO₂ levels (Meder et al. 2010). The *Eucalyptus* plantations have successfully met the demand for raw material of quality required for the pulp and paper, and bioenergy industry. However, the performance in *Eucalyptus* wood as sawn-timber is usually not satisfactory. Selecting trees and improving wood traits seems to be a good strategy for overcoming deficiencies in timber. *Eucalyptus* breeding programs for wood quality may focus on the properties that cannot be manipulated during processing.

Here, we examined the genetic parameters of and correlations between growth traits, wood density, lignin content, wood stiffness and microfibril angle in wood samples from *Eucalyptus* plantations. The findings have shown that wood traits are under moderate to strong genetic control indicating that genetic improvement is possible through breeding. However, most wood properties were unfavorably genetically correlated with growth, although favorable genetic correlations were observed between many *Eucalyptus* wood traits. Because of these unfavorable genetic correlations between wood and growth, selection for increasing density and stiffness or reducing MFA in the absence of selection for growth will result in a reduction (genetic loss) in volume production. Breeders, forest managers and wood producers will have to strike a balance between overall wood and growth traits, and geneticists should develop breeding strategies to deal with such negative, unfavorable genetic correlations, as pointed out by Baltunis et al. (2007) for similar findings in *Pinus*. Indeed, slight reductions in growth may be of little consequence when considering the genetic gains in juvenile wood properties. However, there may be opportunities for selection of correlation breakers for both breeding and deployment, thus improving wood traits without adversely affecting growth traits in *Eucalyptus* plantations. Developing breeding objectives may be the first step in dealing with these unfavorable genetic correlations. If it is possible further understand the genetic basis of these negative genetic correlations using molecular tools (e.g., identifying pleiotropic alleles or genes associated with antagonistically correlated traits), more efficient breeding strategies may be developed to circumvent these antagonistic genetic correlations by crossing genotypes with a desirable suite of alleles.

6 ANNEXES

6.1 Phenotyping the air-dried scantlings of clonal tests

Table 45 lists the descriptive statistics of the density and dynamic properties of air-dried scantlings of *Eucalyptus* wood. Based on early studies on dynamic tests of wood (Hearmon 1961; Ilic 2001; Ilic 2003), we expected to find longitudinal elastic properties higher than the flexural ones. Surprisingly, the flexural elastic moduli were the highest for air-dried scantlings: since the p -value of the t -test was less than 0.01, there was a statistically significant difference between the mean E_{Lad} and E_{Fad} at the 99% confidence level. The environmental effect on the dynamic elastic modulus on longitudinal vibration test is not clear (Figure 48). Because the elastic properties greatly varied between clones, the standard deviations were high and there were no significant differences between sites according to Tukey test.

Table 45 - Descriptive statistics of dynamic properties of the air-scantlings of 6-year-old *Eucalyptus grandis* x *urophylla*, including air-dry density (ρ_{ad} , kg m⁻³), first resonant frequency (f_{lad} , Hz), elastic modulus (E_{ad} , MPa), specific modulus (E'_{ad} , E/ ρ), loss tangent ($tg \delta_{lad}$, 10⁻³) and shear modulus (G_{ad} , MPa) estimated by longitudinal (_L) and flexural (_F) vibration tests

	ρ_{ad}	f_{Lad}	E_{Lad}	E'_{Lad}	$tg \delta_{Lad}$	f_{Fad}	E_{Fad}	E'_{Fad}	G_{Fad}
Mean	596	1,548	12,666	21.2	8.08	101.92	13,292	22.3	652.9
Sd	78	343	2,565	3.0	1.96	47.45	2,697	3.17	170.5
Min	416	984.7	7,237	14.3	2.71	44.1	6,200	12.8	199
Max	827	3,345	20,163	30.7	20.8	366	23,536	32.5	1,419
CV (%)	13.2	22.2	20.2	14.1	24.3	46.5	20.3	14.2	26.1
N	410	410	410	410	339	410	410	410	398

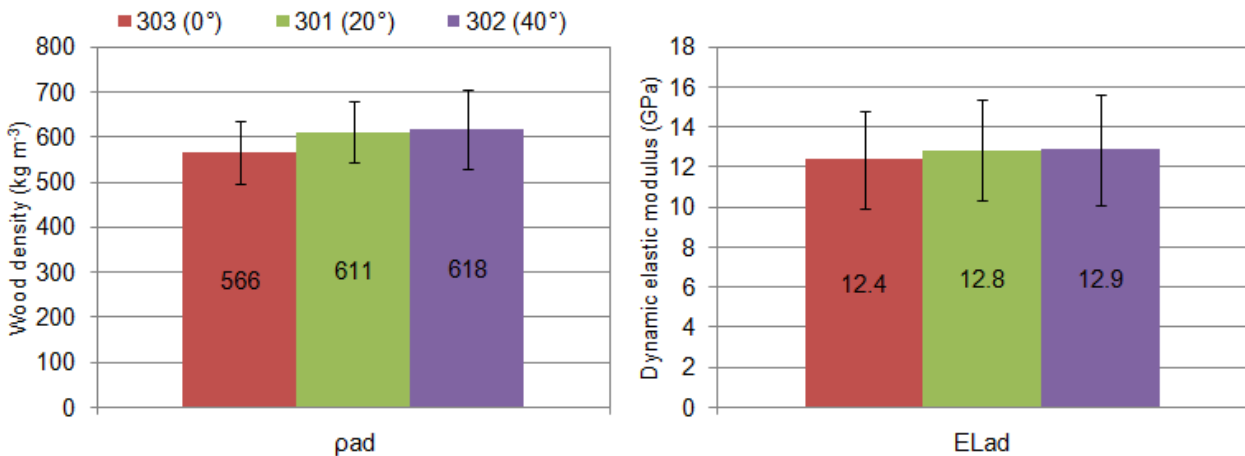


Figure 48 - Mean and standard deviation values of air-dried density and dynamic elastic modulus in air-dried scantlings for each site.

6.2 Correlations between wood traits of air- and kiln-dried scantlings

The correlations among the physical and elastic properties of 395 air-dried and kiln-dried scantlings are presented in Table 46. Correlations between air-dried (ad) and kiln-dried (14) were stronger for both longitudinal and flexural ($r=0.99$) tests.

Table 46 - Correlations among physical and elastic properties of 395 air-dried and 14% dried scantlings of 6-year-old *Eucalyptus grandis x urophylla* wood. The significance level for all relationships was <0.0001

	ρ_{ad}	ρ_{14}	E_{Lad}	E_{Fad}	E_{L14}
ρ_{14}	0.91	1			
E_{Lad}	0.72	0.78	1		
E_{Fad}	0.70	0.74	0.94	1	
E_{L14}	0.71	0.80	0.99	0.94	1
E_{F14}	0.69	0.76	0.91	0.99	0.91

The moisture content of the air-dried scantlings ranged from 14 to 26% but this variation was not high enough to highlight the moisture content effect on these elastic properties. Hence, it appears that short variation in moisture content did not significantly influence the ability of the dynamic tests to estimate the elastic properties of the unseasoned or seasoned wood beams. Accordingly, further studies are required to show the influence of moisture content of wood on dynamic tests.

The correlation between the modulus of elasticity of the kiln-dried (E_{L14}) and air-dried (E_{Lad}) scantlings in the flexural test for the all samples (411 scantlings) is detailed in Figure 49 where the fitted linear regression explained 95.4% of the variability in E_{L14} . The standard deviation of the residuals was 546.5 MPa (Figure 49).

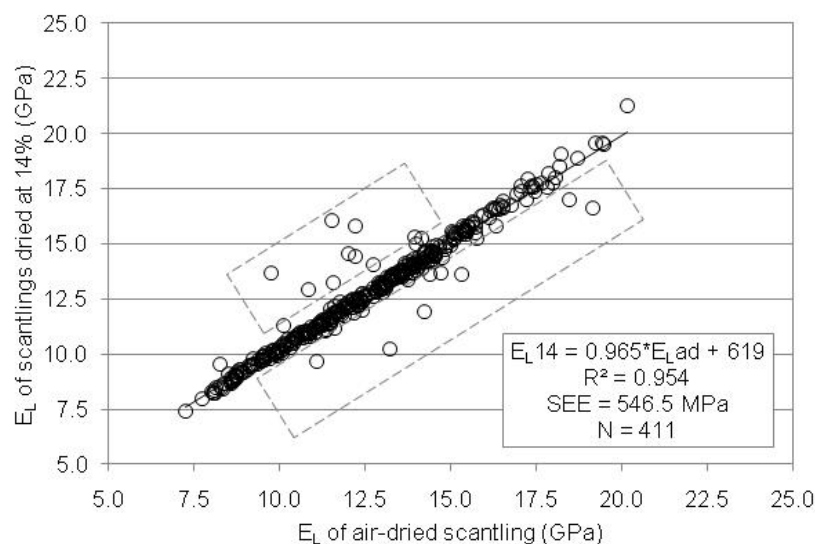


Figure 49 - Correlation between the modulus of elasticity of the kiln- (E_{L14}) and air-dried (E_{Lad}) scantlings obtained in the flexural test for 411 scantlings of *Eucalyptus* showing the samples presenting problems after drying

After kiln-drying process, fifteen (15) scantlings (3.6% of total sampling) presented small cracks. These defects had a negative effect on the vibration test, notably changing the natural frequency and the Young modulus of the scantling. Hence, we considered them as outliers and they were not included in the calculation of correlations presented in Table 46. Figure 50 shows an even stronger correlation between the modulus of elasticity of the kiln-dried (E_{L14}) and air-dried (E_{Lad}) scantlings in the longitudinal test without the 15 outliers (395 scantlings).

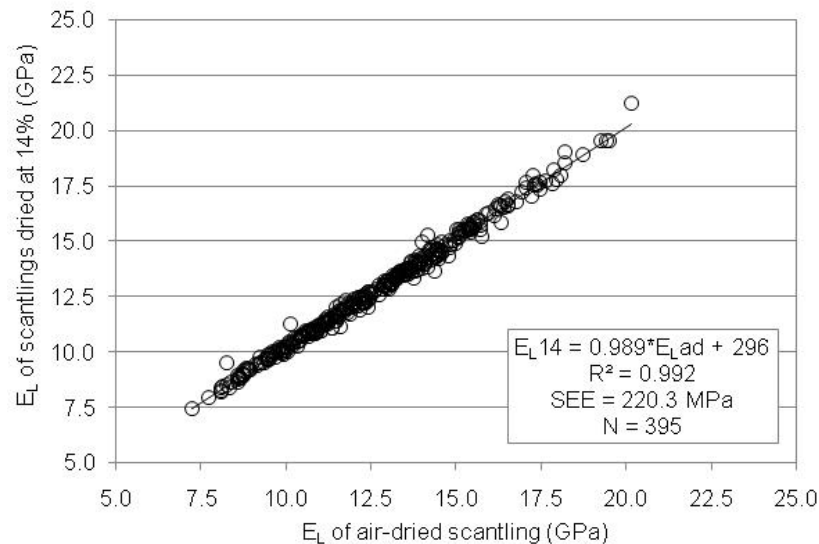


Figure 50 - Correlation between the modulus of elasticity of the kiln- (E_{L14}) and air-dried (E_{Lad}) scantlings obtained in the flexural test for 395 scantlings of *Eucalyptus grandis* x *urophylla* wood with 45 mm x 60 mm cross section

From air- and kiln-dried condition, the scantlings lost around 84 litres of water that corresponded to 8.3% of the total mass (1,013 kg). Considering the high coefficients of determination between these two conditions, these findings indicate that when analyzing elastic properties by means of this resonance method, there is no need to dry the wood pieces in a kiln, which can be expensive, apart from the need to own it. This is a very useful finding for those who need to evaluate their wood samples without owning a wood kiln for large pieces.

It is well known that values of the modulus of elasticity increased with increasing wood density (Kollmann and Côté 1968). According to the Table 46, the density of the kiln-dried scantlings showed good correlation (from 0.74 to 0.80) with their elastic properties. The E_L presented higher correlations with density than the E_F , both for air- and kiln-dried scantlings (Table 46). The main reason for this trend is the lower uncertainty of measurement for longitudinal test.

The correlations (not shown) between air- and kiln-dried values were strong for shear modulus (0.73). The correlation between loss tangent on air- and kiln-dried scantling was weak, but statistically significant (0.47). The modulus of shear and loss tangent had no correlation with elasticity, nor density. Ilic (2001) also did not find statistically significant correlations among these properties.

In the present study, scantlings of different lengths were used. At the outset, we think that this condition would be a limitation, but the tightness of the correlations confirms that the resonance technique is suitable for characterizing wood of any dimensions, with high accuracy and repeatability.

6.3 Environmental and radial position effect on MFA and its correlation with wood traits

The environmental and position effect on correlations among *Eucalyptus* wood traits are listed in Table 47. Taking into account the samples taken from central position (near to the pith), all correlations were higher than those calculated with the samples from external position. For correlation involving MFA, the differences between samples from central or external positions were even stronger.

The $\rho \times E$ correlations were significant, presenting weak variation according to the sites ($0.81 < r < 0.86$) or positions ($0.79 < r < 0.86$) where the samples came from. These results indicate that these traits are not much sensitive to variations in environmental conditions or sampling positions. In other words, the stiffness will be always correlated to the quantity of mass (its density), independently of the sites where the trees were planted or the age at which was considered, at least for these *Eucalyptus* trees. However, for the correlations MFA $\times \rho$ and MFA $\times E$, the coefficients increased as the terrain slope increased, and such correlations varied strongly according to the position.

Table 47 - Correlations among *Eucalyptus* wood traits by site and by radial position. All correlations were statistically significant at $p < 0.01$

correlations	Site effect			Position effect	
	A (0°)	B (20°)	C (40°)	Central	External
MFA $\times \rho$	-0.35	-0.37	-0.51	-0.52	-0.24
MFA $\times E$	-0.58	-0.65	-0.67	-0.76	-0.49
MFA $\times E/\rho$	-0.68	-0.76	-0.67	-0.82	-0.55
MFA $\times MOR$	-0.53	-0.43	-0.53	-0.68	-0.31
$\rho \times E$	0.86	0.81	0.85	0.86	0.79
$\rho \times MOR$	0.66	0.85	0.62	0.74	0.67
E $\times MOR$	0.83	0.87	0.77	0.86	0.76
$\rho/MFA \times E$	0.85	0.87	0.82	0.92	0.78
$\rho/MFA \times MOR$	0.69	0.70	0.56	0.78	0.57

The lower correlations for the samples from external regions can be explained by the possible occurrence of growth stresses, tension wood and grain angle, which are more evident on stem periphery. This indicates that these traits were somewhat correlated when the trees were young, indicating that trees adapt both their stiffness and MFA of their juvenile wood to respond to the specific needs of the young stems, at least, from a phenotypic point of view. However, these relatively close correlations tend to decrease, or disappear, over the years. When the wood reaches certain degree of maturity, variations of other factors (such as density and lignin content) begin to determine its mechanical properties beyond the microfibril angle. These findings outlined the influence of MFA on *Eucalyptus* wood quality. If trees are planted in drastic conditions (sloped areas) or if they are subjected to changing environmental conditions (winds, storms), the trees start developing complementary mechanisms to adapt themselves to the new situation.

In this study, the main difference between sites was the terrain slope, and the results demonstrated that the variation in correlations among traits was stronger for position (age) than for sites (Table 47). In short, specimens taken from central position presented traits and correlations among traits different than those taken from external position. Perhaps, the genetic effects are stronger than the environmental ones in the inner wood. These issues were discussed within the genetic studies section (pg. 109).

6.4 Comparing 3- and 4-points bending tests

After dynamic tests, the wood specimens were tested using a universal testing machine. The modulus of rupture (MOR) of the twin specimens were obtained from three and four points bending tests. Figure 51 shows the correlations between the dynamic flexural elastic modulus and the MOR obtained by tree and four points bending tests for wood samples of *Eucalyptus urophylla* x *grandis* clones.

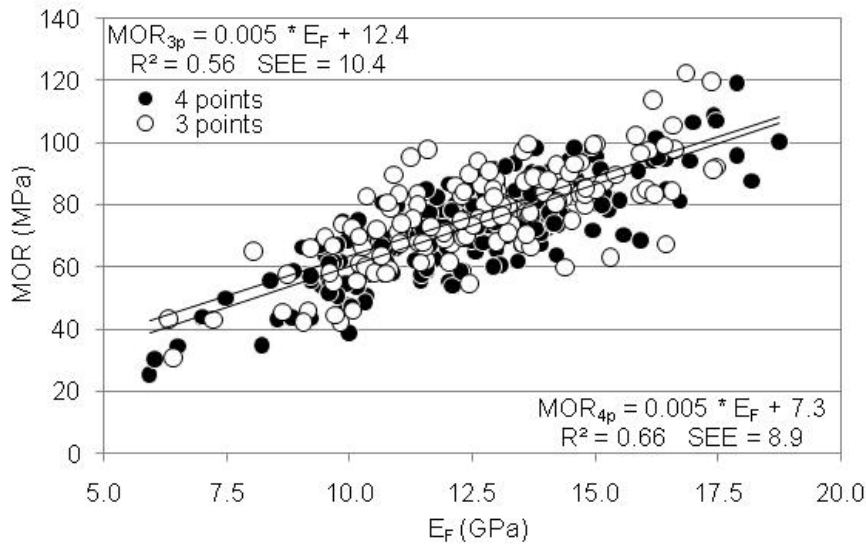


Figure 51 - Linear regression plot between the dynamic flexural elastic modulus and the MOR obtained by tree and four points bending tests using complete sampling of *Eucalyptus* wood. SEE is the standard error of estimation

The correlation between MOR and E_F was higher for four points bending test, while the correlation between MOR and wood density was higher for three points bending test. Two hundred twenty-four (224) samples were considered for correlations concerning MOR_{4p} and 137 specimens were used for three points bending tests. Figure 52 shows the correlations between the wood density and the MOR obtained by tree and four points bending tests for wood samples of *Eucalyptus urophylla* x *grandis* clones.

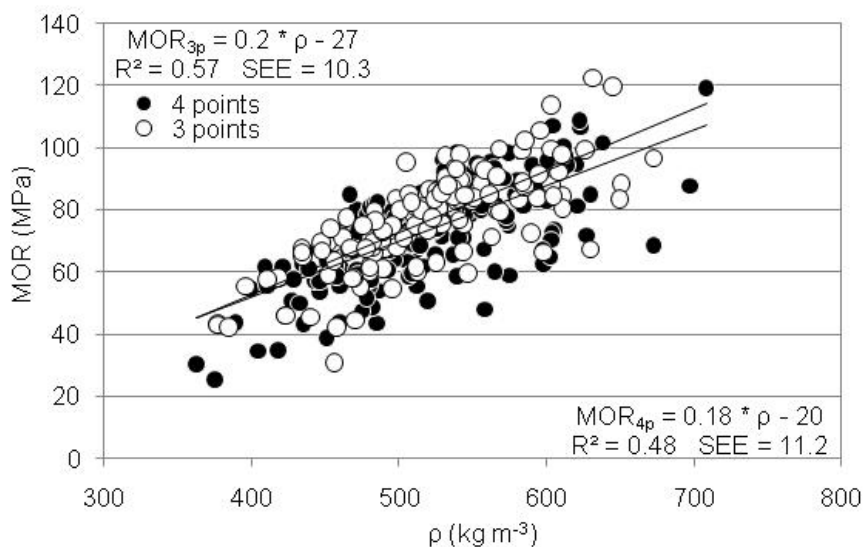


Figure 52 - Linear regression plot between the wood density and the MOR obtained by tree and four points bending tests using complete sampling of *Eucalyptus* wood. SEE is the standard error of estimation

Brancheriau et al. (2002) have compared 3- and 4-point bending tests concerning the longitudinal modulus of elasticity and proposed a crossing analytic formula from a 3-point bending modulus of elasticity to a 4-point bending one, verified by the experimentation. In the present study, an analytic formula for MOR from a 3- to 4-points bending test is proposed: $MOR_{4p} = 0.885 * MOR_{3p} + 5.38$. Figure 53 exhibit the correlation between the modulus of rupture obtained by 3- and 4-points bending tests using twin specimens of *Eucalyptus* wood. As the more commonly methods used for determining the MOE and MOR are the 3- and 4-point bending tests, these findings can be useful when comparing data obtained by different test methods. According to Brancheriau et al. (2002), the analytical study and the experiences have shown that the supports and loading head indentation effect are not negligible but have the same influence as the shear effect. The indentation is the result of the competition between two physical phenomena which are the wood stiffness and the load level applied on the piece of wood during a bending test.

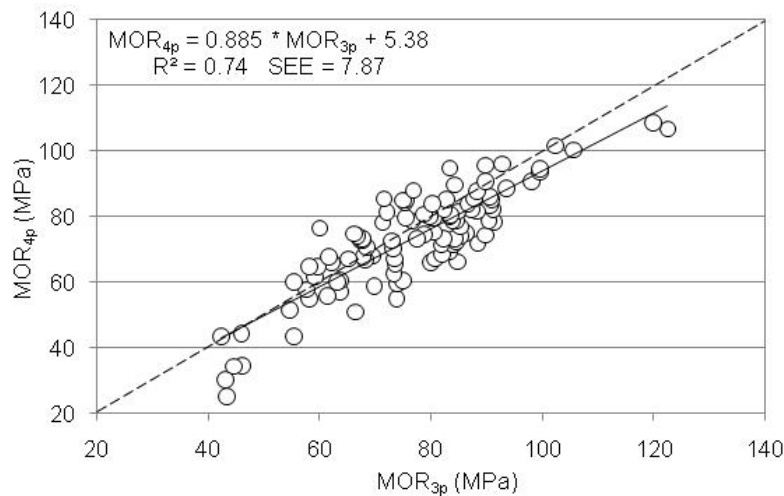


Figure 53 - Linear regression plot between the MOR obtained by tree and four points bending tests. SEE is the standard error of estimation

6.5 Genetic studies from resonance on air-dried scantlings

Table 48 presents the analysis of variance for air-dried density (ρ_{ad}), elastic modulus (E), loss tangent ($tg \delta$) and modulus of shear (G) in air-dried scantlings of the *Eucalyptus* clones from Brazilian plantations. Significant differences between clones were detected for all traits. There were significant differences between clones for all traits, but only for air-dried density and modulus of shear there were significant differences between sites and clones. No significant differences between sites were detected for dynamic modulus of elasticity.

Table 48 - Analysis of variance for density and dynamic traits in air-dried scantlings of 6-year-old *Eucalyptus urophylla* x *grandis* clones

	ρ_{ad}	E_{Lad}	$tg \delta_{ad}$	E_{Fad}	Gad
Clone	$p < 0.0001$	$p < 0.0001$	$p < 0.01$	$p < 0.0001$	$p < 0.0001$
Site	$p < 0.0001$	ns	$p < 0.03$	ns	$p < 0.0001$
interaction	$p < 0.0011$	ns	ns	ns	$p < 0.04$
R^2	0.34	0.20	0.13	0.20	0.20

(* significant at 0.05; ** at 0.01 and *** at 0.001, ns: non-significant)

Table 49 lists the classification of clones and sites for density and dynamic traits of air-dried scantlings. Similarly to Table 33, clones 4494, 4515, 4535, 4557 and 4609 presented the higher mean densities while clones 4426 and 4588 presented the lower densities. For elastic properties, the Tukey (HSD) multiple range tests of air-dried scantlings (Table 49) was less selective than those for kiln-dried scantlings (Table 33). Again, clones 4515 and 4557 produced the stiffest wood samples while clones 4426 and 4579 produced the less stiff ones. Trees growing up on sites 301 and 302 produce the denser woods.

Table 49 - Tukey (HSD) multiple range tests for density and dynamic traits by clone and by site in air-dried scantlings of 6-year-old *Eucalyptus urophylla* x *grandis* clones

Clone	ρ_{ad} (kg m ⁻³)	E _{Lad} (MPa)	tg δ_{ad} (10 ³)	E _{Fad} (MPa)	Gad (MPa)
4426	545.1 ^E	11,100 ^D	8.28 ^{AB}	11,650 ^D	565.4 ^C
4494	614.7 ^{ABC}	13,493 ^{ABC}	8.21 ^{AB}	14,277 ^{ABC}	611.0 ^{BC}
4514	596.7 ^{BCD}	12,758 ^{ABCD}	8.08 ^{AB}	13,433 ^{ABCD}	660.3 ^{ABC}
4515	614.8 ^{ABCD}	13,938 ^A	7.89 ^{AB}	14,482 ^{AB}	695.8 ^{ABC}
4535	632.6 ^A	13,646 ^{AB}	6.78 ^B	14,259 ^{ABC}	731.3 ^A
4541	570.5 ^{CDE}	11,863 ^{CD}	8.17 ^{AB}	12,556 ^{CD}	707.2 ^{AB}
4557	638.8 ^A	13,836 ^{AB}	8.67 ^A	14,576 ^A	625.4 ^{ABC}
4579	582.3 ^{BCDE}	11,597 ^D	8.87 ^A	12,284 ^D	664.5 ^{ABC}
4588	549.7 ^{DE}	12,191 ^{BCD}	7.91 ^{AB}	12,687 ^{BCD}	628.3 ^{ABC}
4609	629.0 ^{AB}	12,570 ^{ABCD}	7.69 ^{AB}	13,069 ^{ABCD}	670.9 ^{ABC}
Site	ρ_{ad} (kg m ⁻³)	E _{Lad} (MPa)	tg δ_{ad} (10 ³)	E _{Fad} (MPa)	Gad (MPa)
301	610.5 ^A	12,846 ^A	7.92 ^B	13,688 ^A	661.4 ^A
302	617.8 ^A	12,864 ^A	8.63 ^A	13,322 ^{AB}	704.9 ^A
303	566.3 ^B	12,394 ^A	7.82 ^B	12,952 ^B	607.0 ^B

Means with the same letter are not significantly different at $\alpha = 0.05$ threshold, using Tukey multiple range tests

The findings obtained from air-dried scantlings (Table 49) and kiln-dried scantlings (Table 33, pg. 108) were basically the same, confirming the repeatability and reliability of the resonance technique as a tool for rapid and low-cost screening technique. Similarly to the Table 49, trees growing up on sites 301 and 302 produce the denser woods and there were no significant differences among sites for modulus of elasticity.

These findings clearly demonstrated that resonance technique is able to simply, rapidly and at such low cost characterize the mechanical properties of wood. The resonance technique permit to rapidly estimate key mechanical properties (such as the modulus of elasticity, the shear modulus and the loss tangent) of the wood even in lumber containing knots, small cracks and also slightly damaged areas. In short, the BING system rapidly provided a large accurate data set of mechanical wood properties as required for high-throughput phenotyping of genetic approaches. These results can be useful for initial classifications, screenings or preliminary selections in breeding programs of *Eucalyptus*. As reported by Burdzik and Nkwera (2002), this method proved to be fast, highly repeatable and does not require heavy equipment, making it the ideal method for on-site determining of MOE at the sawmill.

6.6 Spatial variation of heritability estimates

From the NIR-estimated dataset, the genetic (σ^2_G) and residual (σ^2_E) variance components were estimated by Restricted Maximum Likelihood (REML) method. Thus, broad-sense heritability estimates (H^2) for growth traits and basic density of wood, elastic modulus and microfibril angle at various relative heights and radial positions were calculated. For wood traits, the estimates from the model without GxE interaction (Eq. 38) were similar to those from models with interaction (Figure 45 at pg. 119). Here, the heritability estimates of wood traits were calculated without the variance due to interaction effects.

The patterns of spatial variation in the genetic control over basic density, wood stiffness and microfibril angle within the *Eucalyptus* trees are represented in Figure 54. The coefficient of phenotypic variation, the genetic, residual and interaction variance components and broad-sense heritability estimates (Eq. 38, without GxE interaction) for basic density, wood stiffness and microfibril angle at various relative heights and radial positions are listed in following Tables.

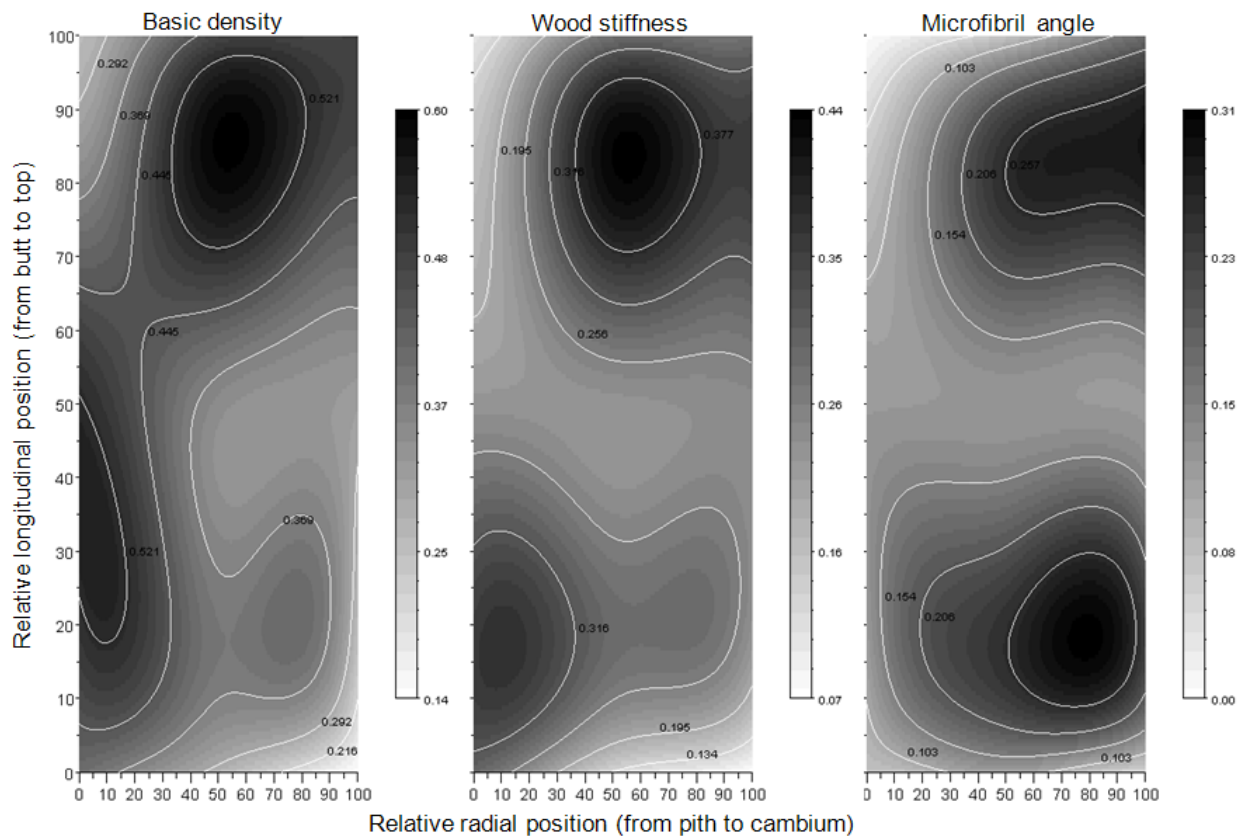


Figure 54 - Spatial variation of heritability estimates over basic density of wood, wood stiffness and microfibril angle within *Eucalyptus* trees (model $y = \mu + G + E$)

Table 50 - Genetic parameters for basic density of the wood in 6-year-old *Eucalyptus urophylla* x *grandis* clones (model $y = \mu + G + E$)

Height	radial position	CV (%)	σ^2_G	σ^2_E	H ²	SE H ²
100%	inner HW ¹⁴	12.5	21.03	35.37	0.261	0.105
	outer HW ¹⁵	11.9	27.75	29.65	0.467	0.135
	SW ¹⁶	10.8	26.04	27.11	0.480	0.129
75%	inner HW ¹¹	12.8	27.83	35.02	0.387	0.122
	outer HW ¹²	10.8	28.80	25.94	0.552	0.139
	SW ¹³	10.3	25.83	29.65	0.431	0.121
50%	inner HW ⁸	10.8	29.19	27.78	0.525	0.129
	outer HW ⁹	9.7	24.66	33.75	0.348	0.111
	SW ¹⁰	12.2	24.52	36.45	0.312	0.118
25%	inner HW ³	11.2	24.84	23.64	0.525	0.135
	middle HW ⁴	8.8	23.04	23.73	0.485	0.135
	outer HW ⁵	11.3	29.41	37.95	0.375	0.126
	inner SW ⁶	11.3	28.65	34.80	0.404	0.134
	outer SW ⁷	12.6	25.43	41.78	0.270	0.112
0%	inner HW ⁰	10.2	26.73	32.39	0.405	0.140
	outer HW ¹	12.7	34.45	55.33	0.279	0.104
	SW ²	11.7	16.86	41.77	0.140	0.080

Table 51 - Genetic parameters for dynamic longitudinal modulus of elasticity of the wood in 6-year-old *Eucalyptus urophylla* x *grandis* clones (model $y = \mu + G + E$)

Height	radial position	CV (%)	σ^2_G	σ^2_E	H ²	SE H ²
100%	inner HW ¹⁴	19.3	694.5	1984.3	0.109	0.069
	outer HW ¹⁵	17.1	1051.7	1711.0	0.274	0.113
	SW ¹⁶	15.4	1029.5	1664.5	0.277	0.122
75%	inner HW ¹¹	17.3	809.5	1750.2	0.176	0.099
	outer HW ¹²	13.1	1052.8	1278.2	0.404	0.130
	SW ¹³	15.0	1232.3	1714.2	0.341	0.111
50%	inner HW ⁸	15.1	772.6	1431.6	0.226	0.100
	outer HW ⁹	12.5	817.0	1508.2	0.227	0.106
	SW ¹⁰	13.1	1009.3	1798.8	0.239	0.092
25%	inner HW ³	16.5	940.4	1314.6	0.339	0.115
	middle HW ⁴	15.7	1010.0	1427.8	0.334	0.117
	outer HW ⁵	14.0	1008.3	1626.7	0.278	0.101
	inner SW ⁶	12.5	1042.7	1658.3	0.283	0.110
	outer SW ⁷	14.4	1142.7	2052.7	0.237	0.099
0%	inner HW ⁰	27.0	1061.9	1645.7	0.294	0.113
	outer HW ¹	21.8	885.0	2258.9	0.133	0.079
	SW ²	16.0	592.2	2103.0	0.073	0.051

Table 52 - Genetic parameters for microfibril angle of cell wall of wood in 6-year-old *Eucalyptus urophylla* x *grandis* clones (model $y = \mu + G + E$)

Height	radial position	CV (%)	σ^2_G	σ^2_E	H ²	SE H ²
100%	inner HW ¹⁴	9.5	0.000	1.217	0.000	0.000
	outer HW ¹⁵	8.4	0.264	0.971	0.069	0.060
	SW ¹⁶	9.4	0.418	0.902	0.177	0.091
75%	inner HW ¹¹	7.8	0.285	0.927	0.087	0.057
	outer HW ¹²	8.7	0.433	0.763	0.244	0.103
	SW ¹³	12.7	0.578	0.988	0.255	0.100
50%	inner HW ⁸	7.7	0.337	0.899	0.123	0.075
	outer HW ⁹	8.2	0.294	0.771	0.127	0.080
	SW ¹⁰	12.2	0.353	0.944	0.123	0.081
25%	inner HW ³	7.6	0.341	0.895	0.127	0.072
	middle HW ⁴	8.5	0.438	0.853	0.209	0.097
	outer HW ⁵	10.3	0.493	0.890	0.235	0.102
	inner SW ⁶	11.2	0.525	0.828	0.286	0.107
	outer SW ⁷	14.0	0.520	0.973	0.222	0.103
0%	inner HW ⁰	8.7	0.309	1.088	0.075	0.050
	outer HW ¹	12.3	0.456	1.242	0.119	0.082
	SW ²	11.0	0.232	0.992	0.052	0.044

It is important to note that in the base of stem it is possible to compare genetic effects on wood developed at the first, third and sixth year of development. Then, the temporal difference between each H² estimate at the base of the stem is approximately of two years whereas the three H² estimates of the top of the tree refer to wood developed at the same year differing only some months.

In short, Figure 54 clearly reveals that heritability estimates for D and E_L exhibited similar patterns of radial variation in the bottom of the tree, and similar trends towards the top. MFA shows opposite trends of spatial variation (mirror effect at radial direction). For density and stiffness, higher H² estimates were found in the higher regions of the tree, especially at the intermediate zone (dark spot at the top of the chart).

7 REFERENCES

1. ABRAF (2010) Associação Brasileira de Produtores de Florestas Plantadas. Statistical Yearbook – Base Year 2009/ ABRAF - Brasília, 127p.
2. Alencar GSB, Barrichelo LEG and Júnior FGSJ (2002) Qualidade da madeira de híbrido de *E. grandis* x *E. urophylla* e seleção precoce. 35º congresso e exposição anual de celulose e papel. Outubro, 2002. São Paulo. Disponível em: <http://www.celuloseonline.com.br/imagembank/Docs/DocBank/dc/dc054.pdf>
3. Alméras T and Fournier M (2009) Biomechanical design and long-term stability of trees: morphological and wood traits involved in the balance between weight increase and the gravitropic reaction. *Journal of Theoretical Biology* 256: 370-381
4. Andersson S, Serimaa R, Torkkeli M, Paakkari T, Saranpfifi P and Pesonen E (2000) Microfibril angle of Norway spruce [*Picea abies* (L.) Karst.] compression wood: comparison of measuring techniques. *Journal of Wood Science* 46: 343-349
5. Apiolaza LA and Garrick DJ (2001) Breeding objectives for three silvicultural regimes of radiata pine. *Canadian Journal of Forest Research* 31: 654-662
6. Apiolaza LA, Raymond CA and Yeo BJ (2005) Genetic variation of physical and chemical wood properties of *Eucalyptus globulus*. *Silvae Genetica* 54: 160-166
7. Apiolaza LA. (2009) Very early selection for solid wood quality: screening for early winners. *Annals of Forest Science* 66: 601
8. Aramaki M, Baillères H, Brancheriau L, Kronland-Martinet R and Ystad S (2007) Sound quality assessment of wood for xylophone bars. *J Acoust Soc Am* 121 (4): 2407-2420
9. Arango B and Tamayo L (2008) Densidad de la madera en clones de *Eucalyptus* por densitometría de rayos X. *Revista Facultad de Ingeniería Universidad de Antioquia* 45: 87-99
10. Archer RR (1986) Growth stresses and strains in trees. Springer-Verlag, Berlin. 240p.
11. ASTM - American Society for Testing and Materials (2007) D 143-94 - Standard test methods for small, clear specimens of timber. 32 p. West Conshohocken, PA, USA
12. ASTM - American Standards and Testing Methods (2002) D2395-02 - Standard test methods for specific gravity of wood and wood-based materials, West Conshohocken, PA, USA
13. Baillères H, Chanson B, Fournier M, Tollier MT and Monties B (1995) Structure, composition chimique et retraits de maturation du bois chez les clones d'*Eucalyptus*. *Annals of Science Forest* 52, 157-172
14. Baillères H, Davrieux F, Ham-Pichavant F. (2002) Near infrared analysis as a tool for rapid screening of some major wood characteristics in a *Eucalyptus* breeding program. *Annals of Forest Science* 59: 479-490
15. Balturis BS, Wu HX and Powell MB (2007) Inheritance of density, microfibril angle, and modulus of elasticity in juvenile wood of *Pinus radiata* at two locations in Australia. *Canadian Journal of Forest Research* 37: 3164-2174
16. Bamber RK, Horne R and Graham-Higgs A (1982) Effect of fast growth on the wood properties of *Eucalyptus grandis*. *Australian Forestry Research* 12(2): 163-167
17. Barnett JR and Bonham VA (2004) Cellulose microfibril angle in the cell wall of wood fibres. *Biol. Rev.* 79: 461-472
18. Bergander A, Brändström J, Daniel G and Salmén L (2002) Fibril angle variability in earlywood of Norway spruce using soft rot cavities and polarisation confocal microscopy. *J. Wood Sci.* 48: 255-263
19. Biblis EJ and Carino HF (1999) Flexural properties of lumber from a 50-year-old loblolly pine plantation. *Wood and Fiber Science* 31(2): 200-203
20. Biblis EJ, Meldahl R and Pitt D (2004) Predicting flexural properties of dimension lumber from 40-year-old loblolly pine plantation stands. *Forest Products Journal* 54: 109-113

21. Binkley D and Stape JL (2004) Sustainable management of eucalyptus plantations in a changing world. In Borralho et al. (2004) *Eucalyptus* in a Changing World. Proc. of IUFRO Conf., Aveiro 11-15 October 2004.
22. Birkett MD and Gambino MJT (1989) Estimation of pulp kappa number with near infrared spectroscopy. *Tappi Journal* 9(72): 193-197
23. Bokobza L (1998) Near infrared spectroscopy. *Journal of Near Infrared Spectroscopy* 6(1): 3-17
24. Bordonné PA (1989) Module Dynamique et Frottement Intérieur dans le Bois, Mesures sur Poutres Flottantes en Vibrations Naturelles. Institut National Polytechnique de Lorraine: 109
25. Bouvet JM, Bouillet JP, Vigneron P and Ognouabi N (1999) Genetic and environmental effects on growth and wood basic density with two *Eucalyptus* hybrids. In: 09/99. Connexion Between Silviculture and Wood Quality through Modelling Approaches and Simulation Softwares, La Londe les Maures, 05 au 12. s.l.: s.n., 2 p. Workshop on Connexion Between Silviculture and Wood Quality Through Modelling Approaches and Simulation Softwares. 3, 1999-09-05/1999-09-12, La Londe-Les Maures, France.
26. Bouvet JM, Saya A and Vigneron P (2009) Trends in additive, dominance and environmental effects with age for growth traits in *Eucalyptus* hybrid populations. *Euphytica* 165: 35-54
27. Bouvet JM, Vigneron P, Gouma R and Saya A (2003) Trends in Variances and Heritabilities with Age for Growth Traits in *Eucalyptus* Spacing Experiments. *Silvae Genetica* 52: 3-4
28. Boyd JD (1950) Tree growth stresses. I Growth stress evaluation. *Australian Journal of Scientific Research B (Biological Sciences)* 3: 270-293.
29. Brancheriau L and Baillères H (2002) Natural vibration analysis of clear wooden beams: a theoretical review. *Wood Science and Technology* 36: 347-365
30. Brancheriau L and Baillères H (2003) Use of the partial least squares method with acoustic vibration spectra as a new grading technique for structural timber. *Holzforschung* 57(6): 644-652
31. Brancheriau L, Baillères H and Guitard D (2002). Comparison between modulus of elasticity values calculated using 3 and 4 point bending tests on wooden samples. *Wood Science and Technology* 36: 367-383
32. Brancheriau L, Kouchade C and Brémaud I (2010) Internal friction measurement of tropical species by various acoustic methods. *Journal of Wood Science* 56(5): 371-379
33. Brémaud I, Gril J and Thibaut B (2011) Anisotropy of wood vibrational properties: dependence on grain angle and review of literature data. *Wood Science and Technology*. on line first
34. Brito JO and Barrichelo LEG (1977) Correlações entre características físicas e químicas da madeira e a produção de carvão vegetal: I. densidade e teor de lignina da madeira de eucalipto. *IPEF* 14: 9-20
35. Bucur V (1995) *Acoustics of wood*. Boca Raton: CRC Press. 284p.
36. Bucur V (2003) *Non-destructive characterization and imaging of wood*. Springer Series in Wood Science, pp. 181-214.
37. Burdzik WMG and Nkwera PD (2002) Transverse vibration tests for prediction of stiffness and strength properties of full size *Eucalyptus grandis*. *Forest Products Journal* 52 (6): 63-67
38. Burgert I and Fratzl P (2009) Plants control the properties and actuation of their organs through the orientation of cellulose fibrils in their cell walls. *Integrative and Comparative Biology* 1-11
39. Burnham KP and Anderson DR (2004) Multimodel inference: Understanding AIC and BIC in model selection. *Sociological Methods and Research* 33(2): 261-304
40. Burns DA and Ciurczak EW (2008) *Handbook of Near-Infrared Analysis*, Third Ed., Marcel Dekker, New York
41. Carvalho AM and Nahuz MAR (2001) Valorização da madeira do híbrido *Eucalyptus grandis* x *urophylla* através da produção conjunta de madeira serrada em pequenas dimensões, celulose e lenha. *Scientia Forestalis* 59: 61-76
42. Cave ID (1966) Theory of X-ray measurement of microfibril angle in wood. *Forest Products Journal* 16(10): 37-42
43. Cave ID (1968) The anisotropic elasticity of the plant cell wall. *Wood Science and Technology* 2(44): 268-278
44. Chaffey I (2000) Microfibril orientation in wood cells: new angles on an old topic. *Trends Plant Science* 5: 360-362

45. Chang HM and Sarkanen KV (1973) Species variation in lignin: Effects of species on the rate of kraft delignification. *Tappi Journal* 56: 132-143
46. Chantre G and Rozenberg P (1997) Can drill resistance profiles (Resistograph) lead to within-profile and within-ring density parameters in Douglas fir wood? In: *Timber management toward wood quality and end-product values*. CTIA/IUFRO International Wood Quality Workshop, p 41-47. 1997.
47. Chen G, Yu Q and Sjöström K (1997) Reactivity of char from pyrolysis of birch wood. *Journal of analytical and applied pyrolysis*, 40(41): 491-499
48. Cilas C, Godin C, Bertrand B and Baillères H. (2006) Genetic study on the physical properties of *Coffea arabica* L. wood. *Trees* 20: 587-592
49. Clair B, Alméras T, Yamamoto H, Okuyama T and Sugiyama J (2006) Mechanical behaviour of cellulose microfibrils in tension wood, in relation with maturation stress generation. *Biophys. Journal* 91: 1128-1135
50. Cogdill RP, Schimleck LR, Jones PD, Peter GF, Daniels RF and Clark A (2004) Estimation of the physical wood properties of *Pinus taeda* L. radial strips using least square support vector machines. *Journal of Near Infrared Spectroscopy* 12: 263-269
51. Costa e Silva J, Borralho NMG, Araujo JA, Vaillancourt RE and Potts BM (2009) Genetic parameters for growth, wood density and pulp yield in *Eucalyptus globulus*. *Tree Genetics and Genomes* 5(2): 291-305
52. Costa e Silva J, Hardner C and Potts BM (2004) Genetic variation and parental performance under inbreeding for growth in *Eucalyptus globulus*. *Annals of Forest Science* 67(6)
53. Costello LR and Quarles SL (1999) Detection of wood decay in blue gum and elm: an evaluation of the Resistograph® and the Portable Drill. *Journal of Arboriculture* 25 (6): 311-318
54. Cown DJ and Clement BC (1983) A wood densitometer using direct scanning with X-rays. *Wood Science and Technology* 17: 91-99.
55. Cown DJ, Ball RD and Riddell MJC (2004) Wood density and microfibril angle in 10 *Pinus radiata* clones: Distribution and influence on product performance. *New Zealand Journal of Forest Science* 34: 293-315
56. Cruz CR (2006) Aplicação de ondas de tensão para a estimativa da umidade em madeira de *Eucalyptus*. Tese (Doutorado em Ciências Florestais) - Universidade Federal do Paraná, Curitiba. 72 p.
57. Decoux V, Varcin E and Leban JM (2004) Relationships between the intra-ring wood density assessed by X-ray densitometry and optical anatomical measurements in conifers. Consequences for the cell wall apparent density determination, *Annals of Forest Science* 61: 251-262
58. Deflorio G, Fink S, and Schwarze FWMR (2008) Detection of incipient decay in tree stems with sonic tomography after wounding and fungal inoculation. *Wood Science and Technology* 42: 117-132
59. Dence CW (1992) The determination of lignin. In: *Methods in Lignin Chemistry*. Eds. Lin, S.Y., Dence, C.W. Springer-Verlag, Berlin. pp.33-61
60. Donaldson L (1993) Variation in microfibril angle among three genetic groups of *Pinus radiata* trees. *New Zealand Journal of Forest Science* 23: 90-100
61. Donaldson L (2008) Microfibril angle: measurement, variation and relationships - a review. *IAWA Journal* 29(4): 345-386
62. Donaldson L and Xu P (2005) Microfibril orientation across the secondary cell wall of *Radiata* pine tracheids. *Trees* 19: 644-653
63. Dungey HS, Matheson AC, Kain D and Evans R (2006) Genetics of wood stiffness and its component traits in *Pinus radiata*. *Canadian Journal of Forest Research* 36: 1165-1178
64. Dutilleul P, Herman M, Avella-Shaw T (1998) Growth rate effects on correlations among ring width, wood density and mean tracheid length in Norway spruce (*Picea abies*). *Canadian Journal of Forestry Research* 28: 56-68
65. Easty DB, Berben SA, Dethomas FA, Brimmer PJ (1990) Near-infrared Spectroscopy for the analysis of wood pulp: quantifying hardwood-softwood mixtures and estimating lignin content. *Tappi Journal* 73(10): 257-261
66. Eklund L and Säll H (2000) The influence of wind on spiral grain formation in conifer trees. *Trees* 14: 324-328

67. Ellis JW and Bath J (1938) Modifications in the near infra-red absorption spectra of protein and of light and heavy water molecules when water is bound to gelatine. *Journal Chem. Phys.* 6: 723-729
68. Evans R (1999) A variance approach to the x-ray diffractometric estimation of microfibril angle in wood. *Appita J.* 52: 283-289
69. Evans R (2006) Wood stiffness by x-ray diffractometry. In: "Characterisation of the Cellulosic Cell Wall", Chapter 11. Proceedings of the workshop 25-27 August 2003, Grand Lake, Colorado, USA. Southern Research Station, University of Iowa and the Society of Wood Science and Technology. D. Stokke and L. Groom, eds. Blackwell Publishing
70. Evans R and Ilic J (2001) Rapid prediction of wood stiffness from microfibril angle and density. *Forest Products Journal* 51(3): 53-57
71. Evans R, Stringer S and Kibblewhite RP (2000) Variation of microfibril angle, density and fibre orientation in twenty-nine *Eucalyptus nitens* trees. *Appita Journal* 53: 450-457
72. Falconer DS (1993) Introduction to quantitative genetics, 3rd edn. Longman Scientific and Technical, New York.
73. Falconer DS and Mackay TFC (1996) Introduction to Quantitative Genetics. 4th Edition. Prentice Hall. Essex, England. 464p.
74. Fang S, Yang W and Tian Y (2006) Clonal and within-tree variation in microfibril angle in poplar clones. *New Forests* 31: 373-383
75. Fang S-Z, Yang W-Z and Fu X-X (2004) Variation of microfibril angle and its correlation to wood properties in Poplars. *Journal of Forest Research* 15(4): 261-267
76. FAO (2006) Global Forest Resources Assessment 2005. Progress towards sustainable forest management. FAO Forestry Paper: 147p. Rome, Italy
77. FAO. State of the World's forests. Food and Agriculture Organization of the United Nations. Viale delle Terme di Caracalla. Rome, 2011. 164p.
78. Berti Filho E (1997) Impact of *Coleoptera cerambycidae* on *Eucalyptus* forests in Brazil. *Scientia forestalis* 52: 51-54
79. Fujimoto T, Kurata Y, Matsumoto K and Tsuchikawa S (2008) Application of near infrared spectroscopy for estimating wood mechanical properties of small clear and full length lumber specimens. *Journal of Near Infrared Spectroscopy* 16: 529-537
80. Gachet C and Guitard (2006) Influence relative de la morphologie cellulaire et de l'angle des microfibrilles sur l'anisotropie élastique tissulaire Longitudinale/Tangentielle du bois sans défaut des résineux. *Annals of forest science* 63(3): 275-283
81. Gantz CH (2002) Evaluating the efficiency of the Resistograph® to estimate genetic parameters for wood density in two softwood and two hardwood species. Raleigh: University of North Carolina State, 88p.
82. Gierlinger N, Schwanninger M and Wimmer R (2004) Characteristics and classification of fourier-transform near infrared spectra of heartwood of different larch species (*Larix* sp.). *Journal of Near Infrared Spectroscopy* 12: 113-119
83. Gierlinger N, Schwanninger M, Hinterstoisser B and Wimmer R (2002) Rapid determination of heartwood extractives in *Larix* sp. by means of Fourier transform near infrared spectroscopy. *Journal of Near Infrared Spectroscopy* 10: 203-214
84. Gilbert EA and Smiley ET (2004) Picus sonic tomography for the quantification of decay in white oak (*Quercus alba*) and hickory (*Carya* spp.). *Journal of Arboriculture* 30: 277-281
85. Gilmour AR, Gogel BJ, Cullis BR, Welham SJ and Thompson R (2005) ASReml user guide release 2.0, VSN international Ltd, Hemel Hempstead HP1 1ES, UK.
86. Glass SV and Zelinka SL (2010) Moisture Relations and Physical Properties of Wood. Cap. 4: 4.1-4.19. Forest Products Laboratory. 2010. Wood handbook - Wood as an engineering material. General Technical Report FPL-GTR-190. Madison, WI: U.S. Department of Agriculture, Forest Service, Forest Products Laboratory. 508p.

87. Gomide JL, Colodette JL, Oliveira RC and Silva CM (2005) Caracterização tecnológica, para produção de celulose, da nova geração de clones de *Eucalyptus* do Brasil. *Árvore* 29(1): 129-137
88. Gominho J, Rodrigues J, Almeida MH, Leal A, Cotterill PP, and Pereira H (1997) Assessment of pulp yield and lignin content in a first-generation clonal testing of *Eucalyptus globulus* in Portugal, in: Proceedings of the IUFRO Conference on Silviculture and Improvement of Eucalypts, Salvador, Brazil, August 24-29, 1997, pp. 84-89.
89. Grabianowski M, Manley B and Walker JCF (2006) Acoustic measurements on standing trees, logs and green lumber. *Wood Science and Technology* 40: 205-216
90. Greaves BL, Borralho NMG, Raymond CA (1997b) Breeding objective for plantation eucalypts grown for production of kraft pulp. *Forest Science* 43: 465-472
91. Greaves BL, Borralho NMG, Raymond CA and Farrington A (1996) Use of a Pilodyn for the indirect selection of basic density in *Eucalyptus nitens*. *Canadian Journal of Forest Research* 26: 1643-1650
92. Greaves BL, Borralho NMG, Raymond CA, Evans R and Whiteman PH (1997a) Age-age correlations and relationships between basic density and growth in *Eucalyptus nitens*. *Silvae Genetica* 46: 264-270
93. Green DW, Gorrnan TM, Evans JW and Murphy JF (2004) Improved grading system for structural logs for log homes. *Forest Products Journal* 54(9): 59-62
94. Green DW, Winandy JE, Kretschmann DE (1999) Mechanical properties of wood, Chapter 4. In: *Wood Handbook – Wood as an Engineered Material*, FPL-GTR-113, USDA Forest Service, Forest Products Laboratory, Madison WI, USA
95. Haines DW, Leban JM and Herbe C (1996) Determination of Young's modulus for spruce, fir and isotropic materials by the resonance flexure method with comparisons to static flexure and other dynamic methods. *Wood science and technology* 30(4): 253-263
96. Hamilton MG and Potts BM (2008) *Eucalyptus nitens* genetic parameters. *New Zealand Journal of Forestry Science* 38(1): 102-119
97. Hamilton MG, Raymond CA, Harwood E and Potts BM (2009) Genetic variation in *Eucalyptus nitens* pulpwood and wood shrinkage traits. *Tree Genetics and Genomes* 5: 307-316
98. Hansen JK and Roulund H (1996) Genetic parameters for spiral grain, stem form, pilodyn and growth in 13 years old clones of Sitka Spruce (*Picea sitchensis* (Bong.) Carr.). *Silva Genetica* 46(2-3): 107-113
99. Harris JM (1989) *Spiral grain and wave phenomena in wood formation*, Springer-Verlag, Berlin, 214 p.
100. Harwood C, Bulman P, Bush D, Stackpole D and Mazanec R (2001) Australian Low Rainfall Tree Improvement Group: Compendium of Hardwood Breeding Strategies. RIRDC Publication No. 01/100. p.31. Rural Industries Research and Development Corporation, Canberra.
101. Hearmon RFS (1961) *An introduction to applied anisotropic elasticity*. Oxford: Oxford University Press, 136 p.
102. Hein PRG, Lima JT and Chaix G (2009) Robustness of models based on near infrared spectra to predict the basic density in *Eucalyptus urophylla* wood. *Journal of Near Infrared Spectroscopy* 17(3): 141-150
103. Hein PRG, Brancheriau L, Lima JT, Rosado AM, Gril J and Chaix G. (2010a) Clonal and environmental variation of structural timbers of *Eucalyptus* for growth, density, and dynamic properties. *Cerne* 16: 74-81
104. Hein PRG, Brancheriau L, Trugilho PF, Lima JT and Chaix G. (2010b) Resonance and near infrared spectroscopy for evaluating dynamic wood properties. *Journal of Near Infrared Spectroscopy* 18(6): 443-454
105. Hein PRG, Clair B, Brancheriau L and Chaix G. (2010c) Predicting microfibril angle in *Eucalyptus* wood from different wood faces and surface qualities using near infrared spectra. *Journal of Near Infrared Spectroscopy* 18(6): 455-464
106. Hein PRG, Lima JT and Chaix G (2010d) Effects of sample preparation on NIR spectroscopic estimation of chemical properties of *Eucalyptus urophylla* S.T. Blake wood. *Holzforschung* 64: 45-54
107. Hein PRG, Brancheriau L, Lima JT, Gril J and Chaix G (2011) Resonance of structural timbers indicates the stiffness even of small specimens of *Eucalyptus* from plantations. *Wood Science and Technology* (DOI: 10.1007/s00226-011-0431-1)
108. Hein PRG and Brancheriau L (2011) Correlations between microfibril angle and wood density with age in 14-year-old *Eucalyptus urophylla* S.T. Blake wood. *BioResources* (submitted)

109. Hein PRG (2011) Relationships between microfibril angle and wood traits in Eucalyptus from fast-growing plantations. *Holzforschung* (submitted)
110. Hein PRG, Bouvet JM Mandrou E, Vigneron P and Chaix G (2011) Genetic control of growth, lignin content, microfibril angle and specific gravity in 14-years Eucalyptus urophylla S.T. Blake wood. *Annals of Forest Science* (submitted)
111. Herman M, Dutilleul P and Avella-Shaw T (1998) Growth rate effects on temporal trajectories of ring width, wood density and mean tracheid length in Norway spruce (*Picea abies* (L.) Karst.). *Wood Fiber Science* 30: 6-17
112. Hirakawa Y and Fujisawa Y (1995) The relationship between microfibril angles of the S2 layer and latewood tracheid lengths in elite sugi tree (*Cryptomeria japonica*) clones. *Journal Japanese Wood Research Society* 41: 123-131
113. Hoffmeyer P (1978) The Pilodyn instrument as a nondestructive tester of the shock resistance of wood. In: *Proceedings, 4th nondestructive testing of wood symposium; 1978 August 28-30; Vancouver, WA.* Pullman, WA: Washington State University: 47-66
114. Hoffmeyer P and Pedersen JG (1995) Evaluation of density and strength of Norway spruce by near infrared reflectance spectroscopy. *Holz als Roh- und Werkstoff* 53: 165-170
115. Hori R, Suzuki H, Kamiyama T and Sugiyama J (2003) Variation of microfibril angles and chemical composition: Implications for functional properties. *J. Mat. Sci. Lett.* 22: 963-966
116. Huang A, Fu F, Fei B and Jiang Z (2008) Rapid estimation of microfibril angle of increment cores of Chinese fir by near infrared spectroscopy. *Chin. For. Sci. Technol.* 7: 52-56
117. Iglesias-Trabado G and Wilstermann D (2008) *Eucalyptus universalis*. Global cultivated eucalypt forests map 2008. Version 1.0.1 In GIT Forestry Consulting's Eucalyptologies: Information resources on Eucalyptus Cultivation worldwide. Retrieved from [March 23th 2011]
118. Ilic J (2001) Relationship among the dynamic and static elastic properties of air-dry *Eucalyptus delegatensis* R. Baker. *Holz als Roh- und Werkstoff* 59: 169-175
119. Ilic J (2003) Dynamic MOE of 55 species using small wood beams. *Holz als Roh- und Werkstoff* 61:167-172
120. Ilic J and Hillis WE (1986) Prediction of Collapse in Dried Eucalypt Wood. *Holzforschung* 40(2): 109-112
121. Innes TC (1996) Pre-drying of collapse prone wood free of surface and internal checking. *Holz als Roh- und Werkstoff* 54(3): 195-199
122. Isik F and Li B (2003) Rapid assessment of wood density of live trees using the Resistograph® for selection in tree improvement programs. *Canadian Journal of Forest Research* 33(12): 2426-2435
123. Jacobs MR (1945) *The Growth of Woody Stems.* Commonwealth Forestry Bureau, Australia, Bulletin No. 28, 67 pp.
124. Jayne BA (1959) Vibrational properties of wood as indices of quality. *Forest Products Journal* 9(11): 413-416
125. Jiang J, Lu J, Ren H, and Long C (2010) Predicting the flexural properties of Chinese fir (*Cunninghamia lanceolata*) plantation dimension lumber from growth ring width. *Journal of Wood Science* 56: 15-18
126. Jones PD, Schimleck LR, Peter GF, Daniels RF and Clark III A (2006) Nondestructive estimation of wood chemical composition of sections of radial wood strips by diffuse reflectance near infrared spectroscopy. *Wood Science and Technology* 40: 708-720
127. Jouan-Rimbaud D, Massart DL and Noord O.E. (1996) Random correlation in variable selection for multivariate calibration with a genetic algorithm. *Chemometrics and Intelligent Laboratory Systems* 35: 213-220
128. Jungnikl K, Koch G and Burgert I (2008) A comprehensive analysis of the relation of cellulose microfibril orientation and lignin content in the S2 layer of different tissue types of spruce wood (*Picea abies* (L.) Karst.). *Holzforschung* 62: 475-480
129. Kärenlampi PP and Riekkinen M (2004) Maturity and growth rate effects on Scots pine basic density. *Wood Science and Technology* 38(6): 465-473
130. Kelley SS, Rials TG, Groom LR and So C-L (2004) Use of Near Infrared Spectroscopy to predict the mechanical properties of six softwoods. *Holzforschung* 58, 252-260

131. Kibblewhite RP, Evans R, Grace JC and Riddell MJC (2005) Fibre length, microfibril angle and wood colour variation and interrelationships for two radiata pine trees with mild and severe compression wood. *Appita J.* 58: 316-322
132. Kien ND, Jansson G, Harwood C and Thinh HH (2009) Genetic control of growth and form in *Eucalyptus urophylla* in Northern Vietnam. *Journal of Tropical Forest Science* 21(1): 50-56
133. Kien ND, Jansson K, Harwood G, Almqvist C, Ha C and Huy T (2008) Genetic variation in wood basic density and pilodyn penetration and their relationships with growth, stem straightness, and branch size for *Eucalyptus urophylla* in northern Vietnam. *New Zealand Journal of Forestry Science* 38: 160-175
134. Klein JI (1995) Multiple-trait combined selection in jack pine family-test plantations using best linear prediction. *Silvae Genetica* 44(5/6): 362-375
135. Koch L and Fins L (2000) Genetic variation in wood specific gravity from progeny tests of ponderosa pine (*Pinus ponderosa* Laws.) in northern Idaho and western Montana. *Silvae Genetica* 49(4): 174-181
136. Kollmann FR and Côté WA (1968) Principles of Wood science and technology. Berlin: Springer-Verlag, 592p.
137. Kretschmann DE, Alden HA and Verrill S (1998) Variations of microfibril angle in loblolly pine: comparison of iodine crystallization and X-ray diffraction techniques. In: Butterfield, B.G., ed. Microfibril angle in wood. New Zealand: University of Canterbury. p.157-176
138. Kube PD and Raymond CA (2005) Breeding to minimise the effects of collapse in *Eucalyptus nitens*. *Forest genetics* 12: 23-34
139. Kube PD, Raymond CA and Banham PW (2001) Genetic parameters for diameter, basic density, cellulose content and fibre properties for *Eucalyptus nitens*. *Forest Genetics* 8: 285-294
140. Lachenbruch B, Johnson GR, Downes G and Evans R (2010) Relationships of density, microfibril angle, and sound velocity with stiffness and strength in mature wood of Douglas-fir. *Canadian Journal of Forest Research* 40: 55-64
141. Lande R (1984) The genetic correlation between characters maintained by selection, linkage and inbreeding. *Genetic Research* 44: 309-320
142. Lapierre C, Pollet B and Rolando C (1995) New insights into the molecular architecture of hardwood lignins by chemical degradative methods. *Res. Chem. Intermed.* 21: 397-412
143. Liang S-Q and Fu F (2007) Comparative study on three dynamic modulus of elasticity and static modulus of elasticity for Lodgepole pine lumber. *Journal of Forestry Research* 18(4): 309-312
144. Lima JT, Breese MC and Cahalan CM (1999) Variation in compression strength parallel to the grain in *Eucalyptus* clones. Proceedings of the Fourth International Conference on the Development of Wood Science, Wood Technology and Forestry, Missenden Abbey, UK, 14-16 July 1999
145. Lima JT, Breese MC and Cahalan CM (2000) Genotype-environment interaction in wood basic density of *Eucalyptus* clones. *Wood Science and Technology* 34: 197-206
146. Lima JT, Breese MC and Cahalan CM (2004) Variation in microfibril angle in *Eucalyptus* clones. *Holzforschung* 58: 160-166
147. Lima JT, Sartorio RC, Trugilho PF, Cruz CR and Vieira RS (2007) Uso do resistógrafo para estimar a densidade básica e a resistência à perfuração da madeira de *Eucalyptus*. *Scientia Forestalis* 75: 85-93
148. Lin C-J and Chiu C-M (2007). Relationships among selected wood properties of 20-year-old *Taiwania* (*Taiwania cryptomerioides*) trees. *Journal of Wood Science* 53: 61-66
149. Lindström H, Harris P, Sorensson CT and Evans R (2004) Stiffness and wood variation of 3-year old *Pinus radiata* clones. *Wood Science and Technology* 38: 579-597
150. MacDonald AC, Borralho NMG and Potts BM (1997) Genetic variation for growth and wood density in *Eucalyptus globulus* ssp. *globulus* in Tasmania (Australia). *Silvae genetica* 46: 236-241
151. Malan FS (1988) Genetic variation in some growth and wood properties among 18 full-sib families of South African grown *Eucalyptus grandis*: a preliminary investigation. *South African Forestry Journal* 146: 38-43.
152. Malan FS (1995) *Eucalyptus* improvement for lumber production. Seminário internacional de utilização da madeira de eucalipto para serraria. 05 e 06 de abril de 1995. IPT, São Paulo, Brazil

153. Mandrou E, Hein PRG, Villar E, Vigneron P, Plomion C and Gion JM (2011) A candidate gene for lignin composition in *Eucalyptus*: Cinnamoyl-CoA Reductase (CCR), Tree Genetics and Genomes (submitted)
154. McKeand SE, Li B, Hatcher AV and Weir RJ (1990) Stability parameter estimates for stem volume for loblolly pine families growing in different regions in the southeastern United States. *Forest Science* 36(1): 10-17
155. McLean J P, Evans R and Moore J R (2010). Predicting the longitudinal modulus of elasticity of Sitka spruce from cellulose orientation and abundance. *Holzforschung* 64:495-500
156. Meder R, Trunga T and Schimleck L (2010) Guest editorial: Seeing the wood in the trees: unleashing the secrets of wood via near infrared spectroscopy. *Journal of Near Infrared Spectroscopy* 18(6): v-vii
157. Megraw RA, Leaf G and Bremer D (1998) Longitudinal shrinkage and microfibril angle in Loblolly pine. In *Microfibril Angle in Wood: Proceedings of the IAWA/IUFRO International Workshop on the Significance of Microfibril Angle to Wood Quality* (ed. B. G. Butterfield), pp. 27-61. Westport, N.Z. University of Canterbury Press, Canterbury, N.Z.
158. Meylan BA (1967) Measurement of microfibril angle by X-ray diffraction. *Forest Products Journal* 17: 51-58
159. Meylan BA (1968) Cause of high longitudinal shrinkage of wood. *Forest Products journal* 18: 75-78
160. Mode CJ and Robinson HF (1959) Pleiotropism and the genetic variance and covariance. *Biometrics* 15: 518-537
161. Mora CR, Schimleck LR (2008) On the selection of samples for multivariate regression analysis: application to near-infrared (NIR) calibration models for the prediction of pulp yield in *Eucalyptus nitens*. *Canadian Journal Forest Research* 38(10): 2626-2634.
162. Mora CR, Schimleck LR and Isik F (2008) Near infrared calibration models for the estimation of wood density in *Pinus taeda* using repeated sample measurement. *Journal of Near Infrared Spectroscopy* 16: 517-528
163. Mrode RA (2005) *Linear models for the prediction of animal breeding values*. 2nd ed. CAB International, Wallingford, Oxon, UK.
164. Muneri A and Raymond CA (2000) Genetic parameters and genotype-by-environment interactions for basic density, pilodyn penetration and stem diameter in *Eucalyptus globulus*. *Forest Genetics* 7: 317-328
165. Murphy JF (2000) Commentary on factors affecting transverse vibration using an idealized theoretical equation. Res. Note FPL-RN-0276. Madison, WI: U.S. Department of Agriculture, Forest Service, Forest Products Laboratory. 4 p
166. Næs T, Isaksson T, Fearn T and Davies T (2002) *A user-friendly guide to multivariate calibration and classification*. Chichester: NIR. 344 p.
167. Nicolotti G, Socco LV, Martinis R, Godio A and Sambuelli L (2003) Application and comparison of three tomographic techniques for detection of decay in trees. *Journal of Arboriculture* 29: 66-78
168. Ohsaki H, Kubojima Y, Tonosaki M and Ohta M (2007) Vibrational properties of wetwood of todomatsu (*Abies sachalinensis*) at high temperature. *Journal of Wood Science* 53: 134-138
169. Osorio LF, White TL and Huber DA (2003) Age-age and trait-trait correlations for *Eucalyptus grandis* Hill ex Maiden and their implications for optimal selection age and design of clonal trials. *Theoretical and Applied Genetics* 106: 735-743
170. Ouis D (1999) Vibrational and acoustical experiments on logs of spruce. *Wood Science and Technology* 33: 151-184
171. Panshin AJ and De Zeeuw C (1980) *Textbook of wood technology*. 4.ed. New York: Mc Graw Hill. 722p.
172. Pasquini C (2003) Near infrared spectroscopy: fundamentals, practical aspects and analytical applications. *Journal of the Brazilian Chemical Society* 14(2): 198-219
173. Peel MC, Finlayson BL and McMahon TA (2007) Updated world map of the Köppen-Geiger climate classification. *Hydrol. Earth Syst. Sci.* 11: 1633-1644
174. Pelletier MC, Henson M, Boyton S, Thomas D and Vanclay J (2008) Genetic variation in shrinkage properties of *Eucalyptus pilularis* assessed using increment cores and test blocks. *New Zealand Journal of Forestry Science* 38(1): 194-210

175. Pereira H, Graça J and Rodrigues JC (2003) Wood chemistry in relation to quality" in Wood Quality and its Biological Basis, Ed by J.R. Barnett and G. Jeronimidis, Blackwell Publishing, Victoria, p.226
176. Petty JA, MacMillan DC and Steward CM (1990) Variation of density and growth ring width in stems of Sitka and Norway spruce. *Forestry* 63: 39-49
177. Peura M (2007) Studies on the cell wall structure and on the mechanical properties of Norway spruce. Report Series in Physics HU-P-D146
178. Poke FS, Potts BM, Vaillancourt RE and Raymond CA (2006) Genetic parameters for lignin, extractives and decay in *Eucalyptus globulus*. *Annals of Forest Science* 63(8): 813-821
179. Polge H (1963) Une nouvelle méthode de détermination de la texture du bois : l'analyse densitométrique de clichés radiographiques. *Annales de Sciences Forestières* 20(4): 531-581
180. Preston RD (1934) The organization of the cell wall of the conifer tracheid. *Philosophical Transactions of the Royal Society B* 224: 131-173
181. R Development Core Team. 2008. R: A Language and Environment for Statistical Computing. Vienna, Austria: R Foundation for Statistical Computing. ISBN 3-900051-07-0. <http://www.r-project.org>.
182. Rabe C, Ferner D, Fink S and Schwarze FWMR (2004) Detection of decay in trees with stress waves and interpretation of acoustic tomograms. *Journal of Arboriculture* 28: 3-19
183. Rayleigh JWS (1877) *The theory of the sound* (Edition of 1945). New York. pp. 243-305
184. Raymond CA (2002) Genetics of Eucalyptus wood properties. *Annals of Forest Science* 59: 525-531
185. Raymond CA and MacDonald AC (1998) Where to shoot your pilodyn: within tree variation in basic density in plantation *Eucalyptus globulus* and *E. nitens* in Tasmania. *New Forests* 15: 205-221
186. Raymond CA, Banham P and MacDonald AC (1998) Within tree variation and genetic control of basic density, fibre length and coarseness in *Eucalyptus regnans* in Tasmania. *Appita Journal* 41(4): 299-305
187. Rinn F (1994) Bohrwiderstandmessungen mit Resistograph®- Mikorbohrungen. *Allgemeine Forst Zeitschrift* 49(12): 652-654
188. Rinn F, Schweingruber F-H and Schär E (1996) Resistograph and X-ray density charts of wood comparative evaluation of drill resistance profiles and X-ray density charts of different wood species. *Holzforschung* 50:303-311
189. Rinn F, Schweingruber H and Schar E. (1996) Resistograph and X-ray density charts of wood comparative evaluation on drill resistance profiles and X-ray density charts of different wood species. *Holzforschung* 50(4): 303-311
190. Rodrigues EAC, Rosado SCS, Trugilho PF and Santos AM (2008) Seleção de clones de *Eucalyptus* para as propriedades físicas da madeira avaliadas em arvores no campo. *Cerne* 14: 147-152
191. Rodrigues J, Alves A, Pereira H, da Silva Perez D, Chantre G and Schwanninger M (2006) NIR PLSR results obtained by calibration with noisy, low-precision reference values: Are the results acceptable? *Holzforschung* 60: 402-408
192. Rodrigues J, Meier D, Faix O and Pereira H (1999) Determination of tree to tree variation in syringyl:guaiacyl ratio of *Eucalyptus globulus* wood lignin by analytical pyrolysis. *Journal of Analytical and Applied Pyrolysis* 48: 121-128
193. Rosado SCS, Brune A and Oliveira LM (1983) Avaliação da densidade básica da madeira de árvores em pé. *Revista Árvore* 7(1): 147-153
194. Ross RJ and Pellerin (1994) Nondestructive testing for assessing Wood members in structures: A review. USDA Forest Service Forest Products Laboratory, General Tech Rep FPL-GTR-70
195. Ross RJ, Geske EA, Larson GL and Murphy JF (1991) Transverse vibration non-destructive testing using a personal computer, Research Paper, FPL-RP-502, Forest Products Laboratory, Forest Service, US Department of Agriculture
196. Rozenberg P and Cahalan C (1997). Spruce and wood quality: Genetic aspects (A review). *Silvae Genetica* 46: 270-279.

197. Rozenberg P and Van de Sype H (1996) Genetic variation of the pilodyn-girth relationship in Norway spruce (*Picea abies* L. Karst). *Annals of Forest Science* 53(6): 1153-1166
198. Ruelle J, Yamamoto H and Thibaut B (2007) Growth stresses and cellulose structural parameters in tension and normal wood from three tropical rainforest angiosperms species. *BioResources* 2(2): 235-251
199. Santos PET, Geraldi IO, Garcia N.G. (2004) Estimates of genetic parameters of wood traits for sawn timber production in *Eucalyptus grandis*. *Genetics and Molecular Biology* 27(4): 567-573
200. Savidge RA (2003) Tree growth and wood quality” in *Wood Quality and its Biological Basis*, Ed by J.R. Barnett and G. Jeronimidis, Blackwell Publishing, Victoria, p.226
201. Savitzky A, Golay MJE (1964) Smoothing and differentiation of data by simplified least-squares procedures. *Anal Chem* 36(8):1627-1639
202. Schimleck L, Jones PD, Peter GF, Daniels RF and Clark III A (2004) Nondestructive estimation of tracheid length from sections of radial wood strips by near infrared spectroscopy. *Holzforschung* 58, 375-381
203. Schimleck LR and Evans R (2002) Estimation of microfibril angle of increment cores by near infrared spectroscopy. *IAWA Journal* 23(3): 225-234
204. Schimleck LR and Evans R (2004) Estimation of *Pinus radiata* D. Don tracheid morphological characteristics by near infrared spectroscopy. *Holzforschung* 58: 66-73
205. Schimleck LR, Evans R and Ilic J (2001) Estimation of *Eucalyptus delegatensis* wood properties by near infrared spectroscopy. *Canadian Journal of Forest Research* 31: 1671-1675
206. Schimleck LR, Evans R and Matheson AC (2002) Estimation of *Pinus radiata* D. Don clear wood properties by near-infrared spectroscopy. *Journal of Wood Science* 48: 132-137
207. Schimleck LR, Evans R, Jones PD, Daniels RF, Peter GF, Clark III A (2005) Estimation of microfibril angle and stiffness by near infrared spectroscopy using sample sets having limited wood density variation. *IAWA Journal* 26(2) 175-187
208. Schimleck LR, Mora C, Daniels RF (2003) Estimation of the physical wood properties of green *Pinus taeda* radial samples by near infrared spectroscopy. *Canadian Journal of Forest Research* 33:2297-2305
209. Shenk JS, Workman JJ and Westerhaus MO (2001) Application of NIR Spectroscopy to Agricultural Products”. In: Burns DA, Ciurezak EW (eds) *Handbook of Near-Infrared Analysis*, Marcel Dekker Inc., New York, p. 419
210. Shield ED (1995) Plantation grown eucalypts: Utilisation for lumber and rotary veneers – primary conversion. *Seminário internacional de utilização da madeira de eucalipto para serraria. 05 e 06 de abril de 1995. IPT, São Paulo, Brazil*
211. Shield ED (2007) Whither eucalypt sawlogs? IUFRO 'Eucalypts and diversity: balancing productivity and sustainability'. Durban, South Africa
212. Silva VL (2006) Caracterização de ligninas de *Eucalyptus* spp. pela técnica de pirólise associada à cromatografia gasosa e à espectrometria de massas. 2006. 85 p. Dissertação - Universidade Federal de Viçosa, Viçosa.
213. Skatter S and Kucera B (1997) Spiral grain - An adaptation of trees to withstand stem breakage caused by wind-induced torsion. *Holz als Roh- und Werkstoff* 55: 207-213
214. Sokal RR and Rohlf FJ (1995) *Biometry: The principles and practice of statistics in biological research*. 3rd edition. W.H. Freeman, New York.
215. Sousa-Correia C, Alves A, Rodrigues JC, Ferreira-Dias S, Abreu JM, Macted N, Ford-Lloyd B and Schwanninger M (2007) Oil content estimation of individuals kernels of *Quercus ilex* subsp. *rotundifolia* [(Lam) O. Schwarz] acorns by Fourier transform near infrared spectroscopy and partial least squares regression. *Journal of Near Infrared Spectroscopy* 15: 247-260
216. Stamm AJ (1964) *Wood and Cellulose Science*. Ronald Press, New York. 509p.
217. Steiglitz K, McBride LE (1965) A technique for the identification of linear systems. *IEEE Trans Automat Contr* 10:461-464
218. Thamarus K, Groom K, Bradley A, Raymond CA, Schimleck LR, Williams ER and Moran GF (2004) Identification of quantitative trait loci for wood and fibre properties in two full-sib pedigrees of *Eucalyptus globulus*. *Theoretical and Applied Genetics* 109(4): 856-864

219. Thibaut B, Gril J and Fournier M (2001) Mechanics of wood and trees: some new highlights for an old story. *Comptes Rendus de l'Academie des Sciences Series IIB Mechanics*. 329(9) 701-716
220. Thumm A and Meder R (2001) Stiffness prediction of radiata pine clearwood test pieces using near infrared spectroscopy. *Journal of Near Infrared Spectroscopy* 9: 117-122
221. Thygesen L (1994) Determination of dry matter content basic density of Norway spruce by near infrared reflectance and transmittance spectroscopy. *Journal of Near Infrared Spectroscopy* 2: 127-135
222. Timoshenko S (1921) On the Correction for Shear of the Differential Equation for Transverse Vibrations of Prismatic Bars. *Philosophical Magazine and Journal of Science XLI - Sixth Series*: 744-746
223. Tomazello Fo M, Brazolin S, Chagas MP, Oliveira JTS, Ballarin AW and Benjamin CA (2008) Application of X-ray technique in non-destructive evaluation of *Eucalyptus* wood. *Maderas. Ciencia y tecnología* 10(2): 139-149.
224. Tonello KC, Cotta MK, Alves RR, Ribeiro CFA and Polli HQ (2008) O desenvolvimento do setor florestal brasileiro. *Revista da madeira* 112
225. Tsuchikawa S (2007) A Review of Recent Near Infrared Research for Wood and Paper. *Applied Spectroscopy Review* 42: 43-71
226. Tsuchikawa S, Hayashi K and Tsutsumi S (1992) Application of near infrared spectrophotometry to wood. 1. Effects of the surface-structure. *Mokuzai Gakkaishi* 38:128-136
227. Tsutsumi J, Matsumoto T, Kitahara R and Mio S (1982) Specific gravity, tracheid length and microfibril angle of sugi (*Cryptomeria japonica* D. Don): Seed grown trees compared with grafts. *Bull. Kyushu Univ. For.* 52: 115-120
228. Turner CH, Balodis V and Dean GH (1983) Variability in pulping quality of *E. globulus* from Tasmanian provenances. *Appita Journal* 36(5): 371-376
229. Verryin SD (2008) Breeding for wood quality - a perspective for the future. *New Zealand Journal of Forestry Science* 38(1): 5-13
230. Verryin SD and Hettasch MH (2006) Synopsis of the "Pine Platform - Global Forest Products Workshop on Pine Tree Traits of Importance in the Solid Wood Value Chain". CSIR, Pretoria, Report Ref. No. CSIR/NRE/FOR/ER/2006/0055/C: 1-40.
231. Via BK, Shupe TF, Groom LH, Stine M and So CL (2003) Multivariate modelling of density, strength and stiffness from near infrared spectra for mature, juvenile and pith wood of longleaf pine (*Pinus palustris*). *Journal of Near Infrared Spectroscopy* 11: 365-378
232. Via BK, So CL, Shupe TF, Groom LH and Wikaira J (2009) Mechanical response of longleaf pine to variation in microfibril angle, chemistry associated wavelengths, density, and radial position. *Composites: Part A* 40: 60-66
233. Via BK, So CL, Shupe TF, Stine M and Groom LH (2005) Ability of near infrared spectroscopy to monitor air-dry density distribution and variation of wood. *Wood Fiber Science* 37: 394-402
234. Villanueva B and Kennedy BW (1990) Effect of selection on genetic parameters of correlated traits. *Theoretical and Applied Genetics* 80(6): 746-752
235. Volker PW, Potts BM and Borralho NMG (2008) Genetic parameters of intra- and inter-specific hybrids of *Eucalyptus globulus* and *E. nitens*. *Tree Genetics and Genomes* 4: 445-460
236. Walker JCF and Butterfield BG (1995) The importance of microfibril angle for the processing industries. *New Zealand Forestry*, November: 35-40.
237. Walker NK and Dodd RS (1988) Calculation of Wood Density Variation From X-ray Densitometer Data. *Wood and Fiber Science* 20: 35-43
238. Wallbacks L, Edlund U, Norden B and Berglund I (1991) Multivariate characterization of pulp using ¹³C NMR, FTIR and NIR. *Tappi Journal* 74(10): 201-206
239. Wang S, Littell RC and Rockwood DL (1984) Variation in density and moisture content of wood and bark among twenty *Eucalyptus grandis* progenies. *Wood Science and Technology* 18(2): 97-100

240. Wang T, Aitken SN, Rozenberg P and Carlson MR (1999) Selection for height growth and Pilodyn pin penetration in lodgepole pine: effects on growth traits, wood properties, and their relationships. *Canadian Journal of Forest Research* 29: 434-445
241. Wang X, Ross RJ, Mattson JA, Erickson JR, Forsman JW, Geske EA and Wehr MA (2001) Several nondestructive evaluation techniques for assessing stiffness and MOE of small-diameter logs. (General Technical Report FPL-RP-600). Madison: U.S.D.A Department of Agriculture, Forest Products Laboratory
242. Wang X, Ross RJ, Mattson JA, Erickson JR, Forsman JW, Geskse EA, Wehr MA (2002) Nondestructive evaluation techniques for assessing modulus of elasticity and stiffness of small-diameter logs. *For Prod J* 52:79-85
243. Wardrop AB (1956) The nature of reaction wood. V. The distribution and formation of tension wood in some species of *Eucalyptus*. *Australian Journal of Botany* 4: 152-166
244. Washusen R and Evans R (2001) Prediction of wood tangential shrinkage from cellulose crystallite width in one 11-year-old tree of *Eucalyptus globulus* Labill. *Australian Forest* 64: 123-126
245. Washusen R, Ades P, Evans R, Ilic J and Vinden P (2001) Relationships between density, shrinkage, extractives content and microfibril angle in tension wood from three provenances of 10-year-old *Eucalyptus globulus* Labill. *Holzforschung* 55: 176-182
246. Washusen R, Baker T, Menz D and Morrow A (2005) Effect of thinning and fertilizer on the cellulose crystallite width of *Eucalyptus globulus*. *Wood Science and Technology* 39: 569-578
247. Wei X and Borralho NMG (1997) Genetic control of wood basic density and bark thickness and their relationships with growth traits of *Eucalyptus urophylla* in south east China. *Silvae Genetica* 46(4): 245-250
248. Wei X and Borralho NMG (1999) Objectives and selection criteria for pulp production of *Eucalyptus urophylla* plantation in south east China. *Forest genetics* 6(3): 181-190
249. Westad F and Martens H (2000) Variable selection in near infrared spectroscopy based on significance testing in partial least square regression. *Journal of Near Infrared Spectroscopy* 8: 117-124
250. White TL, Adams WT and Neale DB (2007) *Forest genetics*. CABI Publishing, CAB International, Wallingford, UK.
251. Whittock SP, Dutkowski GW, Greaves BL and Apiolaza LA (2007) Integrating revenues from carbon sequestration into economic breeding objectives for *Eucalyptus globulus* pulpwood production. *Annals of Forest Science* 64: 239-246
252. Wilkes J (1988) Variations in wood anatomy within species of *Eucalyptus*. *IAWA Journal* 9(1): 13-23
253. Williams PC, Sobering DC (1993) Comparison of commercial near infrared transmittance and reflectance instruments for analysis of whole grains and seeds. *Journal of Near Infrared Spectroscopy* 1:25-33
254. Wold S, Sjöström M and Eriksson L (2001) PLS-regression: a basic tool of chemometrics. *Chemometrics and Intelligent Laboratory Systems* 58: 109-130
255. Workman J and Weyer L (2007) *Practical guide to interpretive near infrared spectroscopy*. Boca Raton: CRC Press. 332p.
256. Wright JA, Birkett MD and Gambino MJT (1990) Prediction of pulp yield and cellulose content from wood samples using near infrared reflectance spectroscopy. *Tappi Journal* 73(8): 164-166
257. Wu HX, Powell MB, Yang JL, Ivkovic M and McRae TA (2007) Efficiency of early selection for rotation-aged wood quality traits in radiata pine. *Annals of Forest Science*. 64(1): 1-9
258. Wu Y-Q, Hayashi K, Liu Y, Cai Y-C and Sugimori M (2006) Relationships of anatomical characteristics versus shrinkage and collapse properties in plantation-grown eucalypt wood from China. *Journal of Wood Science* 52(3): 187-194
259. Wu Y-Q, Hayashi K, Liu Y, Cai Y-C, Sugimoro M and Luo J-J (2005) Collapse-type shrinkage characteristics in plantation-grown eucalypts: I. Correlations of basic density and some structural indices with shrinkage and collapse properties. *Journal of Forestry Research* 16(2): 83-88
260. Yamada T, Yeh T-F, Ching H-M, Li L, Kadla FK and Chiang VL (2004) Rapid analysis of transgenic trees using transmittance near-infrared spectroscopy. *Journal Near Infrared Spectroscopy* 12: 263-269

261. Yamamoto H, Okuyama T and Yashida M (1993) Method of determining the mean microfibril angle of wood over a wide range by the improved Cave's method. *Mokuzai Gakkaishi* 39: 118-125
262. Yamamoto H, Sassus F, Ninomiya M and Gril J (2001) A model of anisotropic swelling and shrinking process of wood. Part 2. A simulation of shrinking wood. *Wood Science and Technology* 35: 167-181
263. Yang JL (2007) Investigation of potential sawlog quality indicators - A case study with 32-year-old plantation *Eucalyptus globulus* Labill. *Holz als Roh- und Werkstoff* 65: 419-427
264. Yang JL and Evans R (2003) Prediction of MOE of eucalypt wood from microfibril angle and density. *Holz als Roh- und Werkstoff* 61: 449-452
265. Yang JL and Waugh G (1996a) Potential of plantation-grown eucalypts for structural sawn products. I. *Eucalyptus globulus* Labill. spp. *globulus*. *Australian Forestry* 59: 90-98
266. Yang JL and Waugh G (1996b) Potential of plantation-grown eucalypts for structural sawn products. II. *Eucalyptus nitens* (Deane & Maiden) Maiden and *E. regnans* F. Muell. *Australian Forestry* 59: 99-107
267. Zamudio F, Baettyg R, Vergara A, Guerra F and Rozenberg P (2002) Genetic trends in wood density and radial growth with cambial age in a Radiata pine progeny test. *Annals of Forest Science* 59: 541-549
268. Zhang SY (1995) Effect of growth rate on wood specific gravity and selected mechanical properties in individual species from distinct wood categories. *Wood Science and Technology* 29(6): 451-465
269. Zobel B and Jett JB (1995) *Genetics of Wood Production*. Berlin: Springer-Verlag. 336 p.
270. Zobel B and Talbert J (1984) *Applied Forest Tree Improvement*. The Blackburn Press, Caldwell, NJ, Reprint of First Edition. 505p.
271. Zobel BJ and Van Buijtenen JP (1989) *Wood Variation: Its Causes and Control*. Springer Verlag, Berlin. 363p.

LIST OF TABLES

Table 1 - Distribution of <i>Eucalyptus</i> and <i>Pinus</i> forest plantations in Brazil by industrial segment in 2009/26	
Table 2 - Components of variance of growth and wood traits (from Falconer (1993))	38
Table 3 - Resume of the main statistics of the NIR-based calibration for estimating wood traits of progeny and clonal tests and the corresponding paper	55
Table 4 - Arrays of parents in the incomplete factorial mating design under controlled crosses.....	57
Table 5 - Description of the environmental information of the clonal tests.....	58
Table 6 - Information about the clones' origin describing their relatives and species	58
Table 7 - Reference of codes relative to radial and longitudinal positions.....	61
Table 8 - Resume of growth and wood traits measurements, methods, sample dimension and number of observations of the trees from Clonal test	68
Table 9 - Resume of growth and wood traits measurements, methods, sample dimension and number of observations of the trees from Progeny test. Chemical properties were done in duplicate	69
Table 10 - Descriptive statistics of growth traits in 14-year-old <i>Eucalyptus urophylla</i> from progeny test and in 6-year-old <i>E. urograndis</i> from clonal test, including circumference at 1.3 meter height (C) and total height (H) by site and considering all samples.....	75
Table 11 - Descriptive statistic for Klason lignin (KL); acid-soluble lignin (ASL) and total lignin content (TL); syringyl to guaiacyl ratio (S/G); and extractive content (EXT) in 14-year-old <i>Eucalyptus urophylla</i> wood	76
Table 12 - Descriptive statistics, including average, standard deviation (Sd), minimum (Min), maximum (Max) and coefficient of variation (CV) for basic density (ρ), <i>T</i> parameter and microfibril angle (MFA) measurements in 14-year-old <i>Eucalyptus urophylla</i> wood	77
Table 13 - Description of tangential sections from the radial wood strips, their influence on the <i>T</i> parameter measurements and the radial variation of MFA and basic density in 14-year-old <i>Eucalyptus urophylla</i> wood. The relative radial position is presented in squared brackets while the range of variation of traits is presented in parentheses.....	79
Table 14 - Descriptive statistics of dynamic properties of the kiln-dried scantlings of 6-year-old <i>Eucalyptus grandis</i> x <i>urophylla</i> , including kiln-dried density (ρ_{14} , kg m ⁻³), first resonant frequency (f_{14} , Hz), elastic modulus (E ₁₄ , MPa), specific modulus (E' ₁₄ , E/ ρ), loss tangent (tg δ_{14} , 10 ⁻³) and shear modulus (G ₁₄ , MPa) estimated by longitudinal (L) and flexural (F) vibration tests.....	80
Table 15 - Descriptive statistics of dynamic properties of the clearwood specimens of 6-year-old <i>Eucalyptus grandis</i> x <i>urophylla</i> , including air-dried density (ρ_{sp} , kg m ⁻³), resonant frequency (f_{sp} , Hz), elastic modulus (E _{sp} , MPa), specific modulus (E' _{sp} , E/ ρ), loss tangent (tg δ_{Fsp} , 10 ⁻³) and shear modulus (G _{sp} , MPa) estimated by longitudinal (L) and flexural (F) vibration tests.....	81

Table 16 - Descriptive statistics of the 4- and 3-points bending test of the specimens of 6-year-old <i>Eucalyptus grandis</i> x <i>urophylla</i> , including force at rupture point (Fmax, N) and modulus of rupture (MOR, MPa).....	83
Table 17 - Descriptive statistics of basic density (ρ_s , kg m ⁻³) and radial and tangential shrinkage (%) of the small samples of 6-year-old <i>Eucalyptus grandis</i> x <i>urophylla</i>	84
Table 18 - Descriptive statistics of the <i>T</i> parameter obtained by X-ray diffraction and microfibril angle estimates by Cave (MFA _C) and Yamamoto (MFA _Y) formulas from the small samples of 6-year-old <i>Eucalyptus grandis</i> x <i>urophylla</i> . Samples were taken from the small wood samples (MFA _{YS}) and from radial strips (MFA _{YRS})	85
Table 19 - Mean and standard deviation (in parentheses) of microfibril angle according to the year of wood formation estimated by Yamamoto (MFA _{YRS} in degrees) formulas from radial strips of 6-year-old <i>Eucalyptus</i> clones from sites 301, 302 and 303.....	86
Table 20 - Correlations between wood traits including wood density (ρ), elastic modulus (E), specific modulus (E'), shear modulus (G), radial (δ_{rd}) and tangential shrinkage (δ_{tg}), microfibril angle, ρ /MFA parameter and modulus of rupture (MOR). The correlations were statistically significant at $p < 0.01$	87
Table 21 - Regression models for predicting modulus of elasticity in longitudinal (E _L) and flexural (E _F) vibrations and modulus of rupture (MOR _{4p}) with MFA, density, and ρ /MFA.....	89
Table 22 - Descriptive statistics of Klason lignin (KL), S to G ratio (S/G), basic density (ρ) and microfibril angle (MFA) of 14-year-old <i>Eucalyptus urophylla</i> woods from progeny test	92
Table 23 - Statistical summary of the overall, calibration and validation sets for air-dry density, basic density, microfibril angle and a range of dynamic properties of the small, clean specimens of <i>Eucalyptus</i> wood from clonal test	92
Table 24 - PLS-R models for Klason lignin (KL, %), syringyl to guaiacyl ratio (S/G, no unit), wood basic density (ρ , kg m ⁻³) and microfibril angle (MFA, degrees) used for estimating phenotypic values for 14-year-old <i>Eucalyptus urophylla</i>	93
Table 25 - PLS-R models for air-dry density (ρ_{sp} , kg m ⁻³), wood basic density (ρ_s , kg m ⁻³), microfibril angle (MFA, degrees), longitudinal and flexural modulus of elasticity (E, MPa), longitudinal and flexural specific modulus (E', MPa/ ρ), first resonance frequency (f_i , MHz) and loss tangent ($\tan\delta_L$, 10 ³) used for estimating phenotypic values for 6-year-old <i>Eucalyptus</i> clones	93
Table 26 - NIR absorption bands normally associated to the main wood components (cellulose, hemicelluloses, lignin, and water) contained in the wood specimens	96
Table 27 - Mean, minimum and maximum values, coefficient of variation and number of observations (N) for measured circumference (C, centimeters) and height (H, meters), and NIR-estimated Klason lignin (KL, %), syringyl to guaiacyl ratio (S/G, no unit), wood density (D, kg m ⁻³) and microfibril angle (MFA, degrees) of the 14-year-old <i>Eucalyptus urophylla</i> population	99
Table 28 - Additive genetic and residual variance components, genetic and residual coefficient of variance and narrow-sense heritability estimates for various traits	100

Table 29 - Estimated additive genetic (r_A , below the diagonal) and residual (r_E , above the diagonal) correlations for various traits, including circumference (C), height (H), microfibril angle (MFA), basic density (D), Klason lignin (KL) and syringyl to guaiacyl ratio (S/G). Standard errors are shown in parentheses	102
Table 30 - Variation with age of additive genetic, residual and phenotypic correlations of density with C, and MFA with C, KL and density. Standard errors are in parenthesis	103
Table 31 - Tukey (HSD) multiple range tests for growth traits by clone and by site in 6-year-old <i>Eucalyptus urophylla</i> x <i>grandis</i> clones	107
Table 32 - Analysis of variance for density and dynamic traits in kiln-dried at 14% scantlings of 6-year-old <i>Eucalyptus urophylla</i> x <i>grandis</i> clones	108
Table 33 - Tukey (HSD) multiple range tests for density and dynamic traits by clone and by site in kiln-dried at 14% scantlings of 6-year-old <i>Eucalyptus urophylla</i> x <i>grandis</i> clones	108
Table 34 - Radial and longitudinal variation for wood basic density (kg m^{-3}) in <i>Eucalyptus</i> clones at three contrasting sites. The means were compared by the Tukey test at $p=0.01$ threshold. Small letters are comparisons between radial positions while capital ones compares sites. Values in brackets are coefficients of variation in percentage	110
Table 35 - Radial and longitudinal variation for modulus of elasticity (MPa) in clones of <i>Eucalyptus</i> wood at three contrasting sites. The means were compared by the Tukey test at $p=0.01$ threshold. Small letters are comparisons between radial positions while capital ones compares sites. Values in brackets are coefficients of variation in percentage	111
Table 36 - Radial and longitudinal variation for microfibril angle (degrees) in clones of <i>Eucalyptus</i> wood at three contrasting sites. The means were compared by the Tukey test at $p=0.01$ threshold. Small letters are comparisons between radial positions while capital ones compares sites. Values in brackets are coefficients of variation in percentage	112
Table 37 - Pith to cambium variation of wood density (kg m^{-3}), stiffness (GPa) and microfibril angle (degrees) at various relative heights.	114
Table 38 - Radial variation at 25% of the stem height for wood basic density (kg m^{-3}) for clones of <i>Eucalyptus</i> wood and sites. The means were compared by the Tukey test at $p=0.05$ threshold. Small letters are comparisons between clones or sites while capital ones compares the radial positions.....	115
Table 39 - Radial variation at 25% of the stem height for elastic modulus (MPa) for clones of <i>Eucalyptus</i> wood and sites. The means were compared by the Tukey test at $p=0.05$ threshold. Small letters are comparisons between clones or sites while capital ones compares the radial positions.....	116
Table 40 - Radial variation at 25% of the stem height for microfibril angle (degrees) for clones of <i>Eucalyptus</i> wood and sites. The means were compared by the Tukey test at $p=0.05$ threshold. Small letters are comparisons between clones or sites while capital ones compares the radial positions.....	118
Table 41 - Genetic parameters for growth traits in 6-year-old <i>Eucalyptus urophylla</i> x <i>grandis</i> clones....	119
Table 42 - Genetic parameters for basic density of the wood in 6-year-old <i>Eucalyptus urophylla</i> x <i>grandis</i>	120

Table 43 - Genetic parameters for dynamic longitudinal modulus of elasticity of the wood in 6-year-old <i>Eucalyptus urophylla</i> x <i>grandis</i>	120
Table 44 - Genetic parameters for microfibril angle of cell wall of wood in 6-year-old <i>Eucalyptus urophylla</i> x <i>grandis</i> clones	121
Table 45 - Descriptive statistics of dynamic properties of the air-scantlings of 6-year-old <i>Eucalyptus grandis</i> x <i>urophylla</i> , including air-dry density (ρ_{ad} , kg m ⁻³), first resonant frequency (f_{lad} , Hz), elastic modulus (E_{ad} , MPa), specific modulus (E'_{ad} , E/ ρ), loss tangent ($tg \delta_{ad}$, 10 ⁻³) and shear modulus (G_{ad} , MPa) estimated by longitudinal (_L) and flexural (_F) vibration tests.....	137
Table 46 - Correlations among physical and elastic properties of 395 air-dried and 14% dried scantlings of 6-year-old <i>Eucalyptus grandis</i> x <i>urophylla</i> wood. The significance level for all relationships was <0.0001	138
Table 47 - Correlations among <i>Eucalyptus</i> wood traits by site and by radial position. All correlations were statistically significant at $p < 0.01$	140
Table 48 - Analysis of variance for density and dynamic traits in air-dried scantlings of 6-year-old <i>Eucalyptus urophylla</i> x <i>grandis</i> clones	142
Table 49 - Tukey (HSD) multiple range tests for density and dynamic traits by clone and by site in air-dried scantlings of 6-year-old <i>Eucalyptus urophylla</i> x <i>grandis</i> clones	143
Table 50 - Genetic parameters for basic density of the wood in 6-year-old <i>Eucalyptus urophylla</i> x <i>grandis</i> clones (model $y = \mu + G + E$).....	145
Table 51 - Genetic parameters for dynamic longitudinal modulus of elasticity of the wood in 6-year-old <i>Eucalyptus urophylla</i> x <i>grandis</i> clones (model $y = \mu + G + E$)	145
Table 52 - Genetic parameters for microfibril angle of cell wall of wood in 6-year-old <i>Eucalyptus urophylla</i> x <i>grandis</i> clones (model $y = \mu + G + E$)	146

LIST OF FIGURES

Figure 1 - Transversal (A), radial (B) e tangential (C) sections of 6-year-old <i>Eucalyptus</i> wood (source: personal image)	29
Figure 2 - Three-dimensional structure of the secondary cell wall of a fibre.....	31
Figure 3 - Relationship between MFA and modulus of elasticity (MOE) of <i>E. globulus</i> , <i>E. nitens</i> and <i>E. regnans</i> wood between 15 and 33 years of age (from Yang and Evans 2003).....	32
Figure 4 - Theoretical model explaining the influence of high microfibril angle (A) and low microfibril angle (B) on longitudinal and transversal components of shrinkage and swelling	33
Figure 5 - Relationship between anisotropic shrinkage (from green to oven-dried) and MFA (from Yamamoto et al. 2001)	34
Figure 6 - The relationship between the angle T derivated from the X-ray intensity variation and the mean microfibril angle measured by iodine staining (A, from Meylan 1967) and by Field-Emission Scanning Electron Microscopy (B, from Ruelle et al. 2007)	36
Figure 7 - Genetic gain from tree breeding programs (A, personal source) and graphs of the regression lines of breeding values on phenotypic values for two hypothetical traits, A and B, with $h^2_A=0.2$ and $h^2_B=0.4$ (B, from White et al. 2007)	37
Figure 8 - Evaluating standing trees with Resistograph (A) and Pilodyn (B). Dotted lines shows in detail the pine penetration (source: personal image).....	44
Figure 9 - Example of tomography analysis; a photograph of the disc (diameter: 90 cm) and the corresponding acoustic tomogram showing the decay (blue parts) in a wood disc (from Rabe et al. (2004))	45
Figure 10 - Portable device for estimating dynamic elastic properties of wood based on sonic resonance frequency (source: personal image).....	46
Figure 11 - Schematic of NIR spectrometer readings	47
Figure 12 - Wood discs from the the progeny and clonal tests and the growth and wood traits under examination in this study (source: personal image)	54
Figure 13 - Differences of field conditions between clonal tests (source: personal image).....	58
Figure 14 - Strategy of wood sampling and wood measurements of the progeny test.....	59
Figure 15 - Strategy of wood sampling and wood measurements of the clonal test and reference of codes relative to radial and longitudinal positions for NIR spectroscopic and genetic analysis	60
Figure 16 - Schema for four-point statistic bending test	64
Figure 17 - Schema for three-point statistic bending test.....	65

Figure 18 - Experimental dispositive for measuring the green volume of the samples (A) and the sample dimensions (B) (source: personal image)	65
Figure 19 - X-ray diffractometer device with CuK α radiation used for measuring XRD patterns (A), detail of the specimen holder (B) and the mini-circular machine used for cutting samples (C) (source: personal image).....	66
Figure 20 - X-ray scattering patterns recorded in 2 mm tangential sections of <i>Eucalyptus</i> samples with low (a) and high (b) T parameter.....	67
Figure 21 - NIR spectrophotometer used for measuring diffuse reflectance of wood samples showing the sintered gold standard (A), cup module for measuring NIR spectra from grounded wood (B), window for NIR spectra scanning - 10 mm of diameter (C) and 2-mm radial section of wood (D) (source: personal image).....	68
Figure 22 - Mean and standard deviation of circumference at breast height (C) and commercial height (H) for each site and considering all samples	75
Figure 23 - Radial strips showing curvature effect by dotted lines and classes by continuous lines	77
Figure 24 - Radial variation of MFA (A) and basic density (B) in 14-year- <i>Eucalyptus urophylla</i> wood for radial strips (N=14)	78
Figure 25 - Mean and standard deviation values of kiln-dried wood density and dynamic elastic modulus in kiln-dried scantlings for each site.....	80
Figure 26 - Mean and standard deviation values of longitudinal and flexural dynamic elastic modulus and 4- and 3-points bending test in small samples of <i>Eucalyptus</i> for each site	82
Figure 27 - Mean and standard deviation values of air-dried density of the specimens (ρ_{sp}) and of the basic density of the small wood samples (ρ_s) and radial and tangential shrinkage from oven-dried to green conditions for each	84
Figure 28 - Mean and standard deviation values of MFA in small wood samples (MFA _{YS}) and radial strips (MFA _{YRS}) of <i>Eucalyptus</i> wood for each site and for all samples	85
Figure 29 - Radial variation of MFA (estimated by Yamamoto's formula) for wood samples taken from radial strips of 6-year-old <i>Eucalyptus</i> clones	86
Figure 30 - Relationship between wood traits in <i>Eucalyptus</i> wood. SEE is the standard error of estimation	88
Figure 31 - NIR absorbance versus wavenumber plot for raw (untreated) NIR spectra from 9,000 to 4,000 cm^{-1} range.	91
Figure 32 - Absorbance versus wavenumber plot for first and second derivative of the NIR spectra	91
Figure 33 - NIR predicted versus measured values plot for Klason lignin (A), S/G ratio (B), basic density (C) and microfibril angle (D) of wood. The calibration set samples are represented by white circles and the validation set samples are represented by black circles	94

Figure 34 - NIR predicted versus measured values plot for air-dry density (A), basic density (B), MFA (C), dynamic elastic modulus (D), first resonance frequency (E) and loss tangent (F) based on NIR spectra for both training (open circles) and test sets (filled rhombs).....	95
Figure 35 - PLS-regression coefficients for NIR-based model for estimating air-dry density (A), basic density (B), microfibril angle (C), dynamic elastic modulus (D), first resonance frequency (E) and loss tangent (F)	98
Figure 36 - Age trends of phenotypic, residual and additive genetic correlations of density with C, and MFA with C, KL and density	104
Figure 37 - Clone x site interaction for mean circumference at 1.3 meters (A) and commercial height (B) of the trees from Clonal test	106
Figure 38 - Clone x site interaction for wood density (A) and longitudinal elastic modulus (B) of the kiln-dried scantlings.....	109
Figure 39 - Spatial variation of wood basic density (kg m^{-3}) in <i>Eucalyptus urophylla</i> x <i>grandis</i> trees	110
Figure 40 - Spatial variation of modulus of elasticity (MPa) in <i>Eucalyptus urophylla</i> x <i>grandis</i> trees	111
Figure 41 - Spatial variation of microfibril angle (degrees) in <i>Eucalyptus urophylla</i> x <i>grandis</i> trees.....	112
Figure 42 - Clone by site interaction for basic density of the inner heartwood (A) and of the outer sapwood (B) at 25% of height	115
Figure 43 - Clone by site interaction for longitudinal elastic modulus of the inner heartwood (A) and of the outer sapwood (B) at 25% of height.....	117
Figure 44 - Clone by site interaction for microfibril angle of the inner heartwood (A) and of the outer sapwood (B) at 25% of height	118
Figure 45 - Spatial variation of heritability estimates over basic density of wood, wood stiffness and microfibril angle within <i>Eucalyptus</i> trees.....	119
Figure 46 - Spatial variation of NIR spectral broad-sense heritability estimates at the base and at 25% of the tree height. The bands normally associated to cellulose, hemicelluloses and lignin are indicated by numbered narrows (these index are presented in Table 26, pg. 97)	123
Figure 47 - Spatial variation of NIR spectral broad-sense heritability estimates at 50, 75 and 100% of the tree height. The bands normally associated to cellulose, hemicelluloses and lignin are indicated by numbered narrows (these index are presented in Table 26, pg. 97)	124
Figure 48 - Mean and standard deviation values of air-dried density and dynamic elastic modulus in air-dried scantlings for each site.	137
Figure 49 - Correlation between the modulus of elasticity of the kiln- (E_{L14}) and air-dried (E_{LD}) scantlings obtained in the flexural test for 411 scantlings of <i>Eucalyptus</i> showing the samples presenting problems after drying	138

Figure 50 - Correlation between the modulus of elasticity of the kiln- (E_{L14}) and air-dried (E_{Lad}) scantlings obtained in the flexural test for 395 scantlings of *Eucalyptus grandis* x *urophylla* wood with 45 mm x 60 mm cross section 139

Figure 51 - Linear regression plot between the dynamic flexural elastic modulus and the MOR obtained by tree and four points bending tests using complete sampling of *Eucalyptus* wood. SEE is the standard error of estimation 141

Figure 52 - Linear regression plot between the wood density and the MOR obtained by tree and four points bending tests using complete sampling of *Eucalyptus* wood. SEE is the standard error of estimation 141

Figure 53 - Linear regression plot between the MOR obtained by tree and four points bending tests. SEE is the standard error of estimation 142

Figure 54 - Spatial variation of heritability estimates over basic density of wood, wood stiffness and microfibril angle within *Eucalyptus* trees (model $y = \mu + G + E$)..... 144